Section 4:
Session 3: Structural Analysis and Fracture Mechanics Issues

Probabilistic Fracture Mechanics Analysis of RPV Top Head Nozzles

U.S. Nuclear Regulatory Commission
Argonne National Laboratory

Conference on Vessel Head Penetration Inspection, Cracking, and Repairs

September 29 – October 2, 2003
Gaithersburg, Maryland

Peter Riccardella, Nathaniel Cofie, Angah Miessi
Structural Integrity Associates
Sept. 30, 2003

EPRI

Structural Integrity Associates, Inc.

Project underway since Sept. 2001 under EPRI / MRP sponsorship

Objectives:

- **Develop generic methodology to determine probabilities of top head nozzle leakage and failure (ejection)**
- **Apply to assortment of U.S. PWRs in support of MRP Safety Assessment**
- **Use to define MRP inspection plan that provides acceptable level of quality and safety**

Elements of Analysis

- Monte-Carlo PFM model
- Applied stress intensity factors for circumferential cracks
- Weibull analysis of plant inspection data (time to leakage or significant cracking)
- Statistical characterization of laboratory PWSCC crack growth rates
- Effect of inspections (interval and probability of detection)

Monte-Carlo PFM Model

- **A time-dependent Monte Carlo analysis scheme**
- **Predicts probability of leakage and nozzle ejection versus time for a specific set of top head parameters:**
  - Deterministic Parameters
  - Statistical Parameters (Random Variables)
- **Two nested Monte Carlo simulation loops**
  - step through time for each nozzle in a head
  - and then for the total number of head simulations specified

Deterministic Parameters

- **Number of top head nozzles**
- **Angle of each nozzle with respect to the head**
- **Nozzle diameter and wall thickness**
- **Number of heats of nozzle material, and number of nozzles from each heat**
- **K-matrices for each of four nozzle angles into which nozzles are lumped**
  - K vs. Crack Length
  - Two Yield Strengths
  - Two Nozzle Interferences

Important Random Variables

- **Head operating temperature**
- **Weibull distribution of time to leakage or cracking (dependent on plant operating time and head temperature)**
- **Stress corrosion crack growth law distribution**
- **Correlation factor between time to crack initiation and crack growth law, and**
- **Critical crack size for each nozzle angle**

  Input as distribution type (normal, triangular, log–normal, log-triangular, Poisson, Weibull, etc.) plus mean and variance

Stress Intensity Factor Calculations

- **Analyses performed for four "characteristic plant types"**
- **Assume that cracking follows planes of maximum stress**
- **Assume through-wall cracks over entire propagation length (30º to 300º)**

	Plant A (B&W)	**Plant B (W 2-Loop)**	**Plant C (W 4-Loop)**	**Plant D (CE)**	
				CEDM	ICI
Top Head: ID (in.) thickness (in)	87.25 6.626	66.3125 5.75	86 7	86 7.6875	
Nozzle: OD (in.) thickness (in)	4.0 0.6175	4.0 0.625	4.0 0.625	4.05 0.661	5.563 0.4065
Total # Nozzles	69	37	96	91	10
Nozzle Angles Analyzed (º)	0, 18, 26, 38.5	0, 13.6, 30, 43.5	48.8	0, 7.8, 49.7	55.3
Nozzle Yield Strengths (ksi)	High:50 Low:37	58	63	High:59 Low:52.5	39.5

Geometric Comparison of Characteristic Plants

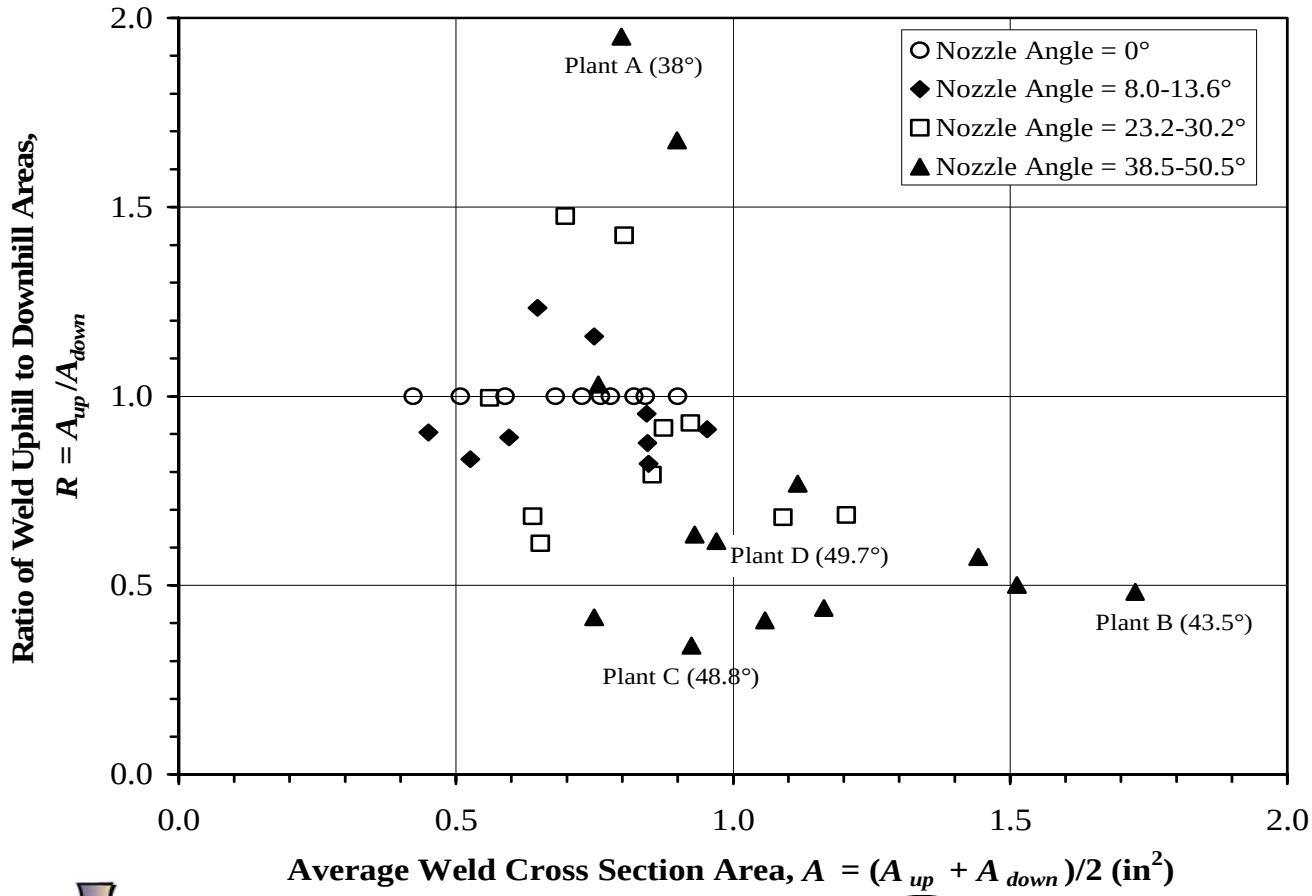

Residual + Operating Stress Analyses of Non-Cracked Nozzles

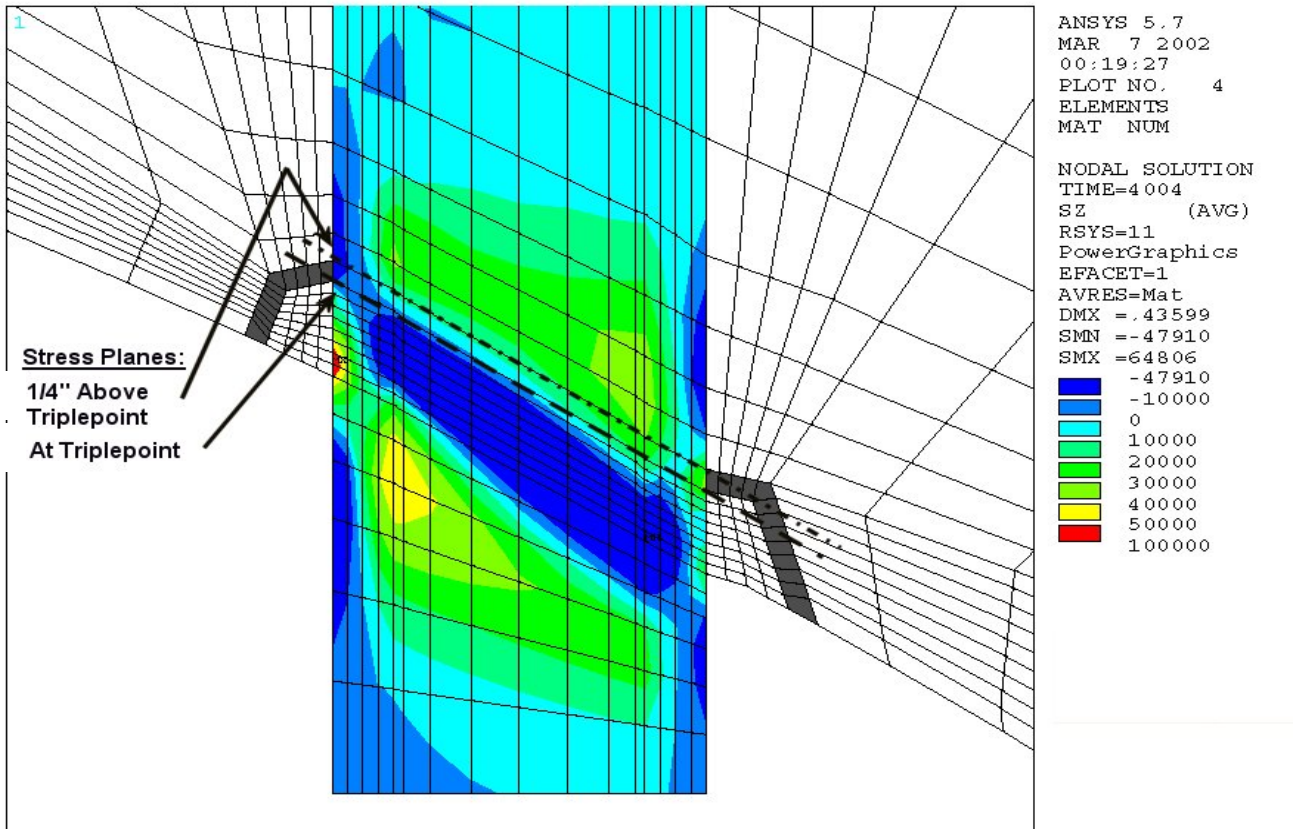

EPRI

Structural Integrity Associates, Inc.

Stresses along Various Stress Planes – Plant A

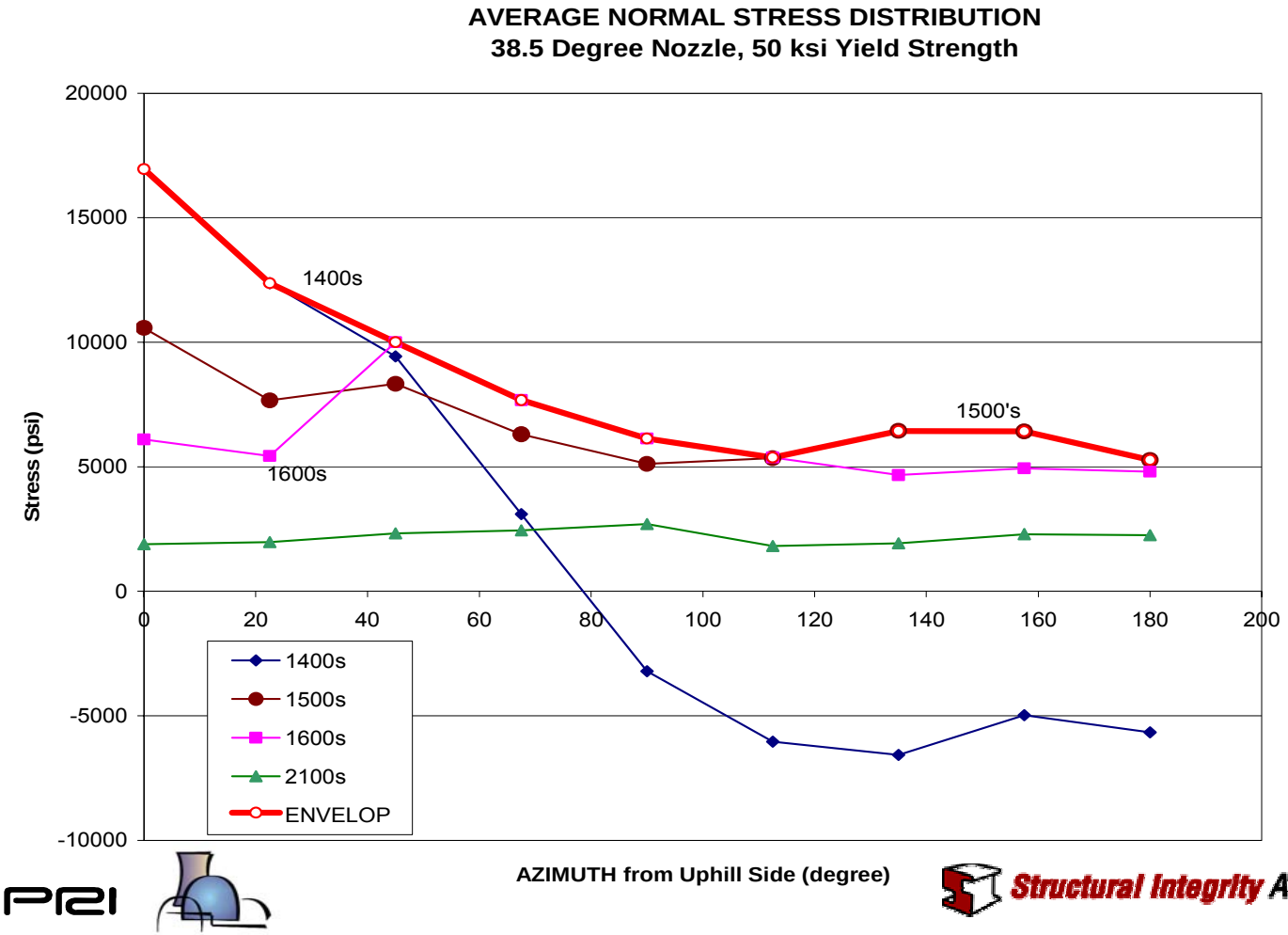

Stresses along Various Stress Planes – Plant C

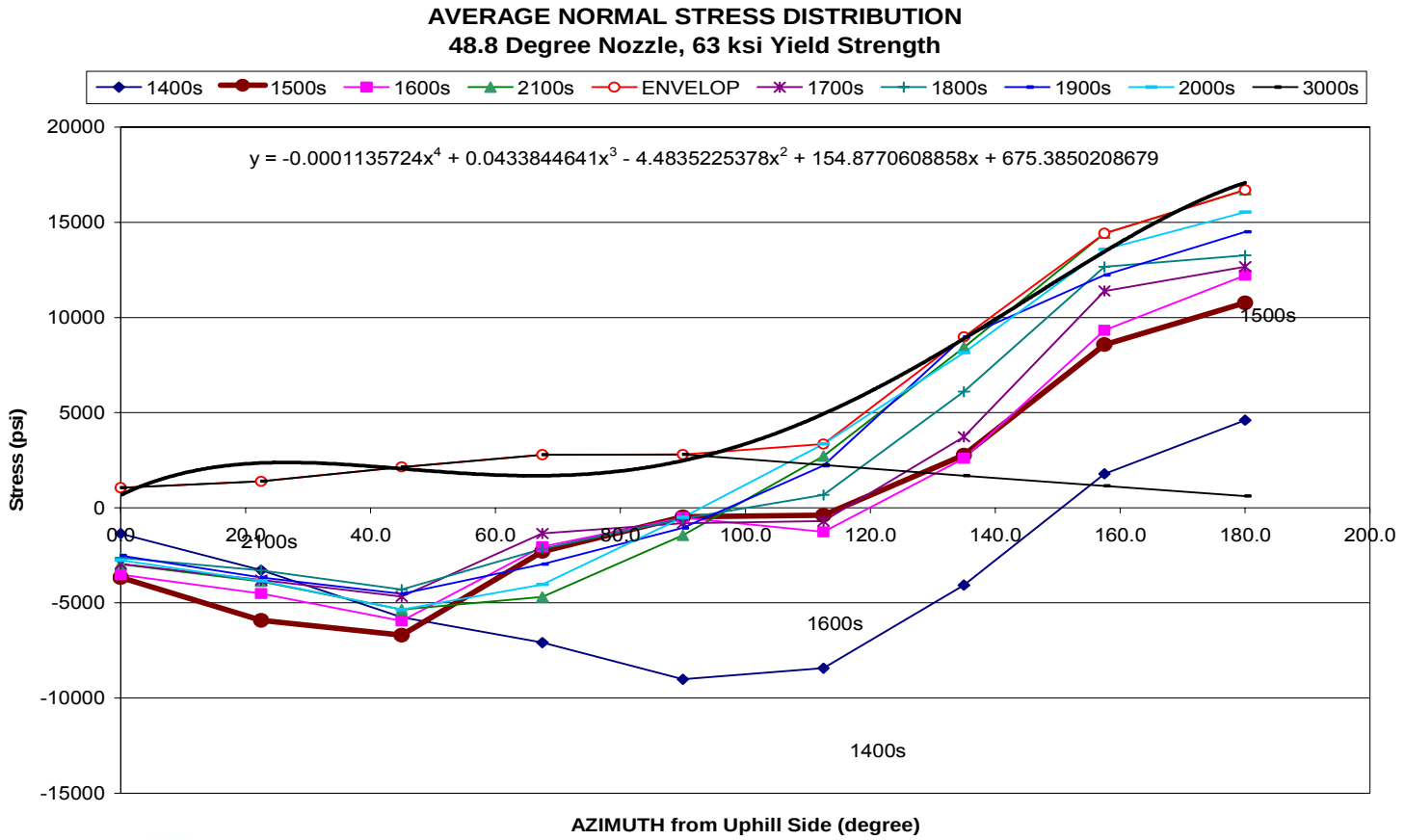

Superposition Approach for K Calculations

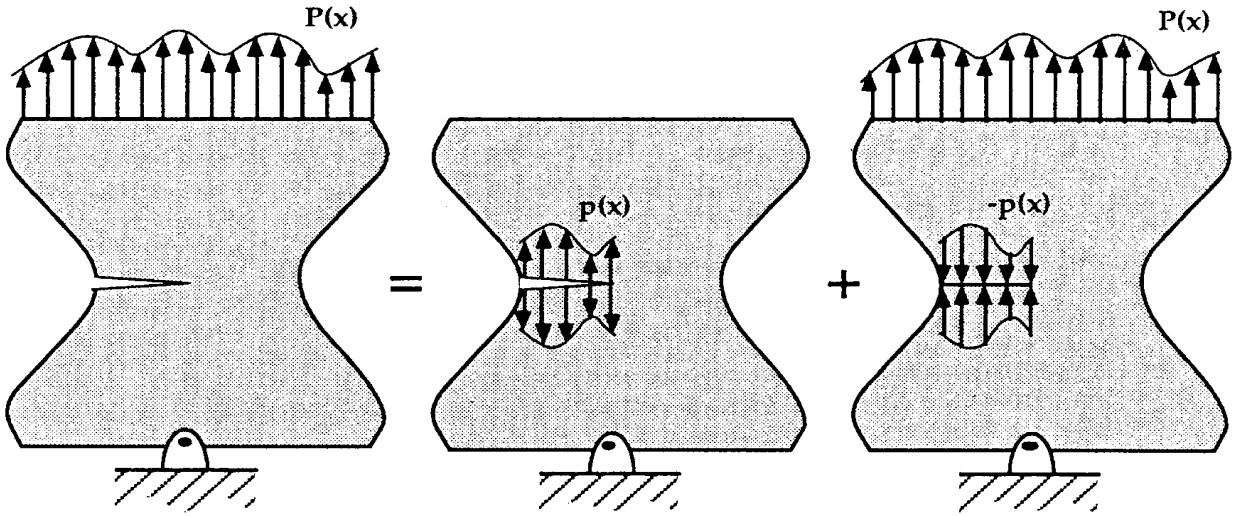

Fracture Mechanics
Through-Wall Crack Model

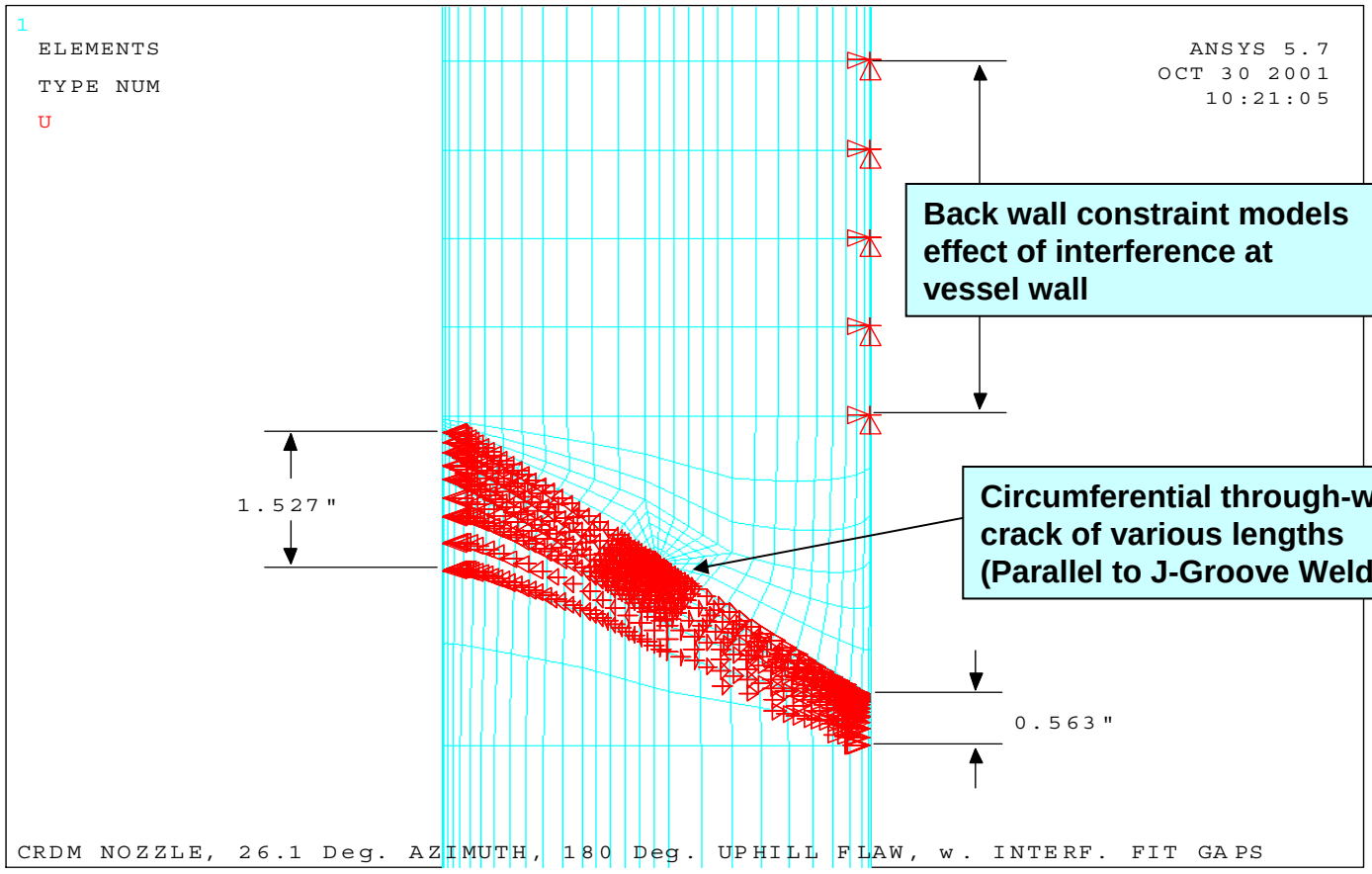

EPRI

Structural Integrity Associates, Inc.

Stress Intensity Factors
Plants A & C - Uphill Cracking

Stress Intensity Factor Comparison - B&W vs. W Heads
Uphill Flaws; Envelop Stress

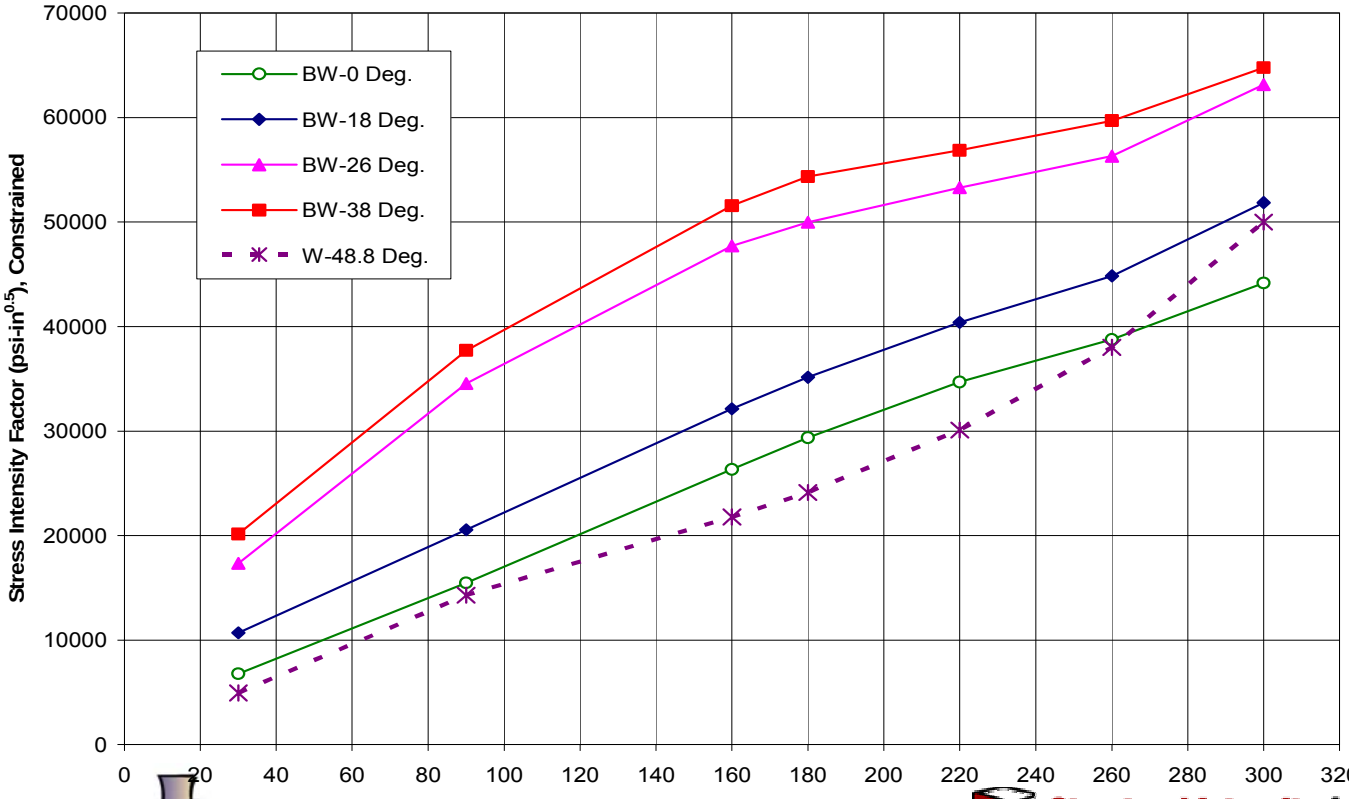

EPRI

Structural Integrity Associates, Inc.

Stress Intensity Factors
Plants A & C - Downhill Cracking

Stress Intensity Factor Comparison - B&W vs. W Heads
Downhill Flaws; Envelop Stress

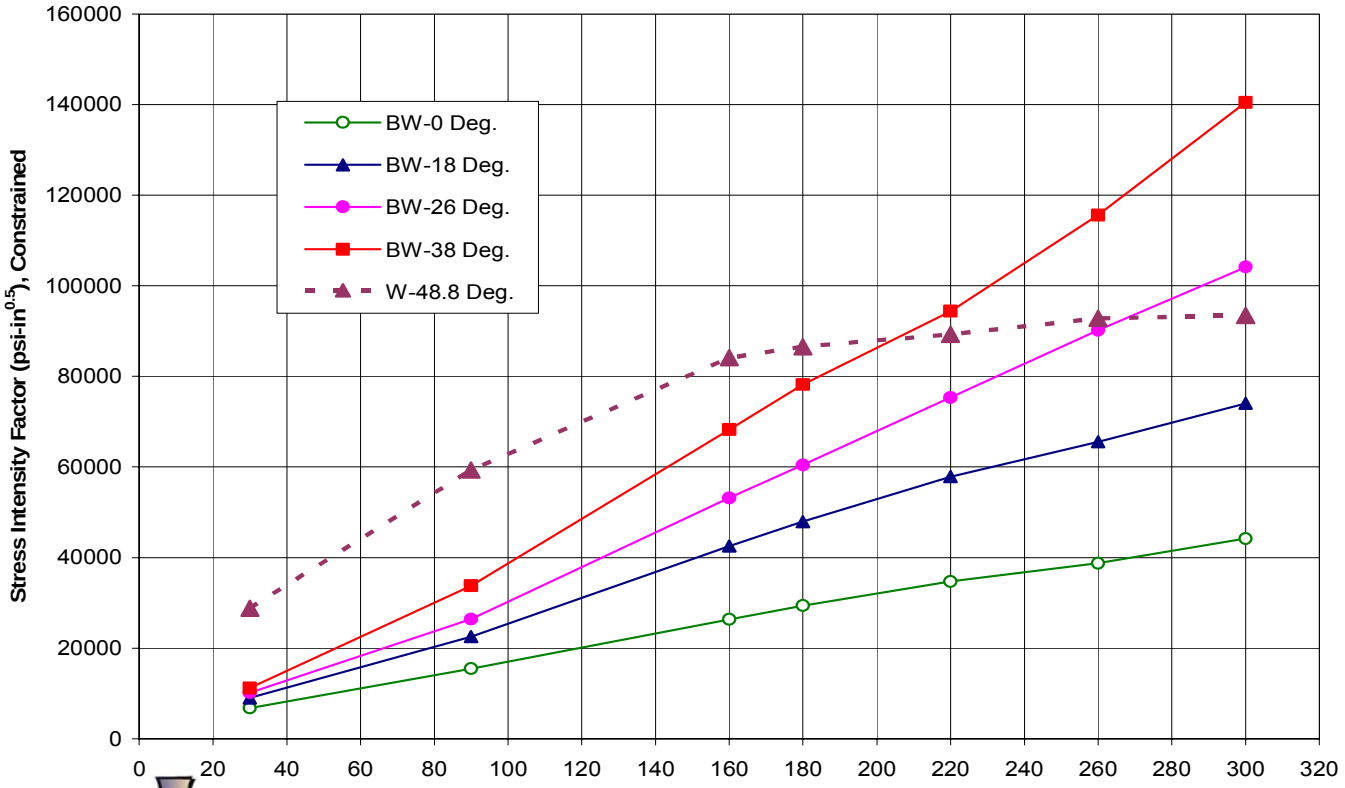

EPRI

Structural Integrity Associates, Inc.

Weibull Model of Time to First Leakage or Cracking

- **"WEI-BAYES" analysis method***
  - Weibull Slope = 3.0 assumed from prior Alloy 600 experience
  - Determine best fit through field inspection results
- **Considers only plants that have performed non-visual NDE thru Spring-03**
  - Population = 30 plants
  - 12 had leaks or significant cracking
  - 18 inspected & clean treated as "Suspensions"
  - Plants that performed only visual examinations excluded
- **Plants w/ multiple cracked or leaking nozzles extrapolated back to time to first leak or crack**
  - w/ same assumed Weibull slope of 3

R. B. Abernathy, "The New Weibull Handbook, Reliability and Statistical Analysis for Predicting Life, Safety, Survivability, Risk, Cost and Warranty Claims," Fourth Edition, Sept. 2000

Summary of Inspections & Results (Thru Spring-03)

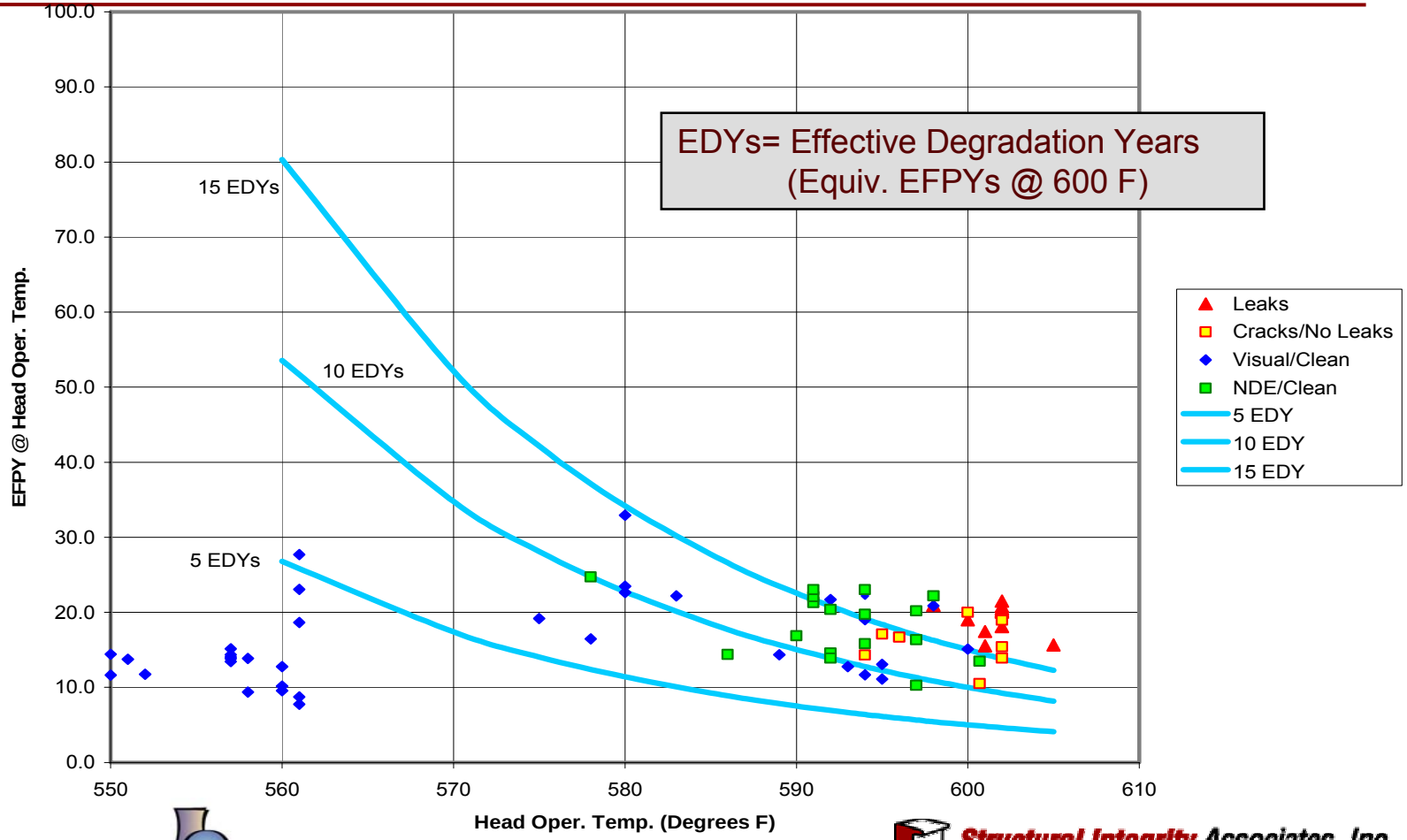

EPRI

Structural Integrity Associates, Inc.

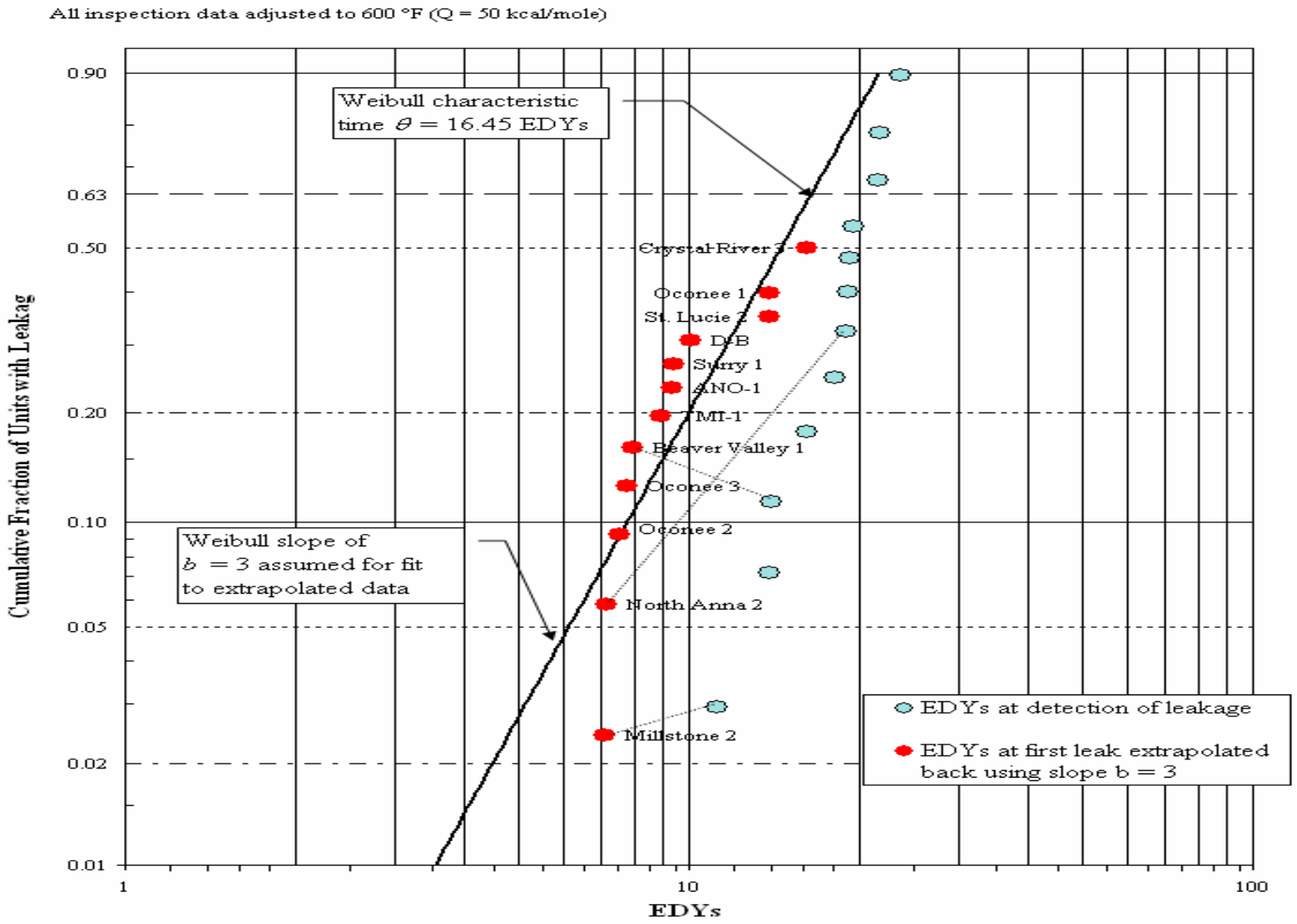
All inspection data adjusted to 600 °F (Q = 50 kcal/mole)
Cumulative Fraction of Units with Leakag
0.90
0.63
0.50
0.20
0.10
0.05
0.02
0.01
1
10
100
EDYs
Weibull characteristic time θ = 16.45 EDYs
Weibull slope of b = 3 assumed for fit to extrapolated data
Crystal River 3
Oconee 1
St. Lucie 2
D.B
Surry 1
ANO-1
TMI-1
Beaver Valley 1
Oconee 3
Oconee 2
North Anna 2
Millstone 2
EDYs at detection of leakage
EDYs at first leak extrapolated back using slope b = 3

Material Crack Growth Rate Statistics

- **Crack growth statistics incorporate latest MRP-55 qualified data set**
  - 26 heats
  - 158 data points
- **Statistical distributions developed for heat-to-heat variation as well as for variability of CGR within a specific heat**
- **Statistical sampling of CGR for PFM analysis assumed to be correlated with Weibull statistics for time to leakage (I.e. nozzles which leak early tend to be sampled from high end of CGR distribution)**

CGR Distributions Based on Heat Data

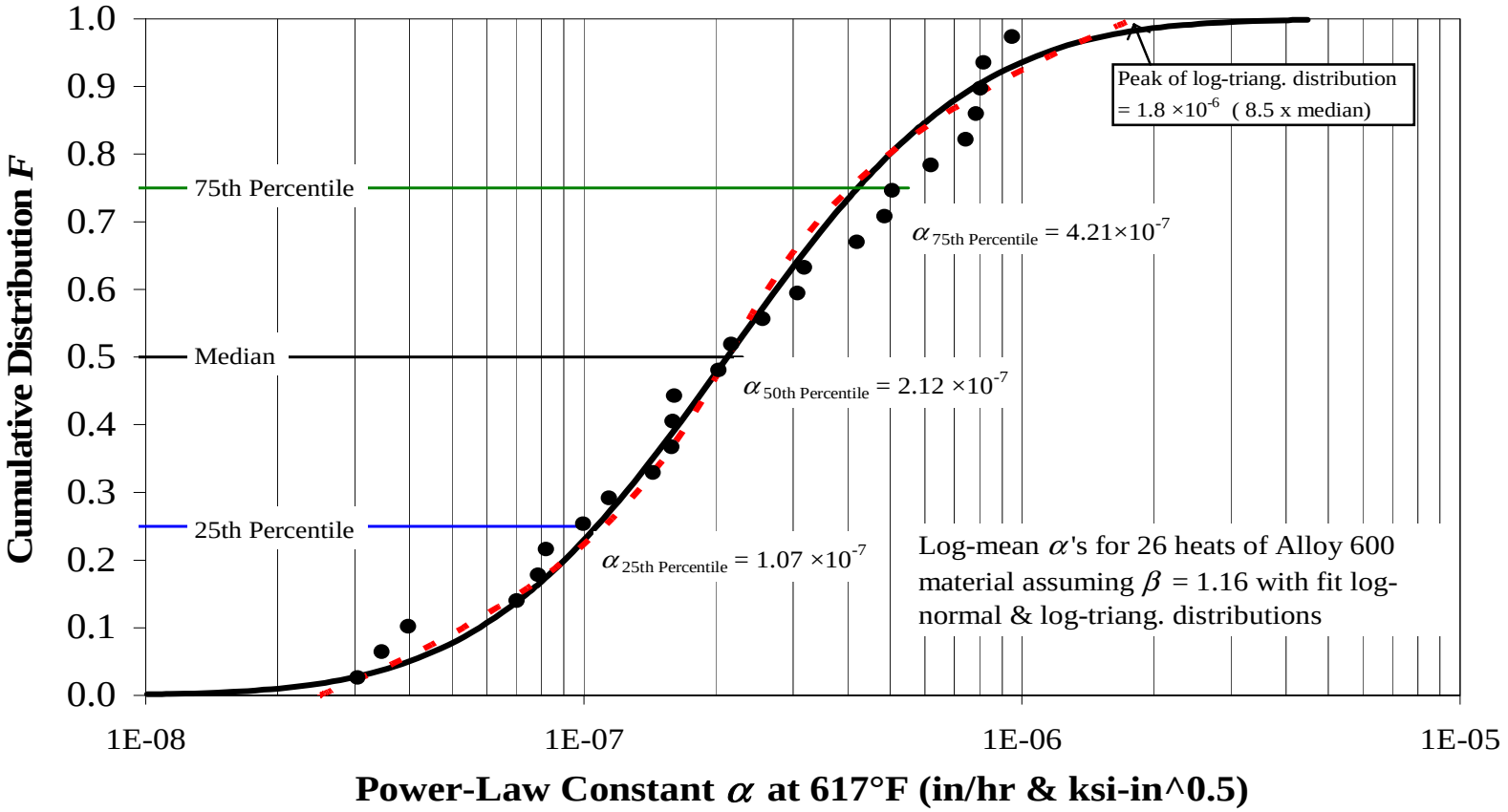

EPRI

Structural Integrity Associates, Inc.

Multiplier on CGR Distribution for Within-Heat Variability

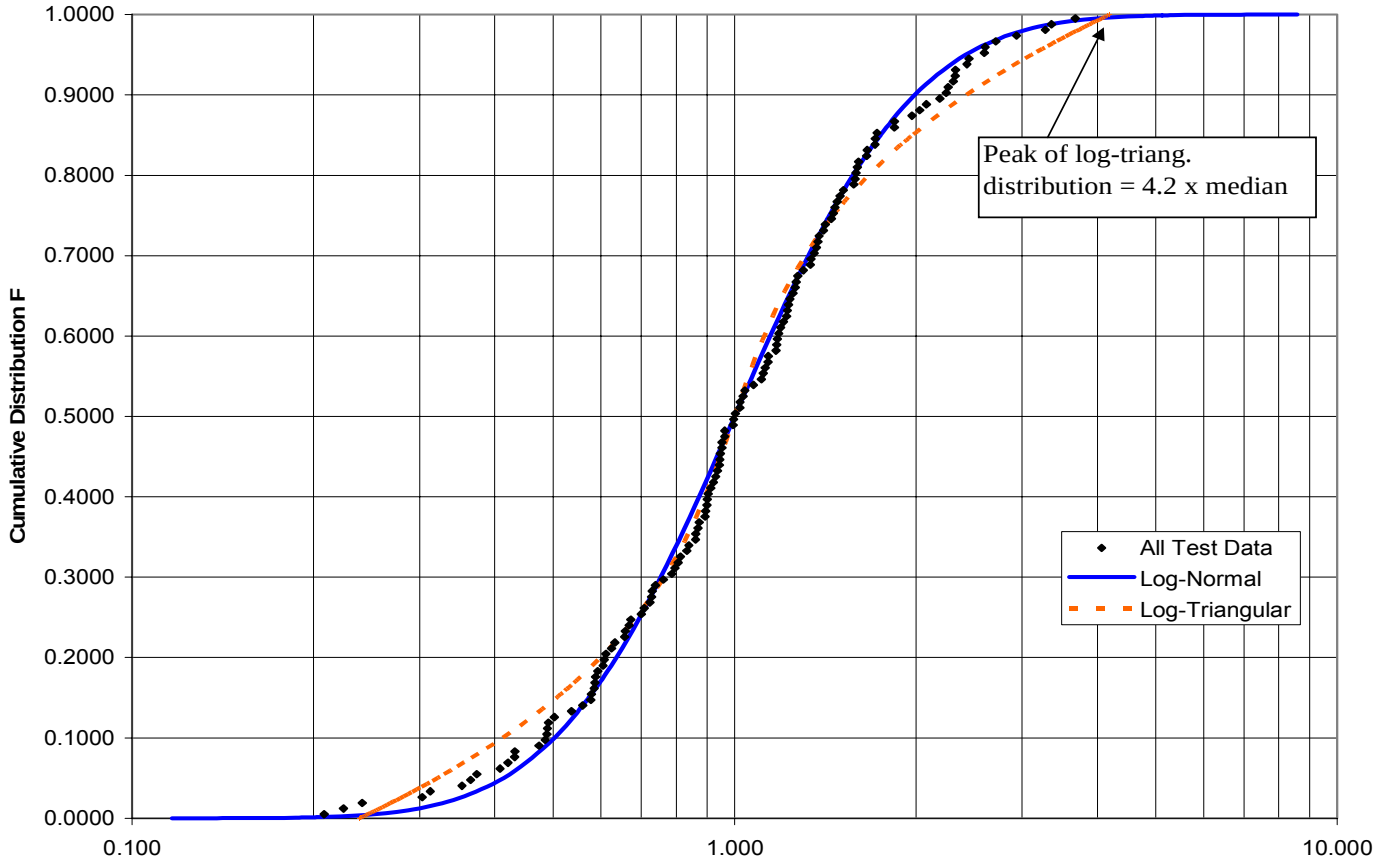

Correlation of CGR with Time-to-Initiation

R=0 Uncorrelated

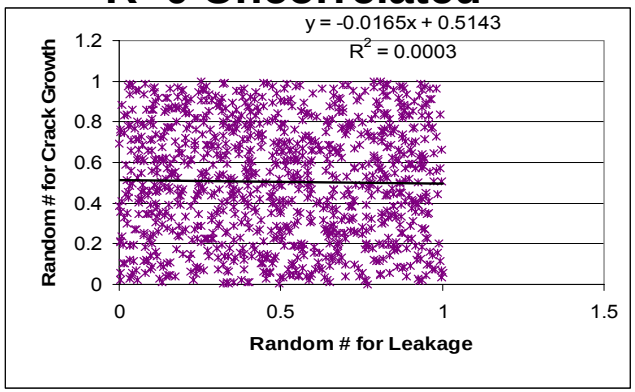

R=-.8 Mod. Corr.

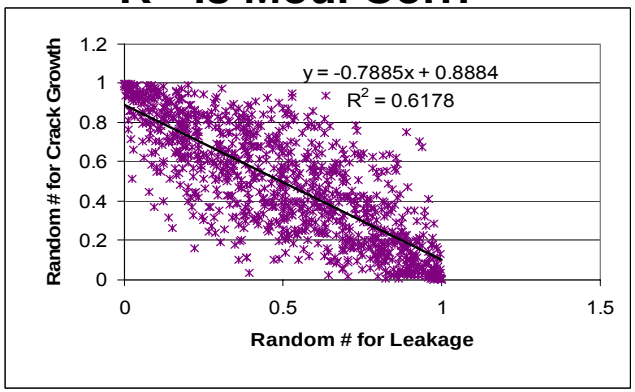

R=-.9 Strong Corr.

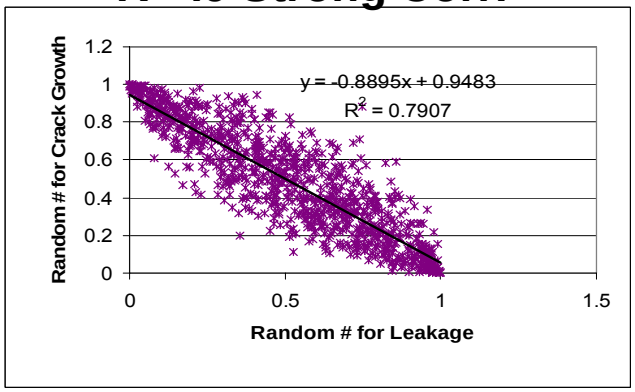

R=0 Totally Correlated

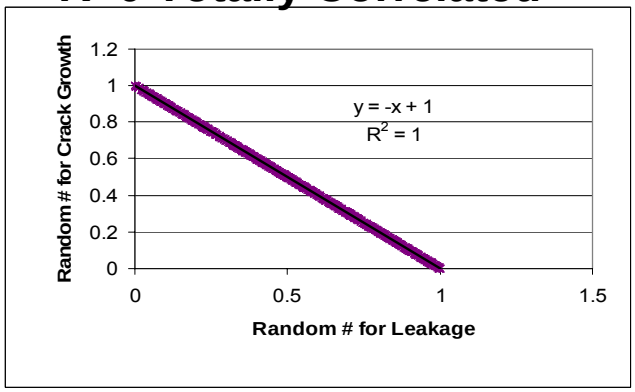

EPRI

Structural Integrity Associates, Inc.

Inspection Interval Analysis
Probability of Detection for NDE

- **Non-Destructive Examinations (NDE)**
  - POD = f(crack depth) per EPRI-TR-102074[1]
  - 80% Coverage Assumed
- **POD Curve Compared to Vendor Inspection Demonstrations**

[1]Dimitrijevic, V. and Ammirato, F., "Use of Nondestructive Evaluation Data to Improve Analysis of Reactor Pressure Vessel Integrity, " EPRI Report TR-102074, Yankee Atomic Electric Co. March 1993

POD Curve for NDE (Illustrating Comparison to Vendor Demonstrations)

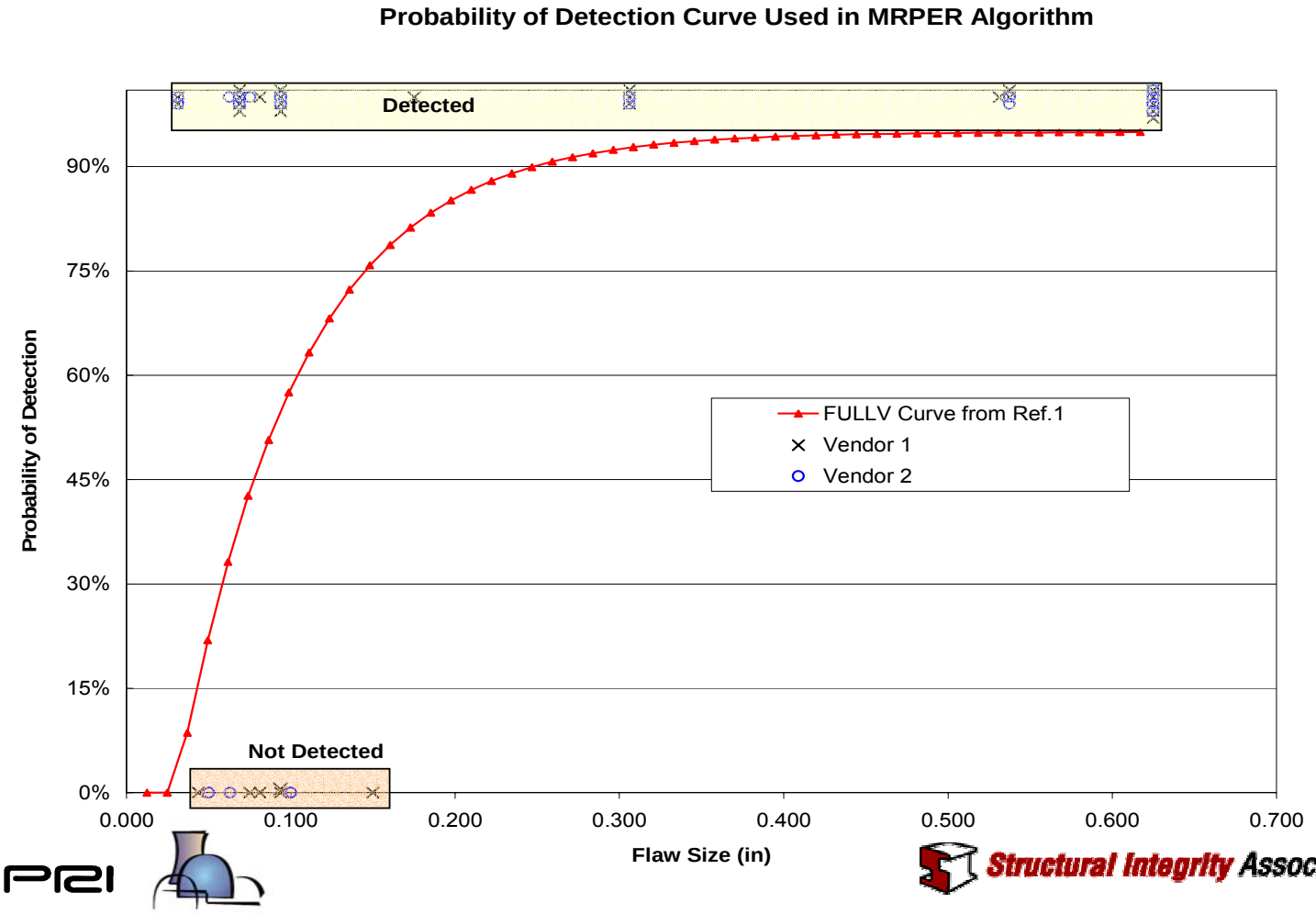

EPRI

Structural Integrity Associates, Inc.

Effect of NDE on Prob. Nozzle Ejection

(Plant A, 600ºF Head, Various Inspection Intervals)

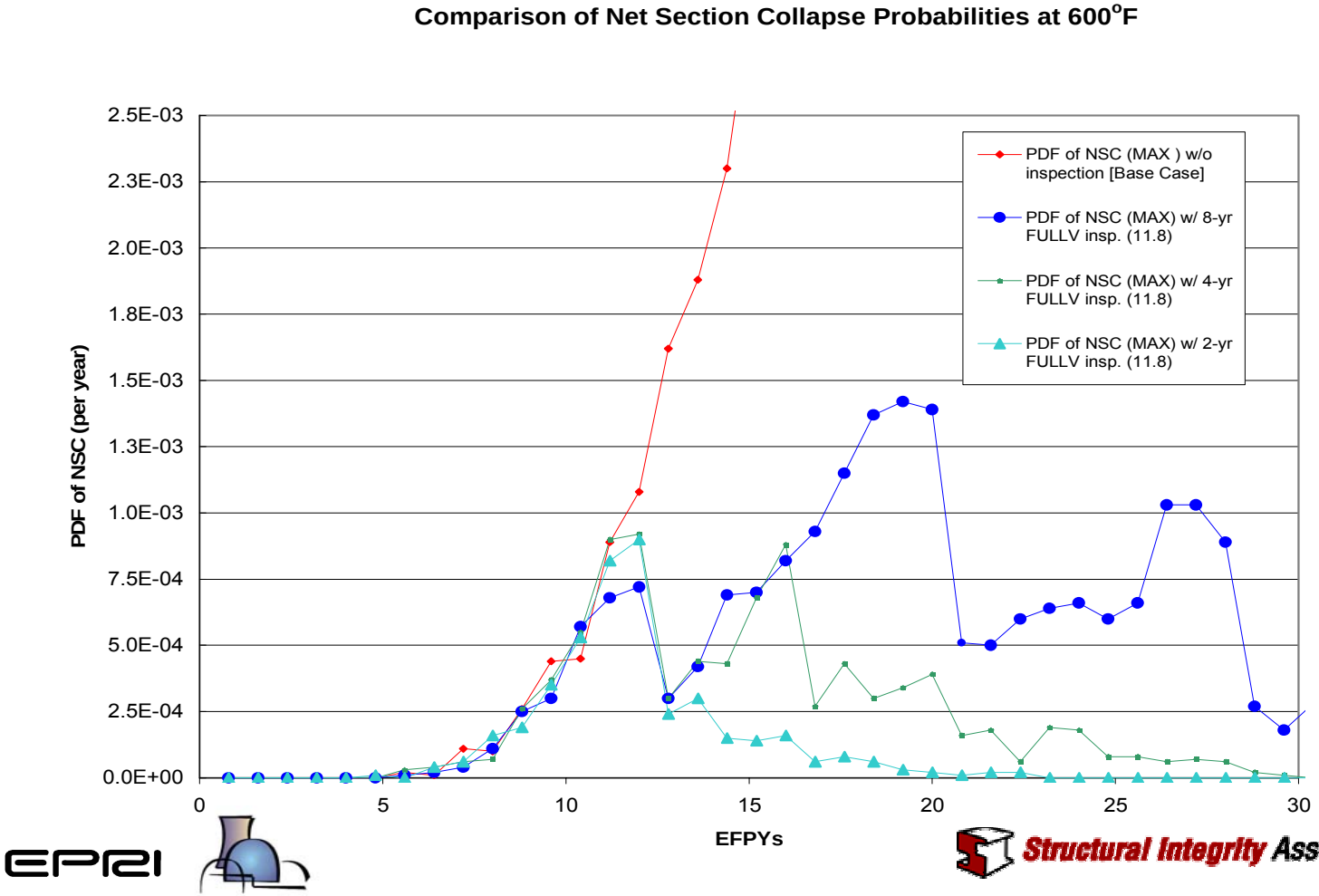

EPRI

Structural Integrity Associates, Inc.

Summary of Results for Characteristic Plants

(Plants A,B,C&D, 600ºF Head, 4-Yr Inspection Intervals)

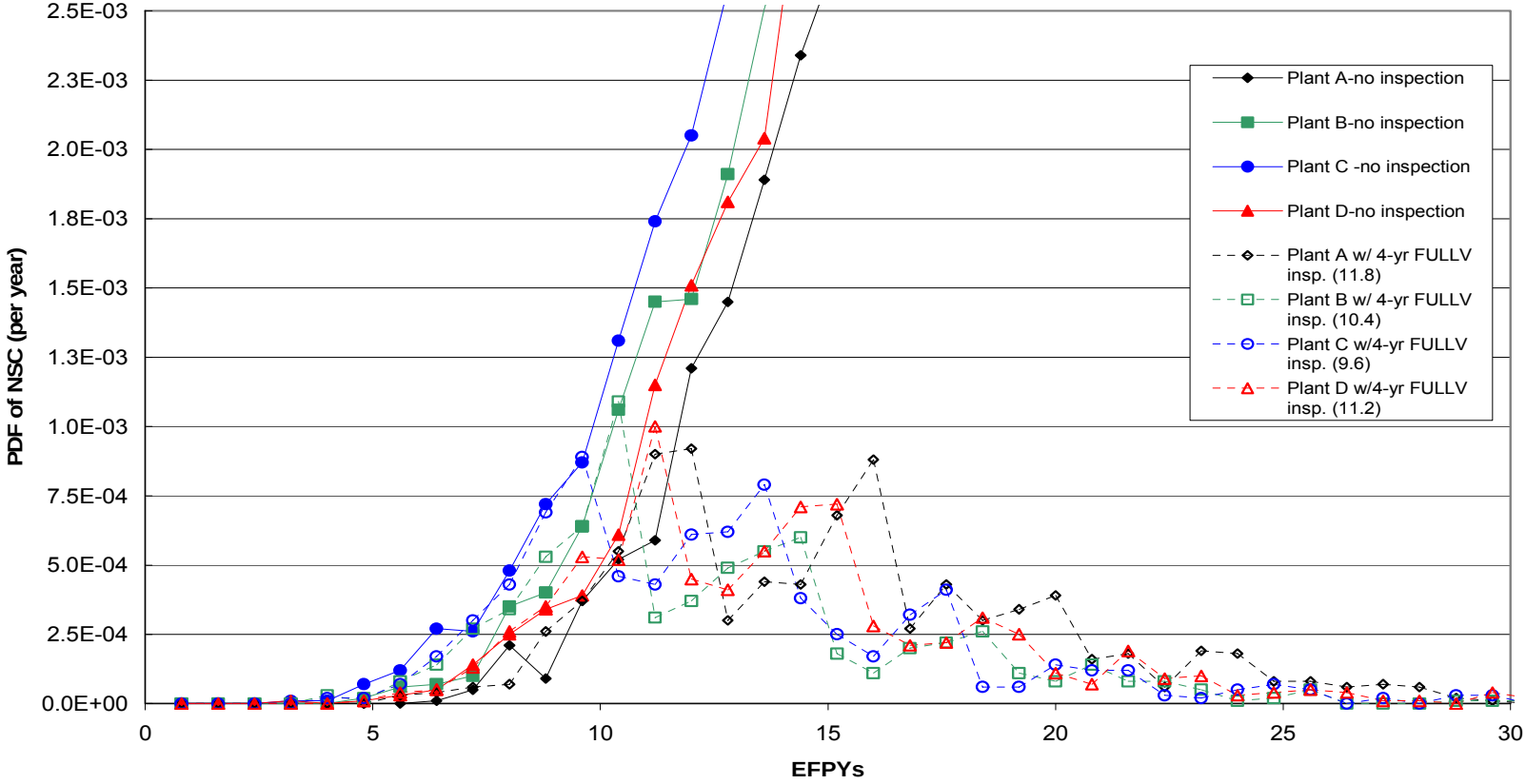

EPRI

Structural Integrity Associates, Inc.

Deterministic Crack Growth Analyses

- MRP-55 CGR correlations used - 75th percentile, with factor of 2 applied for OD connected circumferential flaws (severe environment effect)
- Stress Intensity Factors for envelope stress plane used to compute crack growth from 30° to ASME Section XI allowable crack length (~ 300°)
- Analyses performed for steepest angle (worst case) nozzles in Plants A - D
- Analyses run for various head temperatures using standard activation energy (31.05 kcal/mole) temperature adjustment on crack growth law
- Results Indicate that probabilistic-based inspection intervals are conservative

Deterministic Crack Growth Analysis Results (Plants A & B)

TEMPERATURE °F	UPHILL (EFPH)	UPHILL (EFPY)	DOWNHILL (EFPH)	DOWNHILL (EFPY)
580	218000	24.89	205000	23.40
590	168000	19.18	158000	18.04
600	131000	14.95	123000	14.04
602	125000	14.27	117000	13.36
605	116000	13.24	109000	12.44

Plant A – 38.5º Nozzle

TEMPERATURE °F	UPHILL (EFPH)	UPHILL (EFPY)	DOWNHILL (EFPH)	DOWNHILL (EFPY)
580	468000	53.4	149000	17.0
590	362000	41.3	115000	13.1
600	281000	32.1	90000	10.3
602	267000	30.5	85000	9.7
605	248000	28.3	79000	9.0

Plant B – 43.5º Nozzle

Deterministic Crack Growth Analysis Results (Plants C & D)

TEMPERATURE °F	UPHILL (EFPH)	UPHILL (EFPY)	DOWNHILL (EFPH)	DOWNHILL (EFPY)
580	no growth	no growth	126000	14.38
590	no growth	no growth	97000	11.07
600	no growth	no growth	76000	8.68
602	no growth	no growth	72000	8.22
605	no growth	no growth	67000	7.65

Plant C – 48.8º Nozzle

TEMPERATURE °F	UPHILL (EFPH)	UPHILL (EFPY)	DOWNHILL (EFPH)	DOWNHILL (EFPY)
580	215000	24.54	218000	24.89
590	167000	19.06	169000	19.29
600	130000	14.84	131000	14.95
602	123000	14.04	125000	14.27
605	115000	13.13	116000	13.24

Plant D – 49.7º Nozzle

Highlights of Analysis

- Extensive finite element stress intensity factor computations for set of “characteristic plant types”
- Updated Weibull model of field inspection data including Spring-03 results
- Statistical characterization of latest laboratory PWSCC crack growth rate compilation
- Method to correlate CGRs with crack initiation – early crack initiation => more rapid crack growth
- Effects of inspection POD (correlated with inspection demonstrations) and interval evaluated

Conclusions

- **PFM demonstrates that RPV top head nozzles meet safety limit for nozzle ejection (< 10^{-3} per plant year) with reasonable inspection intervals**
- **Deterministic fracture mechanics analysis supports longer inspection intervals**
- **Several conservatisms in analysis**
  - Envelope stresses used to compute Ks
  - Entire fleet assumed to be from single Weibull population (even though data indicative of a batch effect, with worst heads being replaced)
  - Crack growth rates assumed correlated with time to crack initiation
  - Conservative POD curve assumed, with 80% coverage

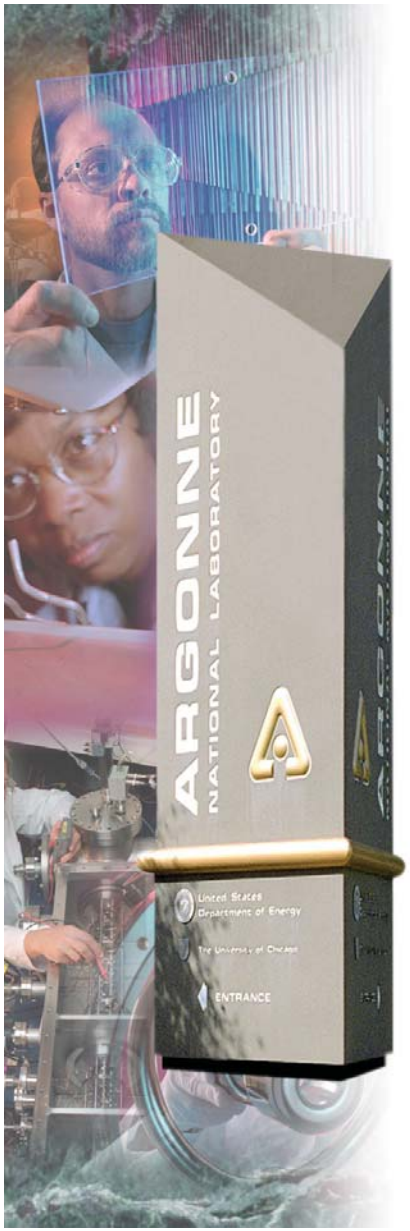

Parametric studies of CRDM Head Failures

W. J. Shack

September 30, 2003

Argonne National Laboratory

Office of Science
U.S. Department of Energy

A U.S. Department of Energy
Office of Science Laboratory
Operated by The University of Chicago

Introduction

- Discuss three types of calculations
  - Distribution of the probability of failure (ejection) of a nozzle
  - Distribution of the probability of failure (nozzle ejection) of a vessel head
  - Expected numbers of leaks, large cracks, nozzle ejections for a population of plants with the same head temperatures, EFPYs, and numbers of nozzles as the 31 operating plants whose inspection data are used to estimate the statistical parameters describing leakage of the nozzles
- Distributions can be interpreted as describing the range of behavior expected in the whole population of nozzles or heads or as the uncertainty in the prediction of the failure of a specific Alloy 600 nozzle or head assuming that we know only its operating temperature and the number of EFPYs of operation
  - Distributions are broad — about 3 orders of magnitude at any given time
- Results are conservative — e.g., true 95th %tile of probability of failure is lower than the estimates presented here

Primary Elements of Model for failure by SCC

- Weibull model for likelihood and initiation time determined from inspection results
  - Initiation assumed to result in a throughwall circumferential crack
  - More detailed modeling of initiation would have to account for growth by multiple initiation and linking and throughwall growth of part–through cracks. Current models assume growth is dominated by fracture mechanics growth of circ cracks.
- K solutions for circumferential cracks and data on crack growth rates used to predict growth
  - EMC^2 solutions for center and sidehill K
  - MRP-55 distribution for base metal (refit by log triangle) used to describe CGRs
- Time to initiation and CGR assume correlated (short initiation time correlated with high CGR); initiation and K uncorrelated

459

Correlation of Initiation and CGR and K values

- Correlation between time to initiation and CGR

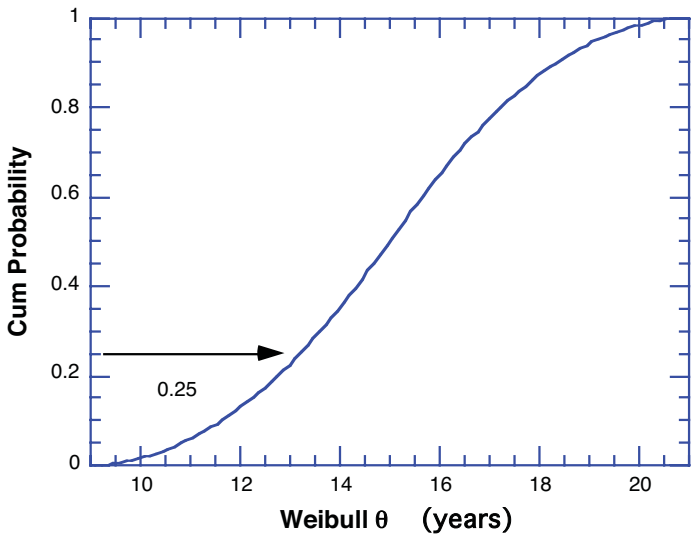

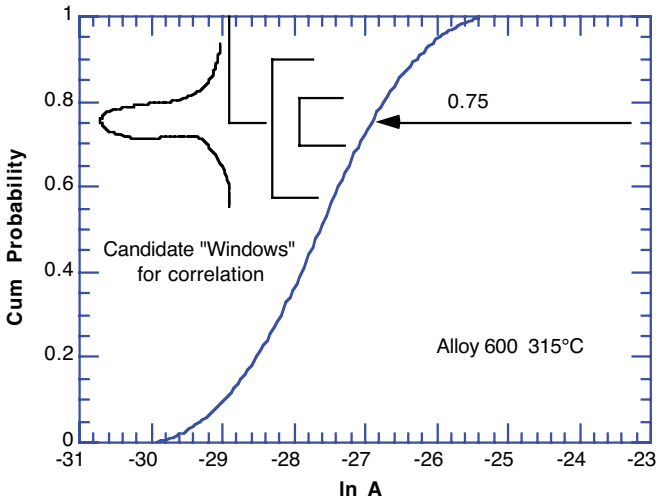

  - Susceptibility to initiation and CGR growth rate are expected to be correlated. Details of the correlation can have a strong impact on results depending on how much the impact of the “high” CGR tail is affected.
  - For specific cases, a conservative distribution for the scale parameter would lead to nonconservative estimates of the CGR (the 25th %tile value in the conservative distribution could be say the 10th %tile value in the realistic case)

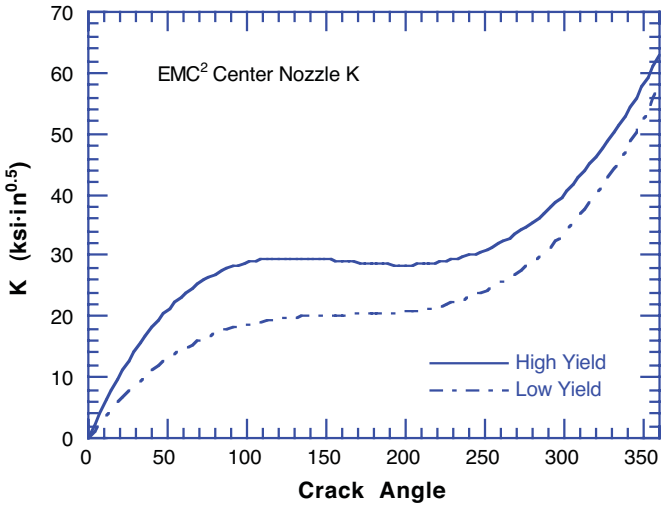

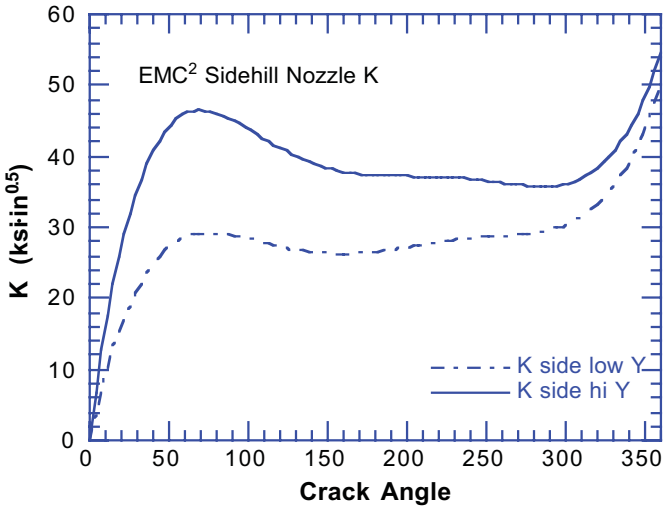

- K values are dominated by welding residual stresses until circumferential cracks are very large
- EMC^2 solutions show strong dependence on yield stress.
- Random variable α used to sample K solutions $K = (1-\alpha)K_{low} + \alpha K_{high}$

Probabilistic initiation models

- Weibull distribution used to describe probability of initiation
  - Staelhe, Gorman et al. have popularized the use of empirical statistical models to describe initiation. Weibull cumulative probability is

$$F(t) = 1 - \exp\left[-\left(\frac{x}{\theta}\right)^{b}\right]$$

where θ is time until cumulative probability of a leak is 0.63 and b characterizes rate of acceleration with age

  - Typical applications of Weibull statistics assume we have data on failures at several times.

    Plot of lnln [1/(1-F)] vs ln t yields straight line from which slope and scale parameter can be determined

  - For CRDM prior knowledge have been used to select b = 3

    Lab data consistent with b = 3, PWSCC in SG tubes gives values ranging from 1.5 to 6 with a median value about 3

    Analysis of CRDM cracking data seems to suggest higher values, but for purposes of predicting initial failures 3 is a conservative choice

- Estimates of population bounds on Weibull scale factor
  - Consider the likelihood function L:

$$L = \prod_{i=1}^{N} \int_0^{\infty} p(\theta) \frac{N_i!}{n_{f_i}!(N_i - n_{f_i})!} \left\{ W(t_i,\theta)^{n_{f_i}} \left(1 - W(t_i,\theta)\right)^{(N_i - n_{f_i})} \right\} d\theta$$

where $p(\theta)$ is the probability distribution function for θ, $W(t_i,\theta)$ is the Weibull cumulative function for time t_i and shape parameter θ, n_{f_i} is the number of leaking nozzles for plant i, N_i is the total number of nozzles for plant i, and N is the total of number of plants considered. The likelihood function is just the usual binomial probability for n_{f_i} items out of a collection of N_i items.

  - Triangular, log-triangular, Weibull, and lognormal distributions for θ were considered. The integrals were evaluated numerically and the distribution parameters varied to find the maximized solution.

Plant	Head Temp °F	EFPYs	EDYs	Nozzles	Leaks/Cracks
ANO 1	602	19.5	19.6	69	8
ANO-2	590	16.8	11.2	81	0
Beaver Valley 1	595	17.2	14.0	65	4
Calvert Cliffs 2	593.7	20.4	15.8	65	0
Cook 1	580	24.8	10.0	79	0
Cook 2	600.7	13.5	13.9	78	0
Crystal River 3	601	15.5	16.2	69	1
Davis-Besse	605	15.7	19.2	69	5
Farley 1	596.5	20.2	17.5	69	0
Farley 2	596.9	17.9	15.8	69	0
Indian Point 2	585.5	14.4	8.0	97	0
Indian Point 3	593.5	20.5	15.7	78	0
Millstone 2	593.9	14.3	11.2	69	3
North Anna 1	600.1	19.9	20.0	65	0
North Anna 2	600.1	19.9	19.0	65	14
Oconee 1	602	20.2	21.9	69	3
Oconee 2	602	21.9	23.7	69	19
Oconee 3	602	20.0	21.7	69	14
Palo Verde 1	592	14.6	10.6	97	0
Palo Verde 2	591.7	14.0	10.0	97	0
Point Beach 1	591.6	20.4	14.5	49	0
Robinson 2	598	22.0	20.3	69	0
San Onofre 2	590.5	22.5	15.3	91	0
San Onofre 3	590.6	22.4	15.3	91	0
Sequoyah 1	580	5.0	1.5	78	0
St. Lucie 1	590.6	23.1	15.7	77	0
St. Lucie 2	595.6	16.7	13.9	91	1
Surry 1	597.8	20.9	19.1	65	6
TMI 1	601	17.4	18.2	69	6
Turkey Point 3	594.4	23.0	18.3	65	0

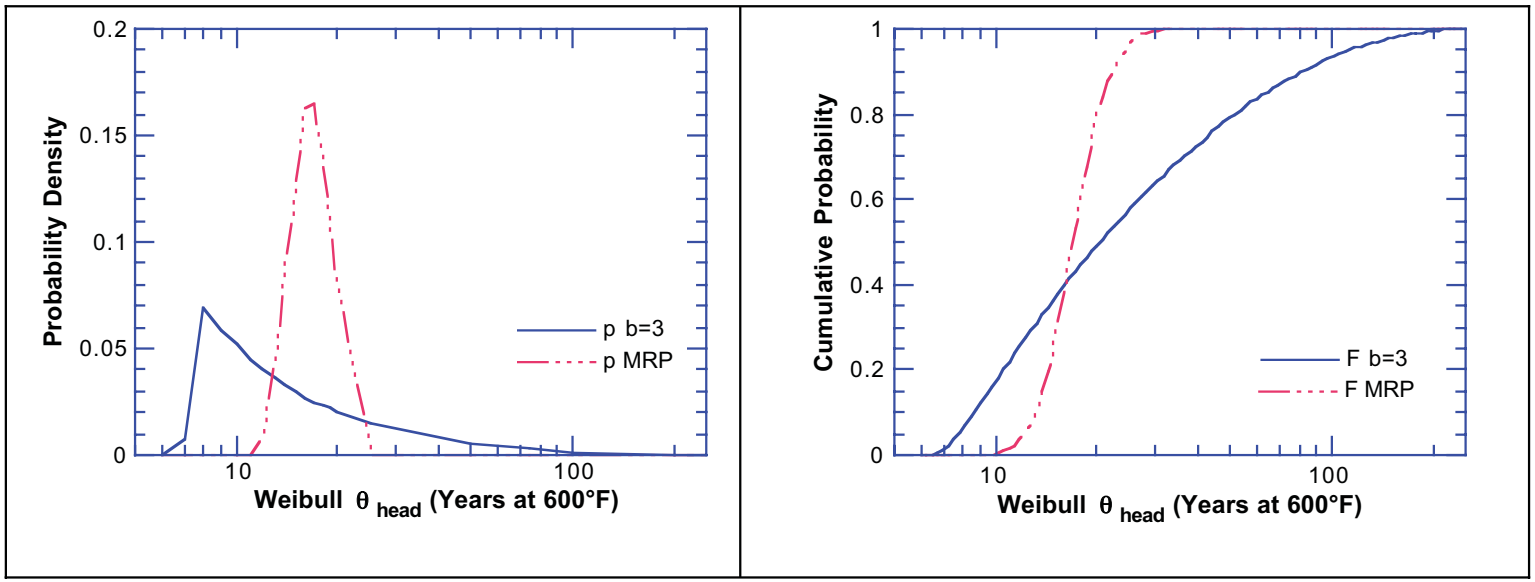

- Calculations actually done to find scale factor for probability of leakage of a nozzle. Presented here in terms of scale factor for a head with 69 nozzles from the same heat. For Weibull distributions $\theta_{head} = \theta_{nozzle} / n^{1/b}$
- Maximum Likelihood Estimate is much broader than MRP 6-03 distribution which is essentially an estimate of an "average" value and the uncertainty on that estimate

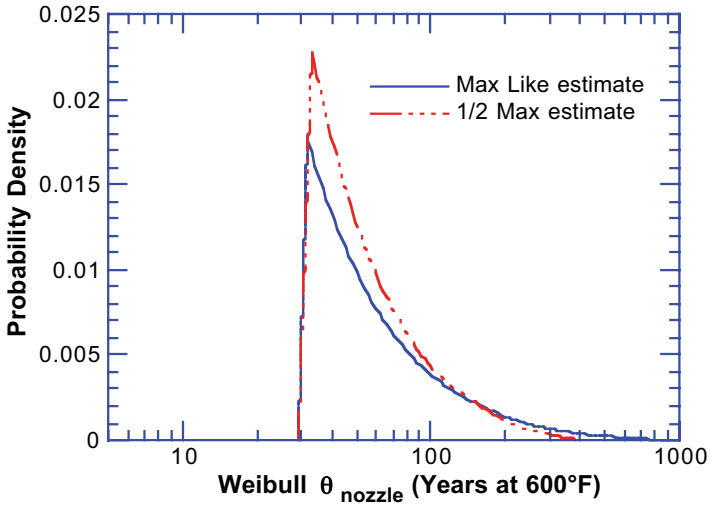

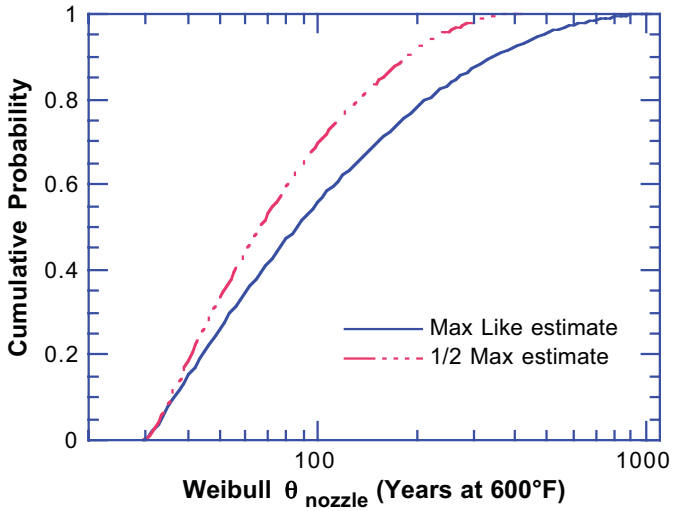

- Maximum is very broad. Value of upper end can be varied significantly with minor effect on the value of likelihood. Physically reasonable. Experience can tell us a lot about the most susceptible nozzles/heads but less susceptible materials involve substantial extrapolation
- Sensitivity calculation was done to determine a distribution where the lower bound value was fixed and the other values adjusted to give a likelihood equal to 1/2 the peak value
- In the 31 plant sample 84 leaks (& large cracks) were observed. For a plant population with the same operating times, temperatures, and number of nozzles as the 31 plant sample, the expected number of leaks are

Weibull scale factor distribution	Expected number of leaks in population
Maximum Likelihood Estimate	55.3 ± 15.3
1/2 Maximum Estimate	69.7 ± 15.7
MRP 6-03	25.6 ± 2.5

467

- Baysian Updates
  - Use generic distributions as prior distributions to get updated distribution

For a plant that has n_f / no failures at time t:

$$\overline{p}(\theta) = \frac{\left(1 - W(t,\theta)\right)^N p(\theta)}{\int_0^\infty \left(1 - W(t,\theta)\right)^N p(\theta)\, d\theta}$$

$$\overline{p}(\theta) = \frac{\left\{W(t,\theta)^{n_f}\left(1 - W(t,\theta)\right)^{(N-n_f)}\right\} p(\theta)}{\int_0^\infty \left\{W(t,\theta)^{n_f}\left(1 - W(t,\theta)\right)^{(N-n_f)}\right\} p(\theta) d\theta}$$

  - One could also develop a “Huntington” or “CE” distribution

$$\overline{p}(\theta) = \frac{\prod_{k=1}^{N}\left\{W(t_k,T_k,\theta)^{n_{fk}}\left(1 - W(t_k,T_k,\theta)\right)^{(N-n_{fk})}\right\} p(\theta)}{\int_0^\infty \prod_{k=1}^{N}\left\{W(t_k,T_k,\theta)^{n_{fk}}\left(1 - W(t_k,T_k,\theta)\right)^{(N-n_{fk})}\right\} p(\theta) d\theta}$$

Probability of leakage for a head

- Probablility of leakage from the head is computed from the probability of leakage for a nozzle. If all nozzles have the same susceptibility to leakage this is just

$$P_{leak} = 1 - (1 - P_{nozzle})^{N}$$

- Most plants appear to have multiple heats of material for nozzles. For the B&W plants the table shows the numbers of nozzles from different heats

ONS–1	ONS–2	ONS–3	ANO–1	Davis Bessie	TMI–1	CR–3
50	2	1	2	32	11	69
1	4	68	21	5	54	
15	27		7	23	1	
	15		36	9	2	
	7		1			
	12		2			
	2					

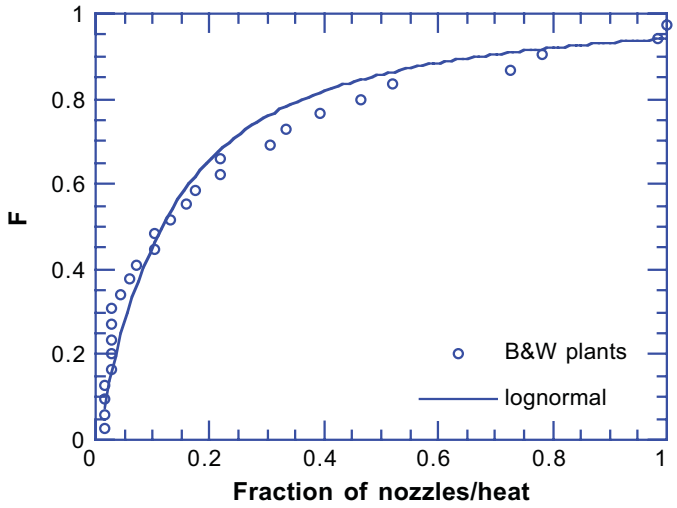

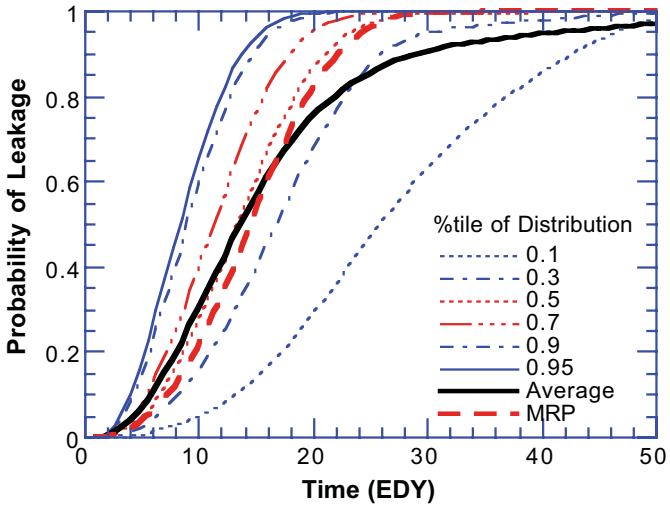

- Vessel head calculations are done assuming that the head contains from 1 to 7 heats of material and that the number of nozzles from a specific heat are distributed approximately lognormally.
- Results suggest a high probability of leakage for most plants after 10-15 EDY. MRP 6-03 Weibull scale factor is fairly close to the average value from the distribution.

Probability of Failure of CRDM Nozzles

- Probability, $P(t_f < T)$, that a nozzle will fail at a time t_f less than T,

$$P(t_f < T) = \int_0^T p(t) P_c(t_f < T - t) dt$$

  - p(t) is the probability that a crack will initiate at a time t
  - $P_c(t_f < T-t)$ conditional probability a crack that initiates at t will fail at a time t_f less than T and is determined by fraction mechanics analysis.
- For a given choice of the Weibull scale factor [which determines p(t)] and stress intensity distribution [which together with the MRP-55 CGR distribution determines $P_c(t_f < T)$], integral gives a probability of failure for a nozzle
- Monte Carlo sampling from the distribution for the scale factor and for the parameter α to determine K gives distributions for the probability of failure of a nozzle

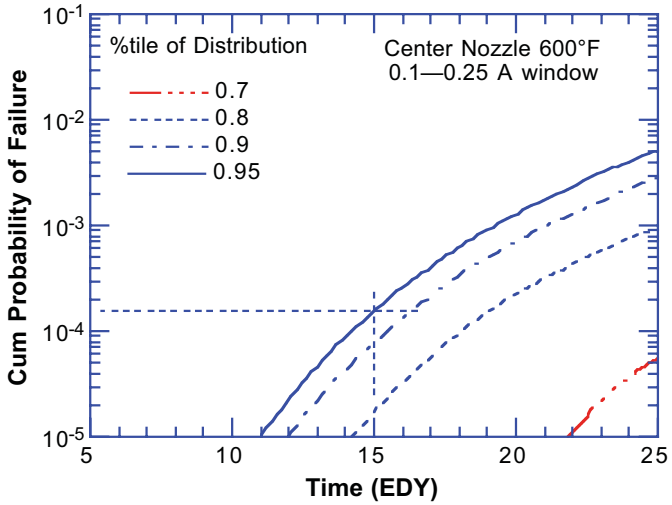

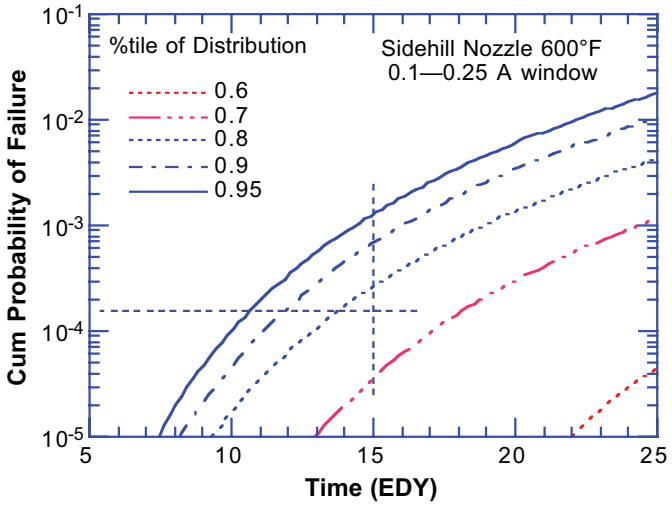

- Probability of failure depends strongly on temperature and choice of correlation window for CGRs
- Sidehill K from EMC^2 is for bounding sidehill angle. POF higher than for center nozzles because of higher K values, but there is overlap in the distributions; interpolation used for head calculations
- If all nozzles are from one heat of material then the POF for the head can be easily calculated from the probability of failure of the nozzles

$$P_{head} = 1-(1-P_{nozzle-c})^{N_c}\,(1-P_{nozzle-s})^{N_s}$$

where N_c and N_s are the number of center and sidehill nozzles, respectively

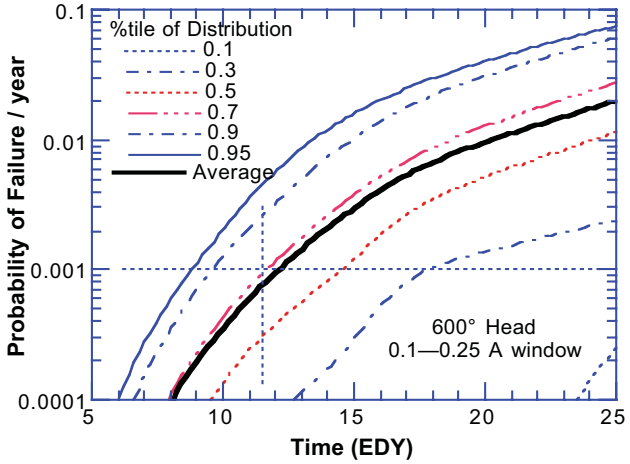

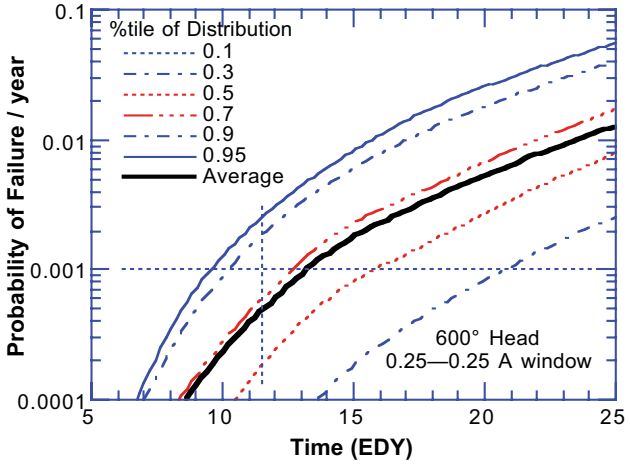

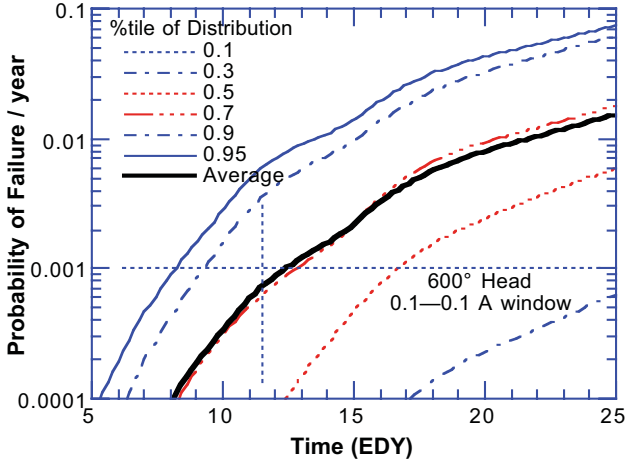

- Calculations for head use multiple heats based on B&W results
- MRP 6-03 POF bounds 70–80% of the population; represents average POF
- $POF_{95th\%tile} \approx 5 \cdot POF_{Average}$

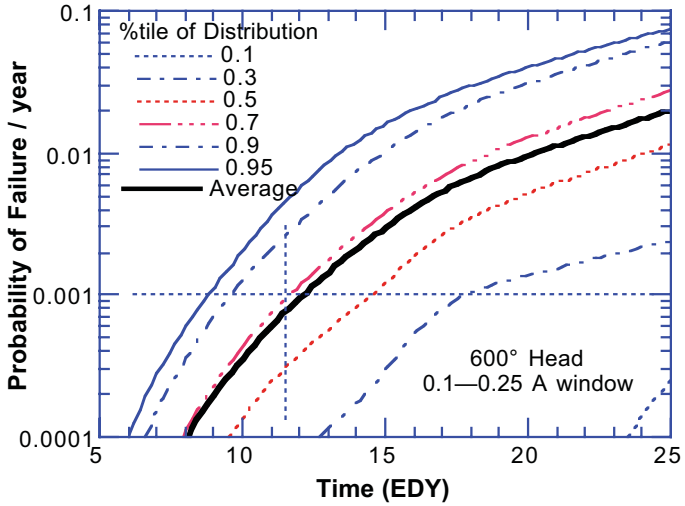

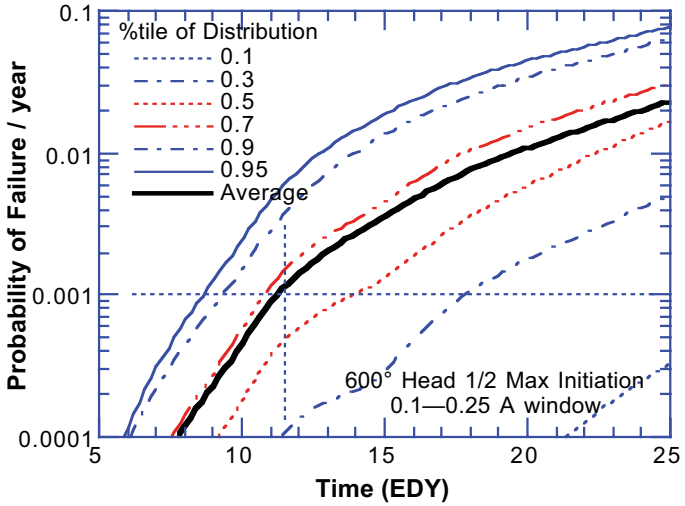

- Using the more conservative 1/2 Maximum Likelihood distribution for the Weibull scale factor shifts the distributions only slightly

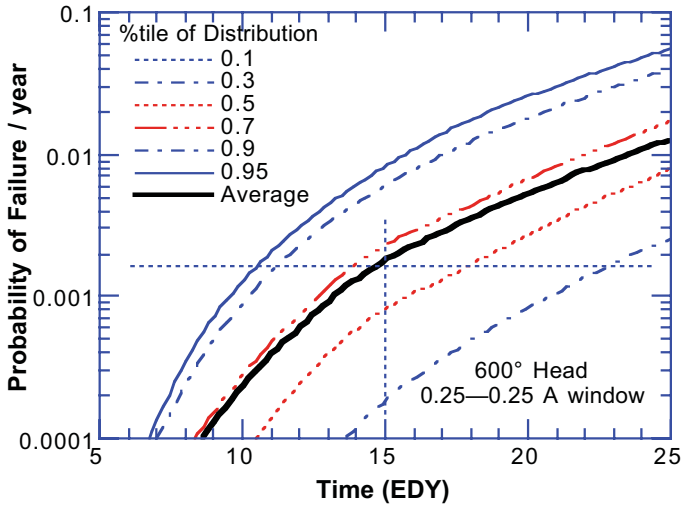

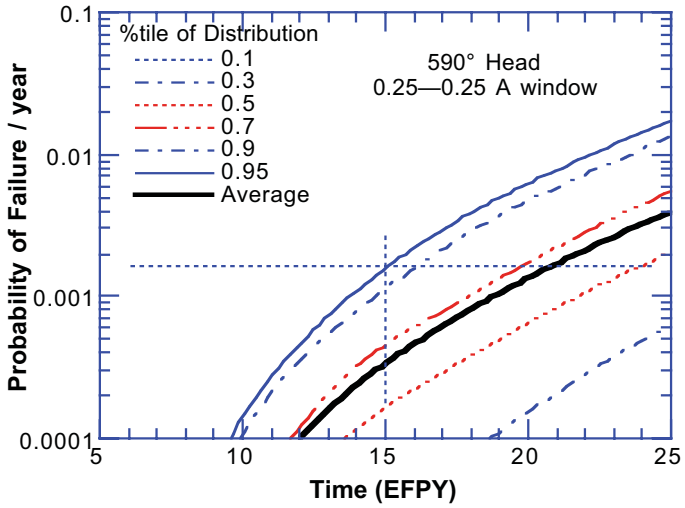

- Decreasing temperature does decrease POF significantly, but there is overlap in the distributions; $POF_{95\%tile}$ at 590°F is comparable to $POF_{average}$ at 600°F

Statistical Checks with operating experience

- For a plant population with the same operating times, temperatures, and number of nozzles as the 31 plant sample, we can compute expected number of large (165°) cracks and nozzle ejections

Model	165°Cracks	Nozzle Ejections
No Interpolation 0.1–0.25 A window	4.1 ± 1.0	1.1 ± 0.53
0.1–0.25 A window	2.8 ± 0.7	0.7 ± 0.33
0.25–0.25 A window	1.8 ± 0.6	< 0.7

- Statistical results suggest all the models are probably conservative. The statistical confidence is higher for the 0.1–0.25 window models.

476

Analysis of Weld Residual Stresses and Circumferential Through-Wall Crack K-solutions for CRDM Nozzles

D. Rudland [(1)], G. Wilkowski [(1)], Y.-Y. Wang [(1)], and W. Norris[(2)]

(1) Engineering Mechanics Corporation of Columbus

(2) U.S. Nuclear Regulatory Commission, Office of Nuclear Reactor Research

Objective of Program at Emc²

- ***Main objective of the Emc² program is to develop a probabilistic computer code to predict the time from detection of leakage to failure for independent assessment of MRP/EPRI analysis.***
  - ***Residual stresses calculated and then circumferential through-wall crack inserted to determine crack-driving force.***
  - ***Dr. Sharif Rahman and B. N. Rao of Univ. of Iowa assisted Emc² in new Visual Fortran probabilistic code.***
- ***Numerous meetings with NRC staff and industry (significant amount of proprietary data).***

RPV Head Geometry Used in FE Analyses was a Westinghouse Design (PV-RUF drawings from ORNL)

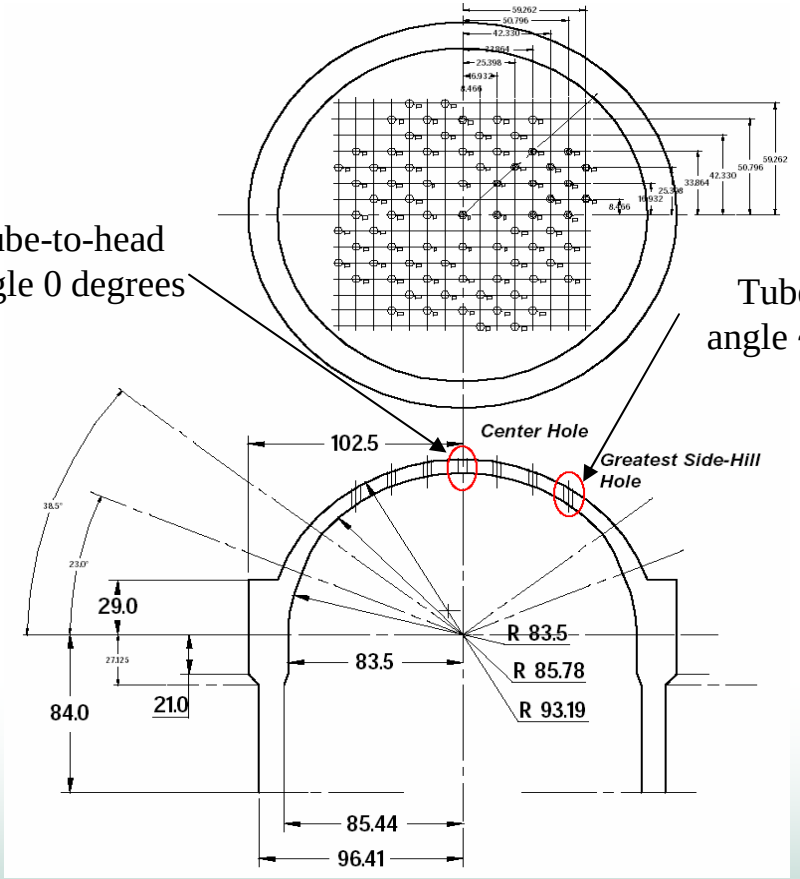

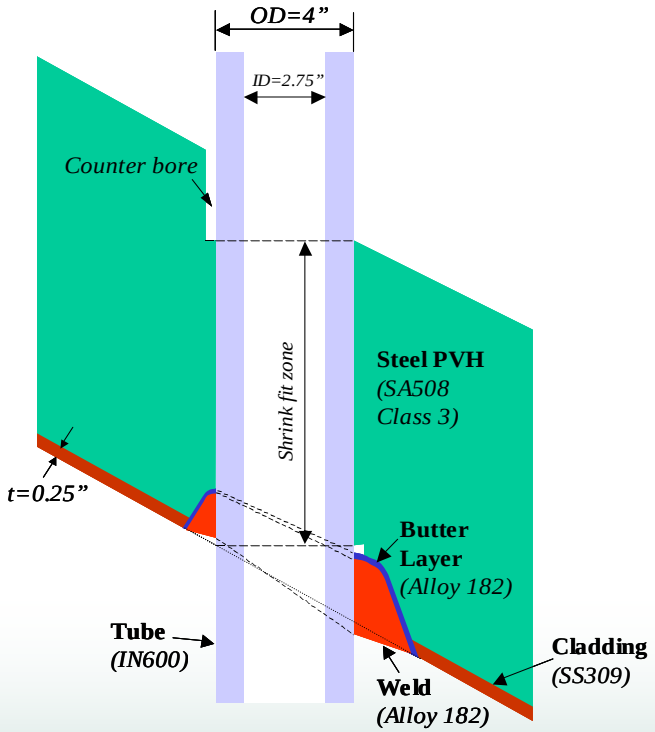

Overall Modeling Strategy

- *Weld Stress Analysis*
  - *heat treatment for stress relieving*
  - *installing tube into RPV head by shrinkage fit*
  - *welding the J-groove*
  - *hydro-testing*
- *Stress Mapping*
  - *Transferring all solution variables (stress tensor, strain tensors, displacement, BC) from weld stress mesh to a crack mesh*
- *K-Solution Analysis*
  - *Applying the service load (pressure and temperature)*
  - *Unzipping the cracked mesh*
  - *Calculation of K-solution*
  - *Curve-fit for use in probabilistic code structure*

"Generic" CRMD Nozzle Fabrication Steps

- *Rough drill the 4" diameter holes in the RPV head*
- *Arc-gouge the groove area away and grind smooth*
- *Butter the groove area with alloy 182 using SMAW process*
- *Stress relieve the head at 1125F +/-25F*
- *Finish machining the groove area*
- *Finish reaming the main hole (interference area), and finish reaming the counter bore region*
- *Install tube by shrinkage fit (tube submerged in liquid nitrogen)*
- *Welding the J-weld with SMAW process and NDE at each 1/4 depth of weld*
- *Hydro-test*
- *Put into service at elevated temperatures*

The FE analyses followed the highlighted essential fabrication steps

Analyses Included Significant Factors Affecting The Crack-Driving Force Solutions

- ***Yield strength level of the tube***
- ***Interference fit***
- ***Weld bead layout sequence (using generic B&W design)***
- ***Weld size and number of weld passes (using generic B&W design)***
- ***Operating temperature of the reactor***
- ***Location of the nozzle penetrations***

Analyses To Date Focused on Parametric Study of Center Hole and a Detailed 3D Model of The Steepest Side-Hill Nozzle

Case #	Interference fit, mm (mils)	Temperature, K (F)	Tube Yield Strength, MPa (ksi)	Weld Bead Layout Sequence	Nozzle Location	Weld Height, mm (in)	Number of Weld Passes
A	0 (0)	616.3 (605)	259 (37.5)	Tube-Head	Head Center	20 (25/32)	13
B	0.2286 (9)	616.3 (605)	259 (37.5)	Tube-Head	Head Center	20 (25/32)	13
C	0.0508 (2)	616.3 (605)	259 (37.5)	Tube-Head	Head Center	20 (25/32)	13
D	0.1143 (4.5)	616.3 (605)	259 (37.5)	Tube-Head	Head Center	20 (25/32)	13
E	0 (0)	566.5 (560)	259 (37.5)	Tube-Head	Head Center	20 (25/32)	13
F	0 (0)	616.3 (605)	259 (37.5)	Head-Tube	Head Center	20 (25/32)	13
G	0 (0)	616.3 (605)	444 (64.5)	Tube-Head	Head Center	20 (25/32)	13
H	0 (0)	616.3 (605)	259 (37.5)	Tube-Head	Head Center	28 (1.10)	20
I	0.2286 (9)	616.3 (605)	259 (37.5)	Tube-Head	Head Center	28 (1.10)	20
J	0.2286 (9)	616.3 (605)	259 (37.5)	Tube-Head	Head Center	36 (1.42)	27
K	0 (0)	616.3 (605)	259 (37.5)	Tube-Head	Greatest Side-hill	Variable	14

Base case analysis

FEM Mesh in Weld Analysis – Center hole

- *Axisymmetric weld analysis*
- *Solution revolved around tube axis for K-solution determination*
- *13 to 20 elements in each weld pass to deal with the temperature and stress gradients in the weld region*

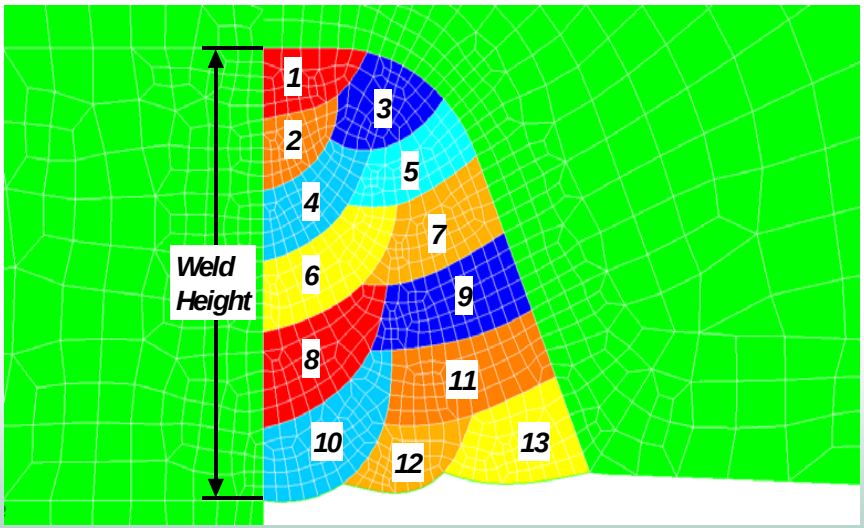

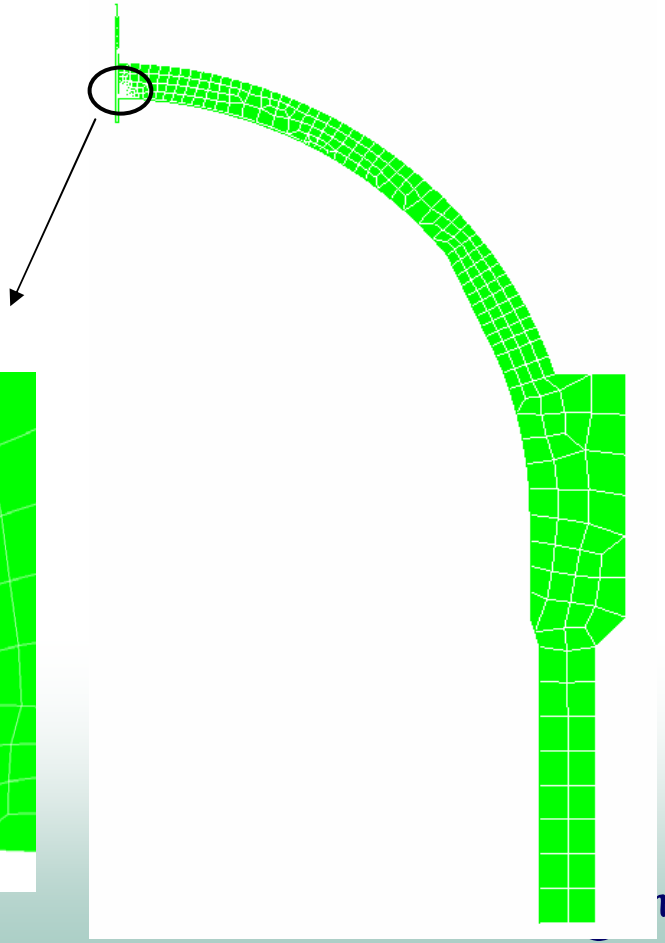

Side-Hill nozzle - Weld Geometry/Meshing

- *As with the centerhole, many factors went into deciding Sidehole geometry*
  - *Used steepest sidehill hole from previous drawing*
  - *Modeled 1/8 of head*
  - *Nozzle/weld details from various trips*
  - *Typical CRDM designs*
  - *Attempted to keep uphill and downhill area similar – Constant volume needed for weld analyses*
  - *Tried to keep some geometry (Bevel angle, etc) same between side-hill and center-hole models*

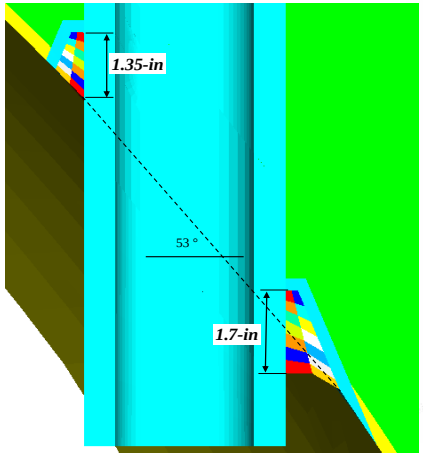

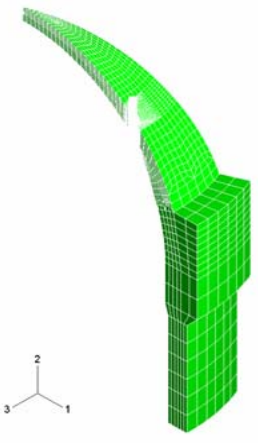

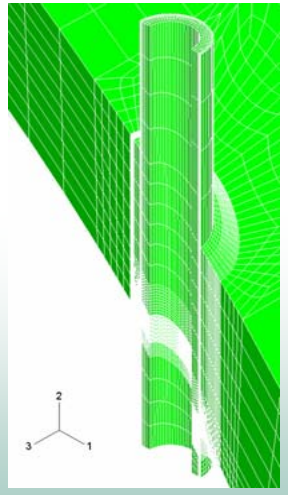

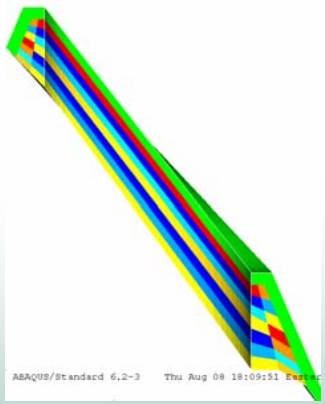

70,000 nodes and 64,000 8-node linear brick elements in the side-hill model.

Weld Analysis Procedure

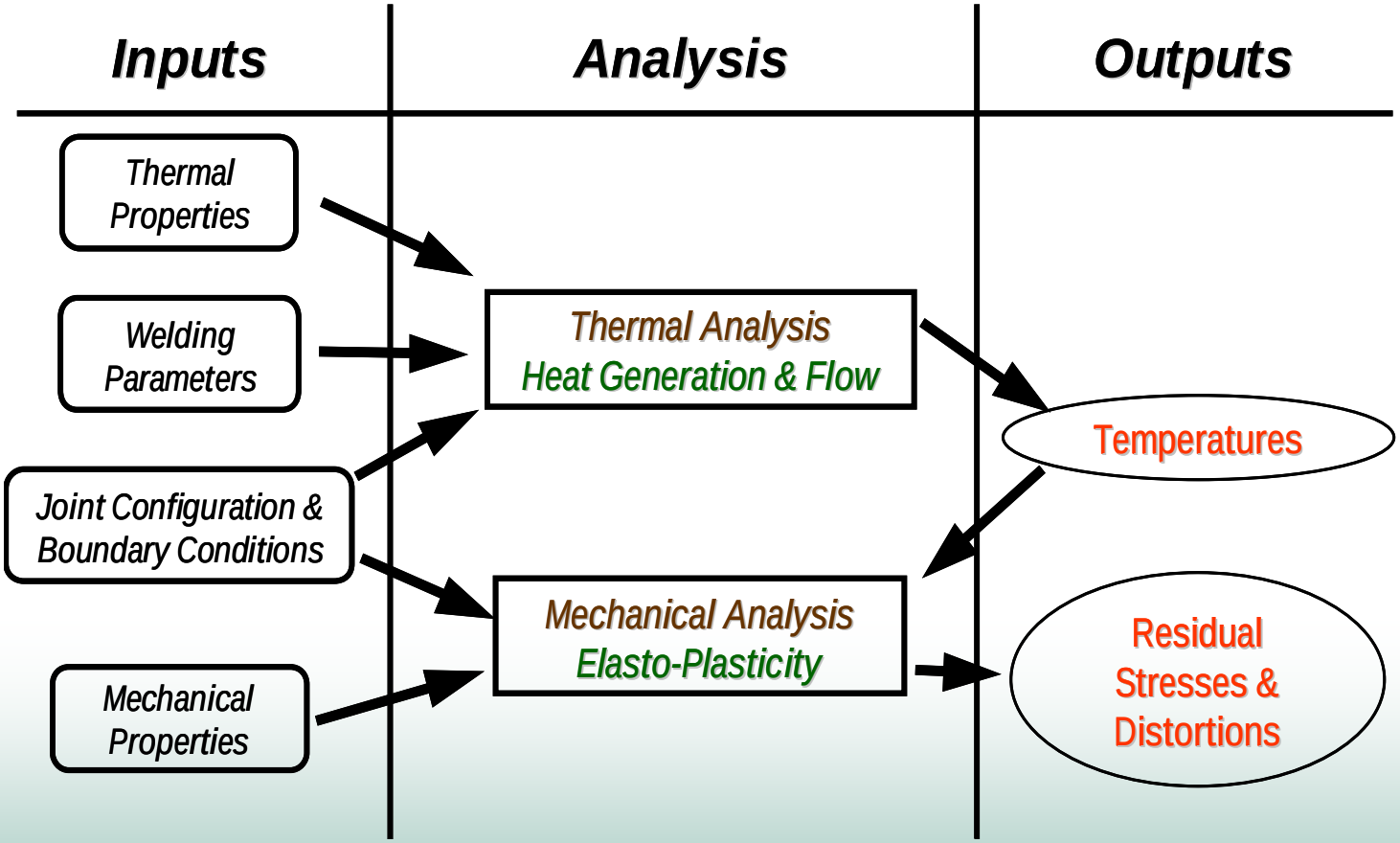

Welding Stress Analysis Procedure (cont.)

- ***Analysis was done using weld pass-by-pass procedure***
  - ***A weld pass is activated only when it is deposited***
  - ***Pass deposition followed the actual welding sequence***
- ***Heat input from the moving welding arc takes Gaussian distribution***

$$q = \frac{6\sqrt{3}\eta EI}{\pi\sqrt{\pi}abc} e^{\left[-3\left(\frac{(\chi-\chi_0)^2}{a^2}+\frac{(\varsigma-\varsigma_0)^2}{b^2}+\frac{(V(t-t_0))^2}{c^2}\right)\right]}$$

- ***Effect of weld solidification on materials constitutive behavior are properly treated with proprietary user subroutines***
- ***ABAQUS is the FE solver, enhanced with various user subroutines***

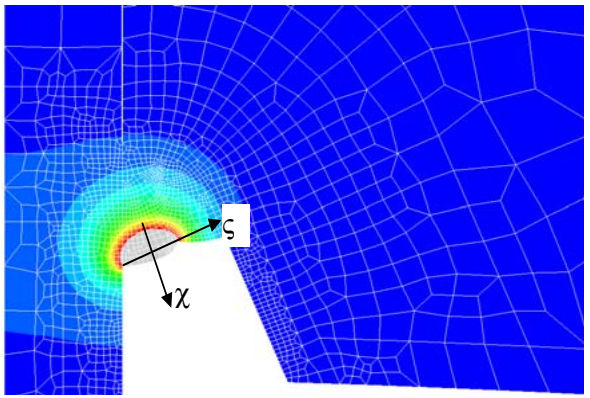

Peak temperature profiles

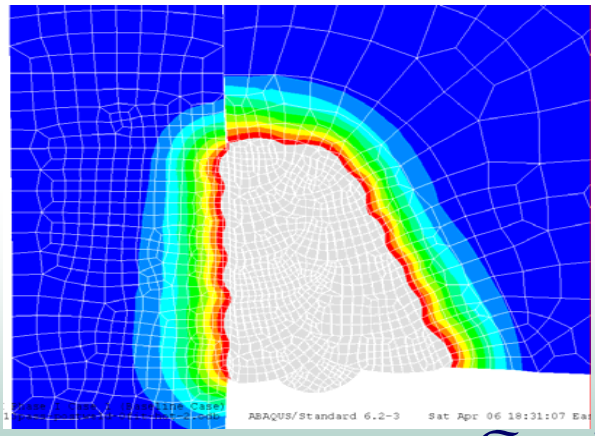

Material Properties

- *Analysis by Emc^2 involves weld simulation of each weld pass*
- *Base and weld metal stress-strain curves needed from room temperature to 1000C (cooling from molten conditions).*
  - *Since plastic strains for weld calculated in our analysis, the weld metal stress-strain curve should be from annealed weld metal, rather than from as-welded weld metal.*
  - *Speed of welding corresponds to an average strain-rate of 10^{-3}.*
  - *ORNL developed annealed Alloy 182 and A508 stress-strain curves at various temperatures and 10^{-3} strain rate. We used Alloy 600 data from literature (slower loading rate).*

Axial residual stress development in a center-hole case – 20 weld passes max (Crack not present during weld simulation.)

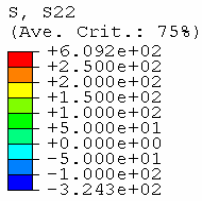

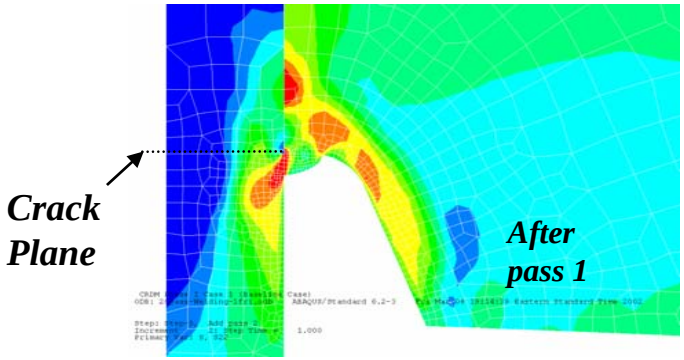

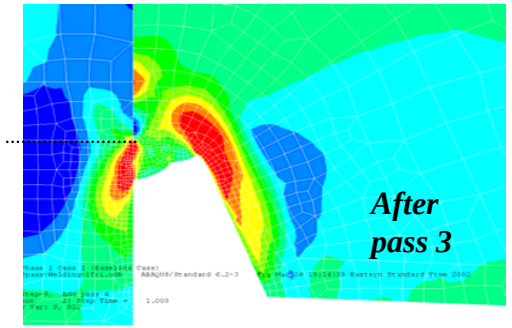

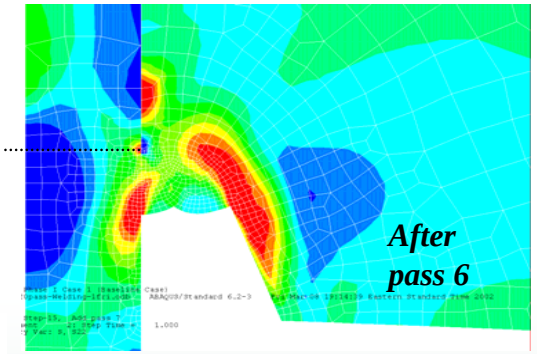

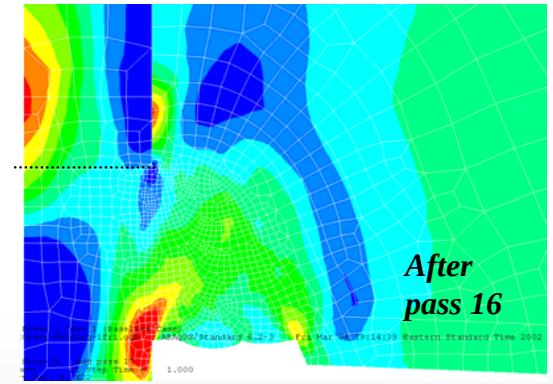

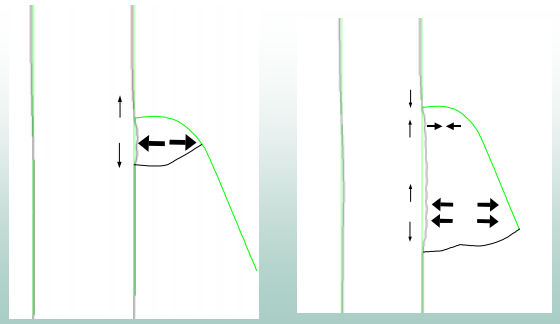

Weld Height Effects on Axial Stress Change is Attributed to "Hinging" Action around Initial Weld Beads

In-Service Stress Distributions of 13-pass J-weld (Design Conditions: 605F and 2,500psi)

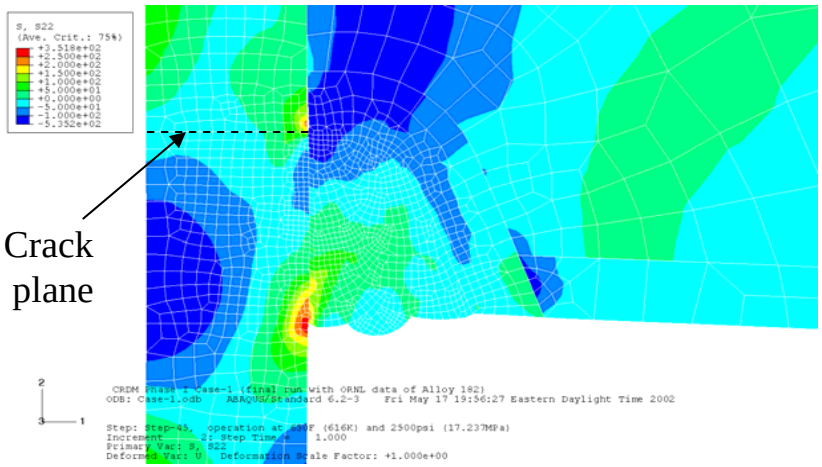

Axial Stress, MPa

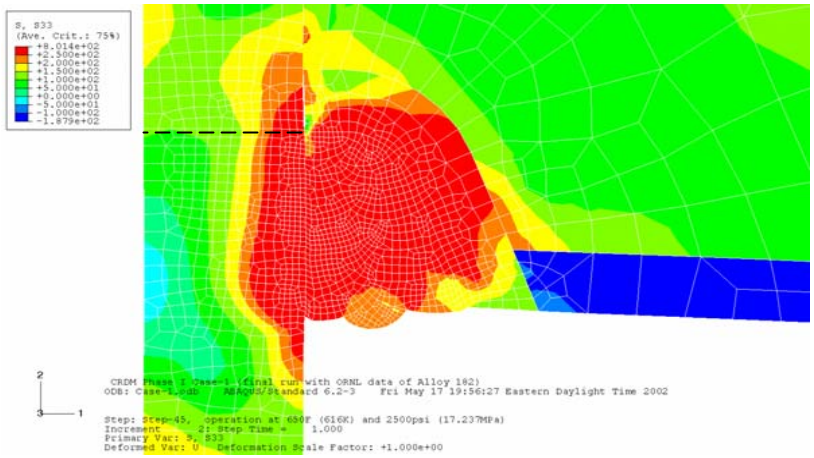

Hoop Stress, MPa

Center-hole model

Side-Hill Weld Residual Stress Model
(Design Conditions: 605F and 2,500psi)

- ***Followed the welding sequence observed in actual fabrication***

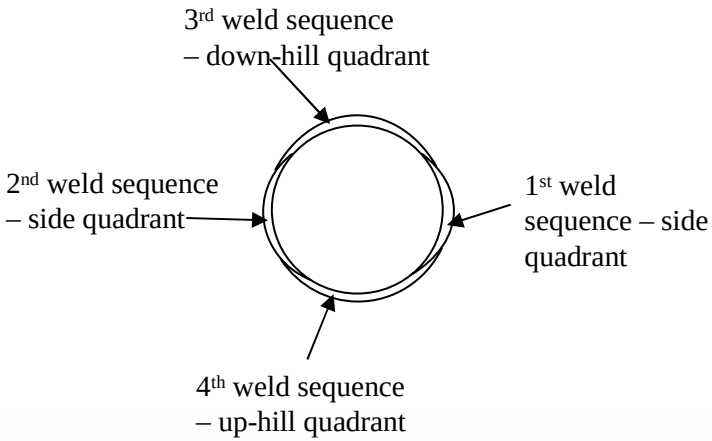

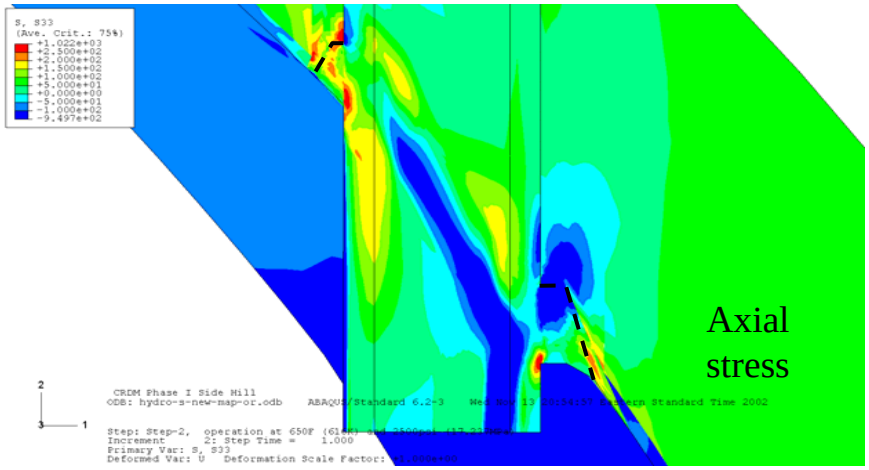

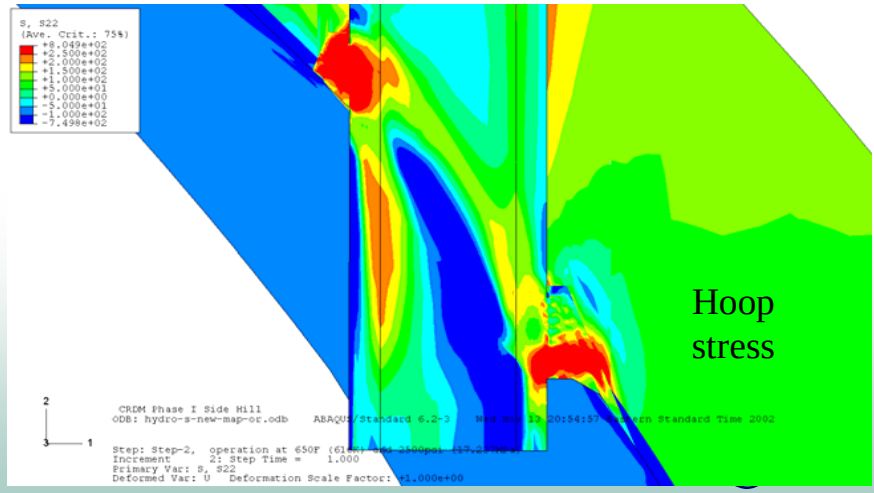

Sectional View of Axial Stresses

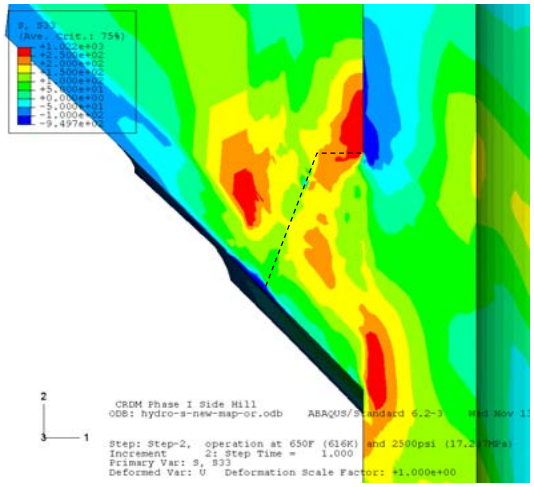

(a) 0-degrees

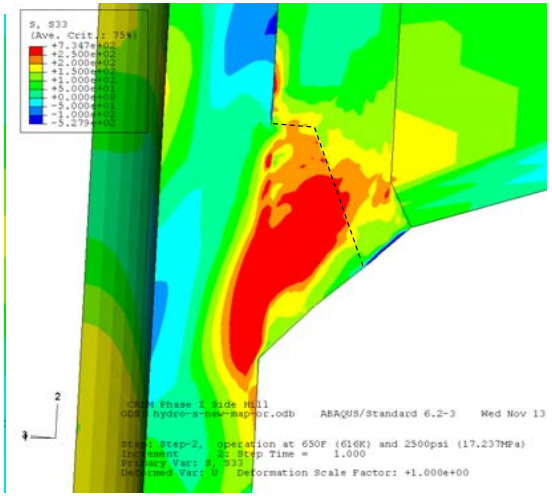

(b) 45-degrees

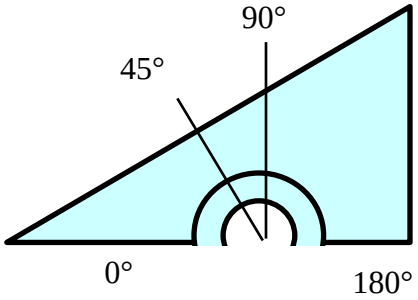

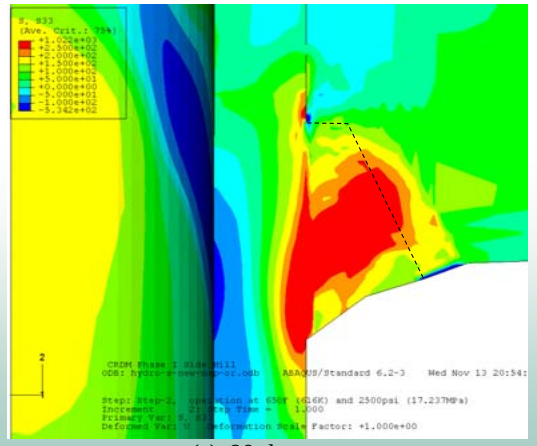

(c) 90-degrees

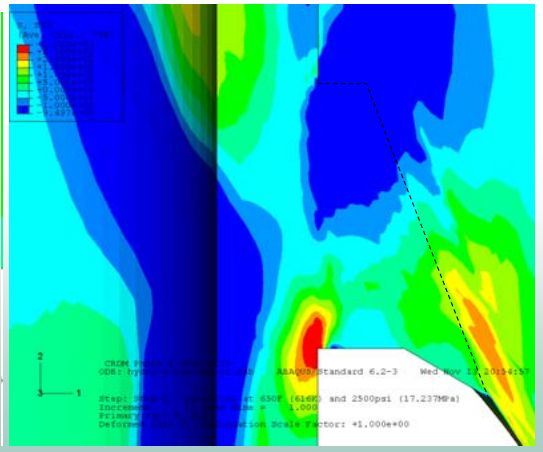

(d) 180-degrees

Observations of Weld Stresses

- *The as-welded stress states are primarily dependent on the J-weld size, and the tube strength levels.*
  - *(Nozzle angle is expected to be a primary factor as well, but the results are not yet available).*
- *There are appreciable differences between the as-welded stress states and the in-service stress state caused by hydro-test and by the pressure and temperature loading from operation.*
- *The hoop stresses in the tube next to the J-weld are high in tension, generally reaching the yield strength level of the tube on the OD and extending above and below the J-weld region.*

Observations of Weld Stresses

- *The axial stress is highly sensitive to the weld height.*
  - *A large J-weld tends to be beneficial for circumferential crack case as it creates compressive axial stresses at the root of the weld.*

- *As the J-weld height increases, the hoop stresses on the ID surface of the tube increase and the axial stresses at the J-weld root decrease.*
  - *There is probably an optimal weld height to minimize both stress components.*

- *The effects of other fabrication variables such as welding sequence and interference fit are secondary to the stress distribution in the J-weld region.*

Cracked Mesh

- ***Replaced original mesh at crack location with focused mesh (crack plane zipped)***
- ***Mapped residual stress solution onto "new" mesh***
- ***Added temperature and operating pressure***
- ***Released crack face restraints***
- ***Calculated K/J at crack tip through thickness***

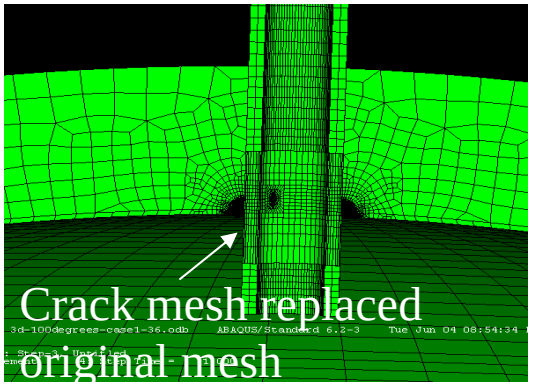

Center hole

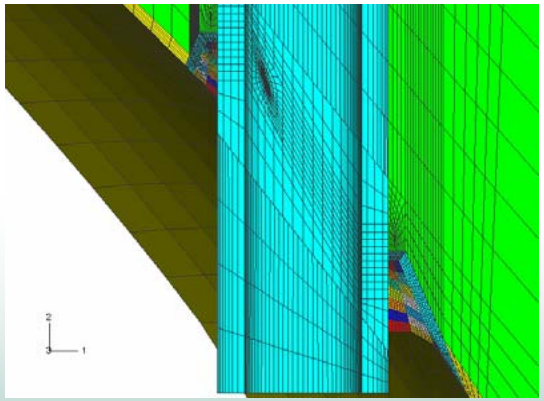

Steepest sidehill

Parametric Analyses

- *10 circumferential through-wall-crack lengths: 40 to 320 degrees*
- *2 tube yield strengths: 37.5 ksi (258.6 MPa) for base case, and 64.4ksi (444 MPa)*
- *3 interference fits: 0, 2 (base case), and 4.5 mils (radial interference at room temperature and P = 0)*
- *Two operating temperatures: 605 F (base case) and 560 F*
- *One operating pressure: 2,500 psi*
- *Center-hole and largest side-hill angle*
  - *Most parametric work completed on center hole – Only baseline case run for largest side-hill angle*
- *Friction between tube and RPV hole included using friction factor of 0.1 (solid lubrication of boric acid crystals)*
  - *With circumferential crack, the tube tips in the hole and contacts the RPV head.*

Mapped Solution for Center-Hole Case

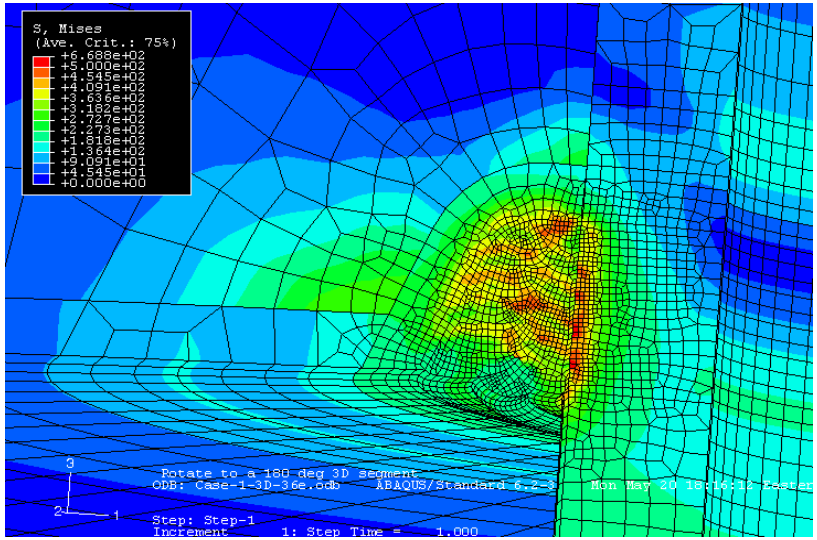

Original

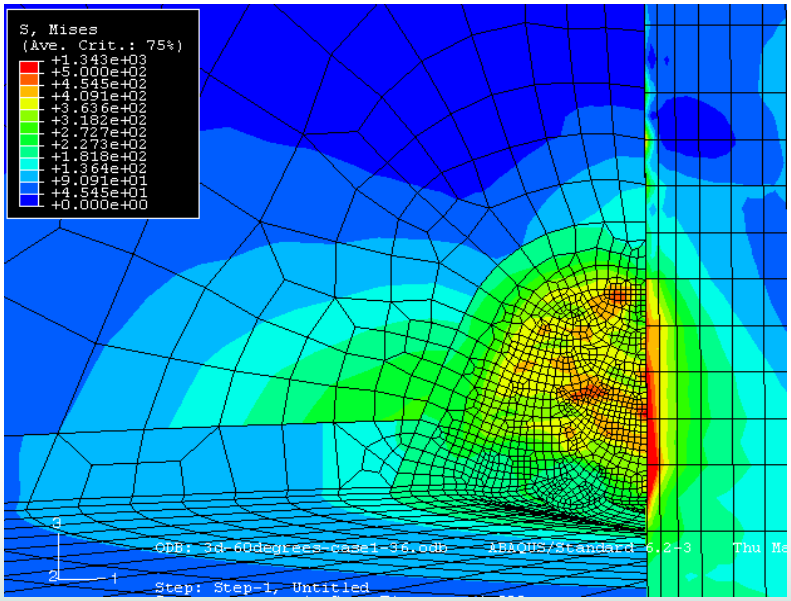

Mapped

Center-hole Cracked Case at Design Conditions

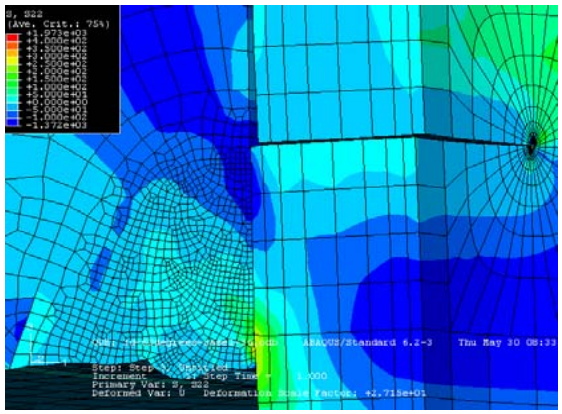

Mode III loading

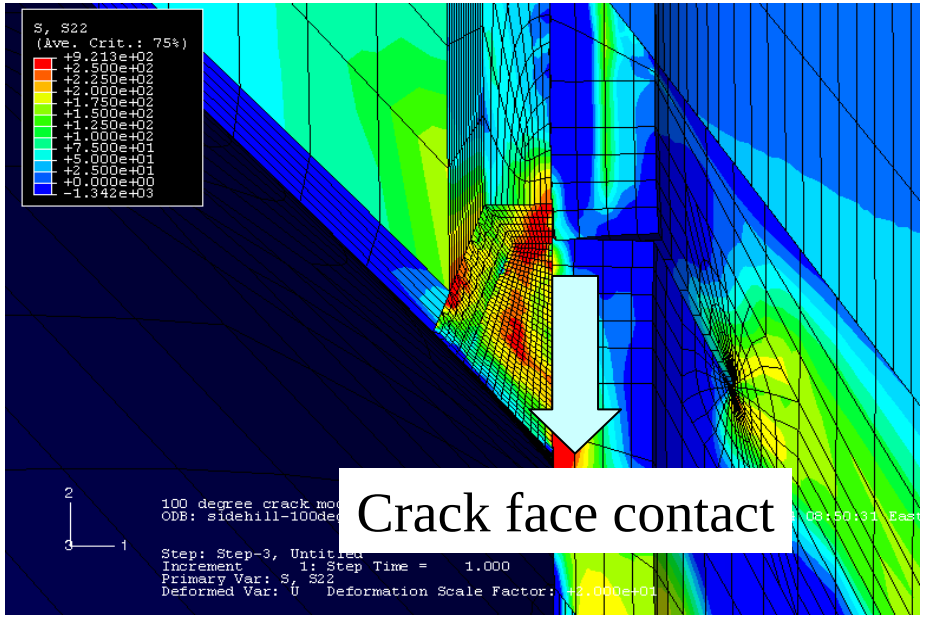

Trend suggests crack will not grow perpendicular to wall thickness – Angled crack growth through the thickness will be investigated in current program

Side-Hill nozzle – Crack face opening

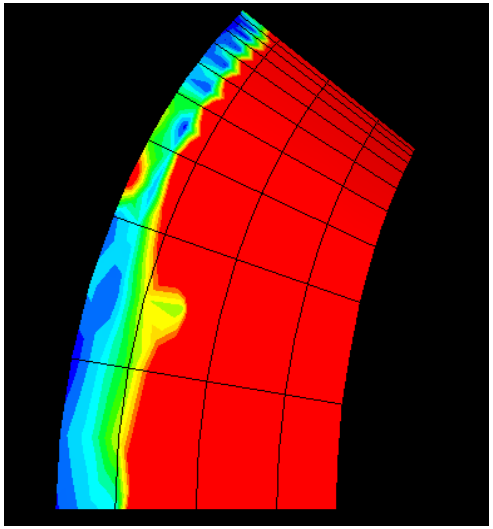

60 degrees

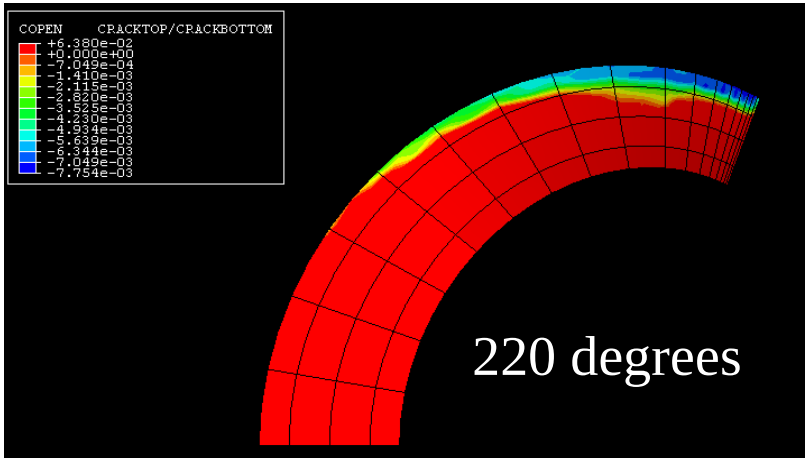

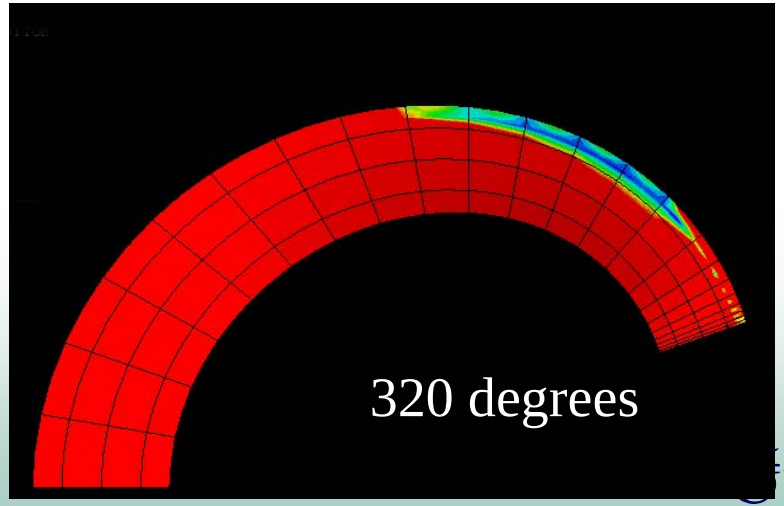

Crack closure exists at all crack lengths

Red – crack open
Other – crack closed

K-solutions from Center hole TWC Analyses

- ***With crack perpendicular to tube surface, large K_{III} and K_{II} component exists.***
  - ***Mode I = opening***
  - ***Mode II = in-plane sliding***
  - ***Mode III = out-of-plane sliding***

- ***Since subcritical cracks grow in maximum Mode I direction, crack angle through the thickness should not be perpendicular to tube surface.***

- ***K_{eq} was calculated from total J.***

Extrapolation technique used for path dependent J/K values

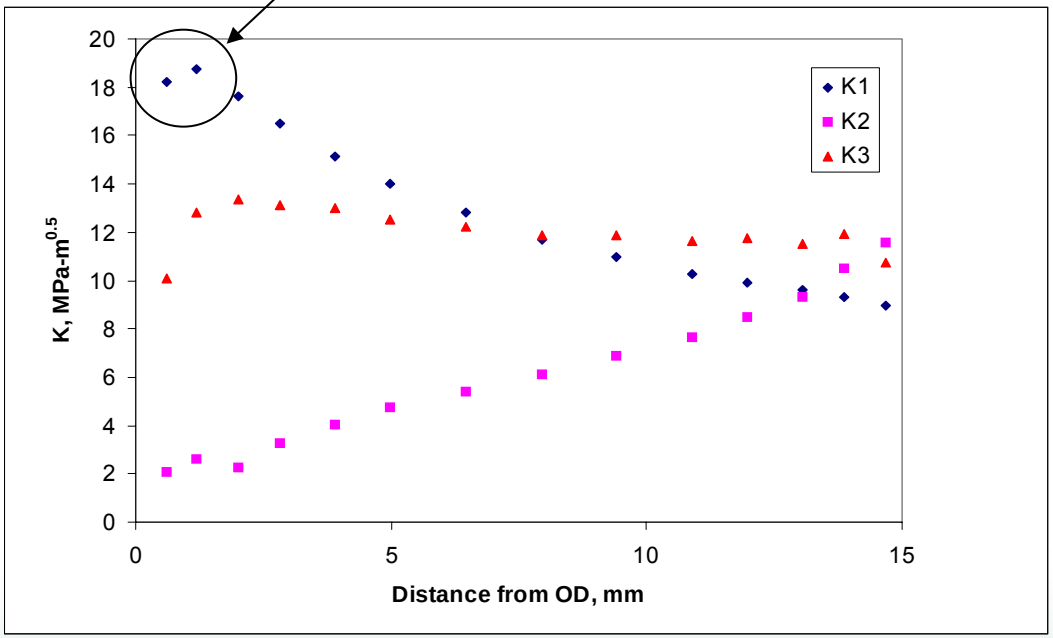

100-degree circumferential through-wall crack case

Side-Hill nozzle – J/K-solutions

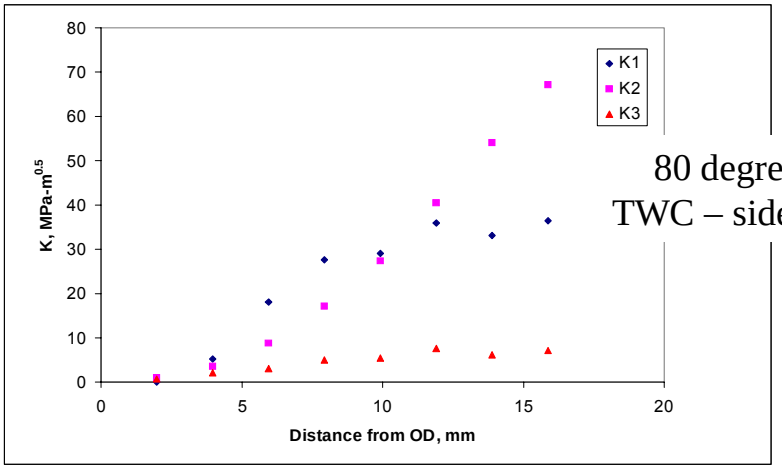

80 degree
TWC – side hill

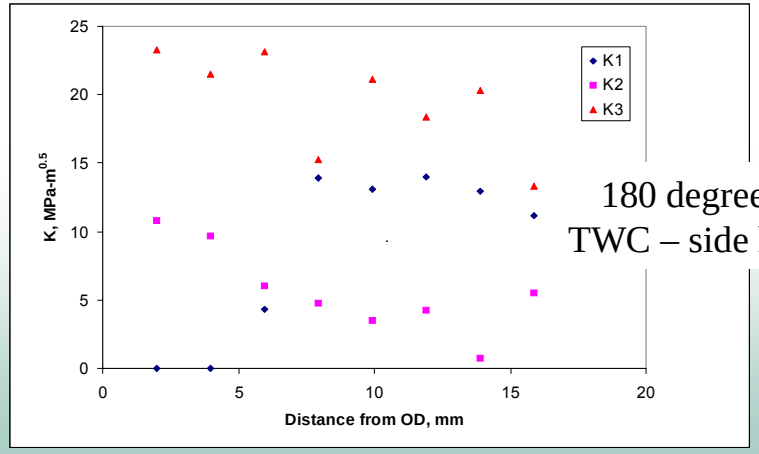

180 degree
TWC – side hill

Huge gradient due
to crack closure

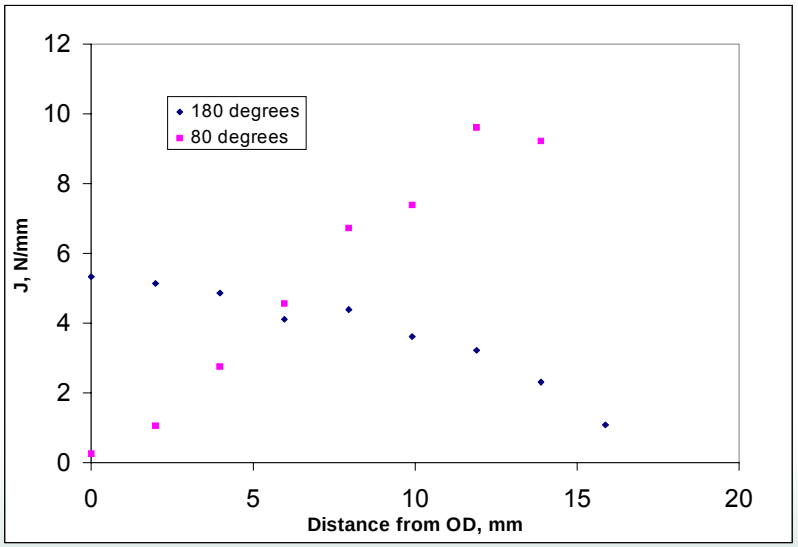

Center Hole $K_{J(average)}$ -solution Comparison

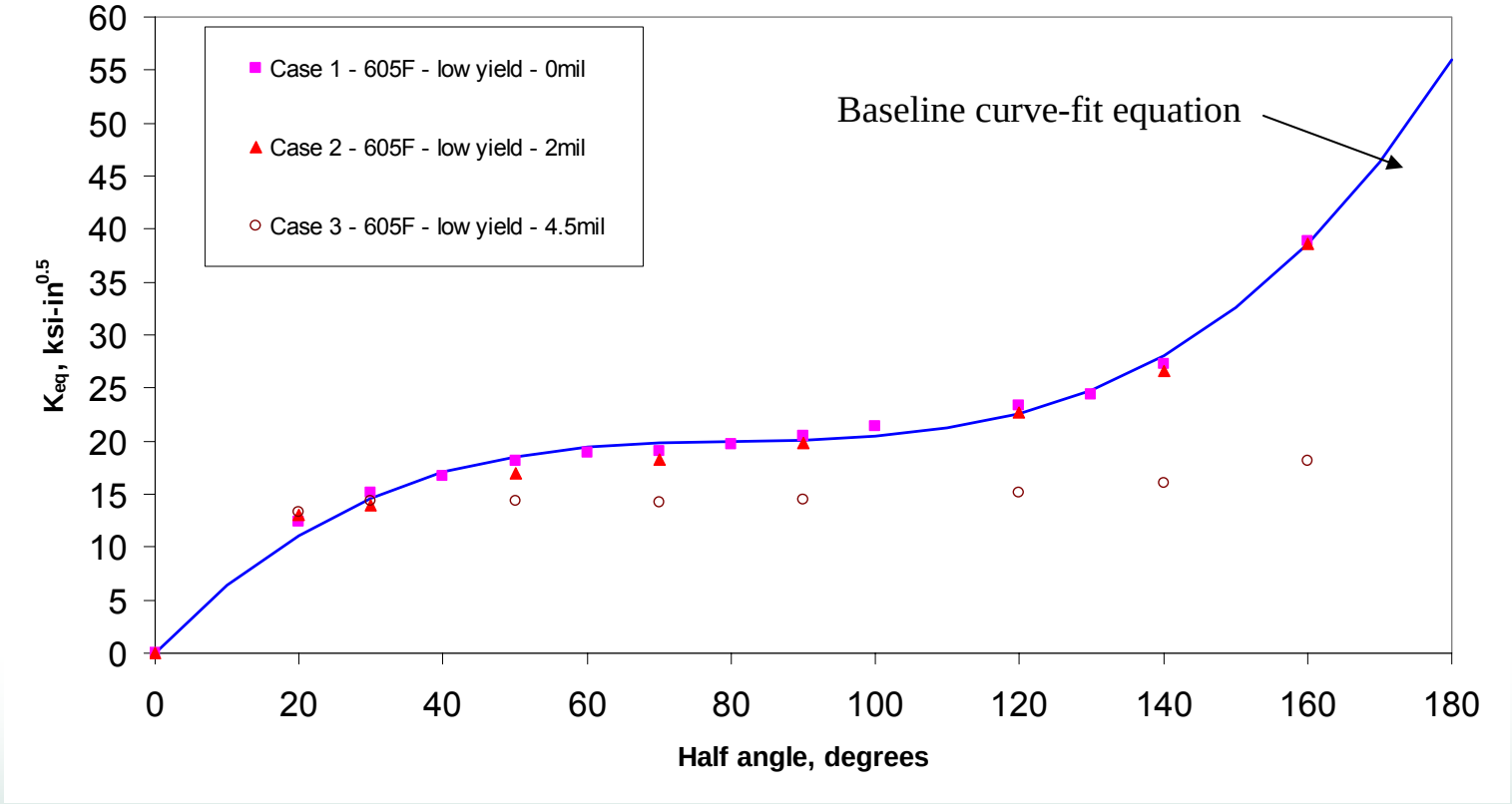

Center-hole circumferential though-wall cracks
(Effect of room temperature interference fit)

Center Hole $K_{J(average)}$ -solution Comparison

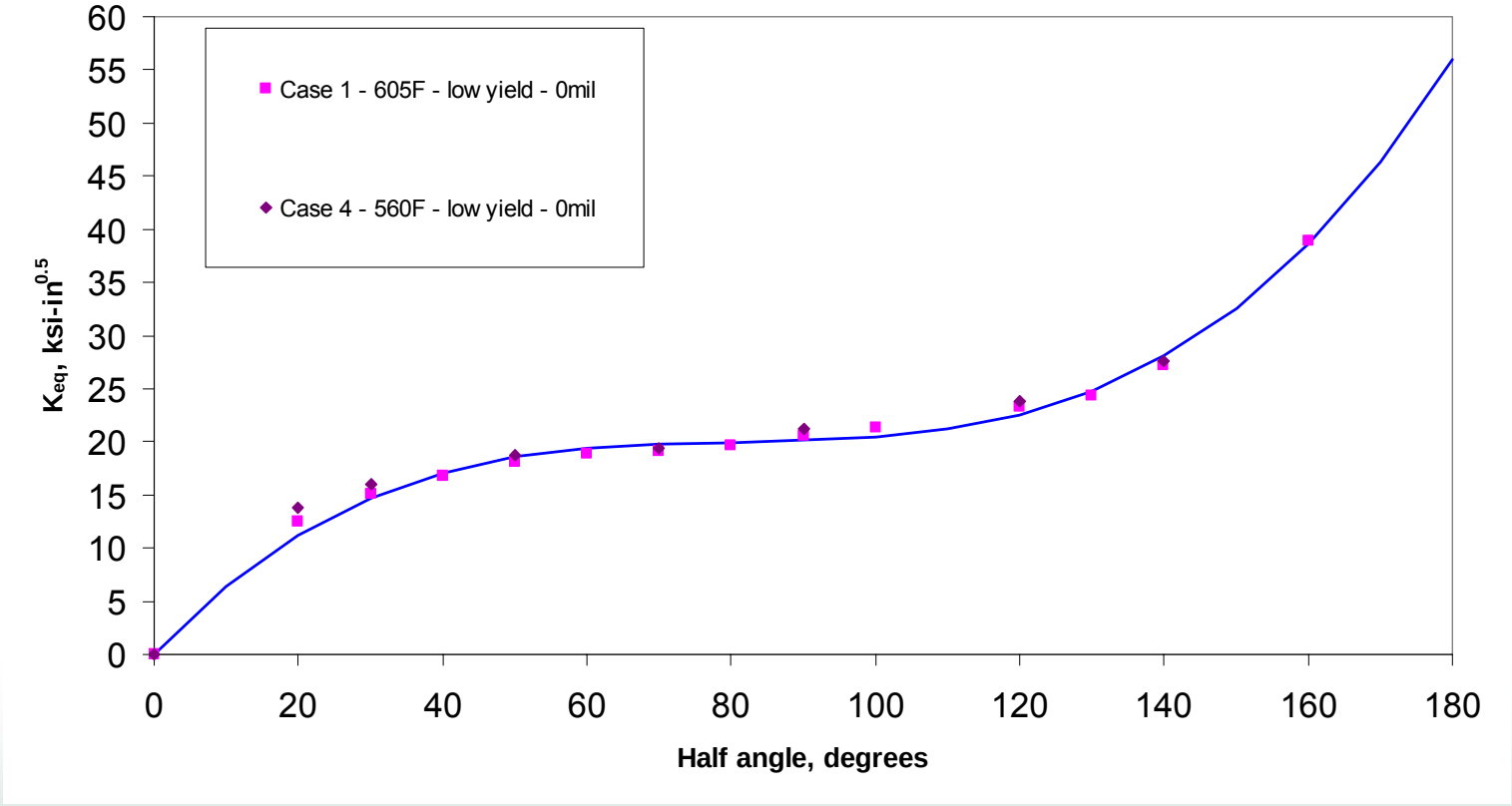

Center-hole circumferential though-wall cracks
(Effect of operating temperature)

Center Hole $K_{J(average)}$ -solution Comparison

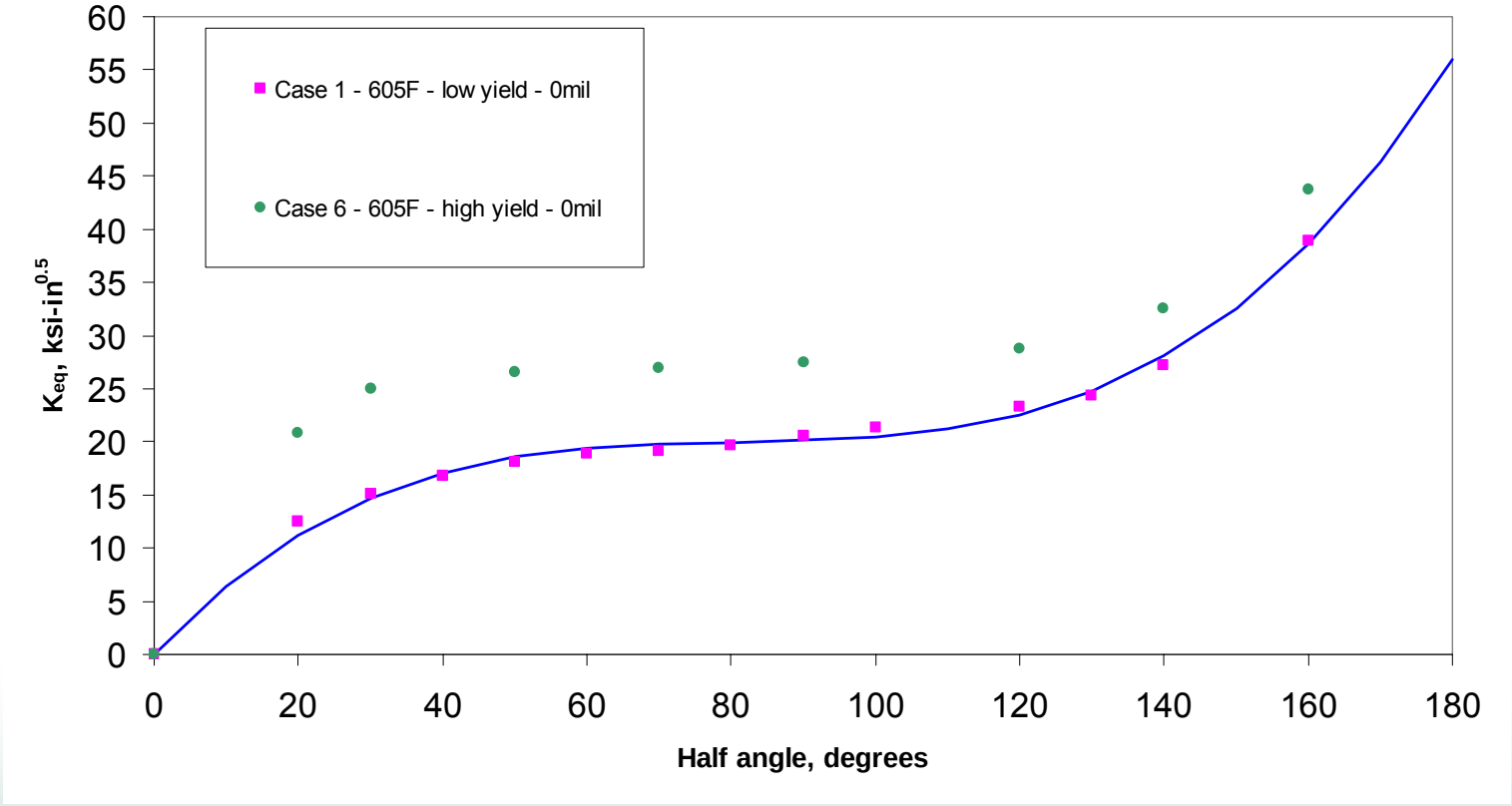

Center-hole circumferential though-wall cracks
(Effect of tube yield strength)

Center Hole $K_{J(average)}$ -solution Comparison

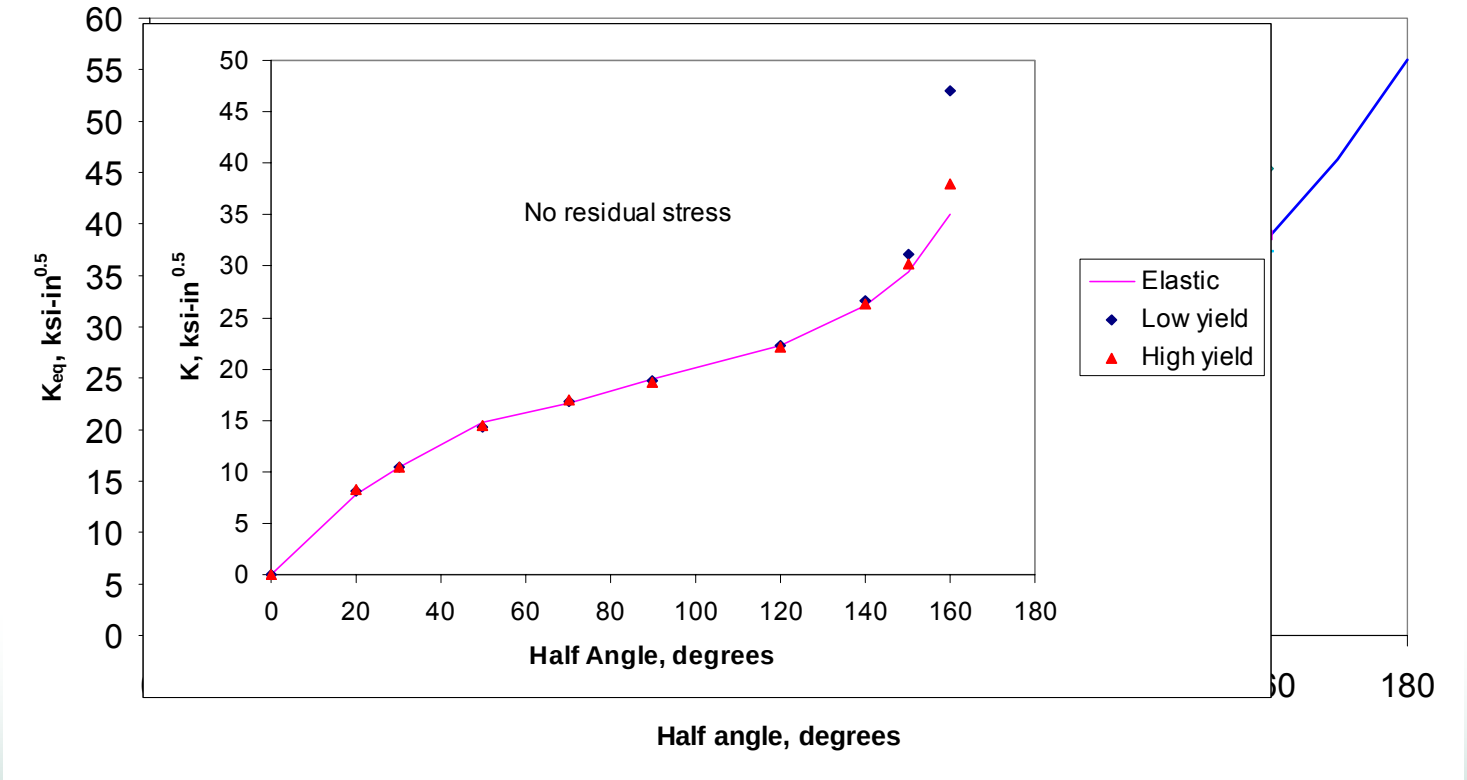

Center-hole circumferential though-wall cracks
(Comparison without residual stresses)

Center Hole $K_{J(average)}$ -solution Comparison

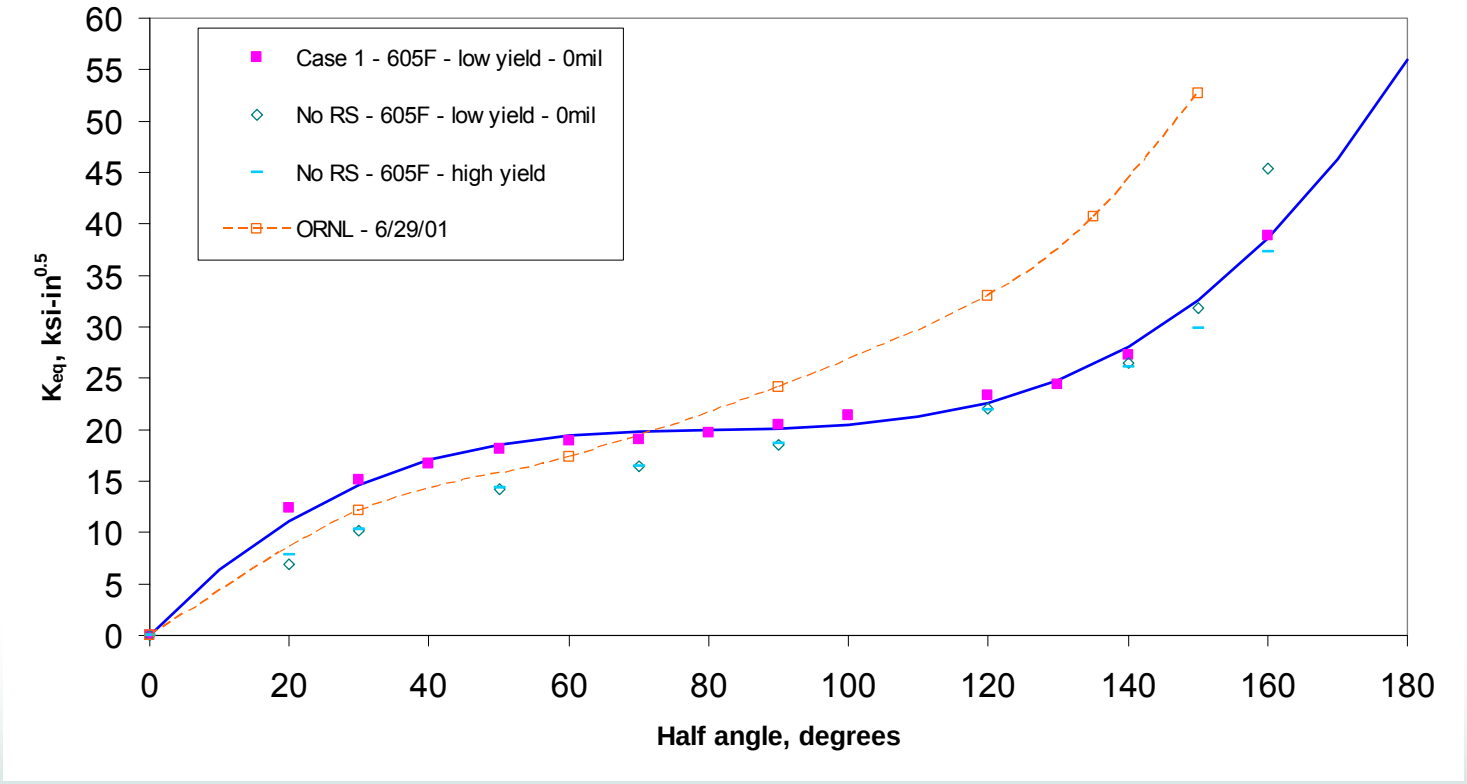

Center-hole circumferential though-wall cracks
(Comparison without residual stresses)

Center Hole $K_{J(average)}$ -solution

K_{max} versus K_{avg}

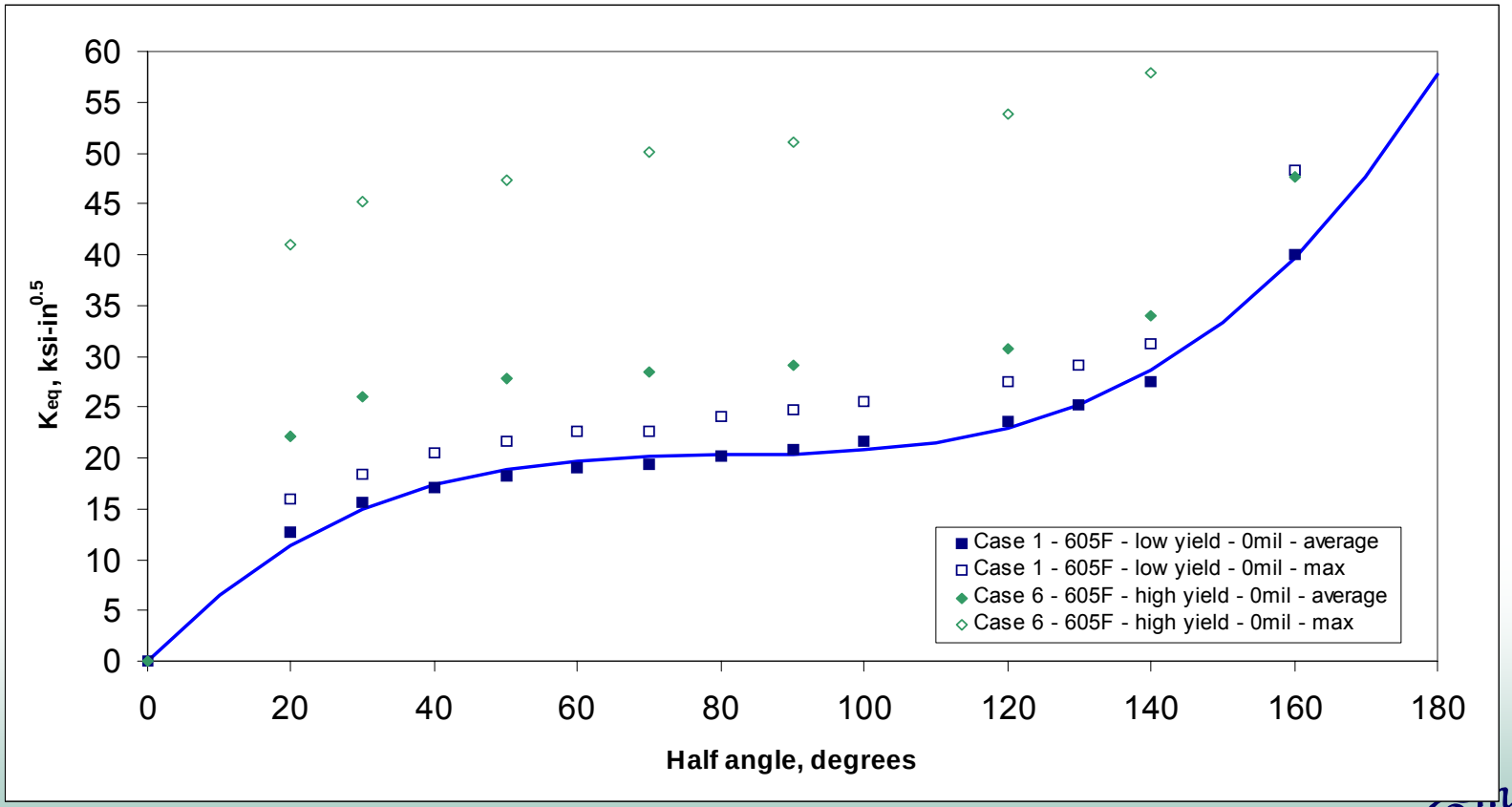

Side-Hill nozzle – $K_{J(average)}$ -solutions

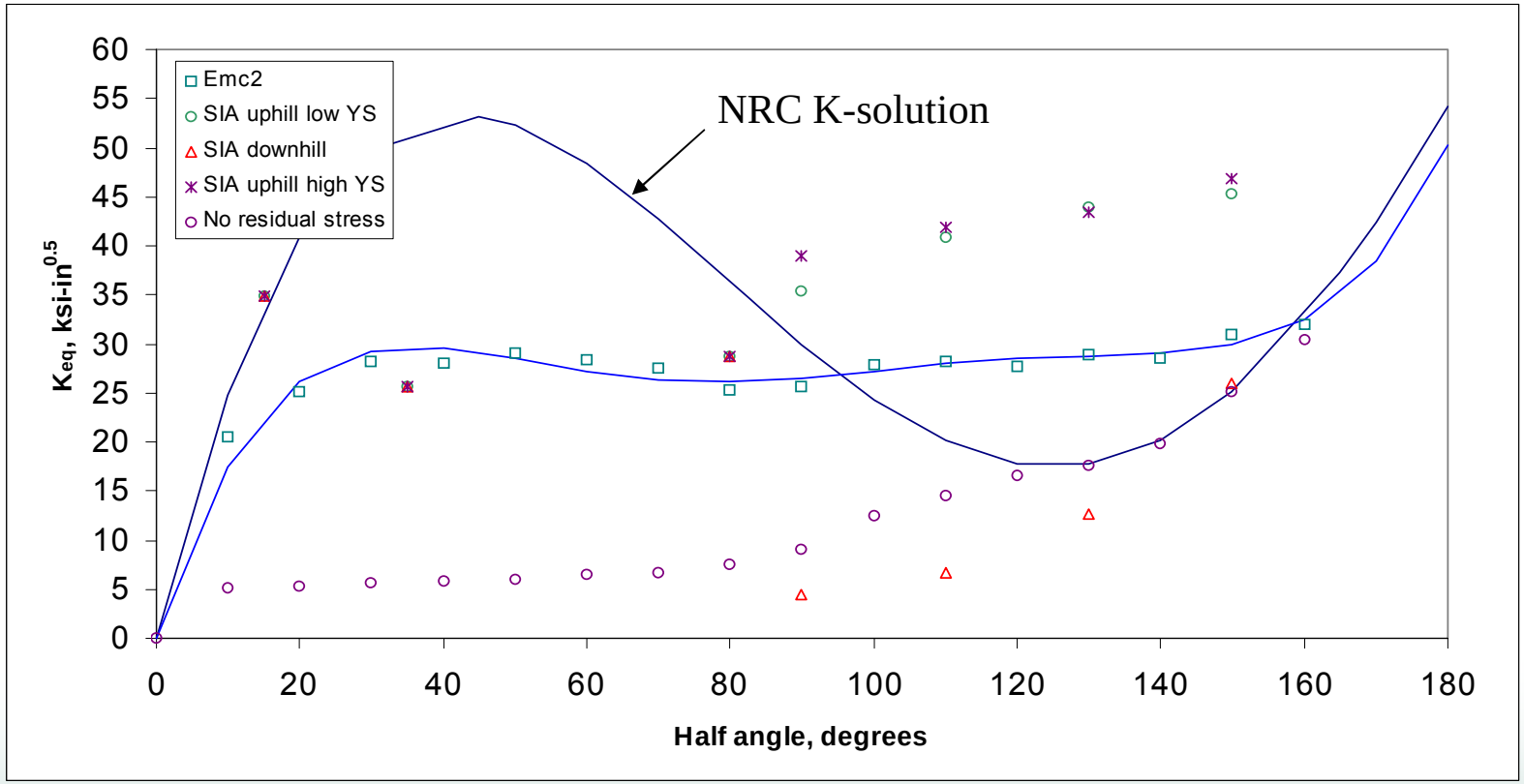

Due to change in J-gradient through the thickness as a function of crack length, the K_{eq} is almost independent of crack length

K-solution Observations

- *Tube yield strength had large effect of K solution – high yield gave large J gradient through thickness.*
- *For low yield, residual stress made no difference in K for cracks greater than 180 degrees.*
- *Large interference fit decreased the K solutions, but intermediate interference fit (2 mil on radius) had no effect on K.*
- *The range of operating temperature considered (560F versus 605F) did not significantly affect the K-solution.*
  - *(Temperature affects the PWSCC crack growth rate, but not the crack driving force.)*
- *The overall results are consistent with past ORNL tube-only K values.*

General Significant Observations

- ***Residual stresses in hoop direction increase with increasing weld size, and stresses in longitudinal direction at J-weld root decrease with increasing weld size.***
  - ***There should be optimum design.***

- ***By mapping entire stress field, it can be seen that there are Mode I, II, and III components when keeping the crack perpendicular to the tube surface.***
  - ***PWSCC crack will probably grow in Mode I direction that would be angled through the thickness.***
  - ***Future work concentrating on optimal crack angle though thickness for maximum K_I contribution!!***

United States Nuclear Regulatory Commission

International Cooperative Project:
PWSCC and NDE in Ni-Base Alloys and Dissimilar Metal Welds

Conference On Vessel Head Penetration Inspection, Cracking and Repairs

October 1, 2003

Carol E. Moyer, Materials Engineer

Office of Nuclear Regulatory Research

301-415-6764 cem3@nrc.gov

Objectives for Research Cooperative

- Document the range of locations and crack morphologies associated with PWSCC. Distinguish PWSCC cracks from similar-appearing features, such as weld hot tears.
- Identify, develop and assess NDE methods for accurately detecting, sizing and characterizing tight cracks such as PWSCC.
- Develop representative NDE mock-ups with cracks to simulate tight PWSCC cracks.

Project Organization

- Task 1 – Atlas of crack morphology for PWSCC
  - Compile existing work
  - Perform new fractography, metallography
- Task 2 – Round Robin of NDE techniques on PWSCC and simulated cracks
  - Assess techniques to detect and size cracks
  - Assess techniques to manufacture test blocks
- Other suggested topics: modeling, effects of surface condition, validation of structural integrity assessment, effects of weld repairs

United States Nuclear Regulatory Commission

What is Needed Next?

- People with common interests, resources
- Crack morphology information (reports, etc.)
- Set of relevant specimens
  - Cracks removed from plant components
  - Components from cancelled plants
  - Simulated or manufactured cracks
- Discussions to define project tasks

United States Nuclear Regulatory Commission

Welding Residual and Operating Stress Analysis
RPV Top and Bottom Head Nozzles

Vessel Head Penetration Inspection,
Cracking and Repair Conference

September 29 – October 2, 2003
Gaithersburg, MD

By:
John Broussard, Dominion Engineering, Inc.
David Gross, Dominion Engineering, Inc.

Dominion Engineering, Inc.
11730 Plaza America Dr.
Reston, VA 20190

Overview

- Development of RPV Head Stress Analysis Model
- Model Description and Validation
- Results for RPV Top Head Nozzles
- Results for RPV Bottom Head Nozzles
- Transient Analyses for Fatigue Analysis
- Additional Weld Residual Stress Modeling
- Fracture Mechanics Modeling with Stress Relaxation

Development of RPV Head Nozzle Stress Analysis Model

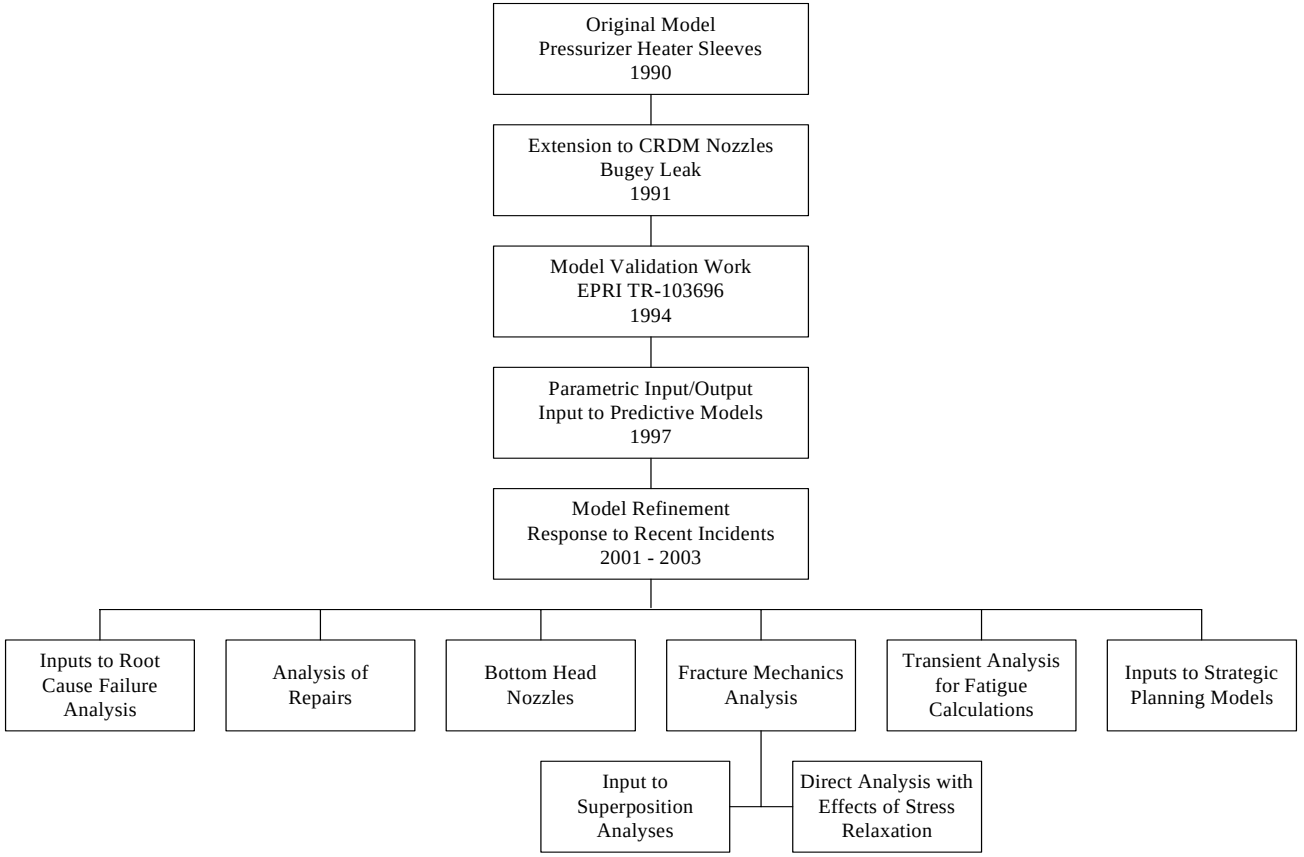

Model Description and Validation
Description

- 3D FEA modeling
  - ANSYS FEA software
  - Parametric input/output modeling
- Multi-pass welding
  - Thermal analysis of each weld pass
  - Structural analysis during weld cooling
  - Alloy 600 tubes have strain hardening properties
  - Welds assumed elastic-perfectly plastic
- Analysis includes
  - Deposition and stress relief of buttering prior to making J-weld
  - Interference fit between nozzle and bore in vessel head
  - Counterbores at top and bottom of head
  - Hydrostatic test pressure
  - Operating pressure and temperature

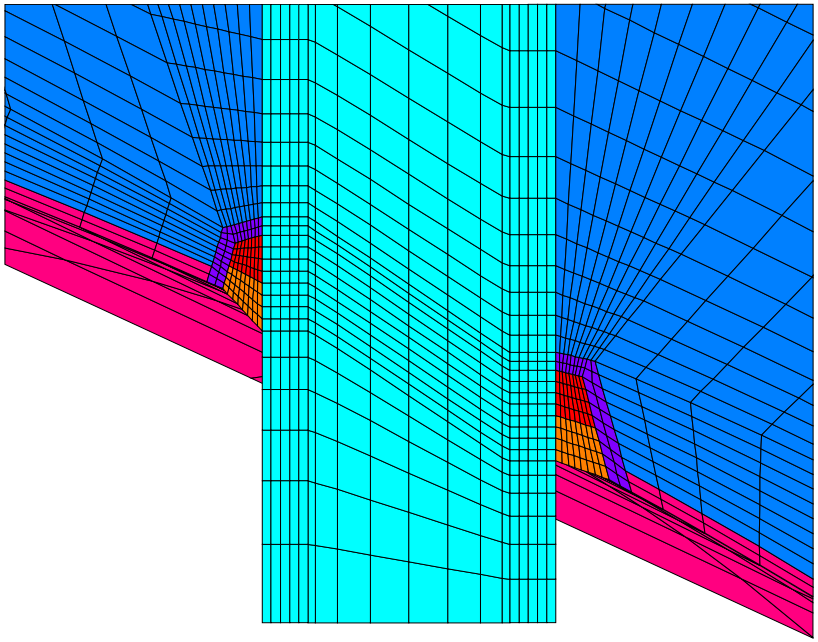

Model Description and Validation
Validation

- Nozzle lateral deflection and ovality
  - Pressurizer heater sleeves
  - CRDM nozzles
  - Bottom head nozzles
- Correlation with reported crack locations and orientations
  - Pressurizer heater sleeves
  - CRDM nozzles
  - Bottom head nozzles
- Correlation with x-ray and strain gauge hole drilling residual stress measurements
  - CRDM nozzle mockups
  - Pressurizer heater sleeve mockups
- Comparison to EMC^2 results
  - Material properties
  - Stresses
- Early validation work reported in EPRI TR-103696

Results for RPV Top Head Nozzles
Typical Hoop and Axial Stresses

- Typical hoop and axial stresses at uphill location

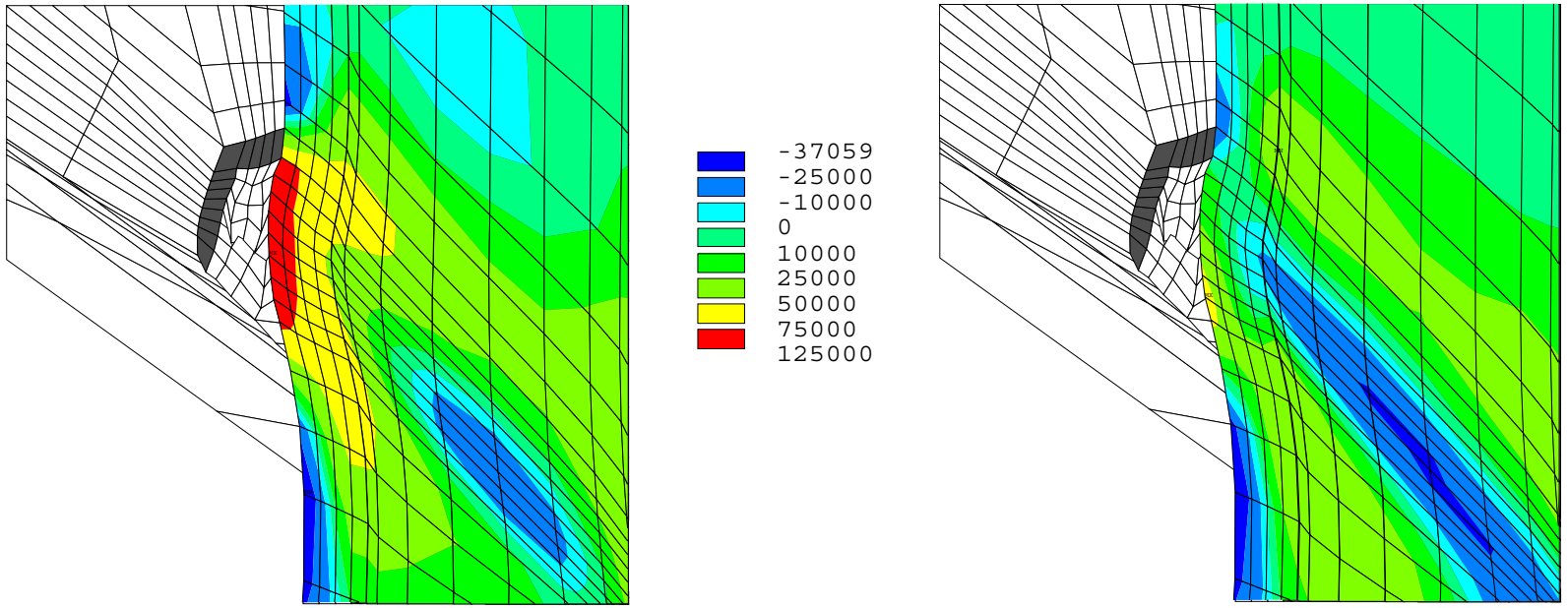

Hoop Stress **Axial Stress**

Results for RPV Top Head Nozzles
Correlation of Crack Orientation with Predictions

- Field experience consistent with typical analysis results
  - Over 90% of cracks have been axial
  - More cracks on the OD surface than on the ID surface
  - Circumferential cracks are more likely to initiate on the OD surface below the J-weld than on the ID surface

		No. of Indications on the Nozzle ID	No. of Indications on the Nozzle OD	*Total*
No. of Axial Tube Indications		112	224	*336*
No. of Circumferential Tube Indications	**Above Weld**	0	7	*7*
	Weld Elevation	0	12	*12*
	Below Weld	6	10	*16*
	Total	*118*	*253*	*371*

Notes
1. 498 Indications in the Database (as of 09/2003).
2. Craze Cracking/Shallow Cracks are not Included.

		% Indications on the Nozzle ID	% Indications on the Nozzle OD	*Total*
% Axial Tube Indications		30%	60%	*91%*
% Circumferential Tube Indications	**Above Weld**	0%	2%	*2%*
	Weld Elevation	0%	3%	*3%*
	Below Weld	2%	3%	*4%*
	Total	*32%*	*68%*	*100%*

Notes
1. 498 Indications in the Database (as of 09/2003).
2. Craze Cracking/Shallow Cracks are not Included.

Results for RPV Top Head Nozzles
Range of J-Weld Geometries

- All J-welds are not the same design
  - Weld cross section areas vary
  - Ratio of uphill-to-downhill areas vary
- Analyses show differences in stress and stress distribution with J-weld geometry
- As-built weld sizes determined by UT inspections differ from design dimensions
  - Oversize downhill welds can reduce maximum OD stresses at weld toe due to lower restraint

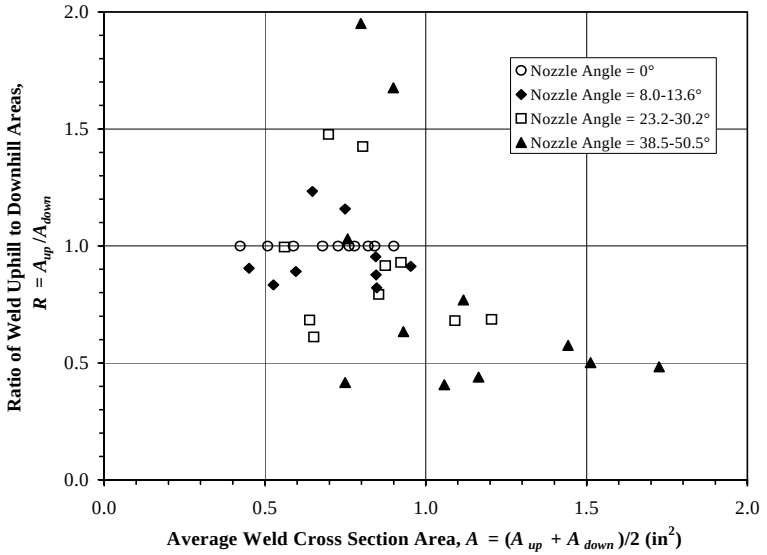

Results for RPV Bottom Head Nozzles
Typical Westinghouse BMI Nozzle

- Nozzles typically have lower D/T ratio than CRDM nozzles
- Typical results show
  - Ovalization is lower than in CRDM nozzles which have higher D/T ratio
  - Stresses are higher than in CRDM nozzles due to larger relative weld size
  - Hoop stresses in nozzle exceed axial stresses at high stress locations
  - Straightening the nozzle by plastic deformation does not increase total operating condition stresses

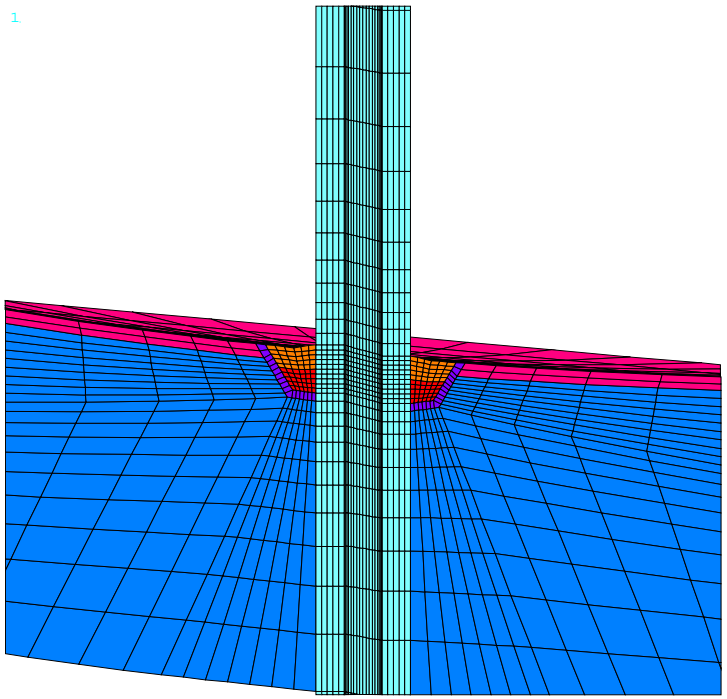

Results for RPV Bottom Head Nozzles
Typical B&W IMI Nozzle

- B&W IMI nozzles repaired
  - Original nozzles and J-welds stress relieved with vessel
  - Prior to plant operation the part of the nozzle inside the vessel was removed and replaced by larger diameter nozzle
- Typical results show
  - Peak stresses in nozzle are higher than in CRDM nozzles due to larger relative weld size
  - Hoop stresses in nozzle exceed axial stresses at high stress locations
  - Stresses in repaired part of nozzle trend to be lower due to less restraint during welding

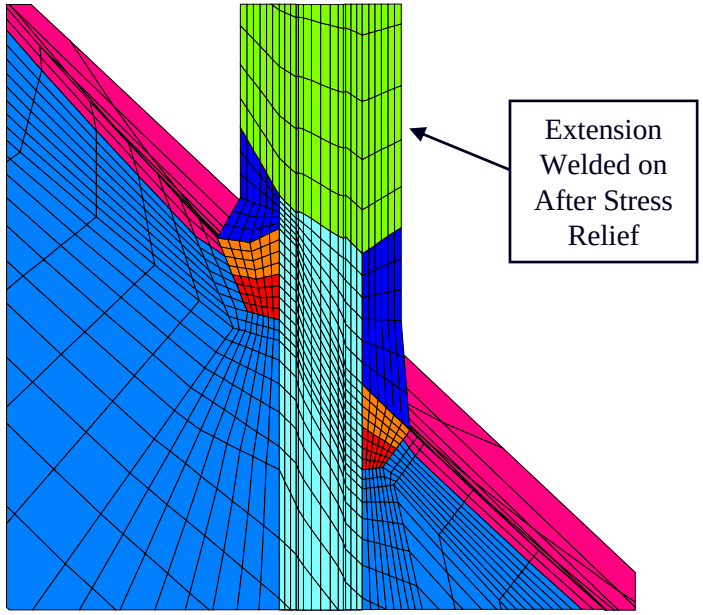

Transient Analyses for Fatigue Evaluation

- Representative transients selected for analysis
- Thermal transient analysis followed by structural analysis with temps and pressures
- Typical results show:
  - Stress trends consistent throughout model
  - Crack growth rates dominated by PWSCC

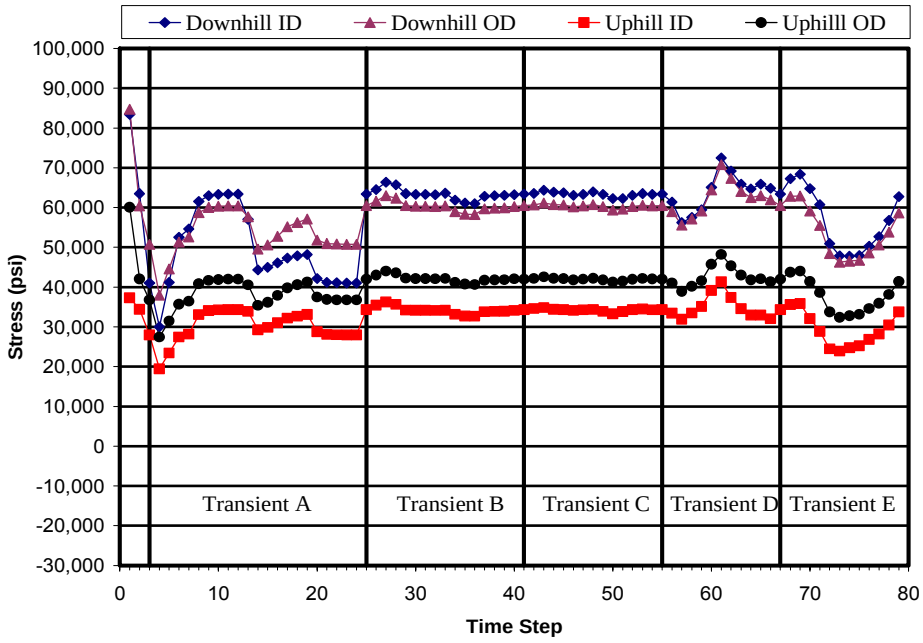

Additional Weld Residual Stress Modeling

- Various nozzle repair techniques simulated with stress results used as inputs to fracture mechanics models
  - Nozzle removal repair
  - Embedded flaw repair
- Other penetrations being analyzed
  - Pressurizer side shall penetrations
  - Hot leg nozzle penetrations
  - Pressurizer top and bottom head penetrations

Fracture Mechanics Analyses with Stress Relaxation
Background

- Stress intensity factors are often calculated using superposition method
- For cases with high residual stresses, superposition
  - Conservatively applies residual stresses as primary loads
  - Does not allow for stress relaxation and redistribution with crack growth
- Development work was performed to modify the existing stress analysis model to calculate stress intensities for circumferential flaws above the J-weld including the effects of stress relaxation with crack growth

Fracture Mechanics Analyses with Stress Relaxation
Calculation Methodology

- Initial application is for through-wall crack in outer row CRDM nozzle parallel to weld contour with variable distance above top of weld
- Custom fracture mechanics code added to DEI welding residual finite-element stress model for J-groove nozzles
- Stress redistribution from intact to cracked conditions modeled
  - Redistribution modeled as an elastic unloading problem amenable to LEFM
- Equivalent stress intensity factor (K) calculated from J-integral
  - J-integral calculated using numerical volume integration
  - J-integral averaged across nozzle wall
  - J-integral approach captures effect of Mode II and III contributions

$$K_{eq} = \sqrt{\frac{J_{avg} E}{1-\nu^2}}$$

Fracture Mechanics Analyses with Stress Relaxation
Fracture Mechanics Model

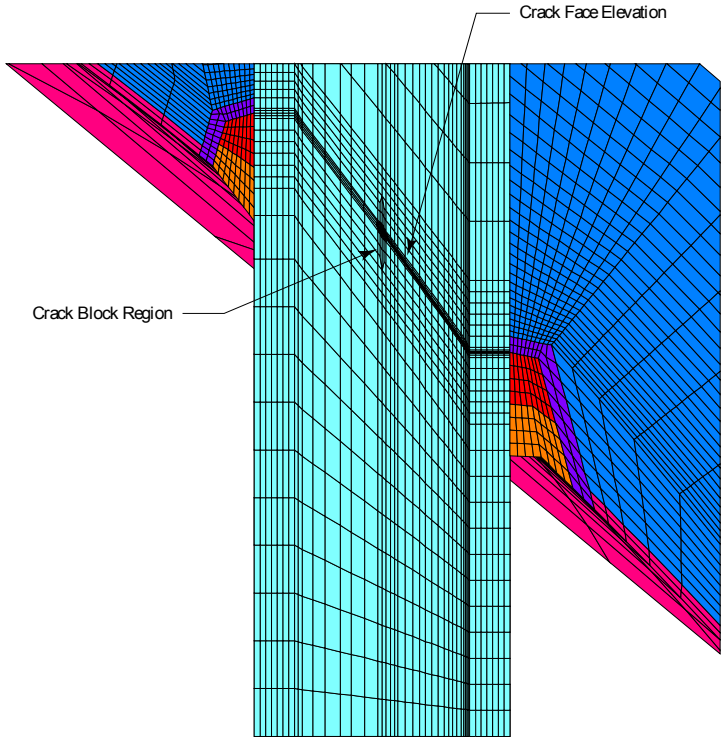

180° Downhill-Centered Crack

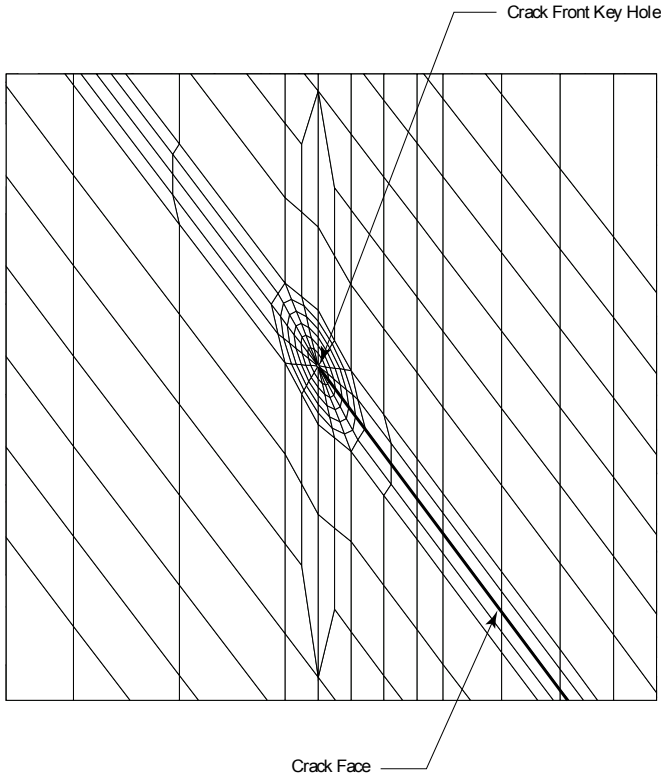

Crack Mesh Detail

Fracture Mechanics Analyses with Stress Relaxation

Relief of Axial Stress With Crack Growth

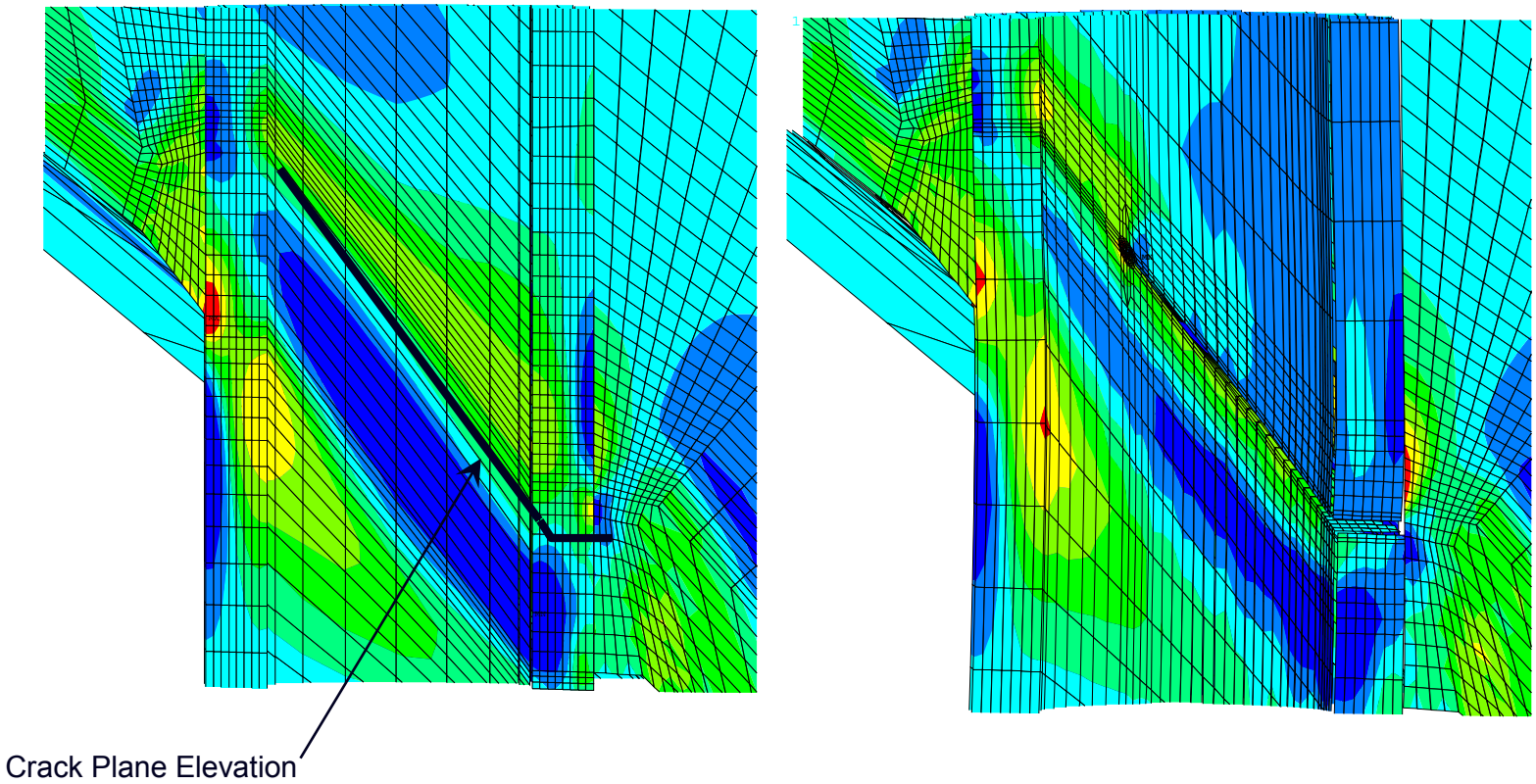

Operating Condition Axial Stress

Fracture Mechanics Analyses with Stress Relaxation

Stress Intensity: Downhill-Centered Cracks

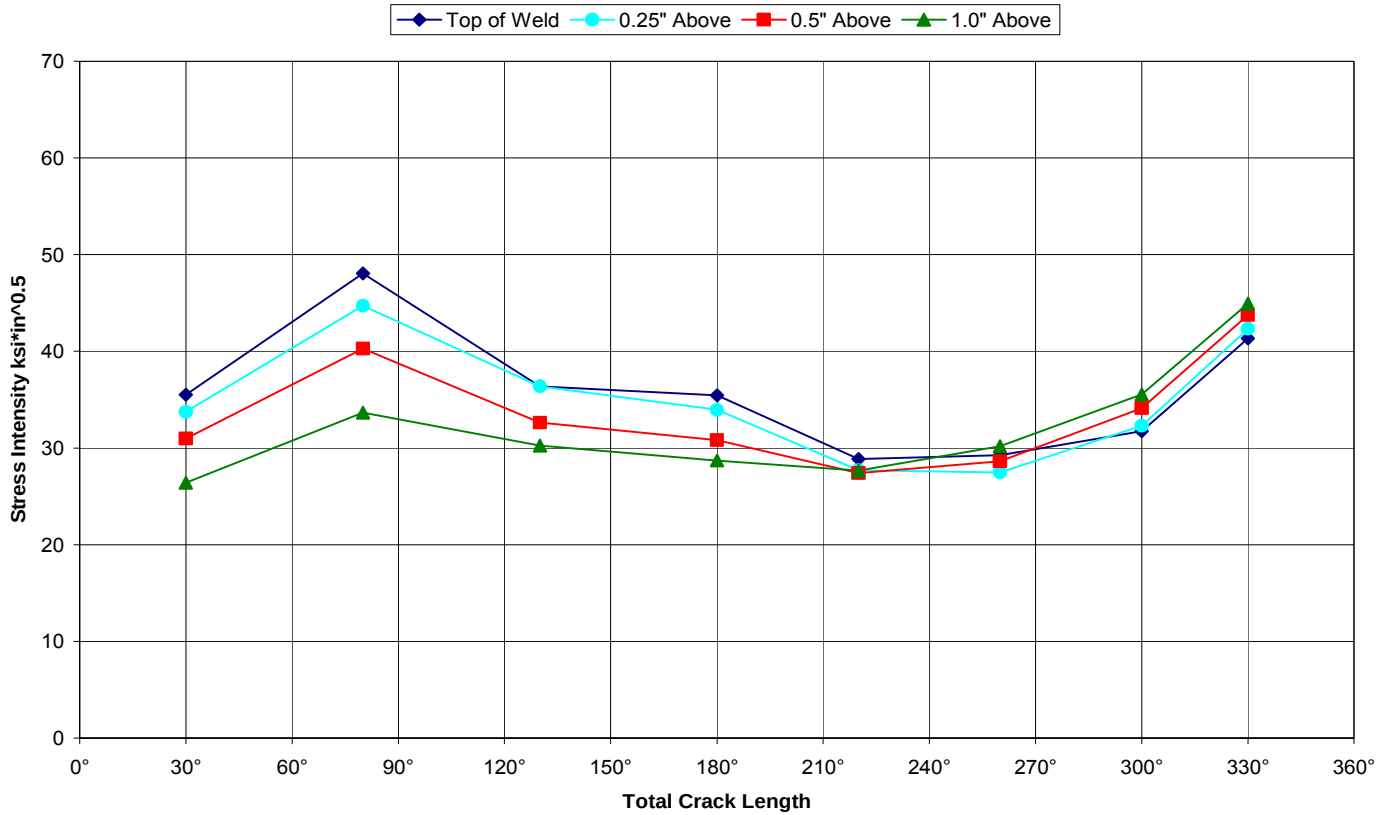

Fracture Mechanics Analyses with Stress Relaxation

Stress Intensity: Uphill-Centered Cracks

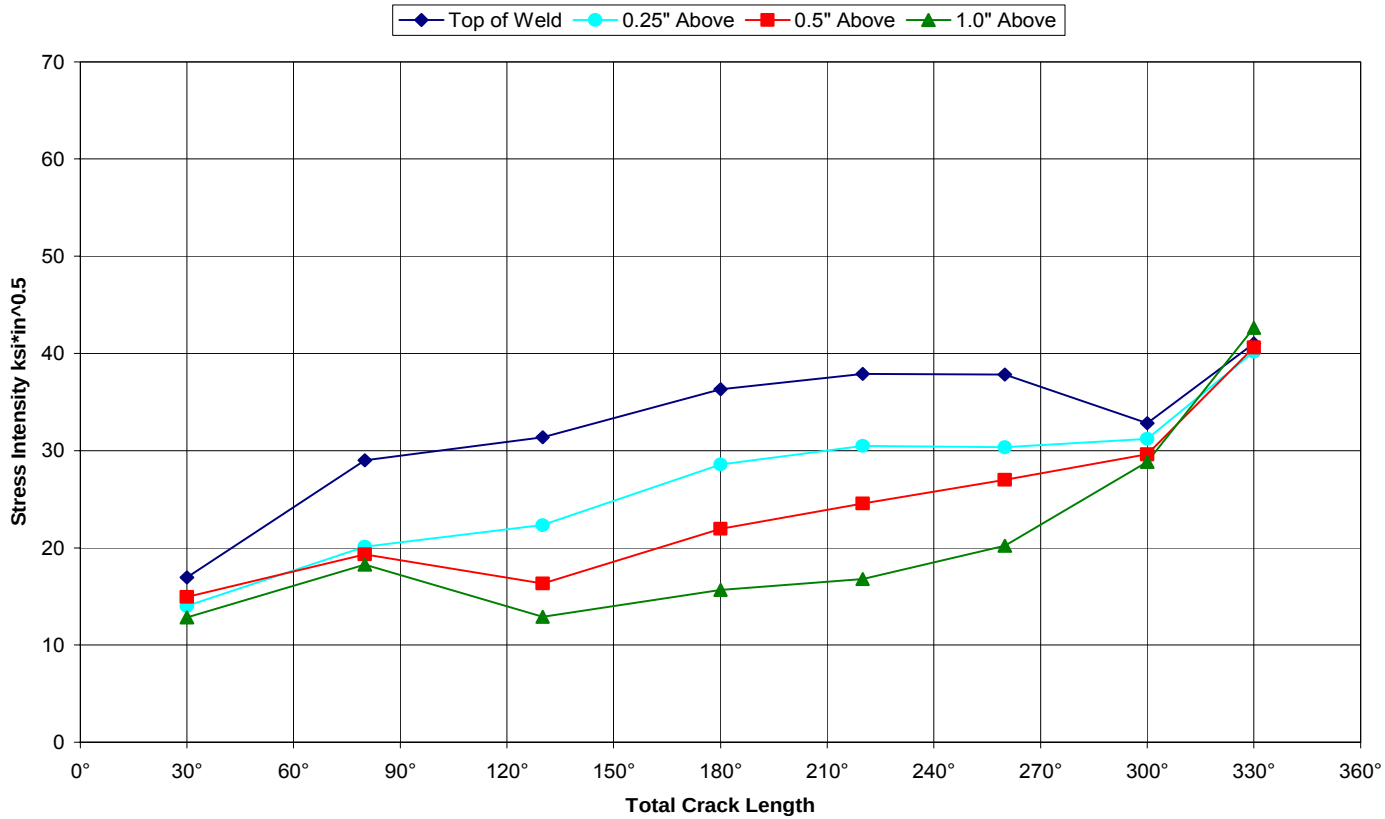

Fracture Mechanics Analyses with Stress Relaxation
Comparison to Other Data: Downhill-Centered Cracks

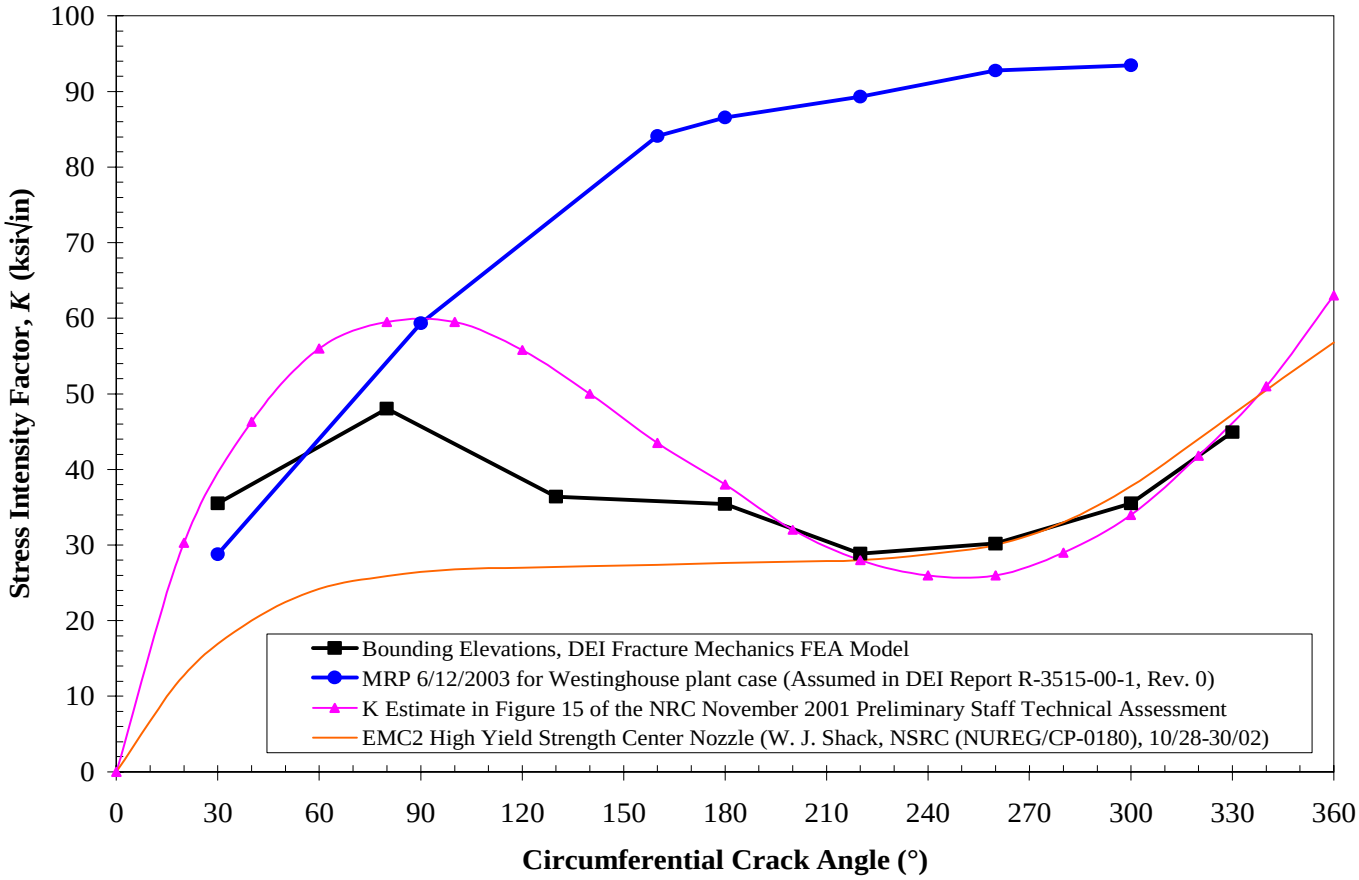

Fracture Mechanics Analyses with Stress Relaxation
Comparison to Other Data: Uphill-Centered Cracks

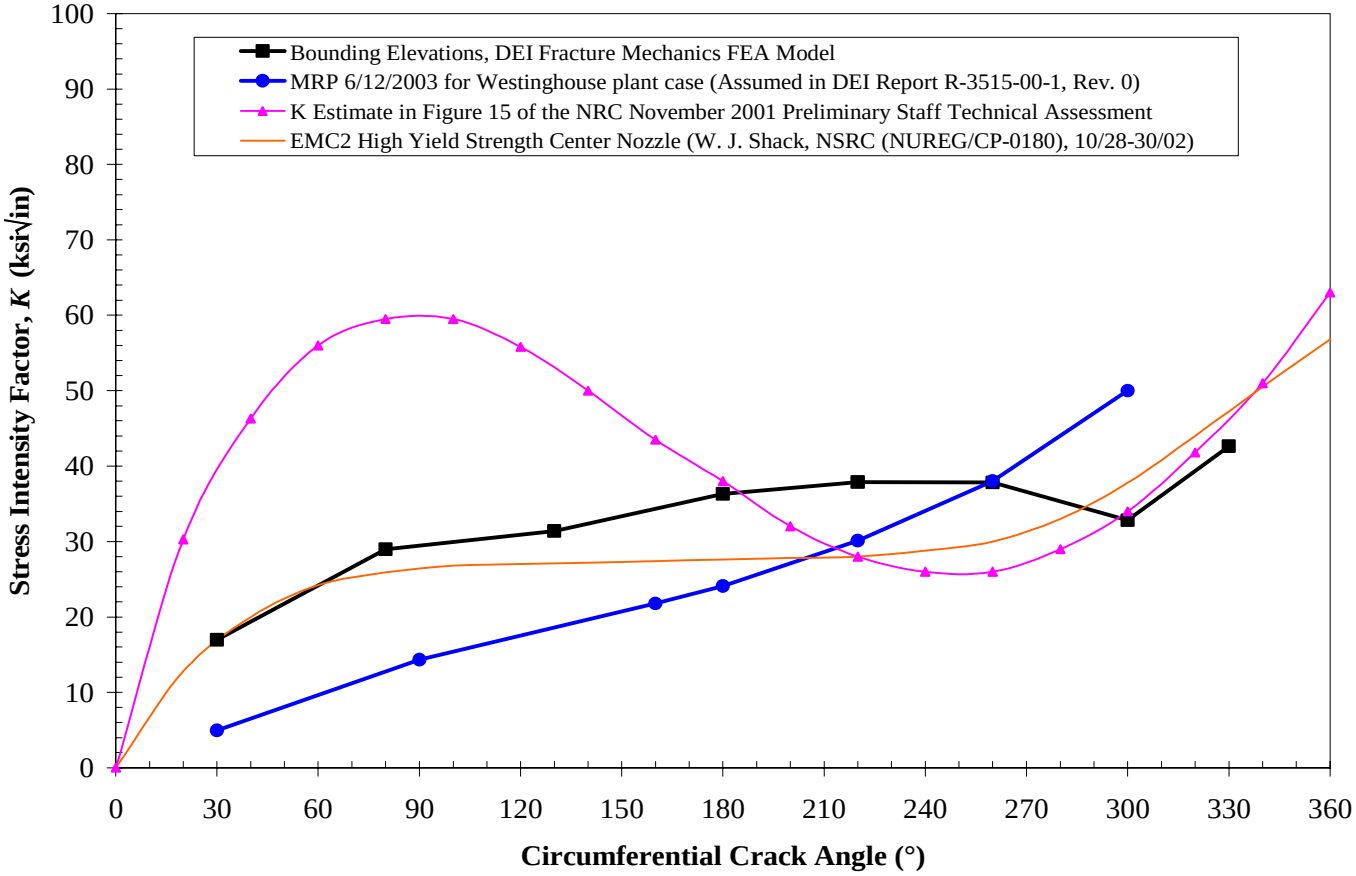

Fracture Mechanics Analyses with Stress Relaxation
Model Validation Case 1: Pipe with Axial Tension

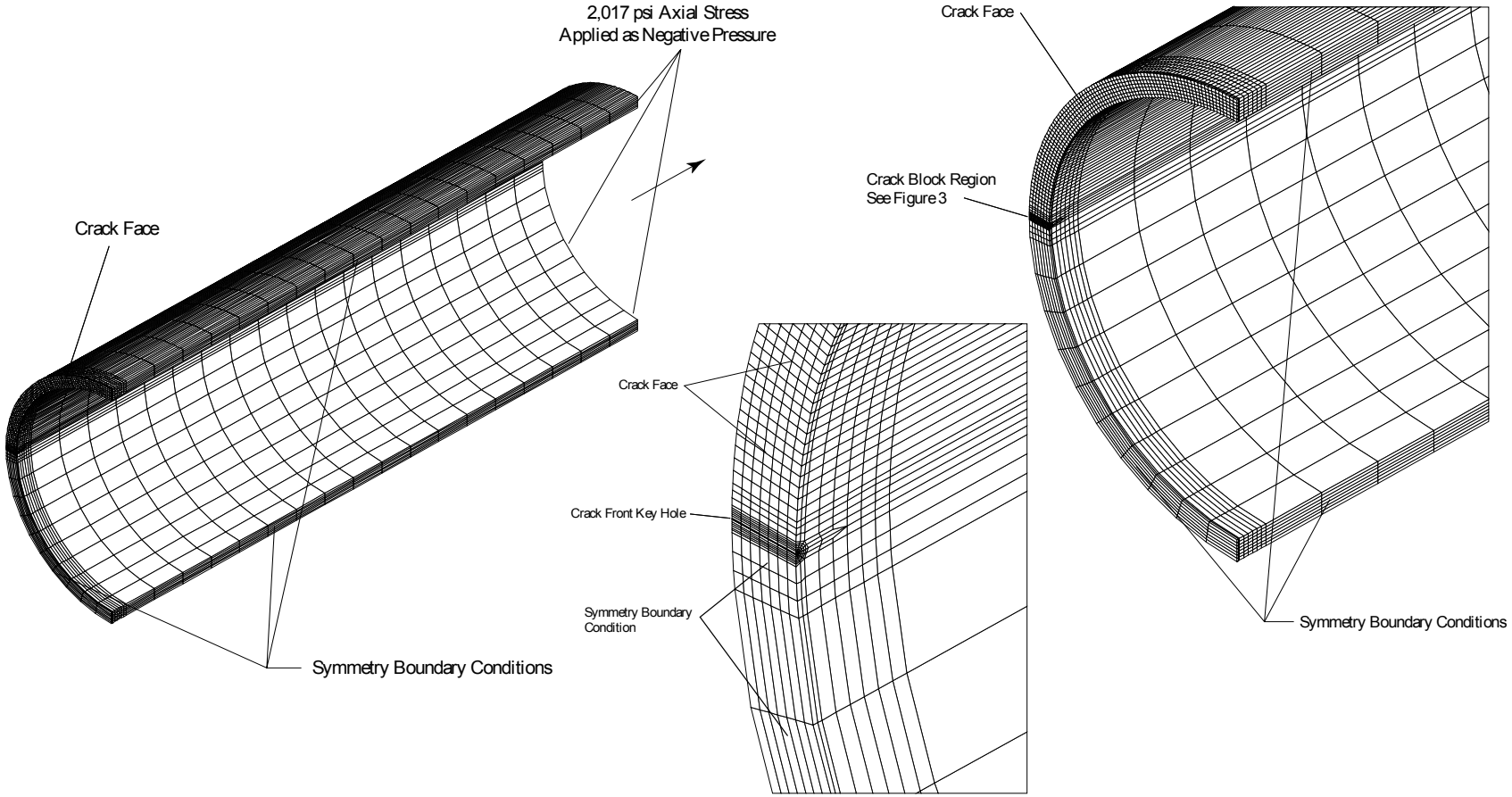

Fracture Mechanics Analyses with Stress Relaxation
Validation Case 1: Pipe with Axial Tension

- The stress intensity factor calculated for this model was compared to the results published by Zahoor[1] for a mean radius to wall thickness ratio of 10 and a maximum total crack arc of 180°:
  - Results agree within about 10%

Crack Length	K_I Calculated Using Zahoor[1]	K Calculated per FEA Model Test Case
30°	2.9 ksi√in	2.9 ksi√in
80°	6.6 ksi√in	7.1 ksi√in
130°	12.7 ksi√in	13.6 ksi√in
180°	24.0 ksi√in	26.5 ksi√in

[1]**A. Zahoor, *Ductile Fracture Handbook, Volume 1*, EPRI, Palo Alto, CA: 1989. NP-6301-D.**

Fracture Mechanics Analyses with Stress Relaxation Model
Validation Case 2: Through-Wall Center Crack in Plate

- For large crack sizes, the residual stresses are mostly relieved and the pressure stress determines the stress intensity factor

- A published solution[2] for a through-wall crack in a finite plate for all *a*/*b* and large *h*/*b* was compared to the results for large circumferential cracks
  - The remote axial stress σ was based on the axial pressure loading including pressure on the crack face

$$K_0 = \sigma\sqrt{\pi a}; \qquad \frac{K_I}{K_0} = \frac{1 - 0.5\frac{a}{b} + 0.326\left(\frac{a}{b}\right)^2}{\sqrt{1-\frac{a}{b}}}$$

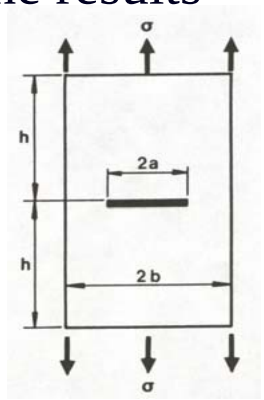

Note: *a* is taken as the projection of the crack midwall half-length on a horizontal plane.

[2]D. P. Rooke and D. J. Cartwright, *Compendium of Stress Intensity Factors*, Her Majesty's Stationery Office, London, 1976, p. 10.

Fracture Mechanics Analyses with Stress Relaxation Model
Validation Case 2: Through-Wall Center Crack in Plate

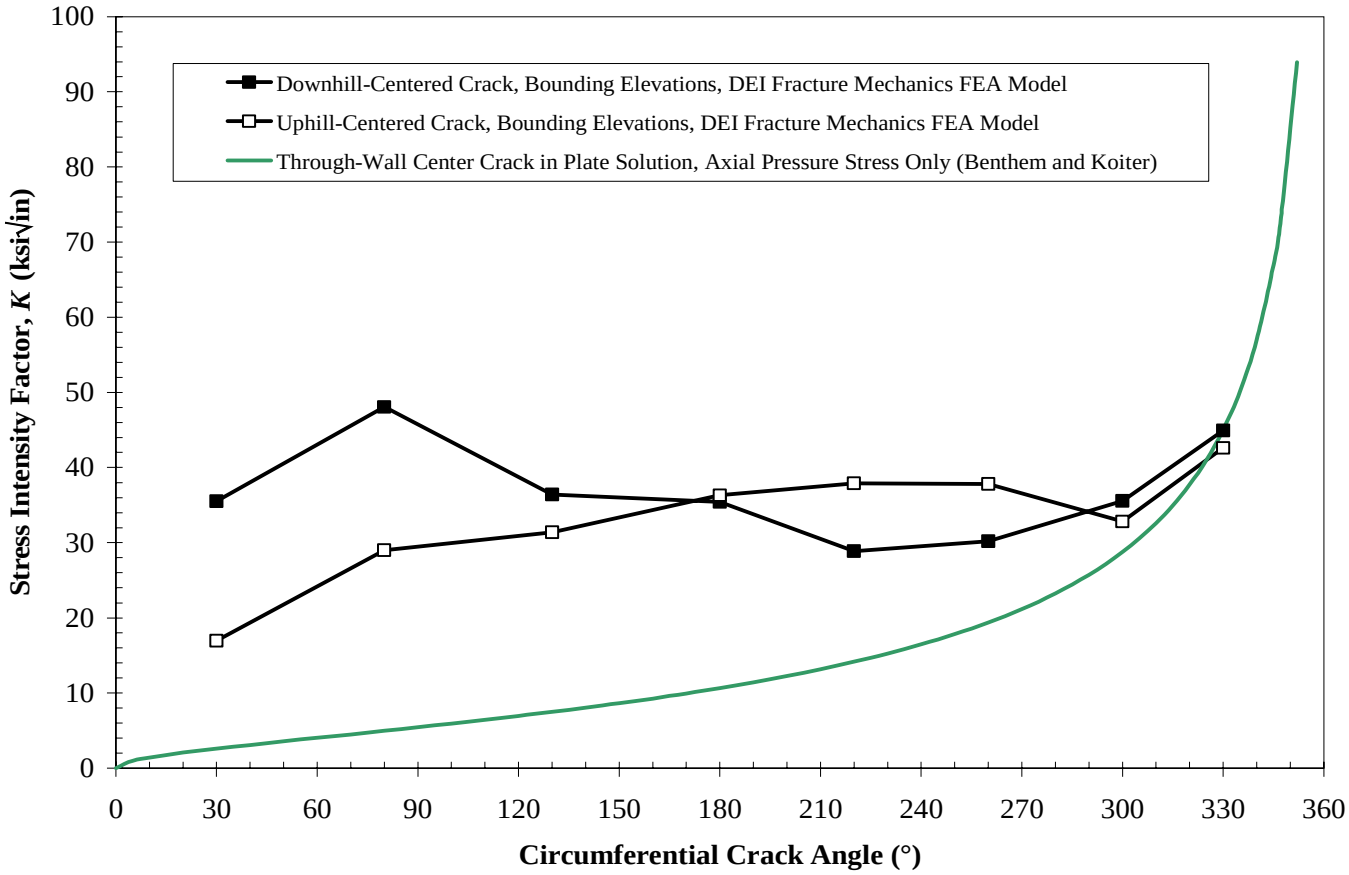

Fracture Mechanics Analyses with Stress Relaxation
Conclusions

- Analysis work shows that stress intensities calculated by superposition without the effect of stress relaxation can be conservative

RPV Penetration Stress Analysis and Fracture Mechanics
Future Efforts

- Continued comparisons of welding residual stress and fracture mechanics model results with others
- New opportunity for comparison between model and as-built results in North Anna RPV head
- Additional fracture mechanics applications:
  - Through-wall axial cracks for wastage analyses
  - J-groove weld cracks for time to grow to leak as well as leak rate calculations

Predicting the First Failure

Roger W. Staehle
Adjunct Professor, University of Minnesota

Vessel Penetration Conference
September 29-October 2, 2003
Washington, D. C.

Objectives and Scope

- Predict the first failure as it occurs in a statistical distribution. The first failure is usually the most important and often cannot be readily obtained
- Predict statistical distribution of SCC *a priori* based on physical variables from prior experience.
- Combine statistical distribution with physical variables of pH, potential, species, alloy composition, alloy structure, temperature, stress.
- Integrate multiple environments and submodes using product of reliabilities.
- Can apply to initiation and propagation.
- Evaluate in environments.

Weibull Distribution (Constant θ, Variable β)

Probability density function

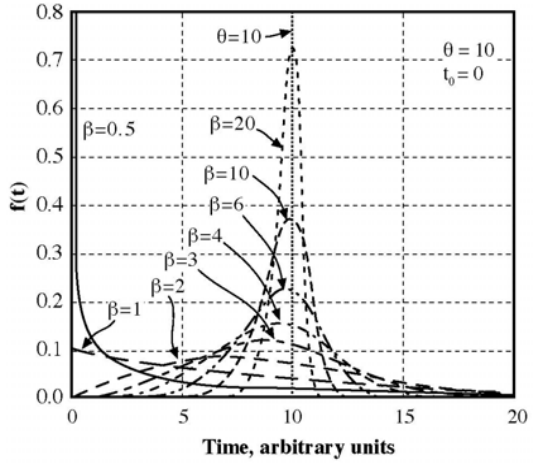

Cumulative distribution function

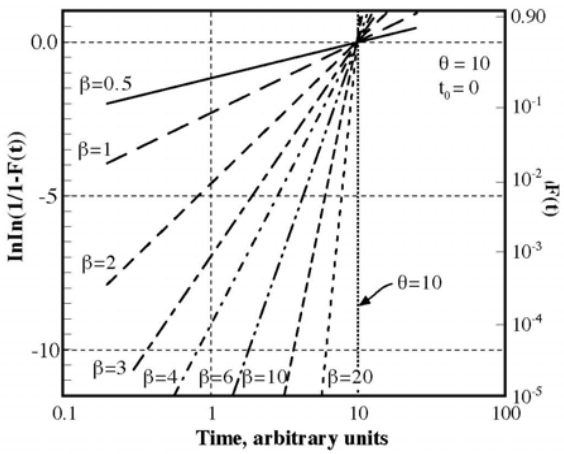

Hazard function

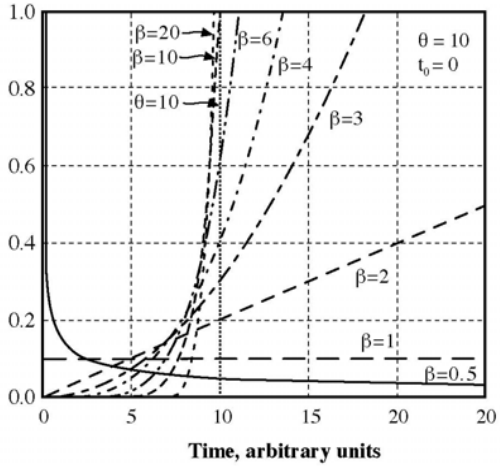

$$f(t)=\left[\frac{\beta}{(\theta-t_o)^{\beta}}\right](t-t_o)^{\beta-1}\exp\left[-\left(\frac{t-t_o}{\theta-t_o}\right)^{\beta}\right],\ t>t_o \quad (1)$$

$$F(t)=P\{t\le t\}=\int_0^t f(t)dt \quad (2)$$

$$F(t)=1-\exp\left[-\left(\frac{t-t_o}{\theta-t_o}\right)^{\beta}\right] \quad (3)$$

$$\ln\left[\ln\left(\frac{1}{1-F(t)}\right)\right]=\beta\left[\ln(t-t_o)-\ln(\theta-t_o)\right] \quad (4)$$

$$h(t)=\frac{f(t)}{1-F(t)} \quad (5)$$

$$h(t)=\left(\frac{\beta}{\theta-t_o}\right)\left(\frac{t-t_o}{\theta-t_o}\right)^{\beta-1}=\frac{\beta}{(\theta-t_o)^{\beta}}(t-t_o)^{\beta-1} \quad (6)$$

θ=Scale parameter
β=Shape parameter
t_o=Location parameter

Magnitudes of cdf Depending on Shape Parameter And Number in Sample

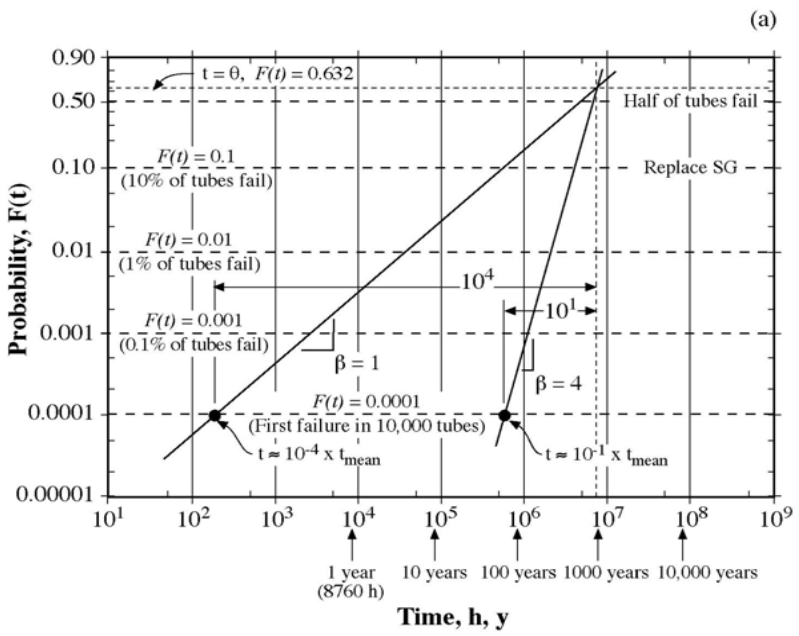

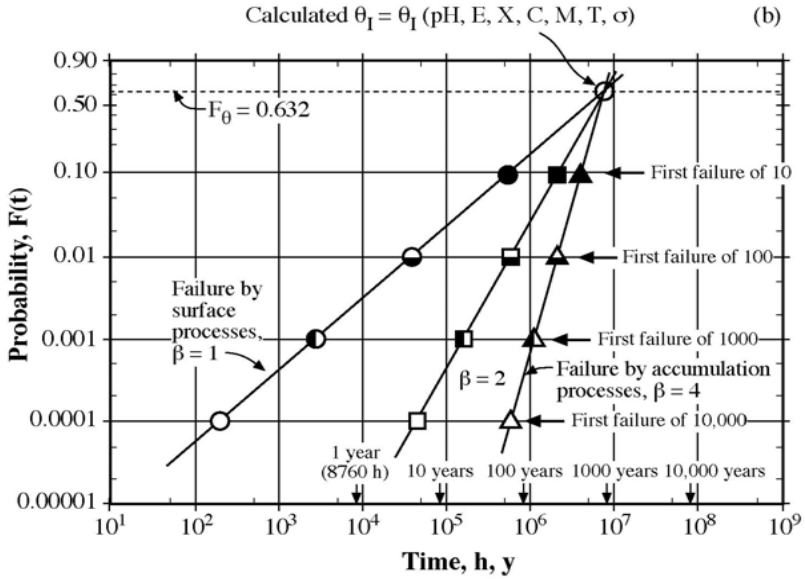

Probability of SCC vs. Time in Large (4 inch diameter) and Small (2 inch diameter) of Welded Stainless Steel Piping in BWR Water (Easton and Shusto)

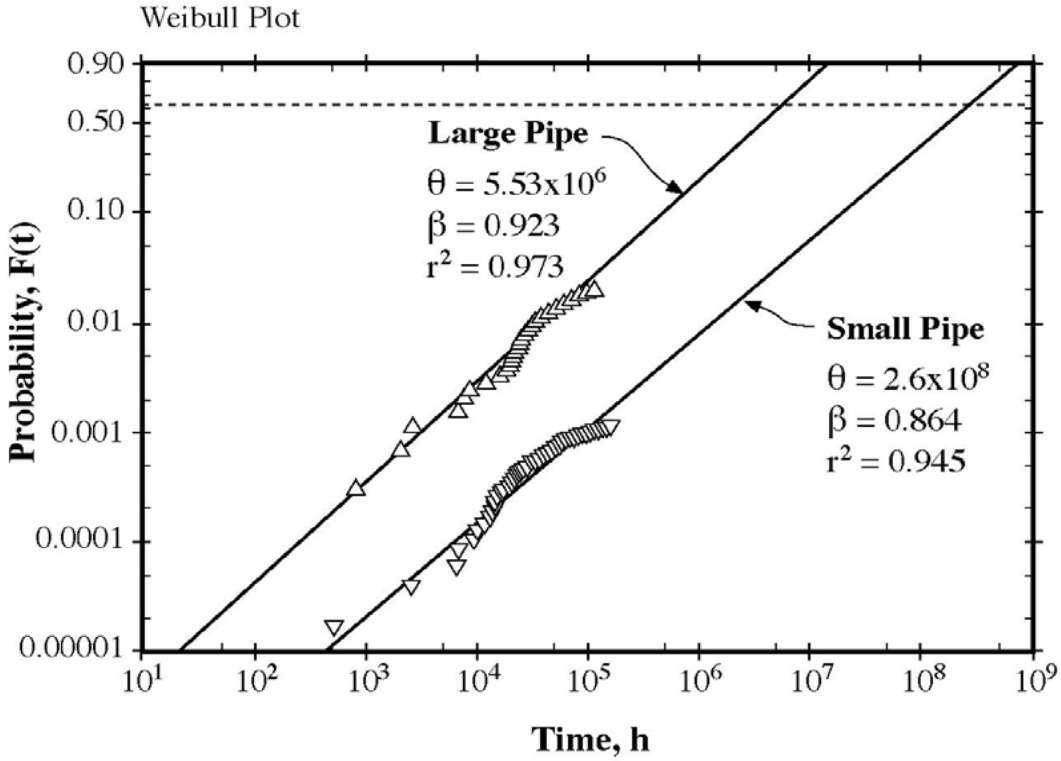

Probability vs. EFPY for Alloy 600 Tubing in Ringhalls-4 PWR Steam Generator (Gorman and Bjornquist)

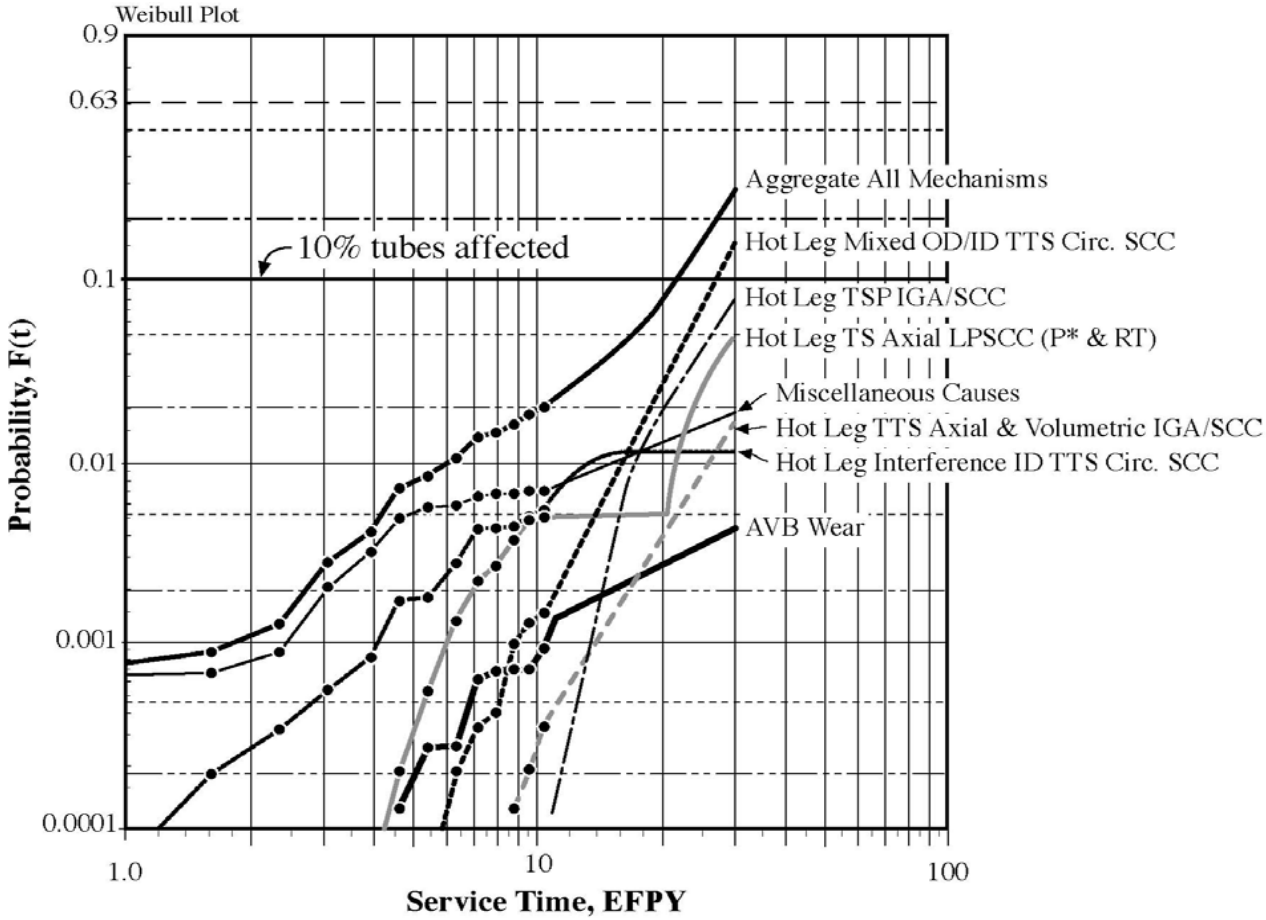

Shape Parameter, β, vs Mean Failure Time in NaCl solutions
Using Sensitized Stainless Steel and No Crevices 30-80°C
(Akashi and Nakayama)

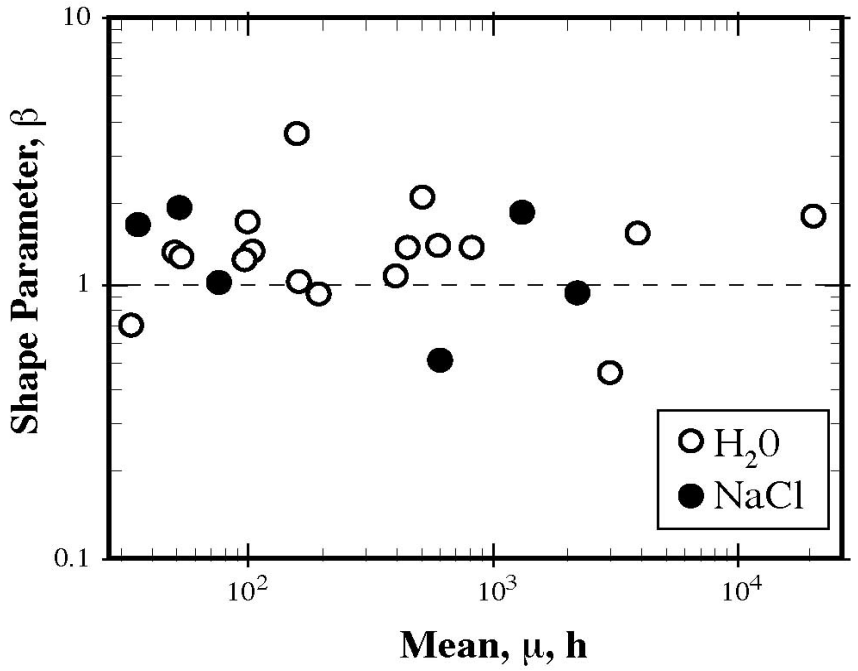

Progressive Development of Prediction from Early Data Using Weibull cdf

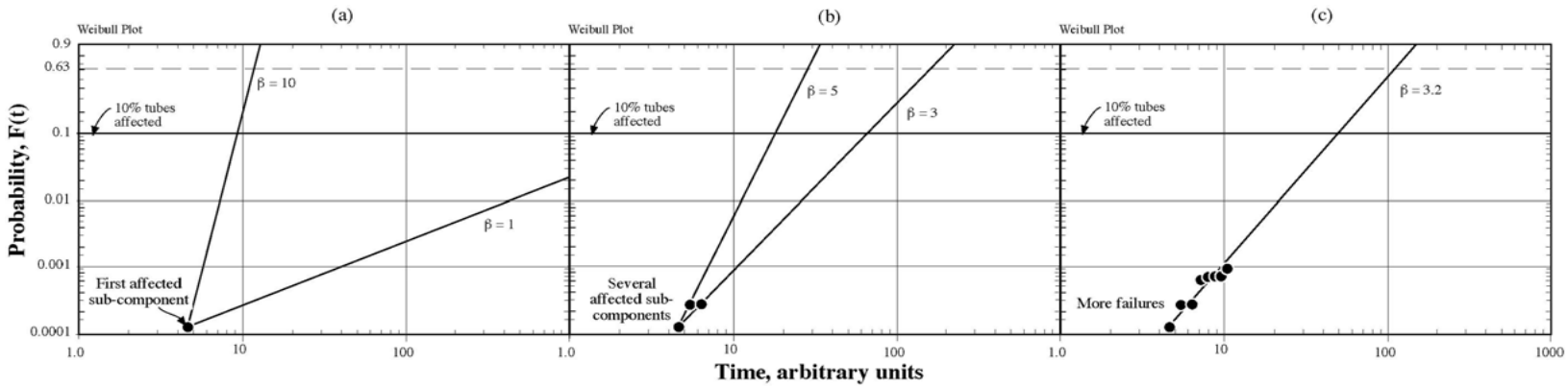

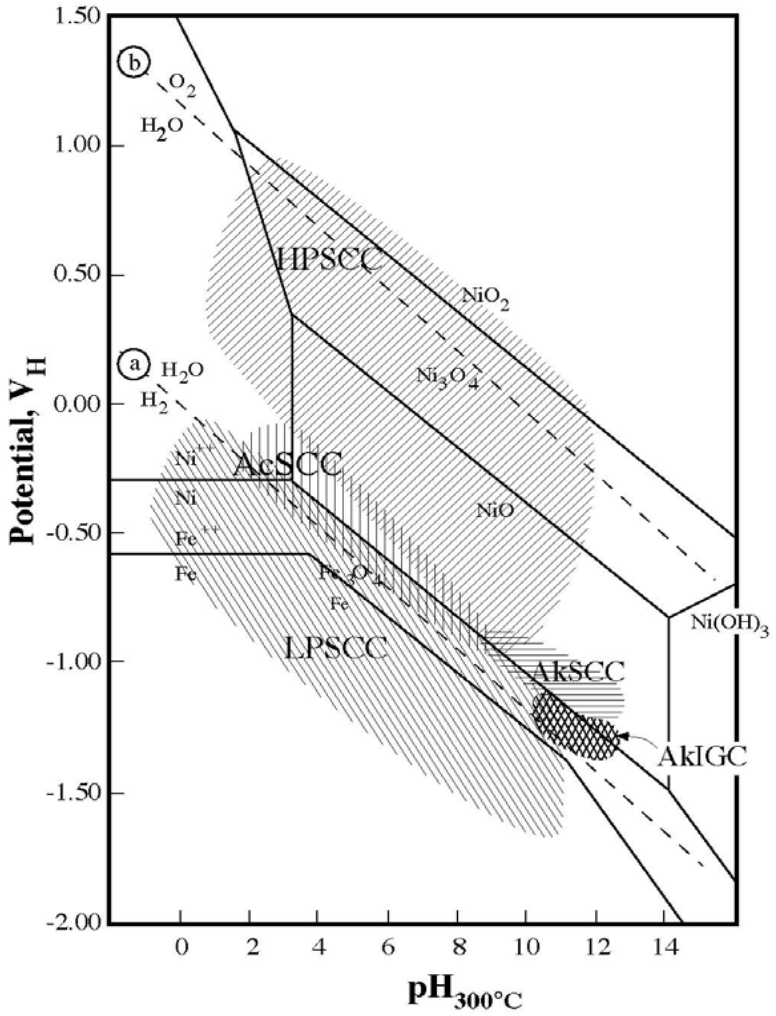

Mode Diagram for SCC of Alloy 600 in 300-350°C Range in Pure Water Applied to PWR Steam Generators

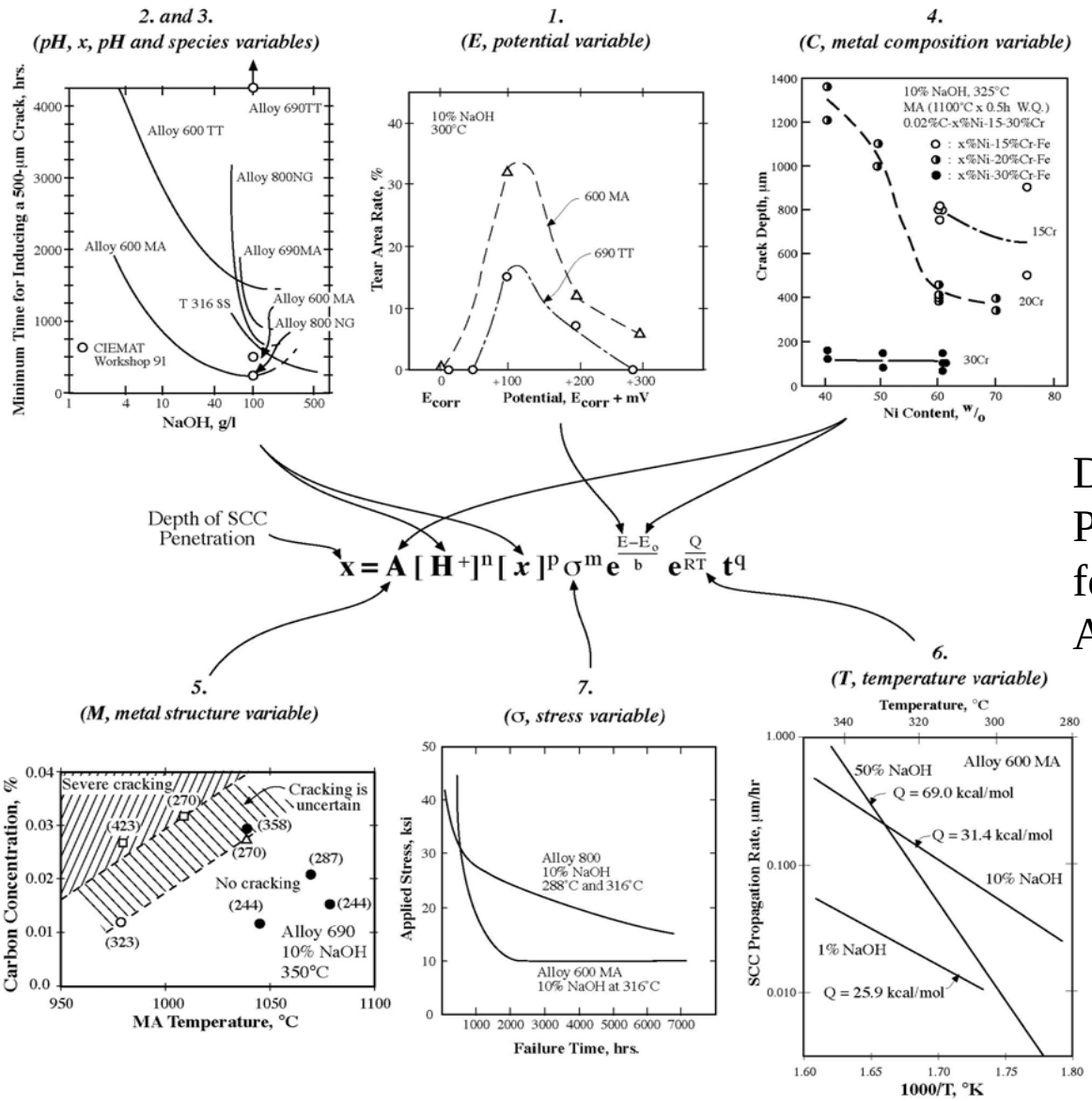

Dependencies of SCC on Primary Variables for Alloy 600 in Alkaline Environments

Nine Stages of SCC

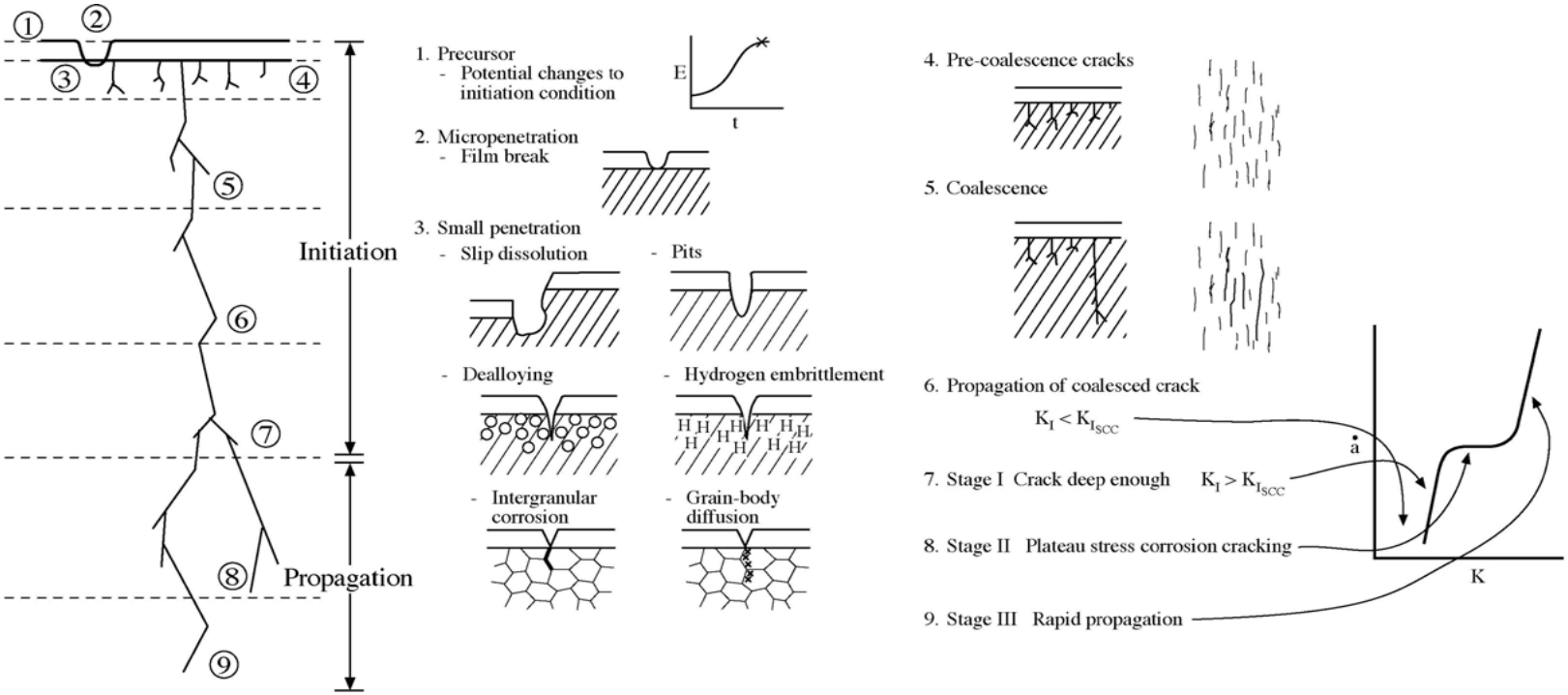

Estimation of Depth of Transition from Initiation to Propagation

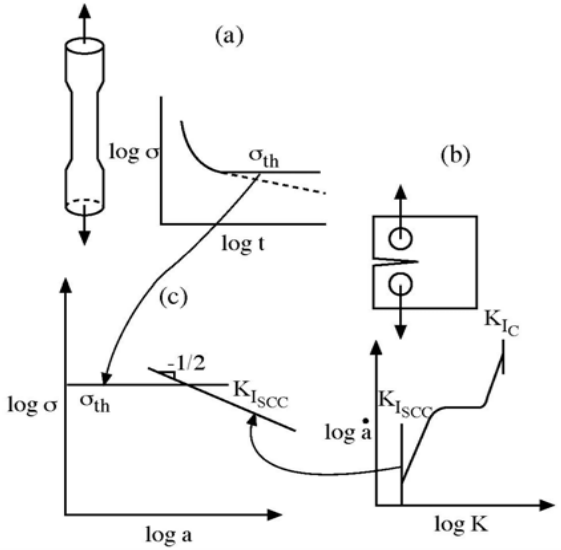

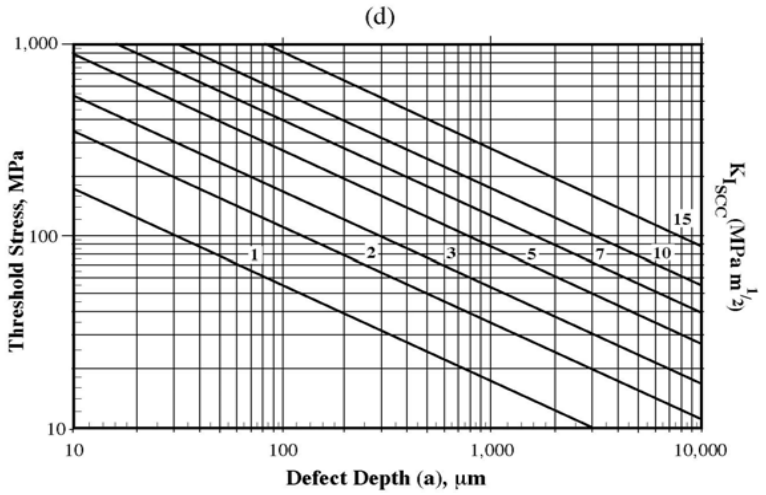

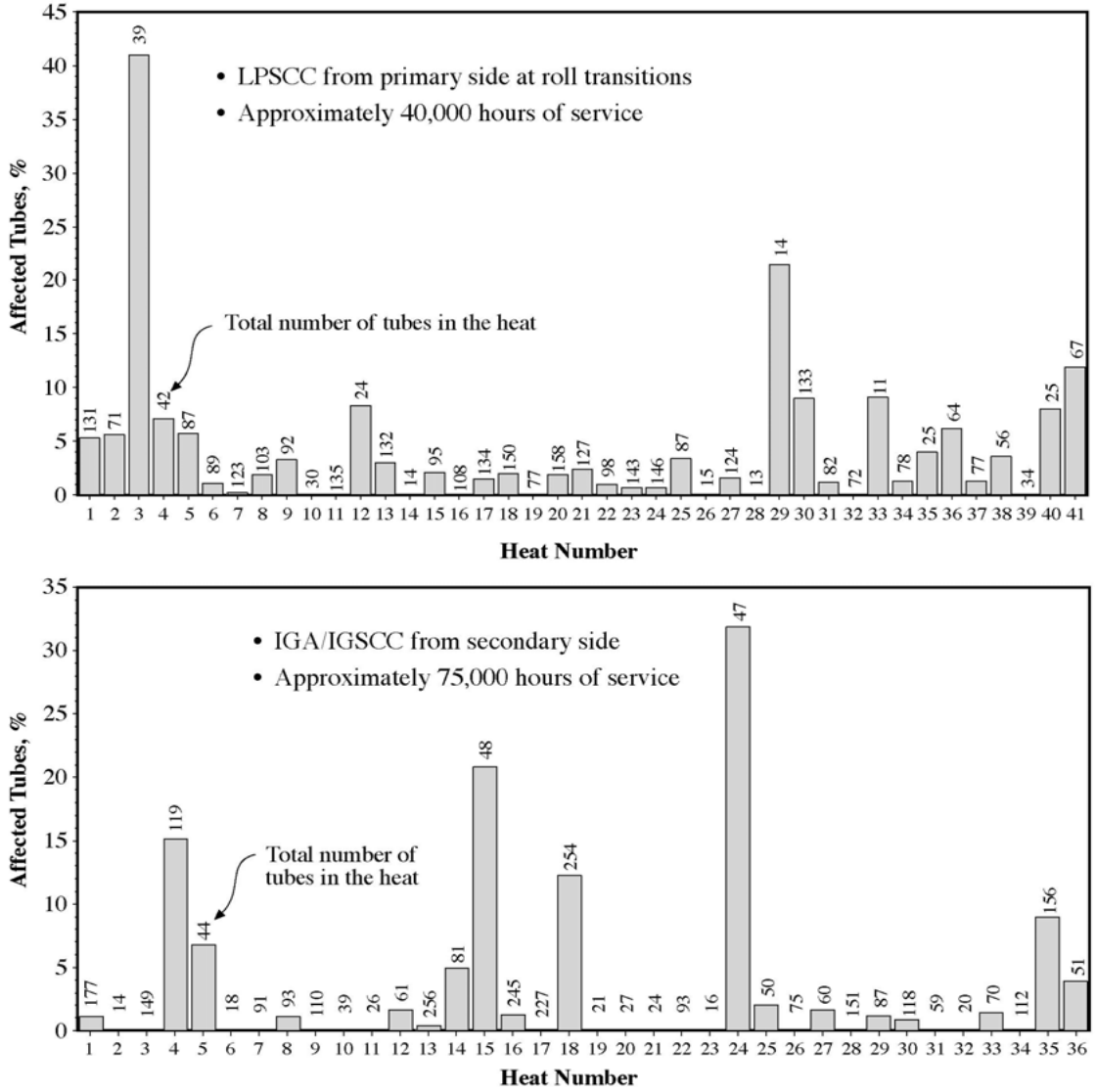

Percent Failure of SG Tubes per Heat for Primary (Upper) and Secondary (Lower) Sides vs.. Heats Produced by Single Manufacturer in Chronological Sequence. (Number of tubes from each heat used shown)

Complexity of Environments in Heat Transfer Crevices

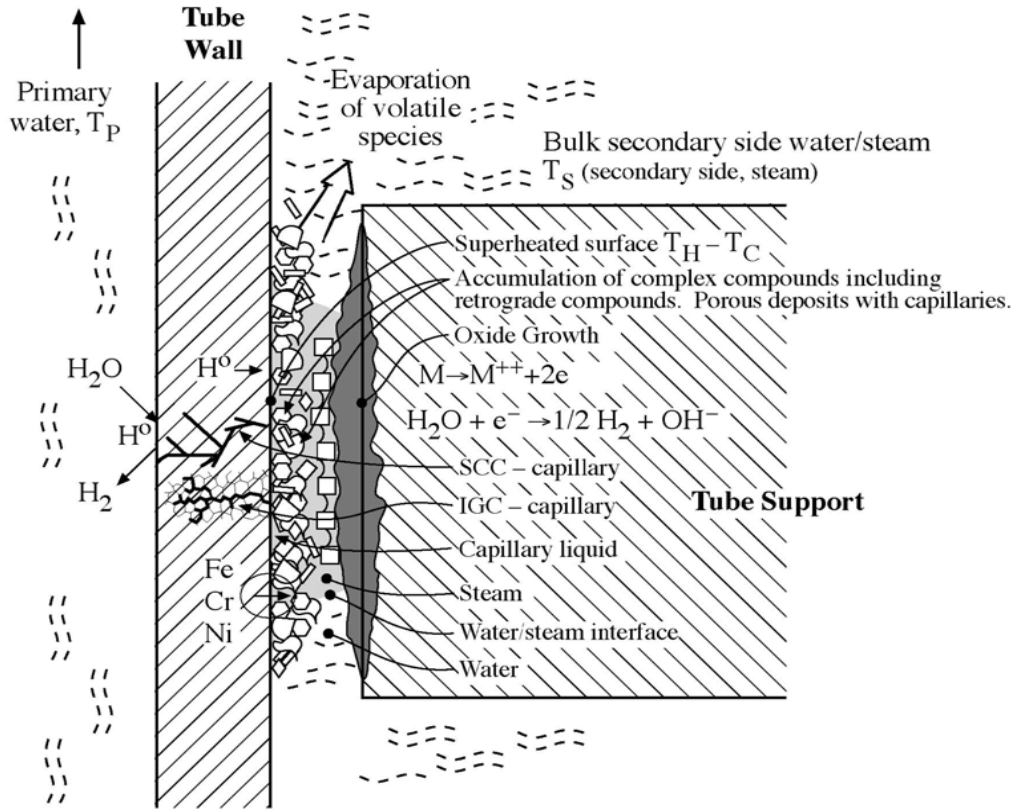

Chemistry, Location, and Depth of Deposits from Heated Crevice from PWR SG (Cattant, Sala)

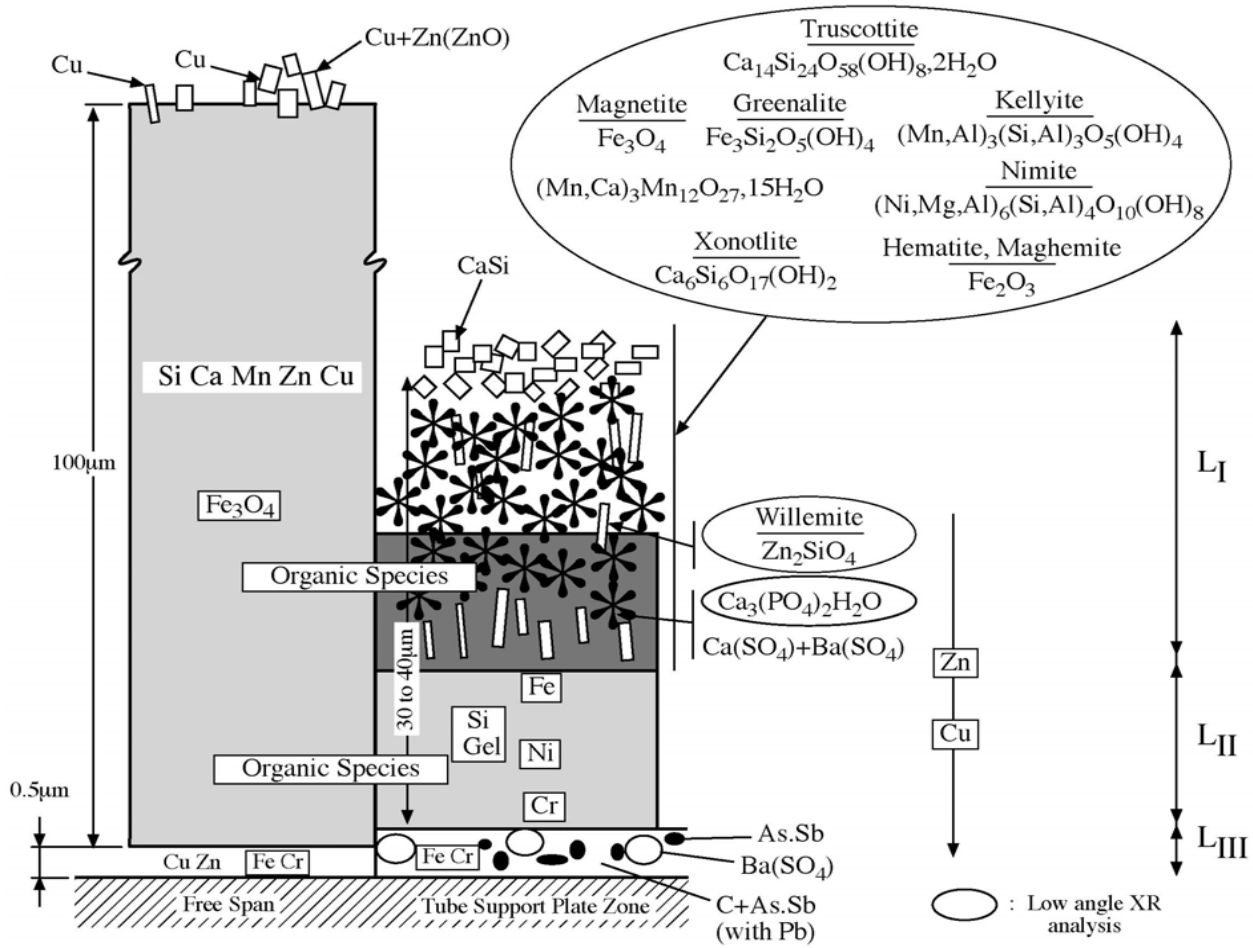

Probability vs. Time for LPSCC of Alloy 600 as a Fuction of Temperature
(Data from Webb, Jacko);
Dependencies of Statistical Parameters on 1/T

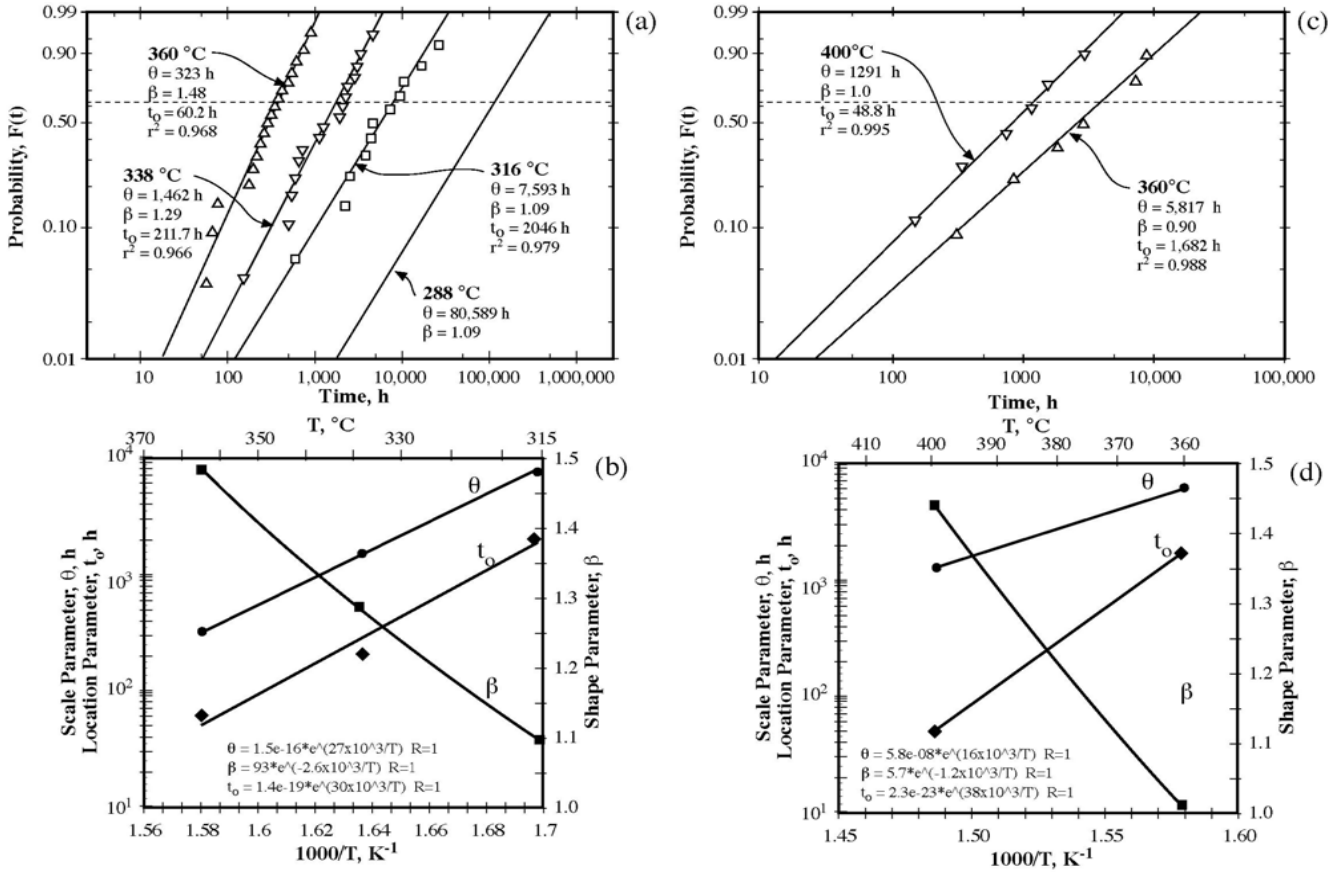

Probability vs. Time as a Function of Stress for Sensitized Type 304 Stainless Steel Exposed at 288°C in Pure Oxygenated Water (Clark and Gordon, Akashi and Ohtomo);
Dependence of Statistical Parameters on Stress

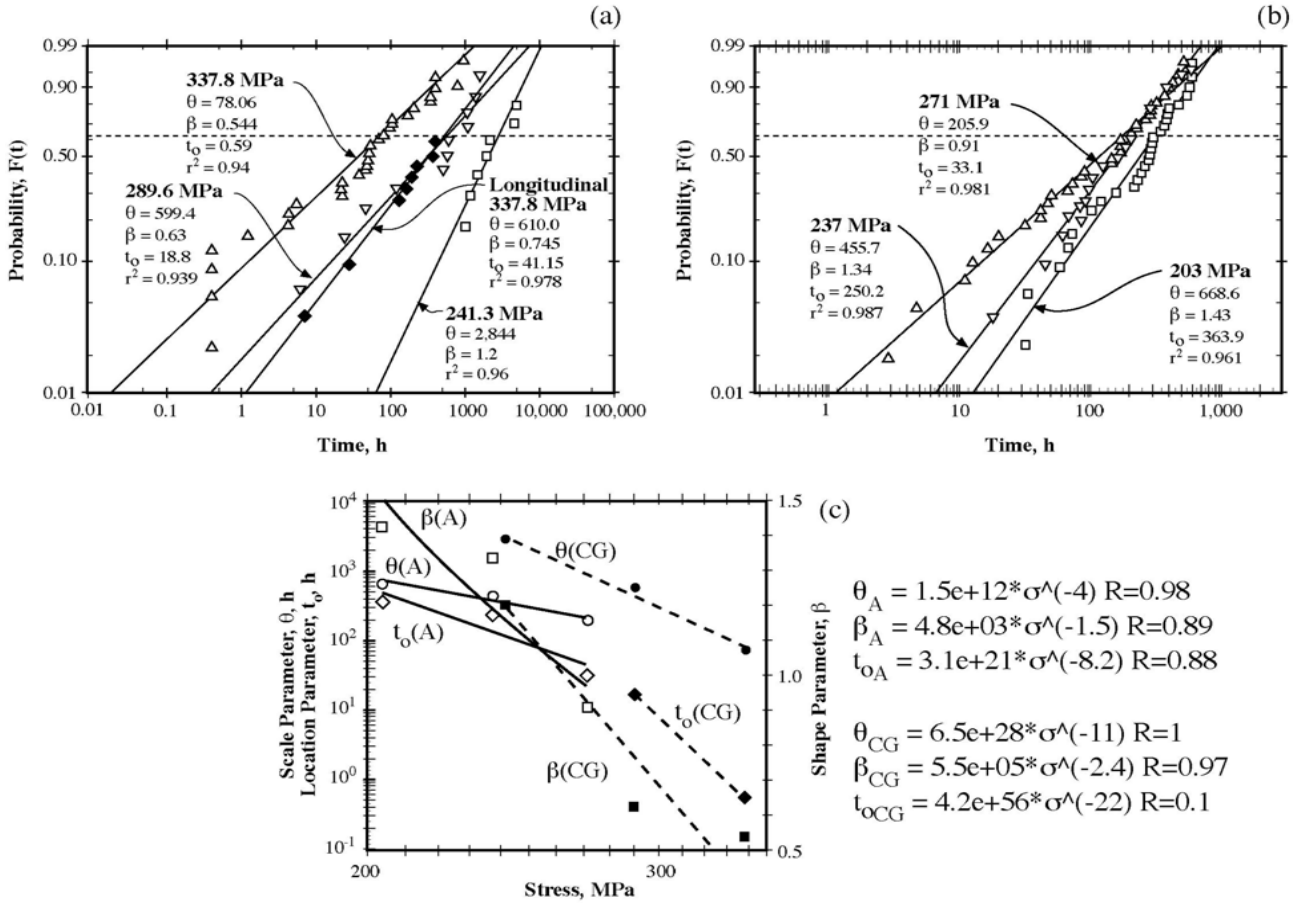

θ_A = 1.5e+12*σ^(-4) R=0.98
β_A = 4.8e+03*σ^(-1.5) R=0.89
t_{oA} = 3.1e+21*σ^(-8.2) R=0.88

θ_{CG} = 6.5e+28*σ^(-11) R=1
β_{CG} = 5.5e+05*σ^(-2.4) R=0.97
t_{oCG} = 4.2e+56*σ^(-22) R=0.1

Probability vs. Time for Stainless Steel in Boiling $MgCl_2$ at 154°C
as a Function of Stress (Shibata and Takeyama, Cochran and Staehle);
Dependence of Statistical Parameters on Stress

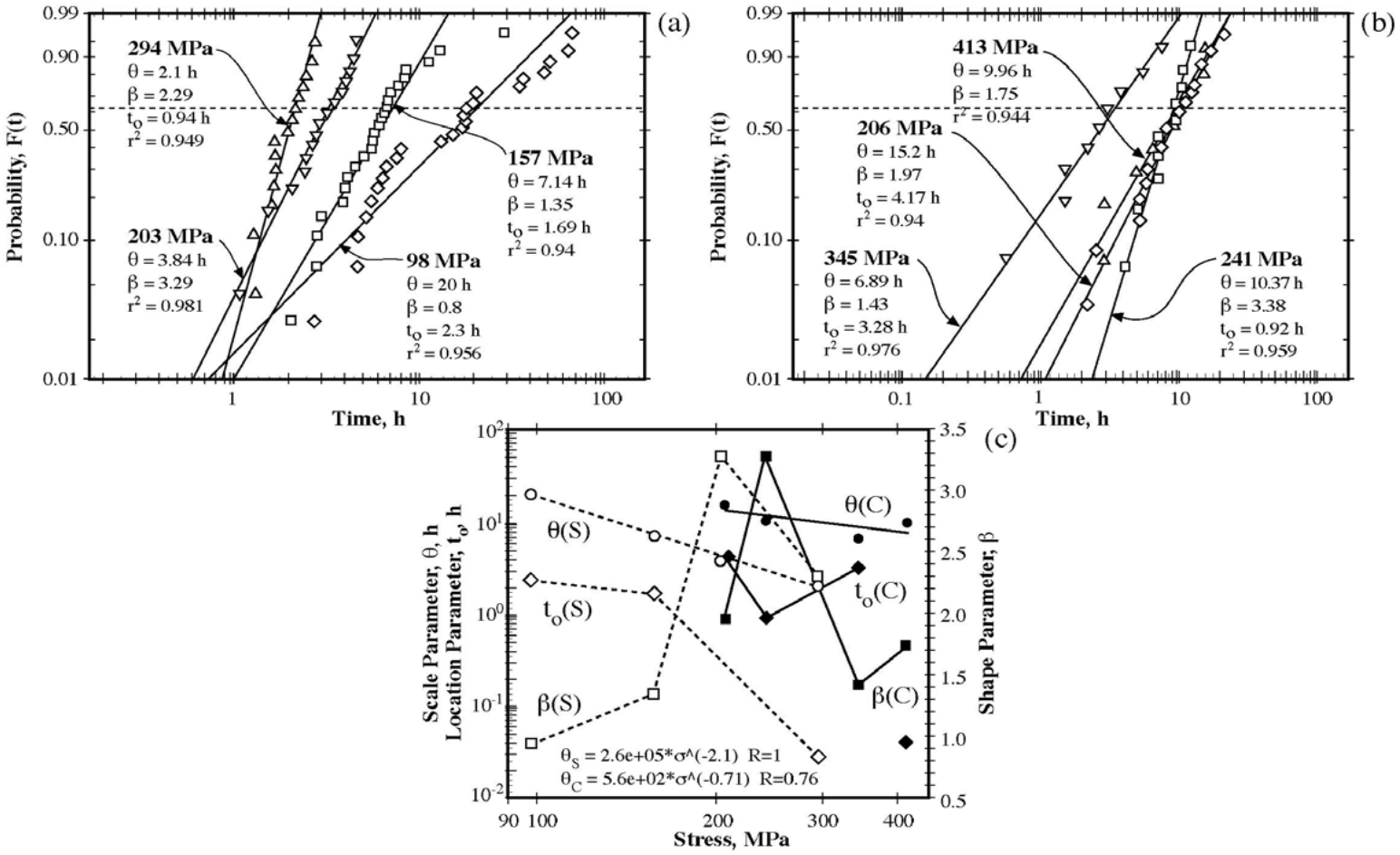

Probability vs. time for SCC ofTtype 304 Exposed to
Dilute and Concentrated Chloride Solutions as a Function of Concentration
(Nakayama et al. 1.75 Sy at 80°C Crevice; Shibata et al. 200MPa at 100°C)
Dependence of Statistical Parameters on Concentration

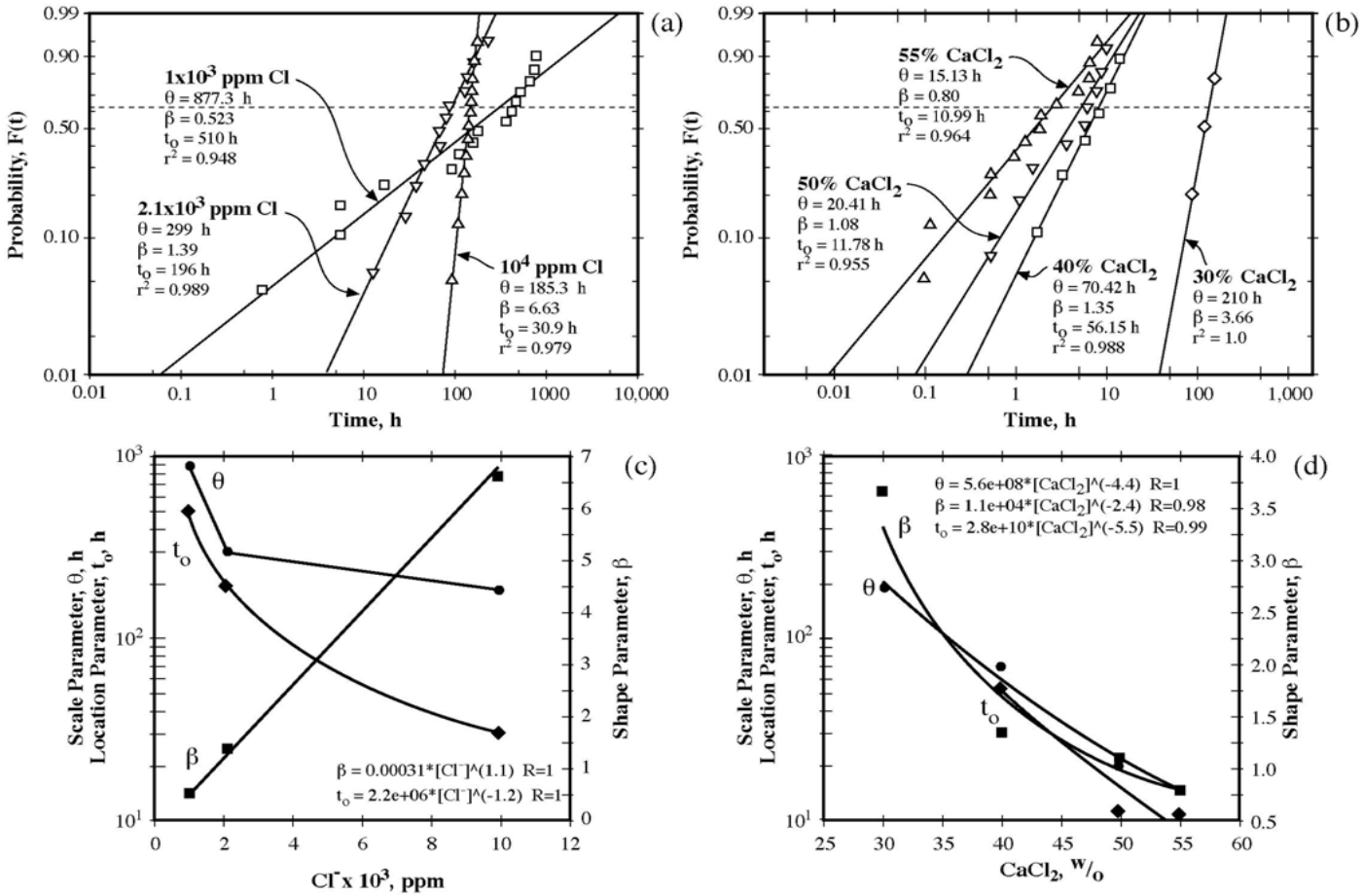

Effects of Physical Conditions on the Shape Parameter;
Comparing Suruface and Time Dependent Processes;
Comparing with Cumulative Distribution and Hazard Function

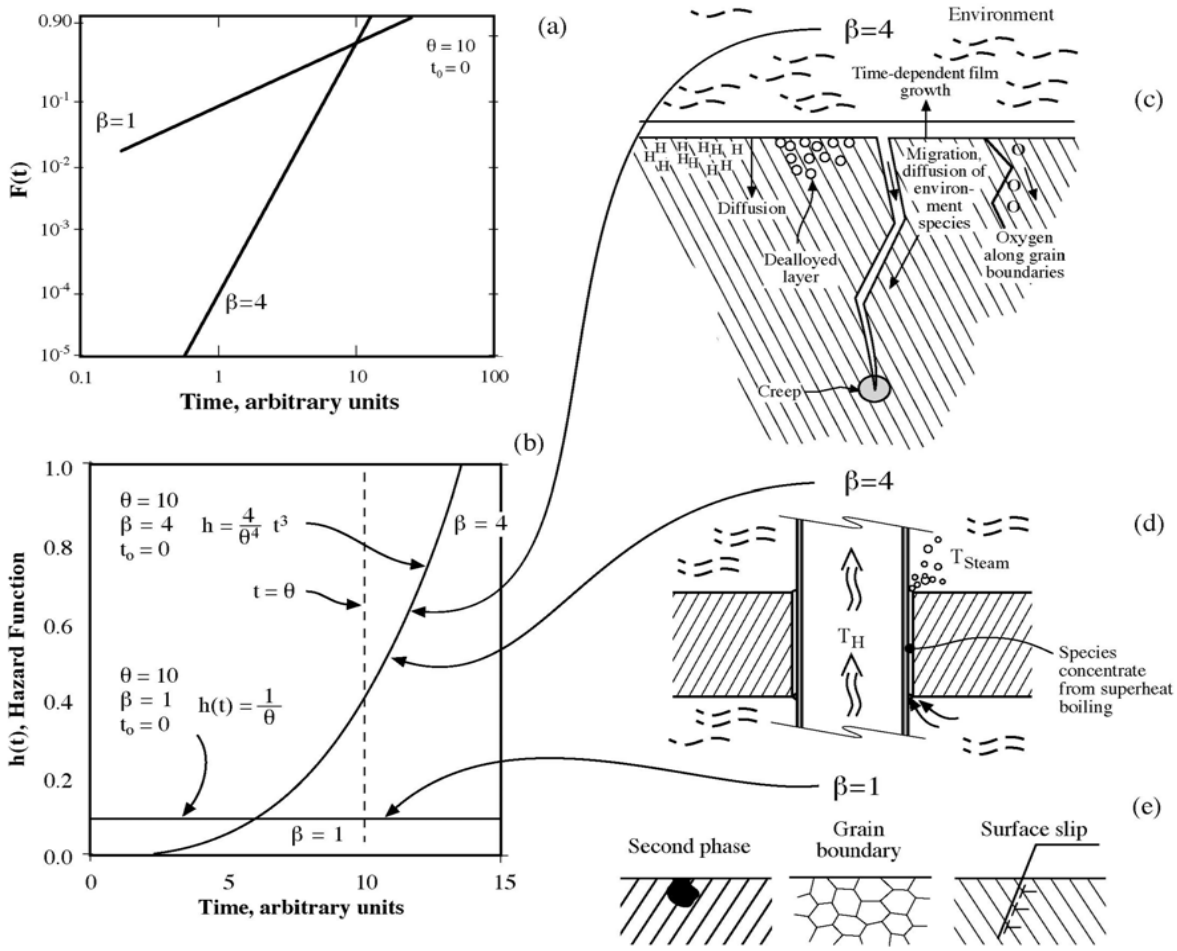

Probability of SCC vs. Time as a Function of Stress for Zircaloy 2 in Iodine Gas at 350°C; Statistical Parameters vs. Hoop Stress (Shimada and Nagai)

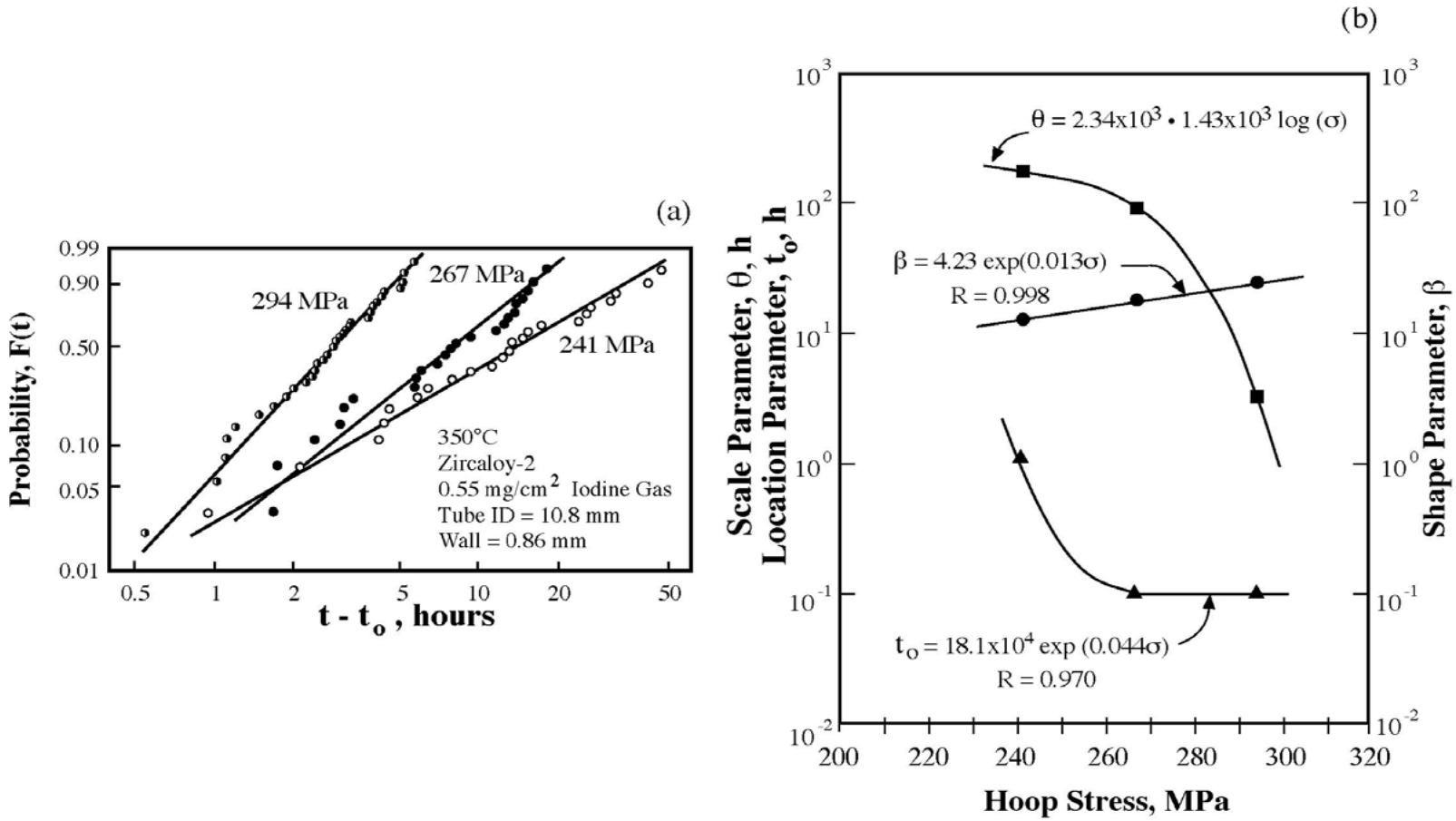

Probability vs. Time for Different Applied Stresses for
Type 304 Stainless Steel Exposed to MgC_{l2} at 154°C;
Shape Parameter vs. Applied Stress (Shibata and Takeyama)

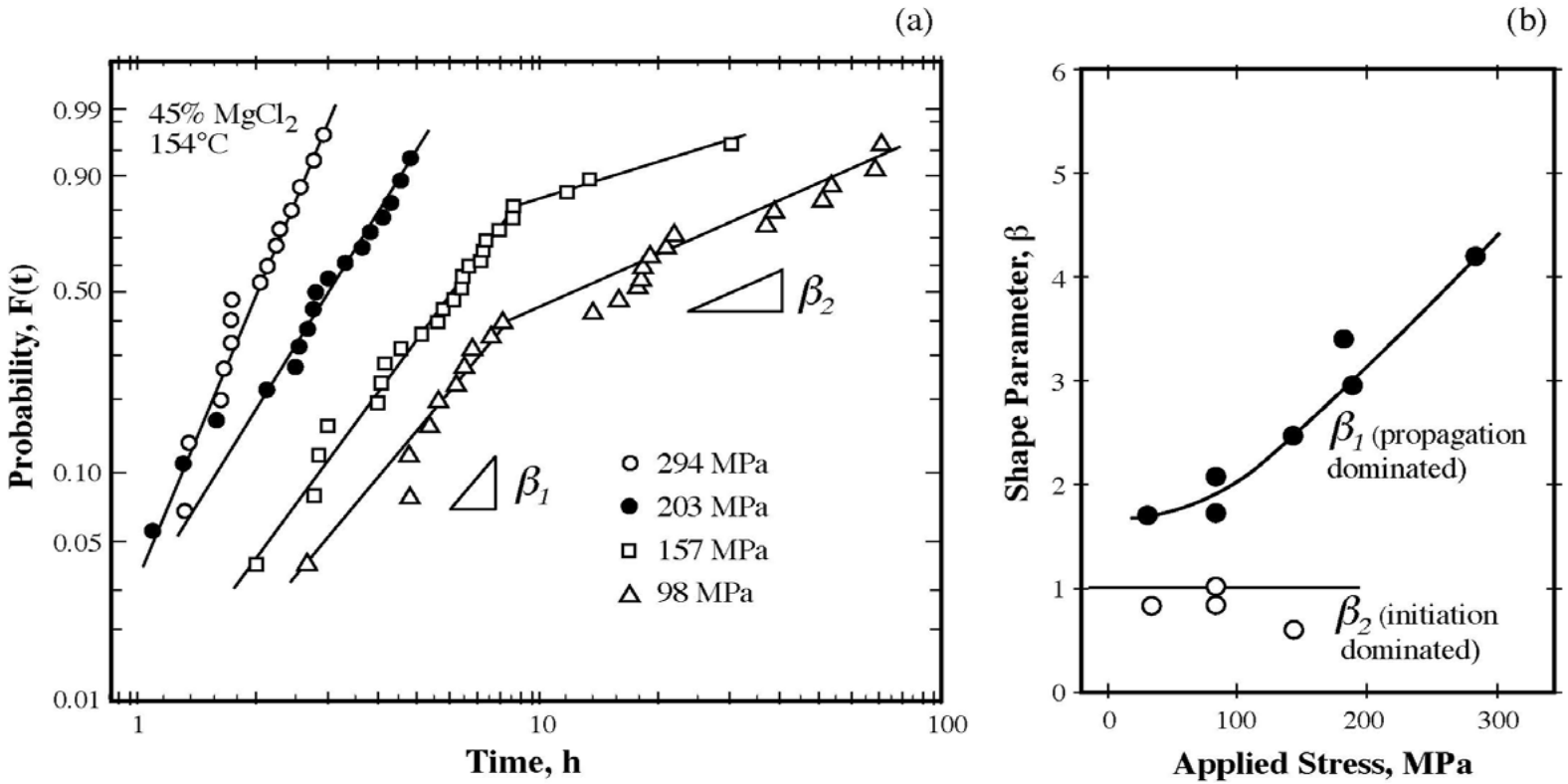

Probability vs. Time for Initiation and Propagation of SCC in a High Strength Steel in 3.5% NaCl at 40°C. (Ichikawa et al.)

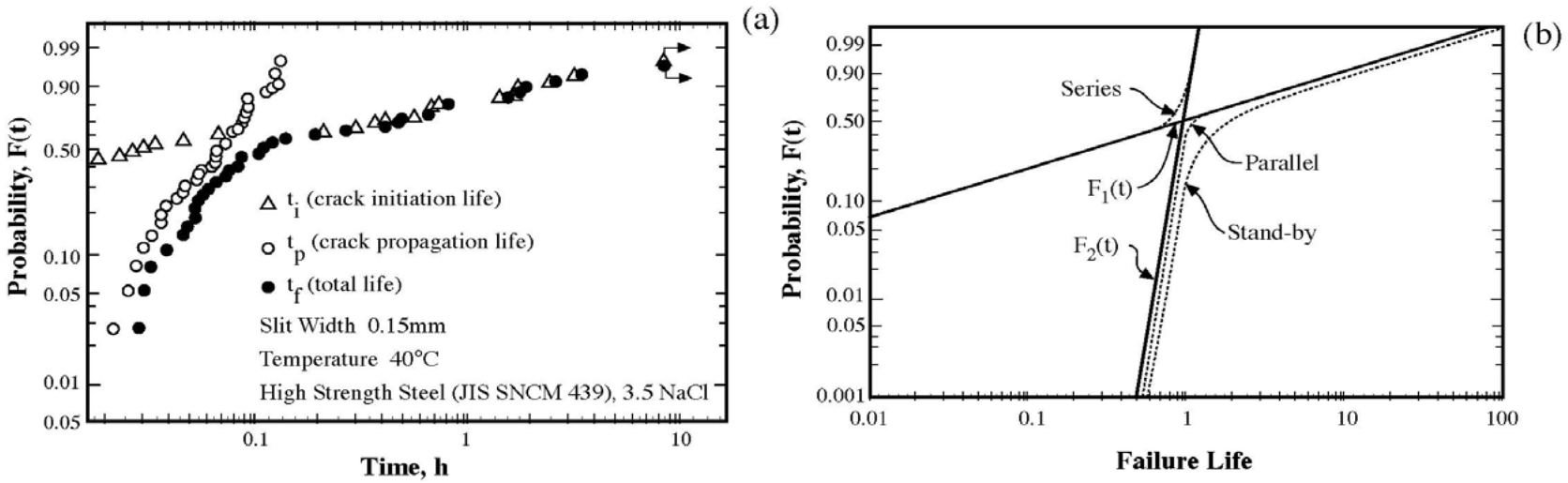

Probability vs. Time for the LPSCC of Alloy 600 in High Purity Water
with Hydrogen Additions Using RUB Specimens at 365°C from Different Heats.
(Estimated Data Points from Norring)
Aggregate of All Specimens

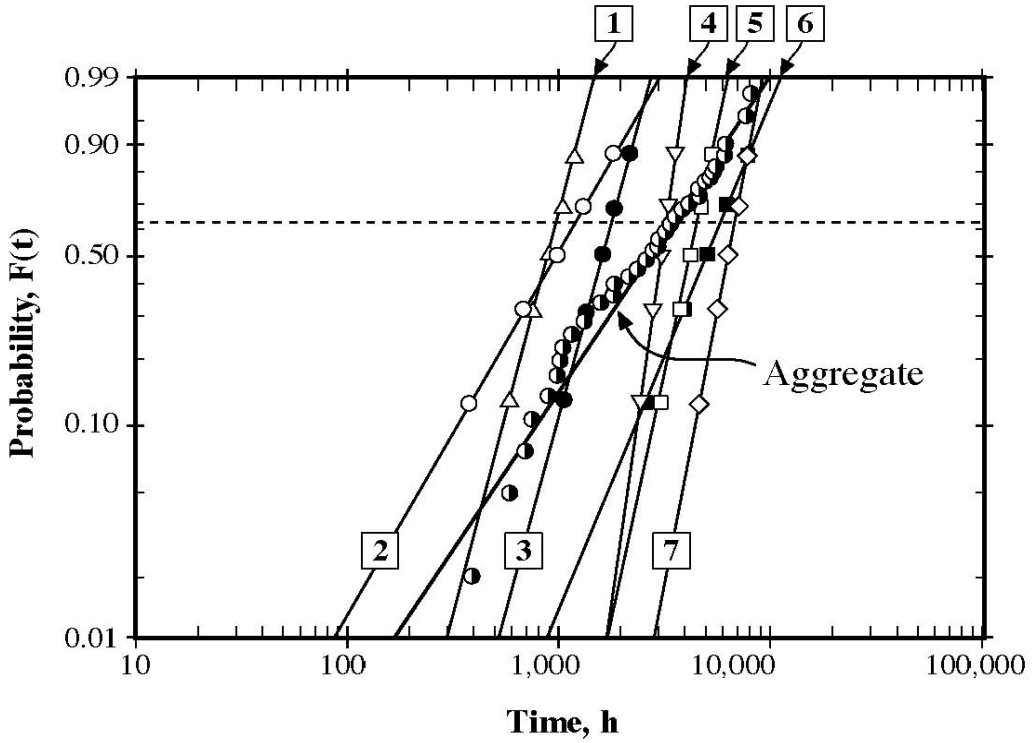

1. **B&W 927 °C**
   θ = 987
   β = 3.84
2. **Ringhalls 2**
   θ = 1,225
   β = 1.73
3. **Alloy 600 MA**
   θ = 1,815
   β = 3.64
4. **Huntington 927 °C**
   θ = 3,225
   β = 7.1
5. **Sandvik 927 °C**
   θ = 4,599
   β = 4.64
6. **Ringhalls 4**
   θ = 6,950
   β = 2.41
7. **Ringhalls 3**
   θ = 6,958
   β = 5.18

Aggregate
θ = 3,509
β = 1.50

Dependence of Shape Parameter on the Ratio of Scale Parameters for Four Assumed Distributions and Constant Initial Shape Factor

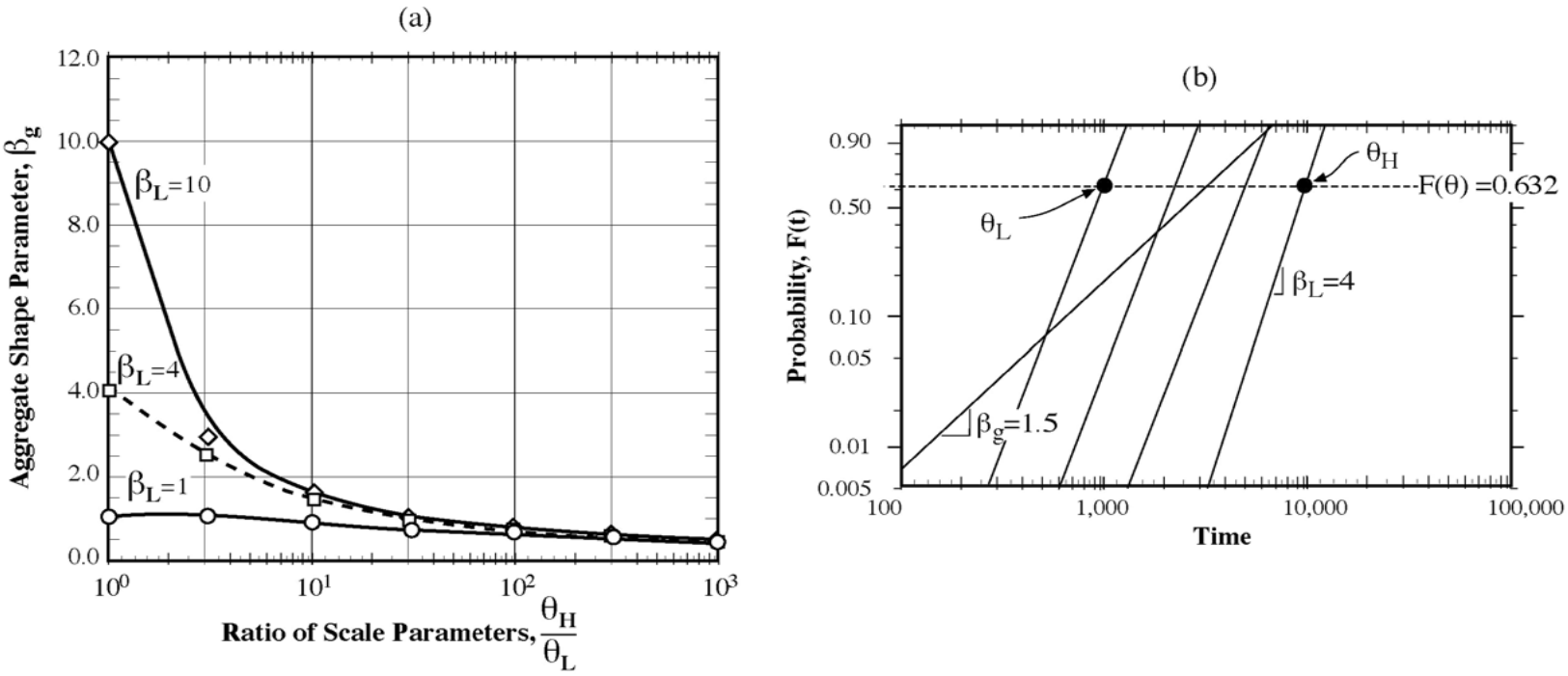

Probability vs. time for SCC of Type 304 Compared with Field Experience for Various Methods of Testing (Sato et al.)

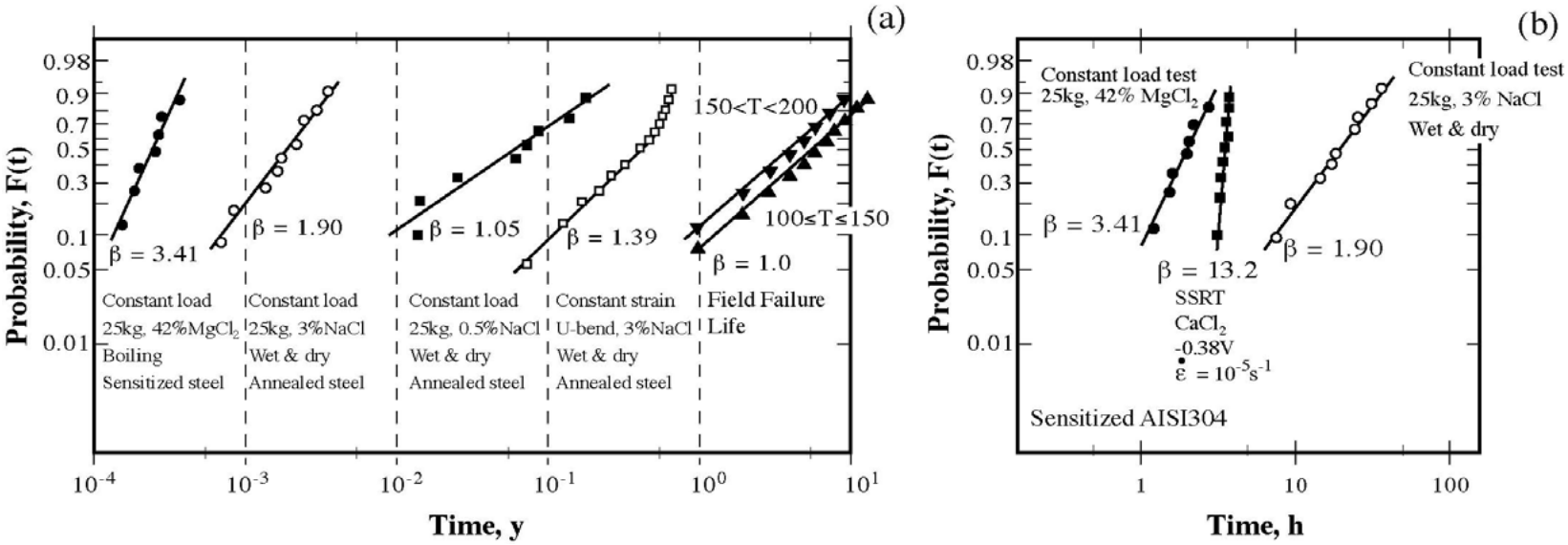

Probability vs. Service Time for Examples of Accelerated Test and Actual Conditions

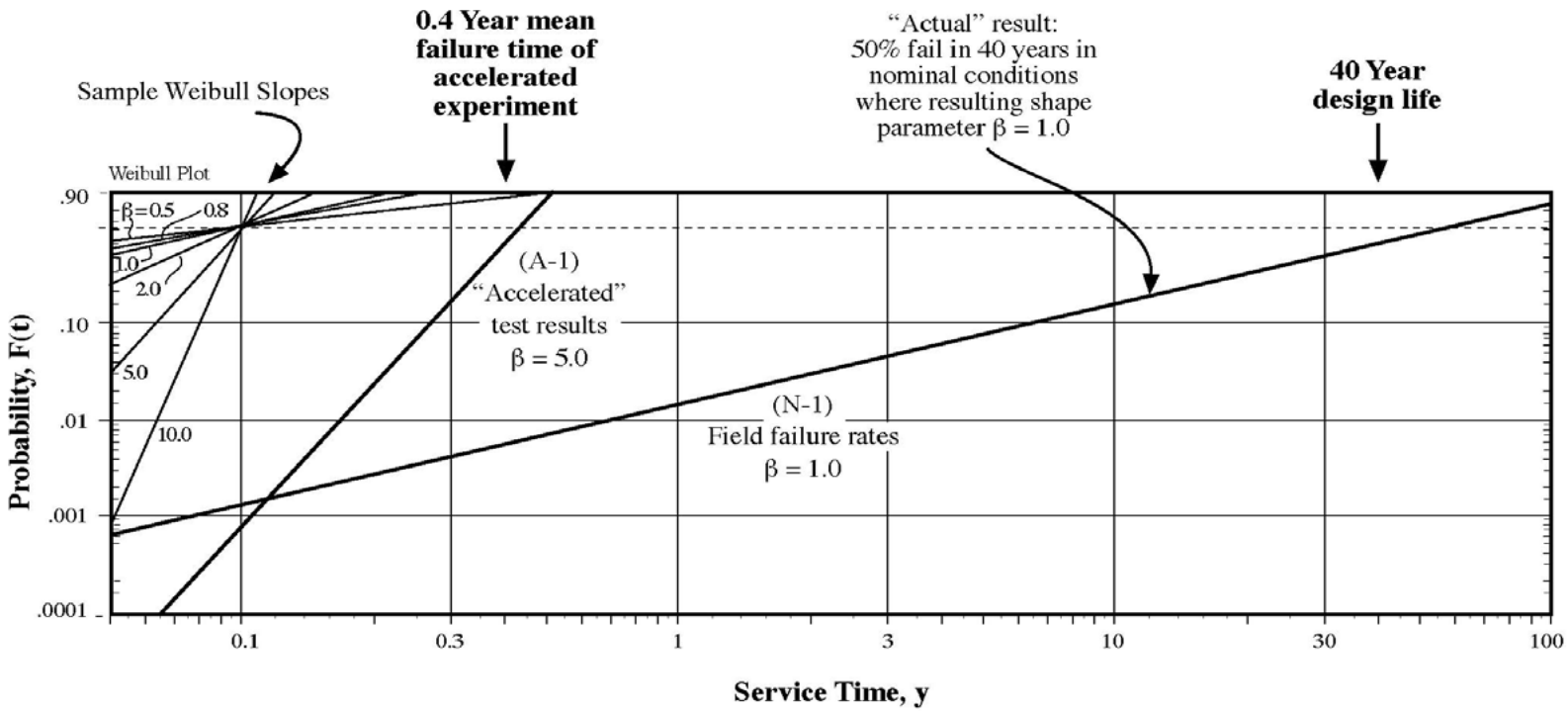

Insert Dependencies on the Seven Primary Variables into Statistical Parameters

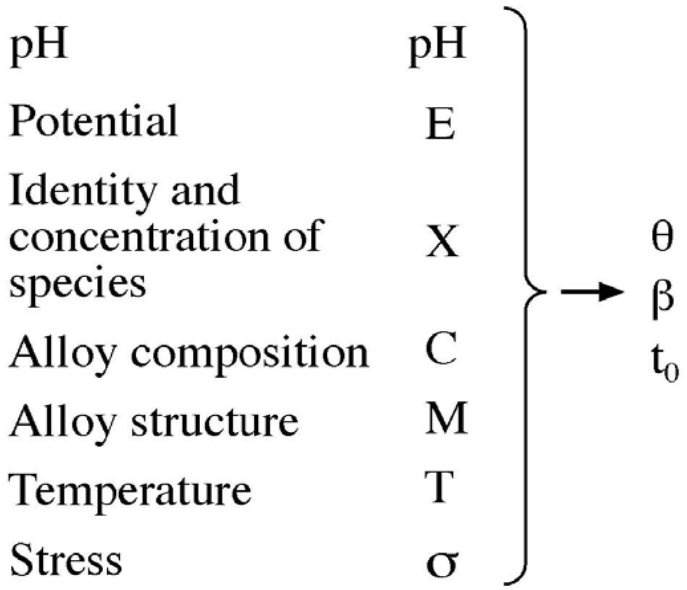

$$\theta, \beta, t_0 = \theta, \beta, t_0\,(E, pH, X, C, M, T, \sigma)$$

$$F(t) = F(\theta, \beta, t_0)$$

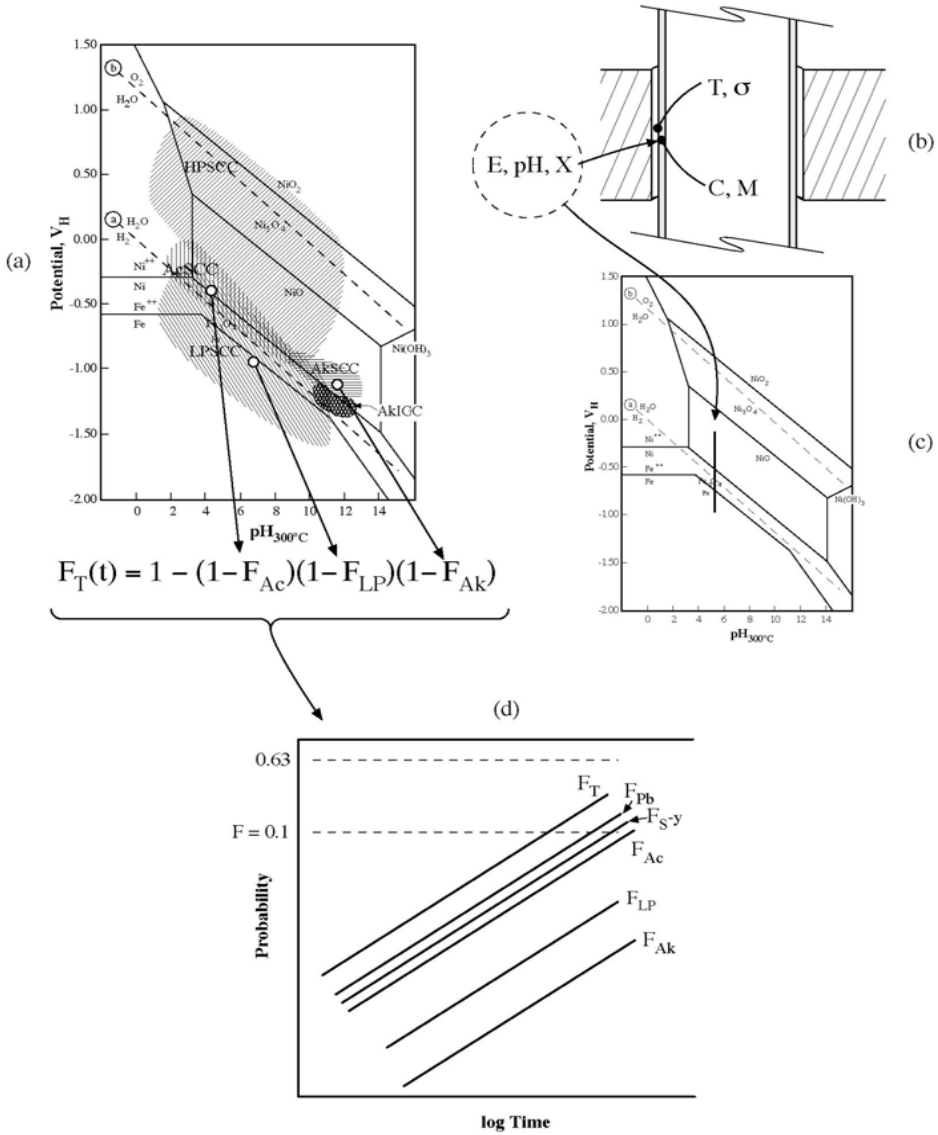

- Evaluate Each of the cdfs of the Submodes for the Dependencies on the Seven Primary Variables;
- Develop the Total Probabililty of Failure from Product of Reliabilities, e.g. $R_T = R_{AkSCC} \times R_{LPSCC} \times R_{AcSCC} \times \ldots$
- Evaluate at Selected Environment.

Conclusions

1. It is possible to predict the occurrence of the first failure by using past experience together with a statistical distribution for which the parameters are evaluated with primary variables.

2. This methods enables predicting the occurrence of first failures that do not occur at the same conditions as previous ones.

3. This method enables accounting for the multiple sets of submodes that may occur.

4. There are naturally difficulties of interactions of variables in this approach; however, a first approach is probably much more useful than nothing.

Elevated Temperature Grain Boundary Embrittlement and Ductility-Dip Cracking in Ni-base Weld Metals

John C. Lippold
The Ohio State University

Welding and Joining Metallurgy Group

Conference on Vessel Penetration Inspection, Cracking, and Repairs
September 29-October 2, 2003, Gaithersburg, MD

Weldability Issues with Austenitic Materials

Cracking Mechanism	Location	Factors that Promote
Solidification Cracking	Solidification Grain Boundary	Impurity segregation Continuous liquid films
Weld Metal Liquation Cracking	Solidification Grain Boundary Migrated Grain Boundary	Impurity segregation Large grain size High heat input
Ductility-Dip Cracking	Migrated Grain Boundary	Large grain size Grain boundary mobility
Reheat, or Strain-age, Cracking	Migrated Grain Boundary	Relaxation of residual stress Intragranular precipitation Impurity segregation
Copper-Contamination Cracking	Migrated Grain Boundary	Cu abraded on surface Temperature > 1093°C
Hydrogen-Assisted Cracking	Migrated Grain Boundary	Grain boundary precipitation Threshold H concentration

Weld Metal Boundaries

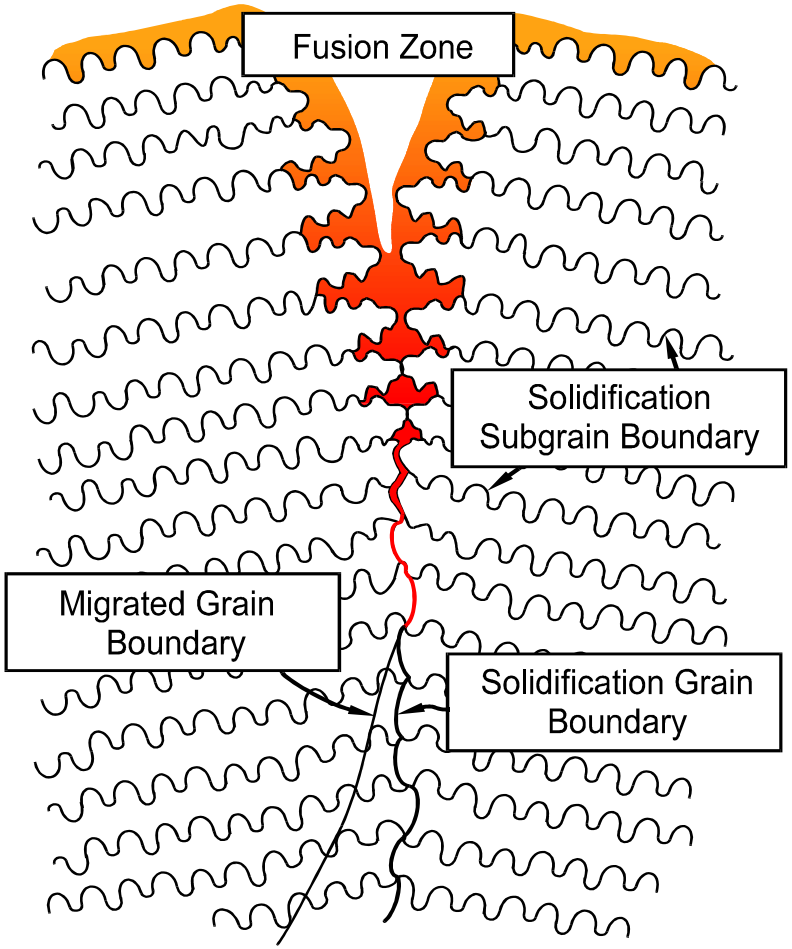

- **Differentiated by**
  - **Composition**
  - **Structure**
- **Solidification subgrain boundaries (SSGBs)**
  - **Composition (Case 2)**
  - **Low angle misorientation**
- **Solidification grain boundaries (SGBs)**
  - **Composition (Case 3)**
  - **High or low angle misorientation**
- **Migrated grain boundaries (MGBs)**
  - **Local variation in composition**
  - **High angle misorientation**

Solidification Grain Boundary

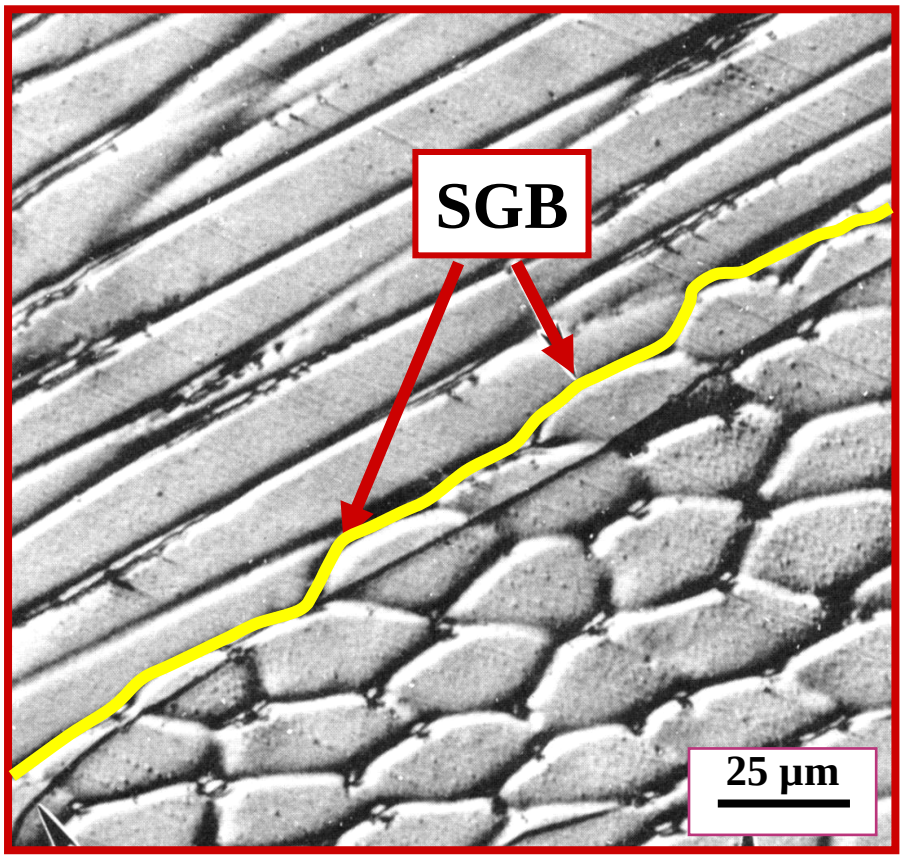

- Boundary between packets of subgrains
- Results from competitive growth
- Composition dictated by Case 3 solute redistribution
- Large misorientation across boundary at end of solidification - high angle boundary
- Most likely site for solidification cracking

Migrated Grain Boundary

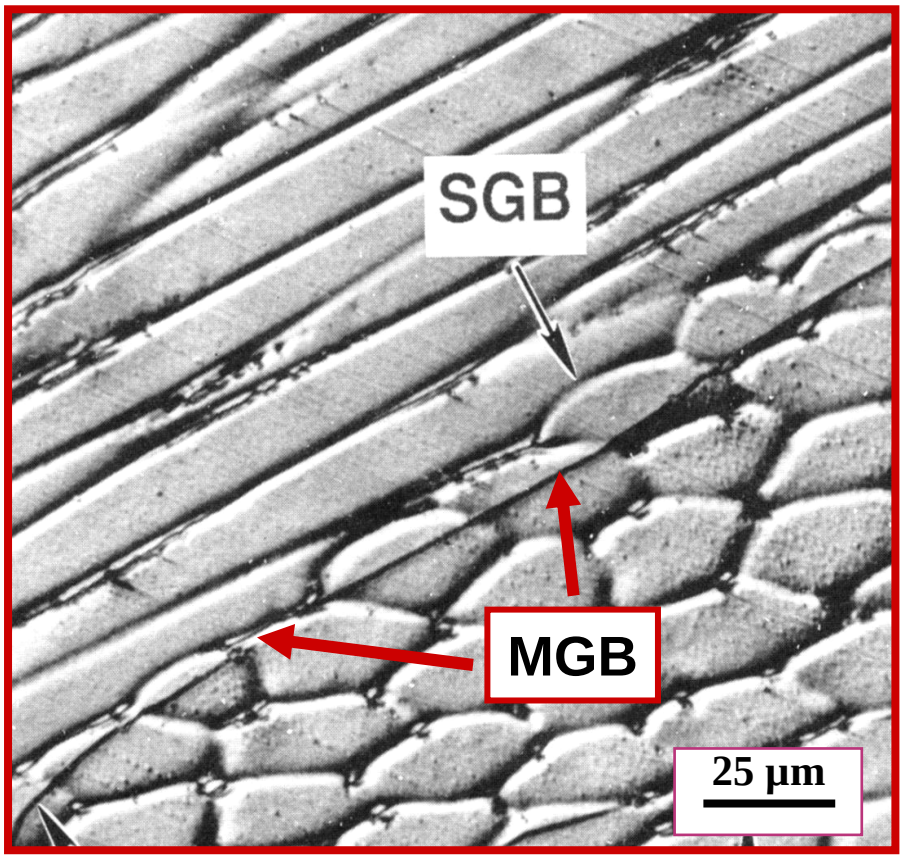

- Crystallographic component of SGB
- Migrates away from SGB in the solid state following solidification or during reheating
- Large misorientation across boundary - high angle boundary
- Composition varies locally
- Possible boundary “sweeping” and segregation
- Liquation and ductility dip cracking

Migrated Grain Boundaries in Filler Metal 82

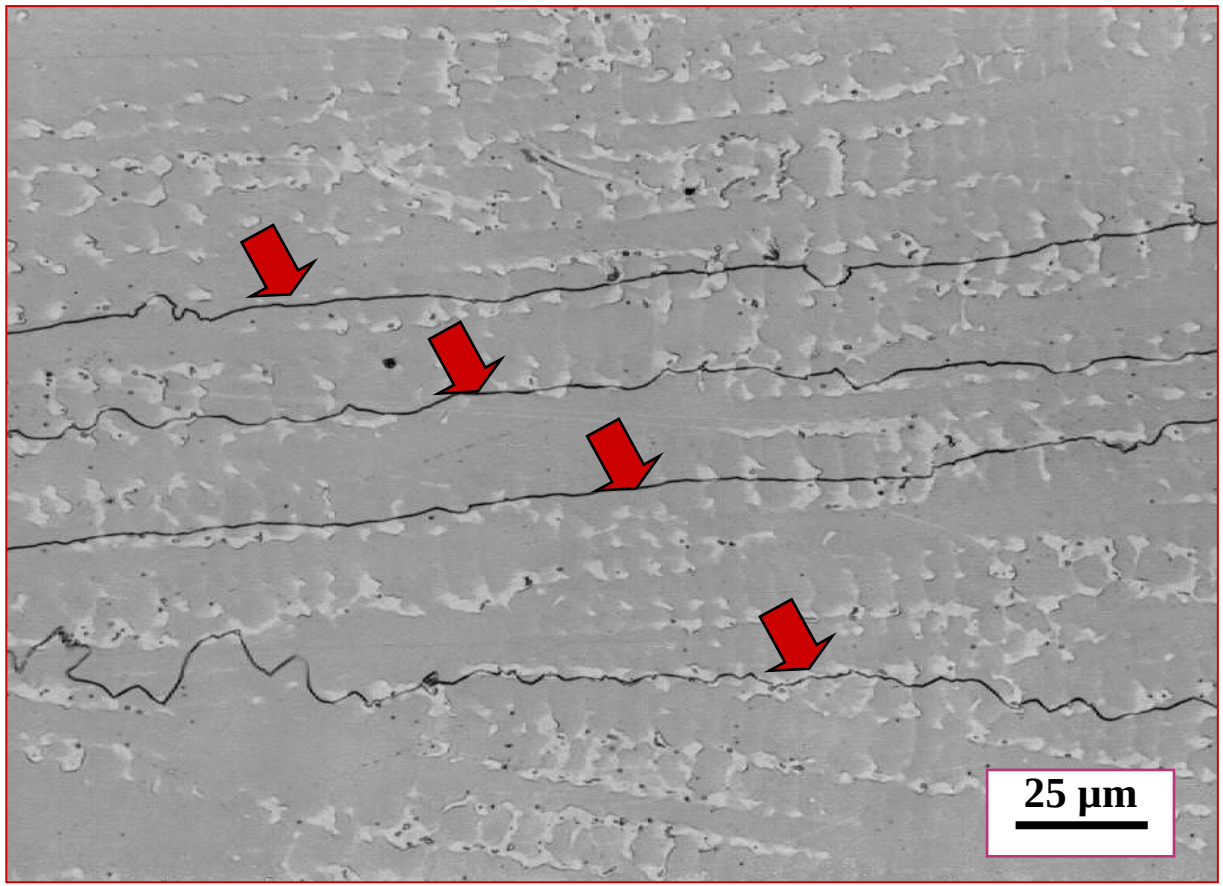

Ductility-dip Cracking

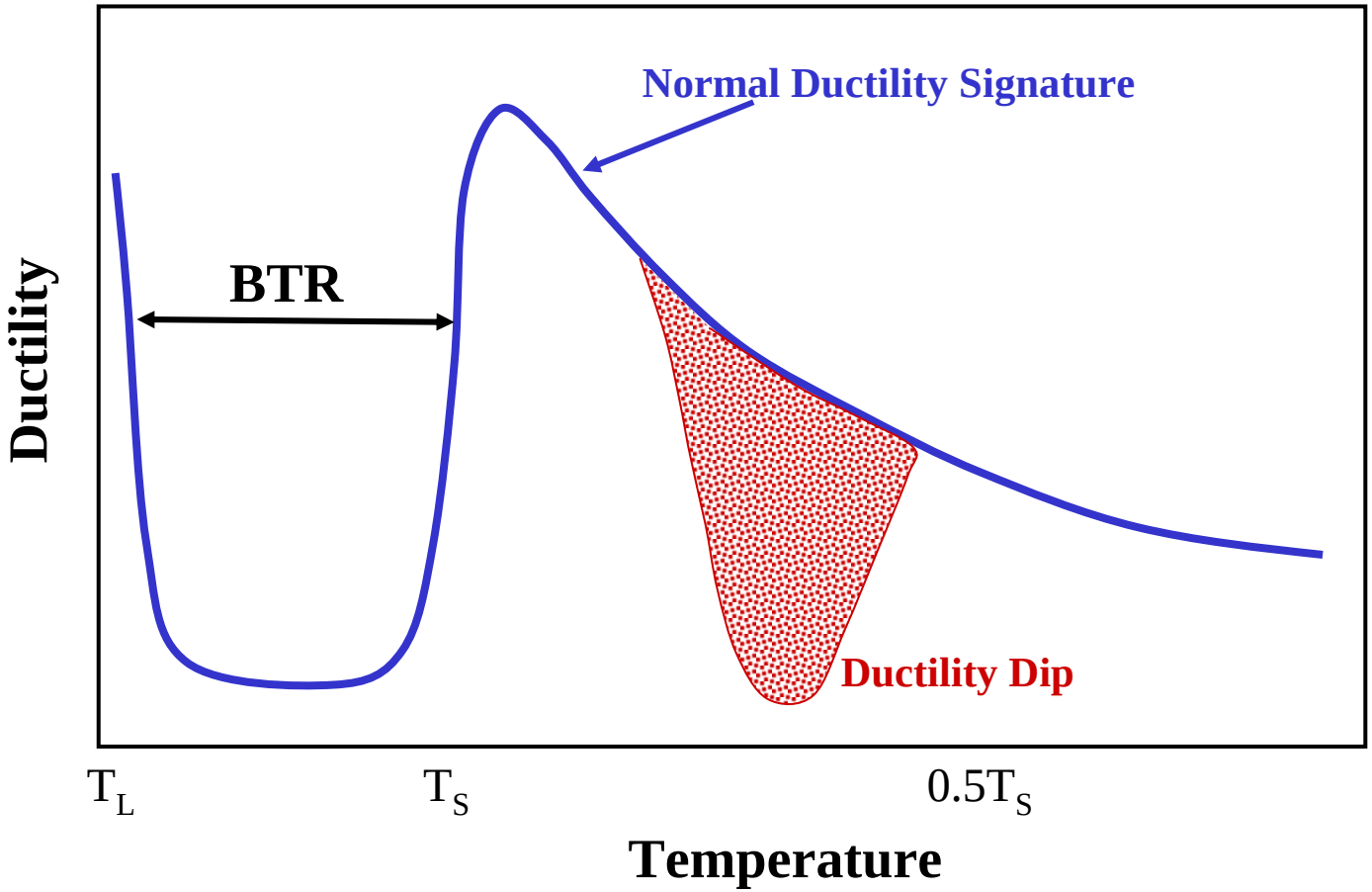

Weld Metal DDC Characteristics

- Sharp drop in elevated temperature ductility
- Solid state cracking
- Austenitic (FCC) Alloys
- Large grain size
- High restraint levels
- Intergranular along migrated grain boundaries

Ductility-dip cracking in Filler Metal 52 multipass weld deposit

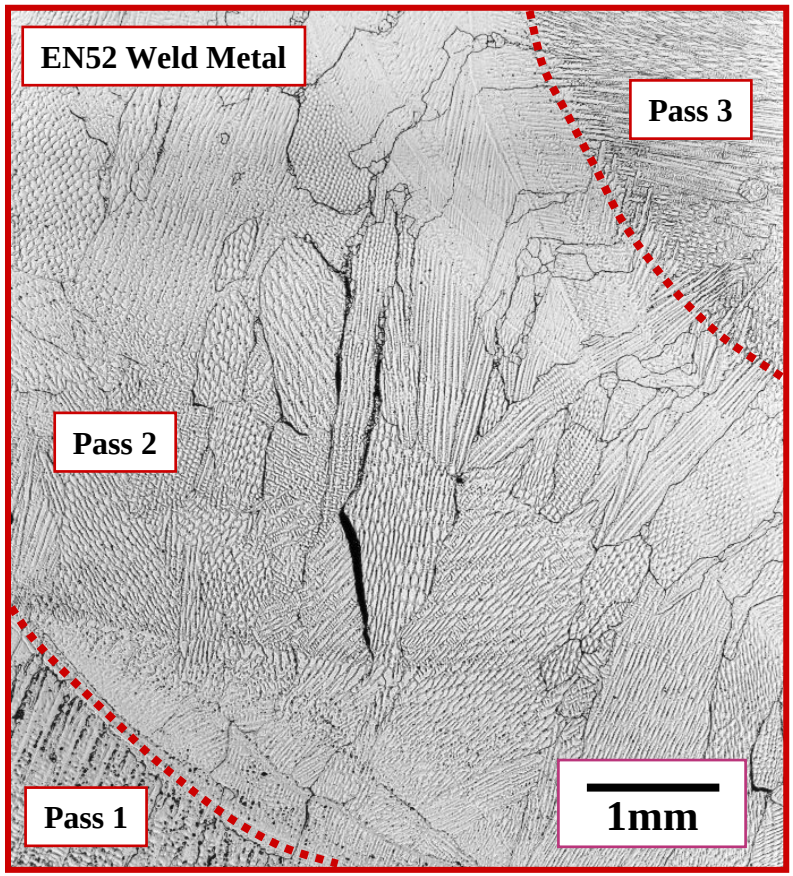

Ductility-dip cracking along migrated grain boundaries in Filler Metal 52 butter layer

- Large grain size
- Ductility “exhaustion” at grain boundaries
- Recrystallization along grain boundaries due to high local strains (arrows)

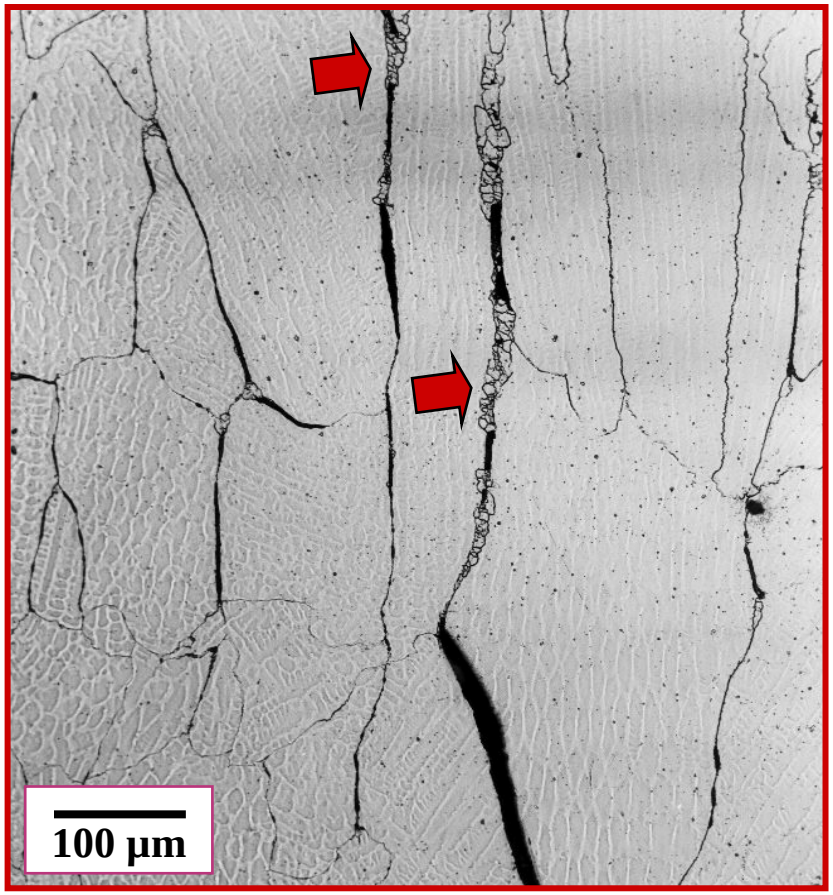

Migrated grain boundaries in re-heated weld metals

- Crystallographic component of SGB
- High angle boundary
- Migrates on-cooling after solidification and during re-heating (multi-pass welds)
- Large grain size

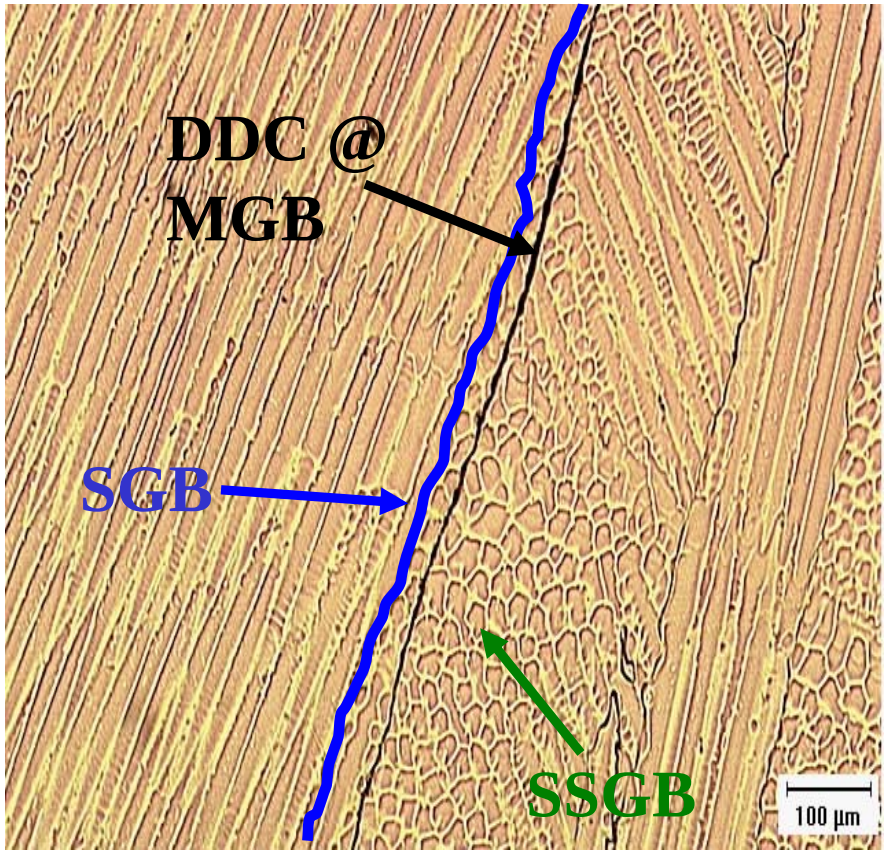

Factors Influencing DDC

- Strain concentration at Grain Boundaries (GB) and Triple Points
- GB orientation relative to the applied strain
- GB tortuosity
- Temperature
  - GB sliding inoperable at low Temperature
  - Recrystallization at high temperature
- Precipitates
- Impurities segregation (Sulfur)
- Hydrogen
  - H induced decohesion
  - H enhanced local plasticity

Strain-to-Fracture DDC Test

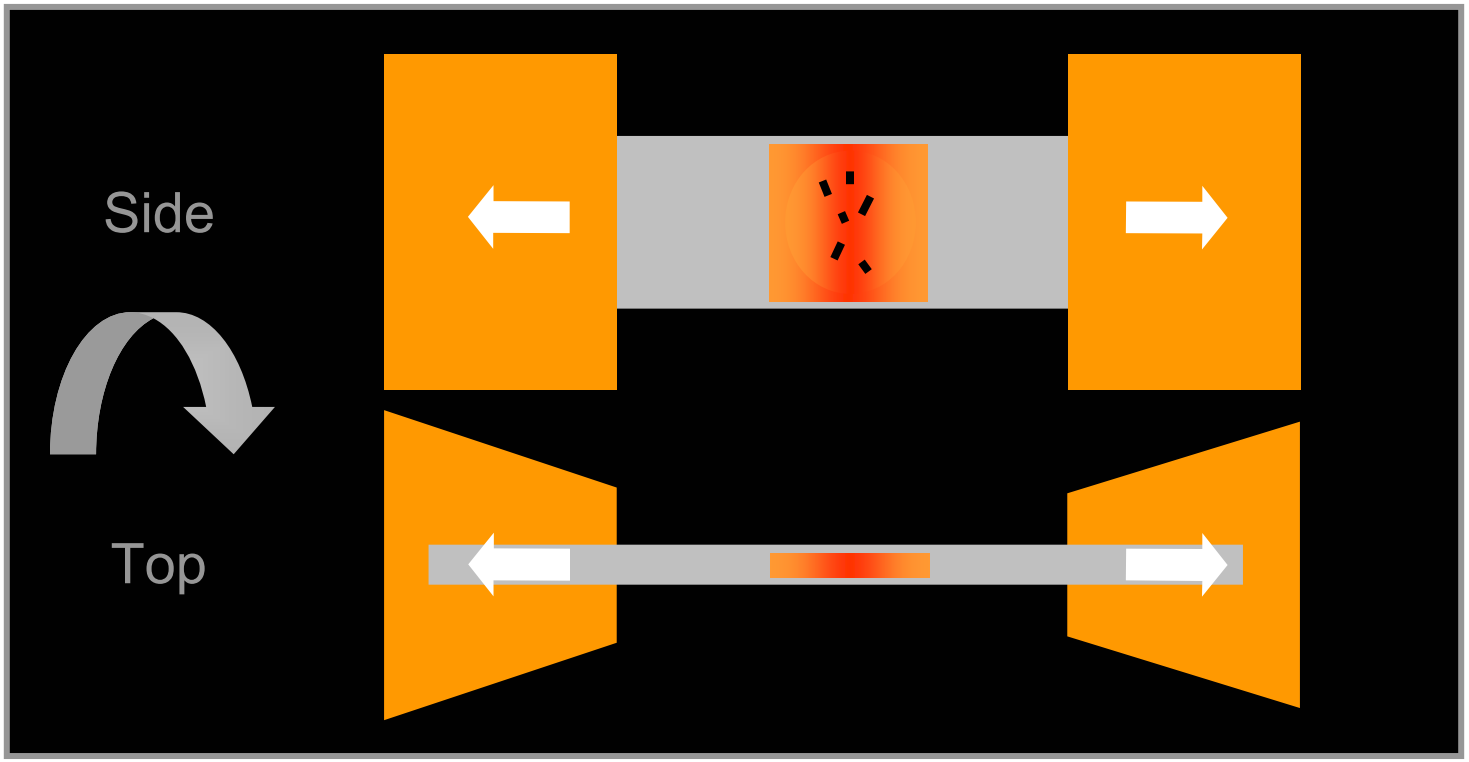

Testing filler metals - sample preparation

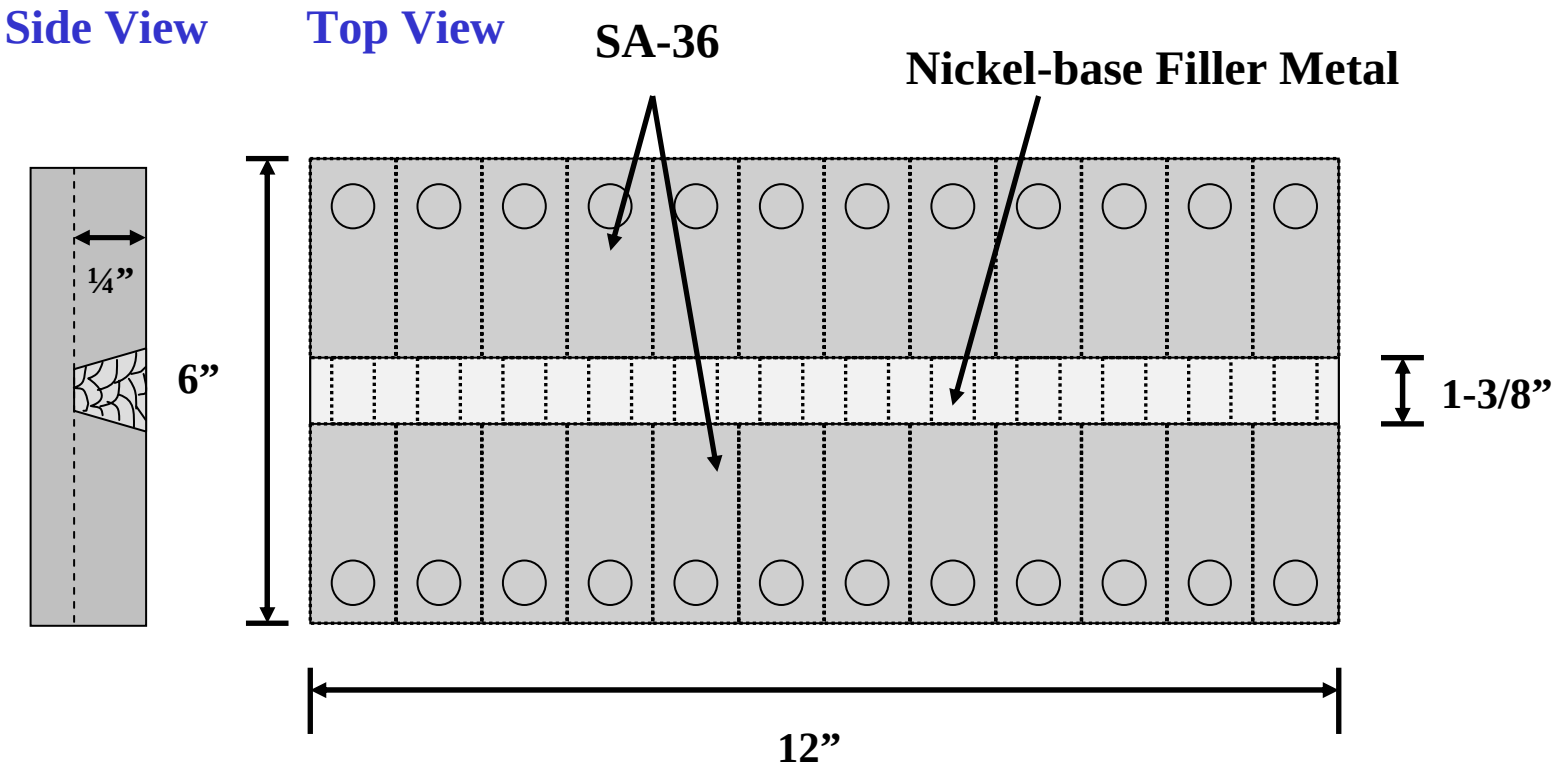

Filler Metal 52 STF Test Results

Welding and Joining Metallurgy Group

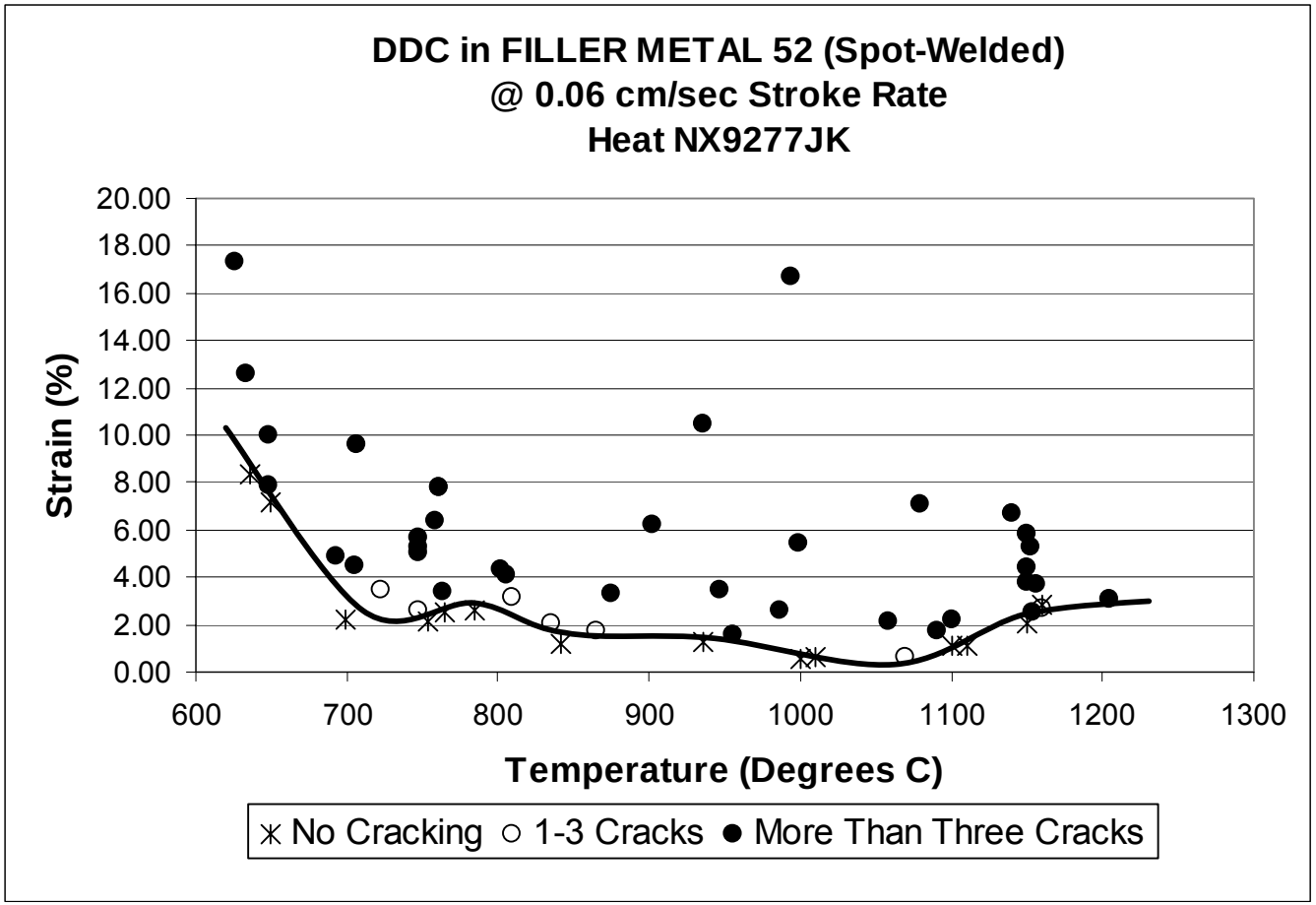

Filler Metal 52 STF Test Results

Welding and Joining Metallurgy Group

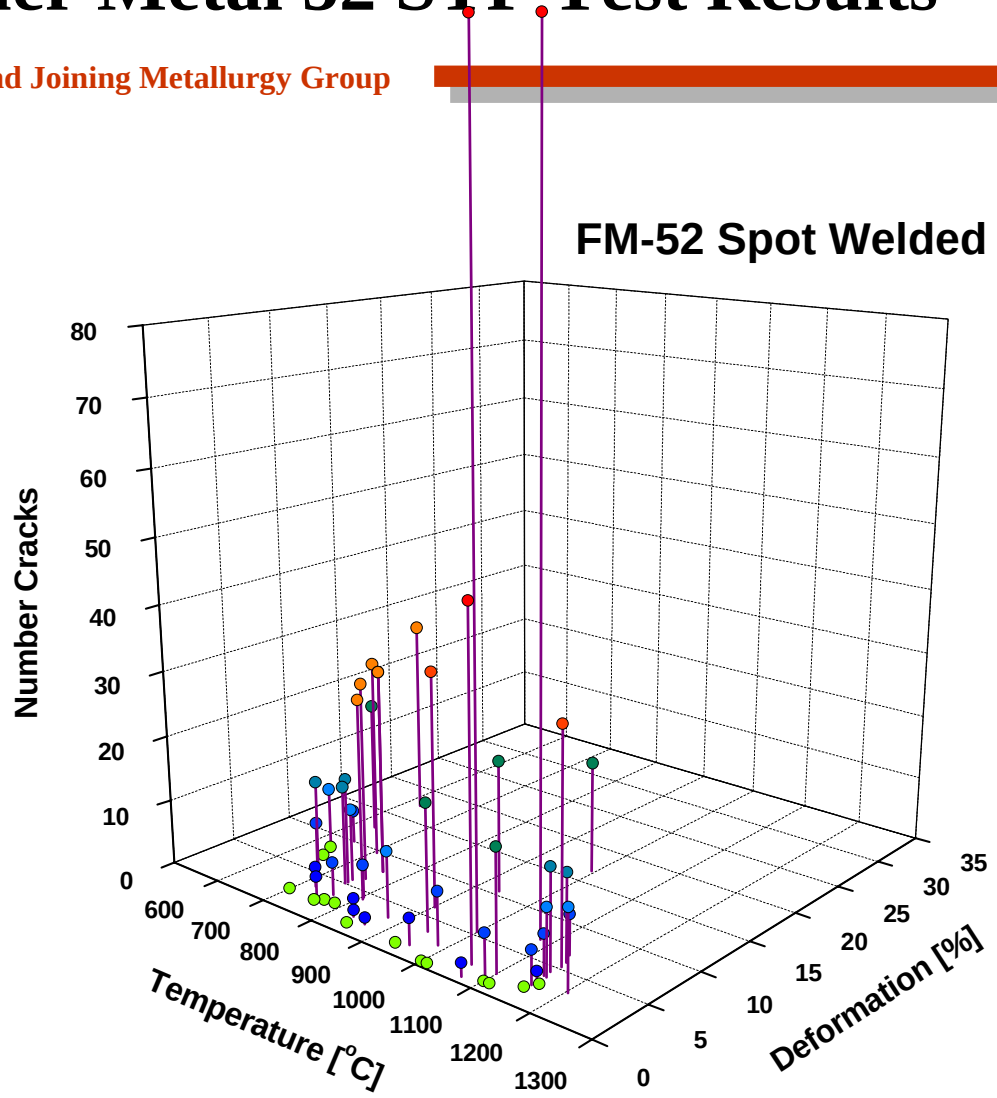

Filler Metal 52 vs. Filler Metal 82

Welding and Joining Metallurgy Group

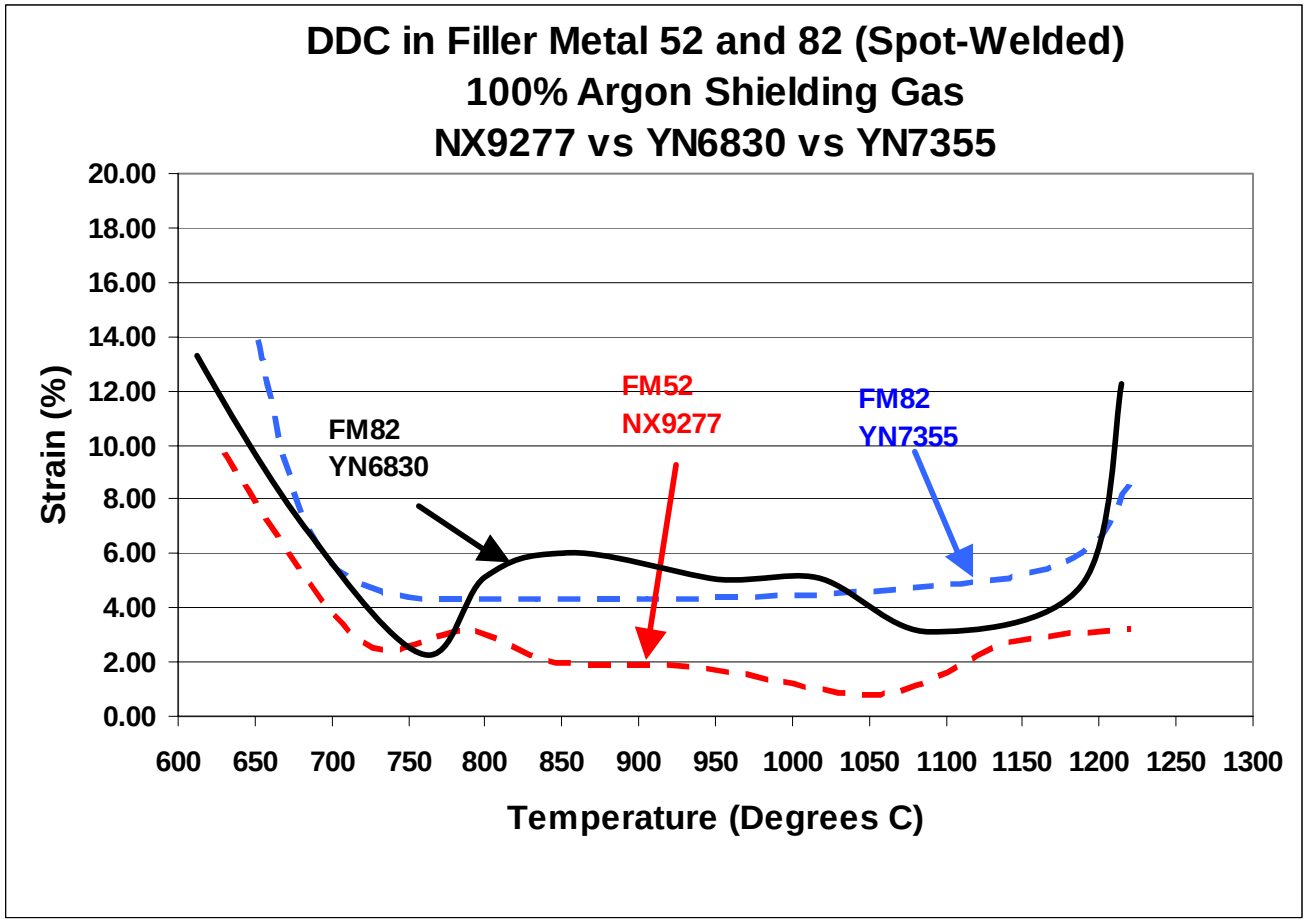

Filler Metal 82 – H_2 additions

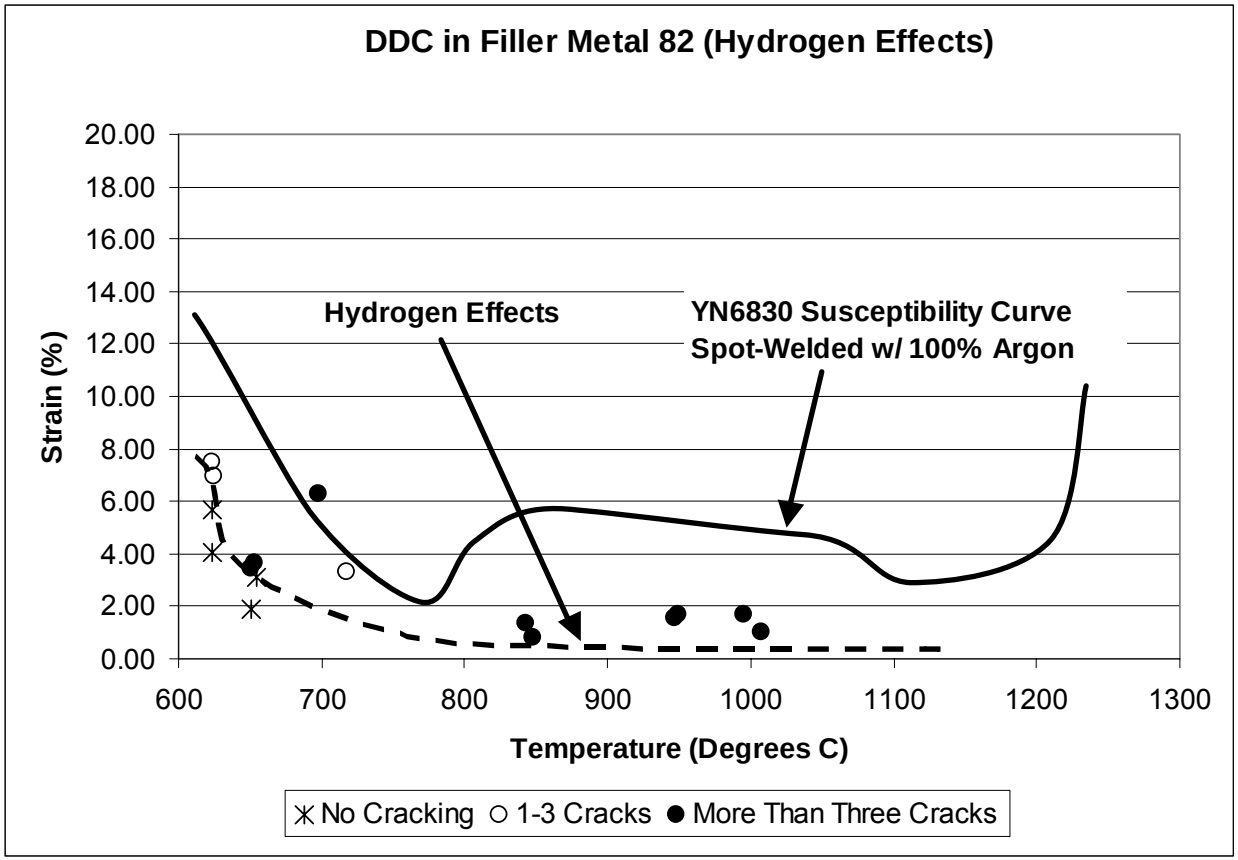

Ductility-dip cracking

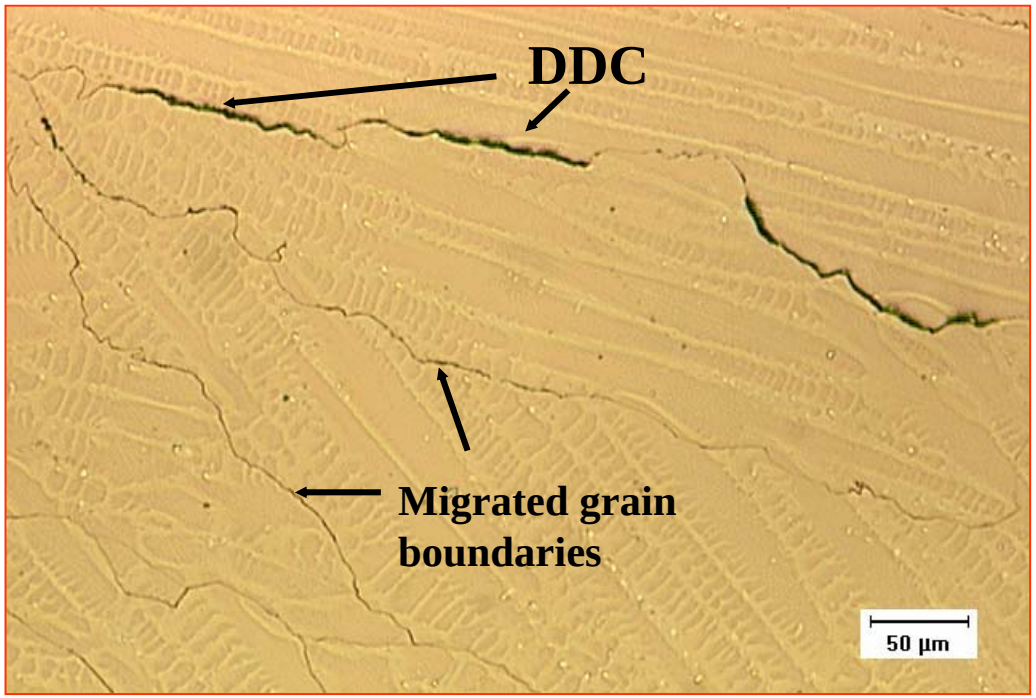

Characteristics

- Fully austenitic
- Large grain size
- Straight, smooth boundaries
- Low impurity content
- High restraint

DDC Fracture Surface in Filler Metal 52

Ductile intergranular fracture along migrated grain boundaries

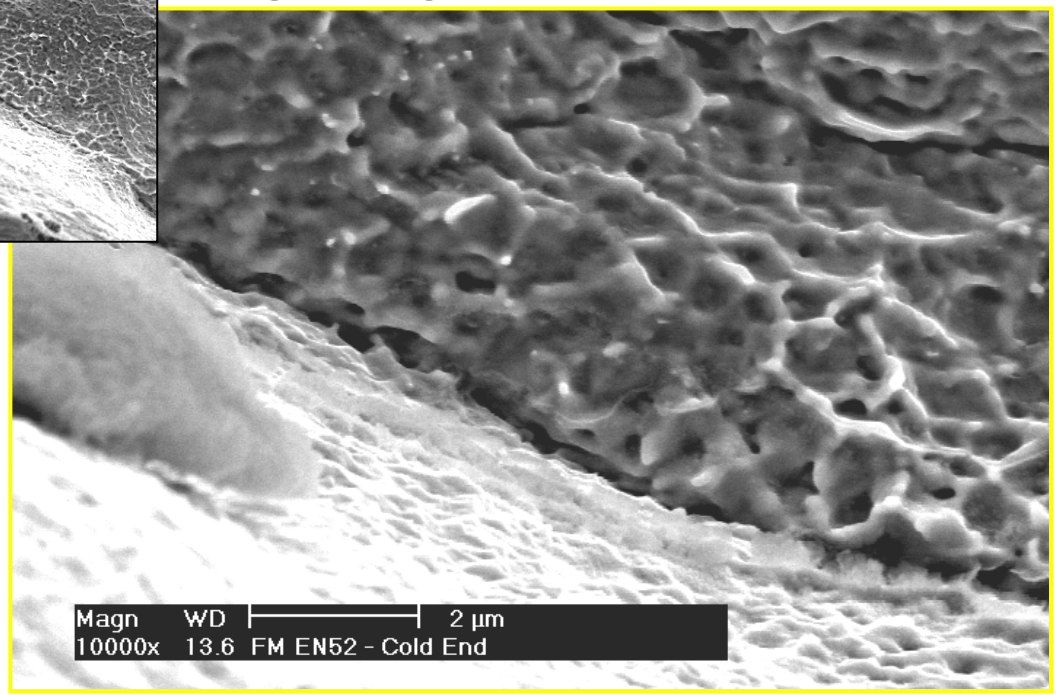

Grain boundary characteristics – Filler Metal 52

Long, straight, “clean” MGB in Filler Metal 52 at 986°C

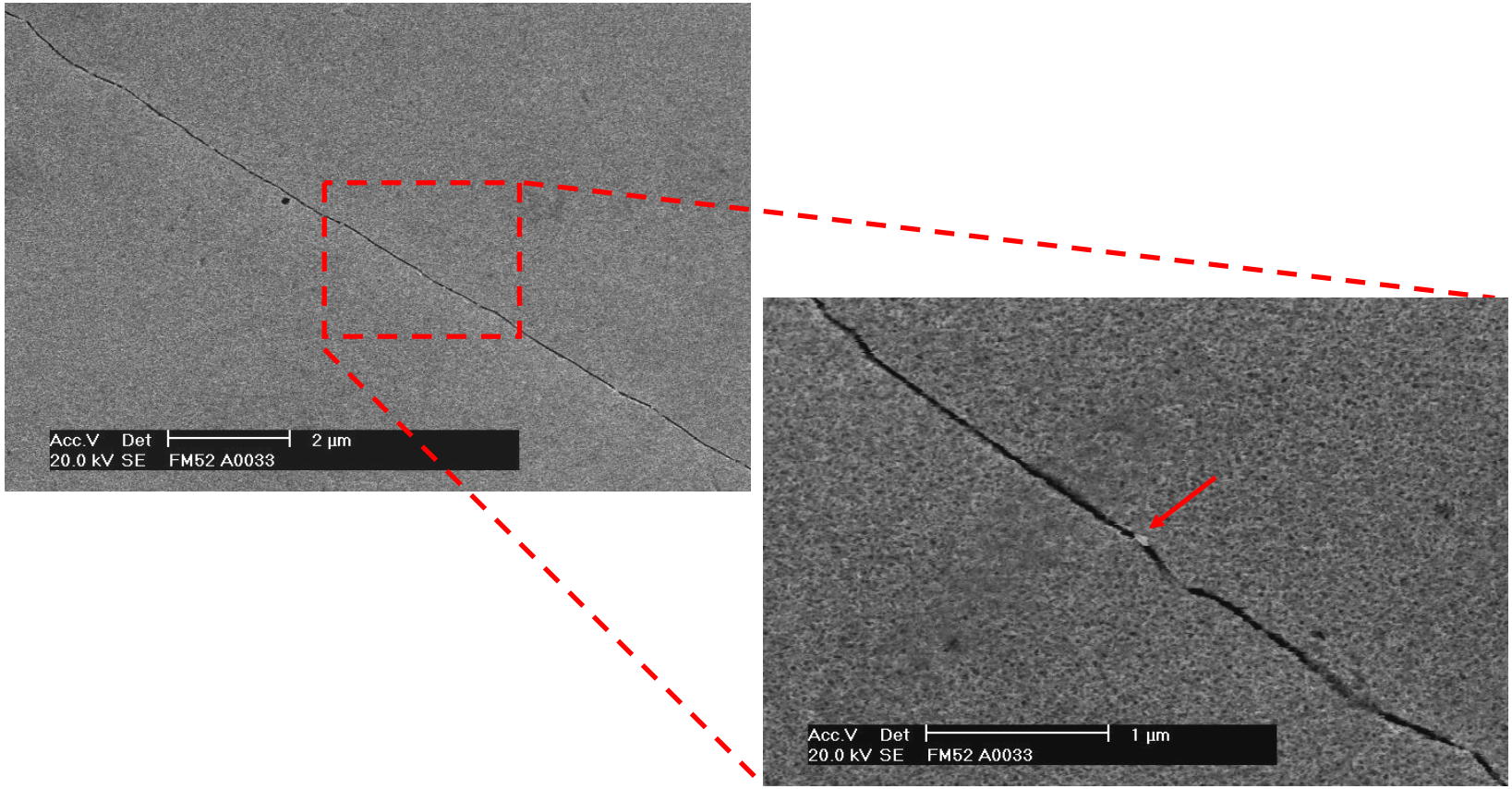

Intergranular Precipitation - FM 52

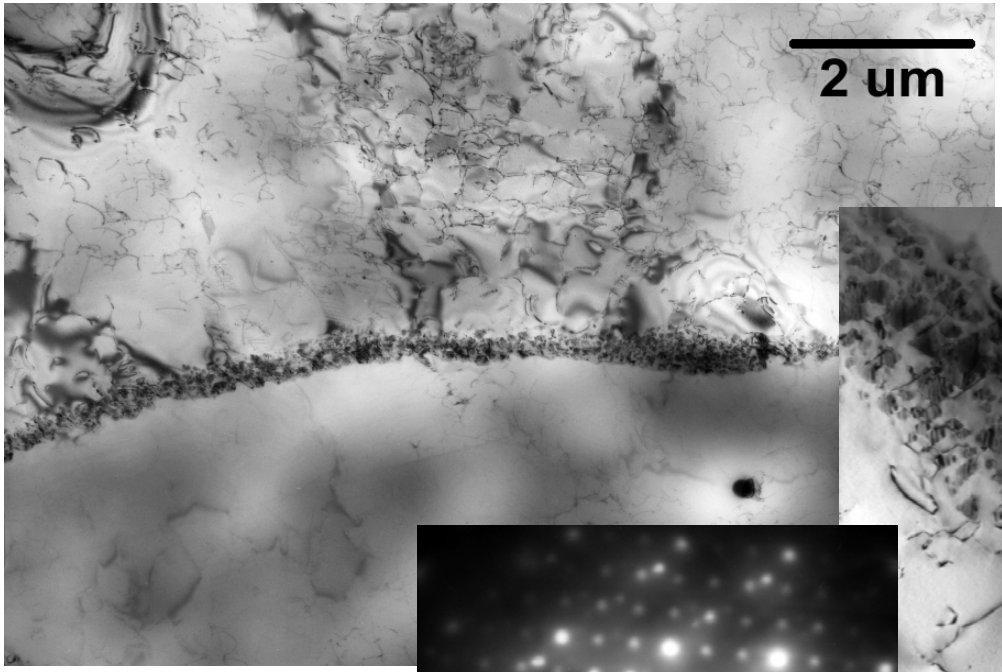

990 °C
Strain: 1.6%

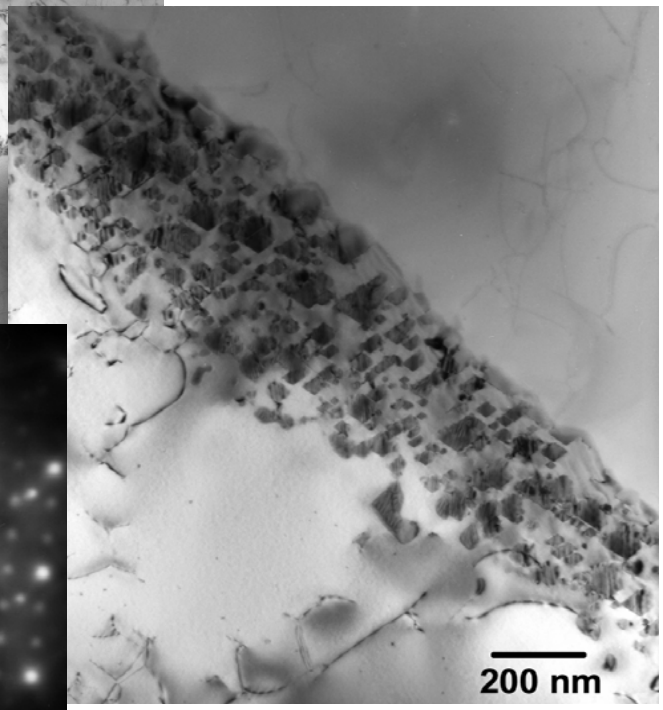

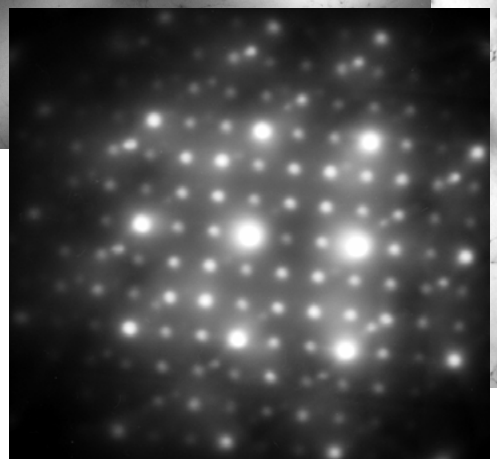

$M_{23}C_6$

10 - 50 nm

Cube-on-Cube
Orientation Relationship

GB Pinning -Filler Metal 82

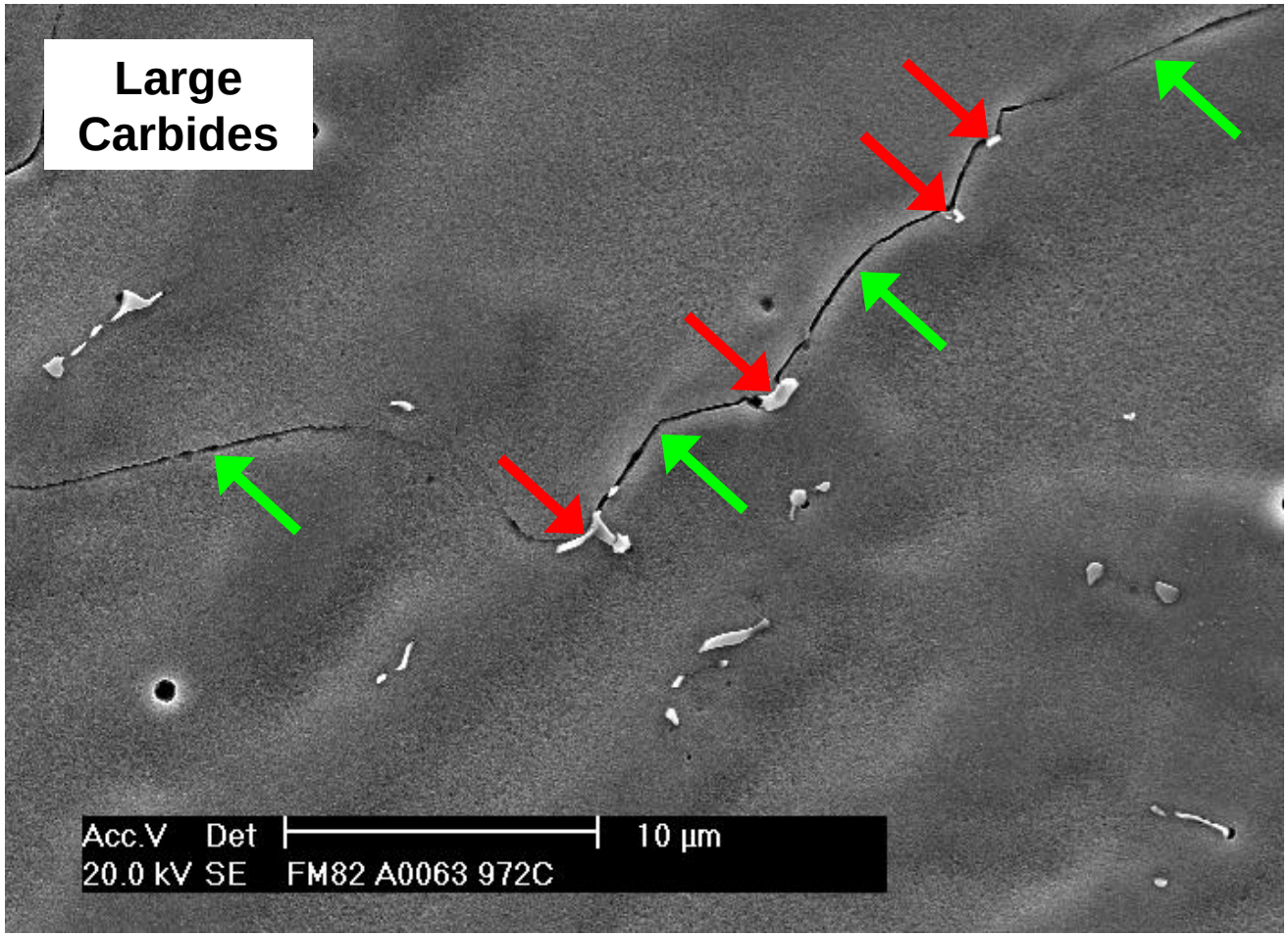

970 °C
Strain: 7.5%

Precipitates in Filler Metal 82

Welding and Joining Metallurgy Group

1150 °C
Strain: 11.3%

Heat – YN6830

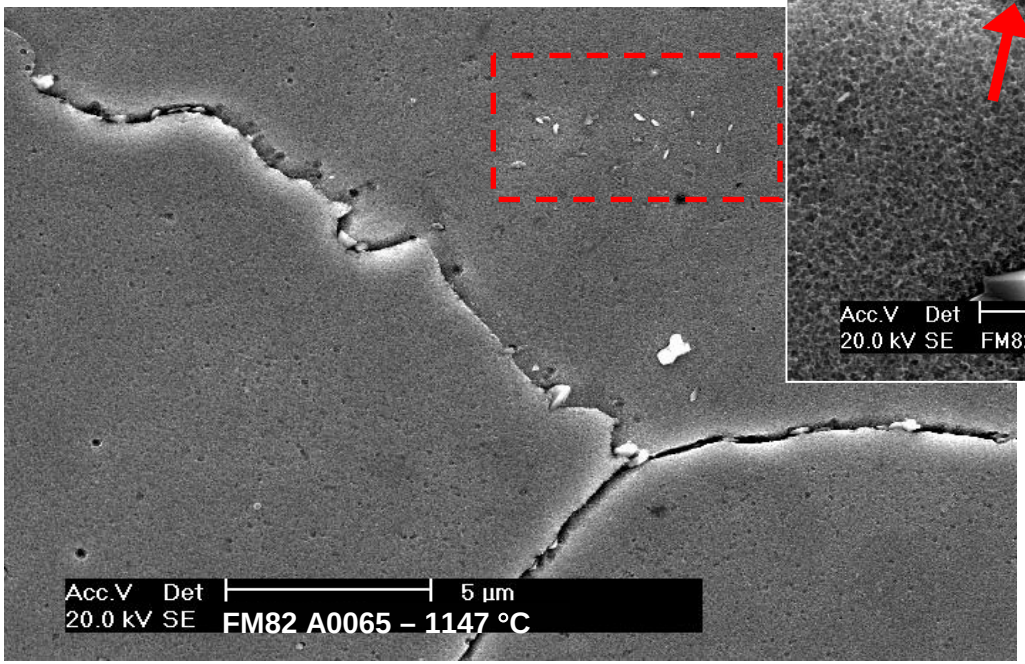

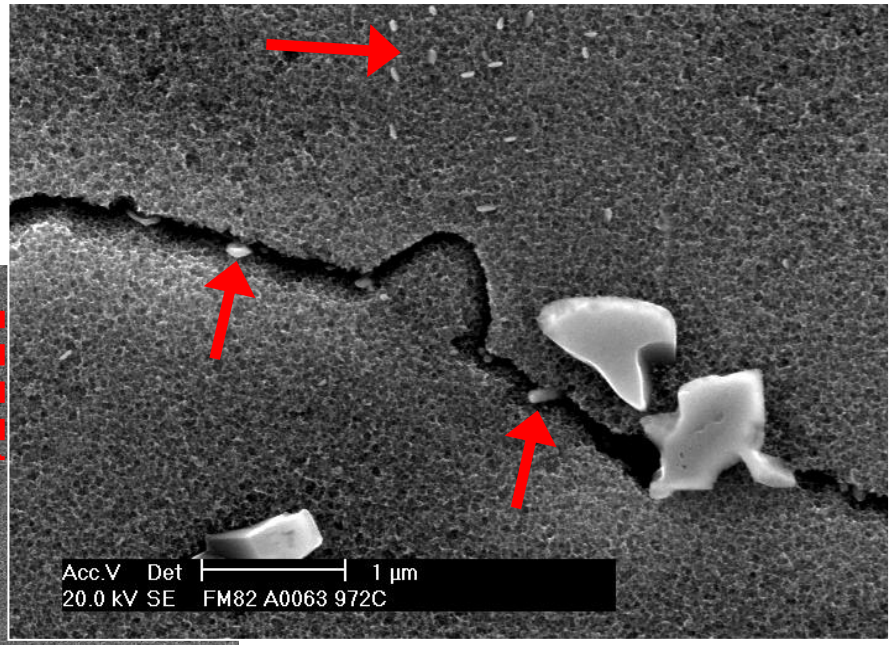

970 °C
Strain: 7.5%

Heat – YN6830

Precipitates on Fracture Surface

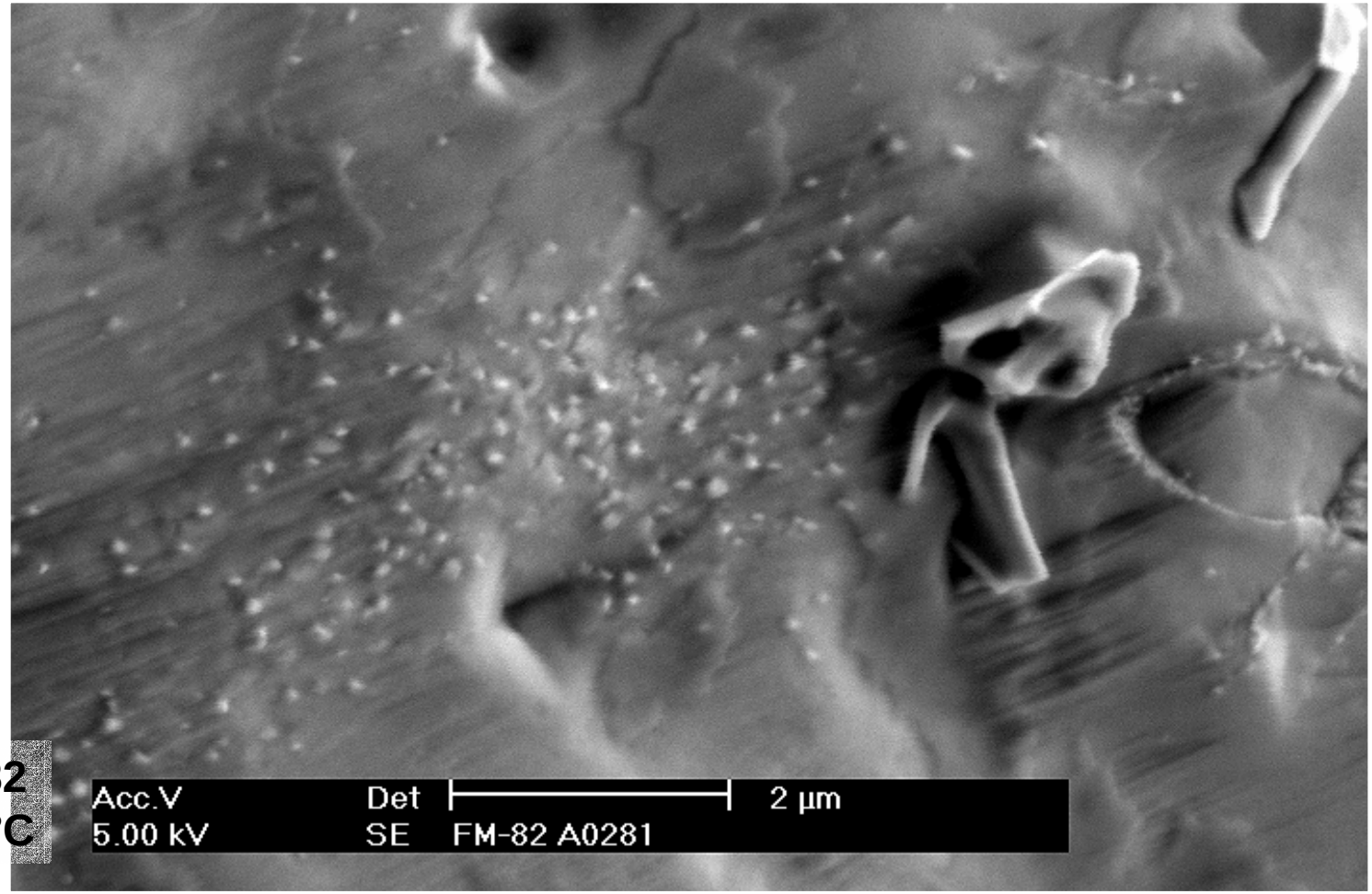

FM-82
950 °C

Medium Size (Nb,Ti)C Precipitates Filler Metal 82

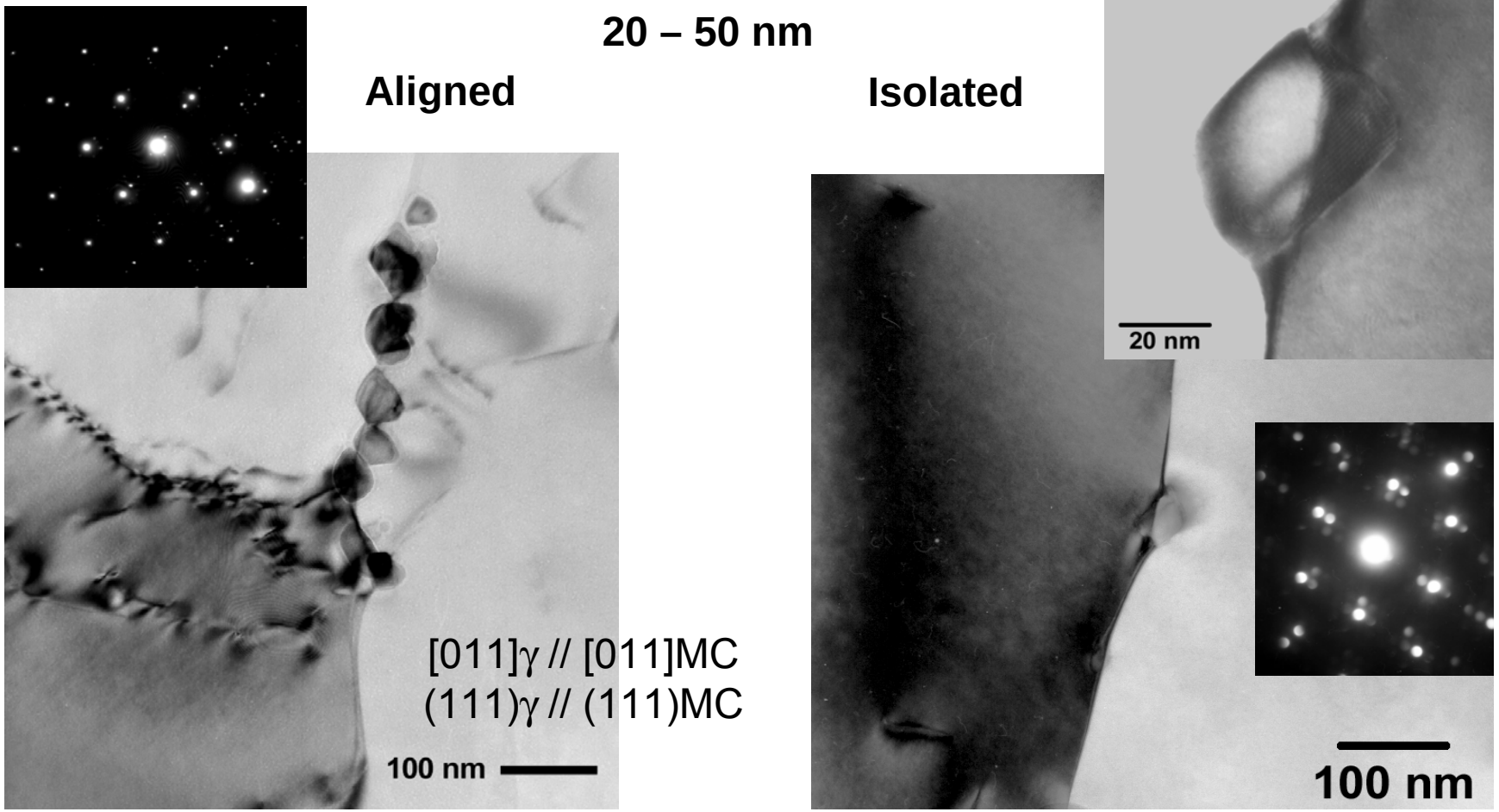

Small Precipitates - Filler Metal 82

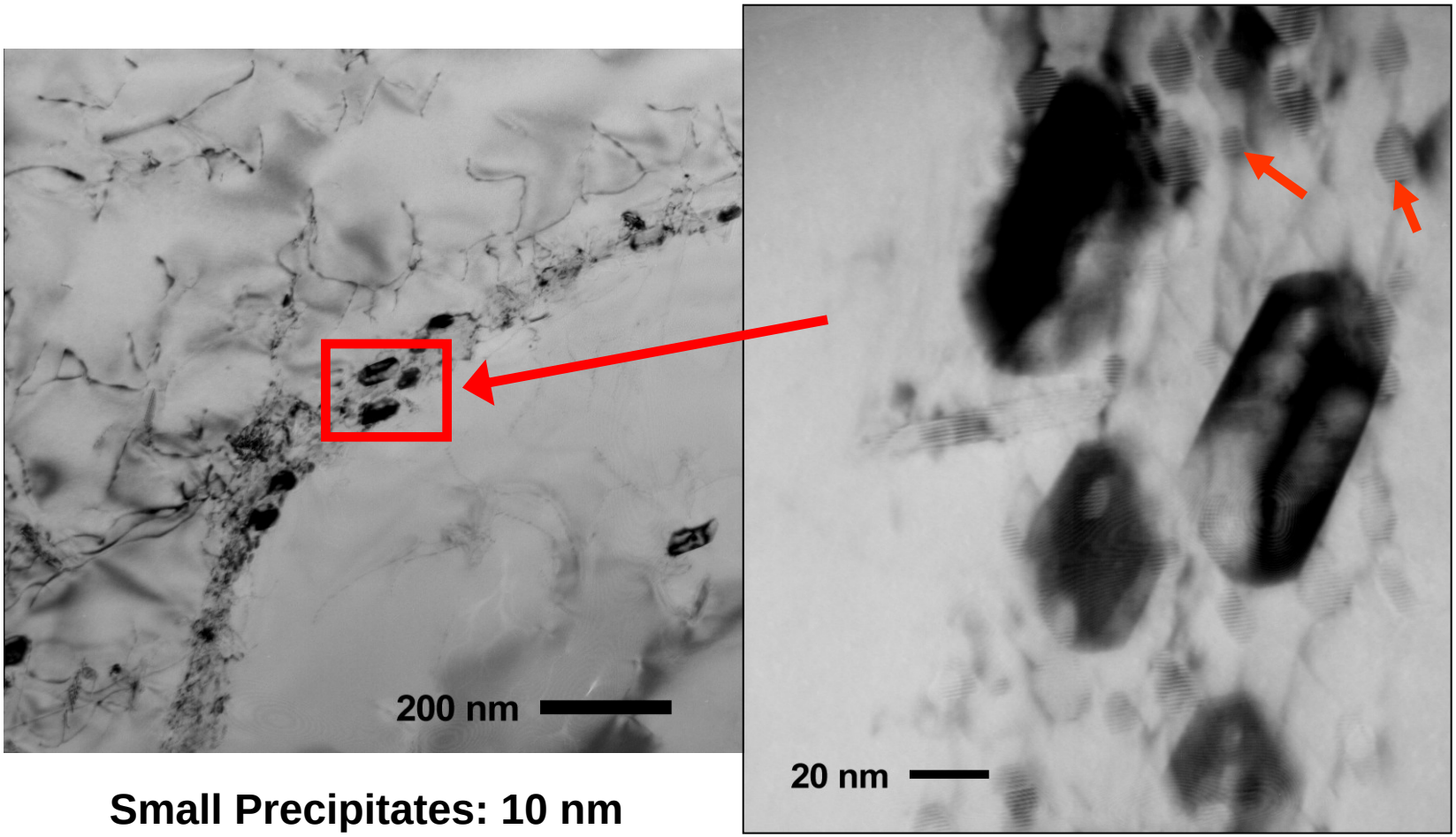

Small Precipitates: 10 nm

Strain Distribution

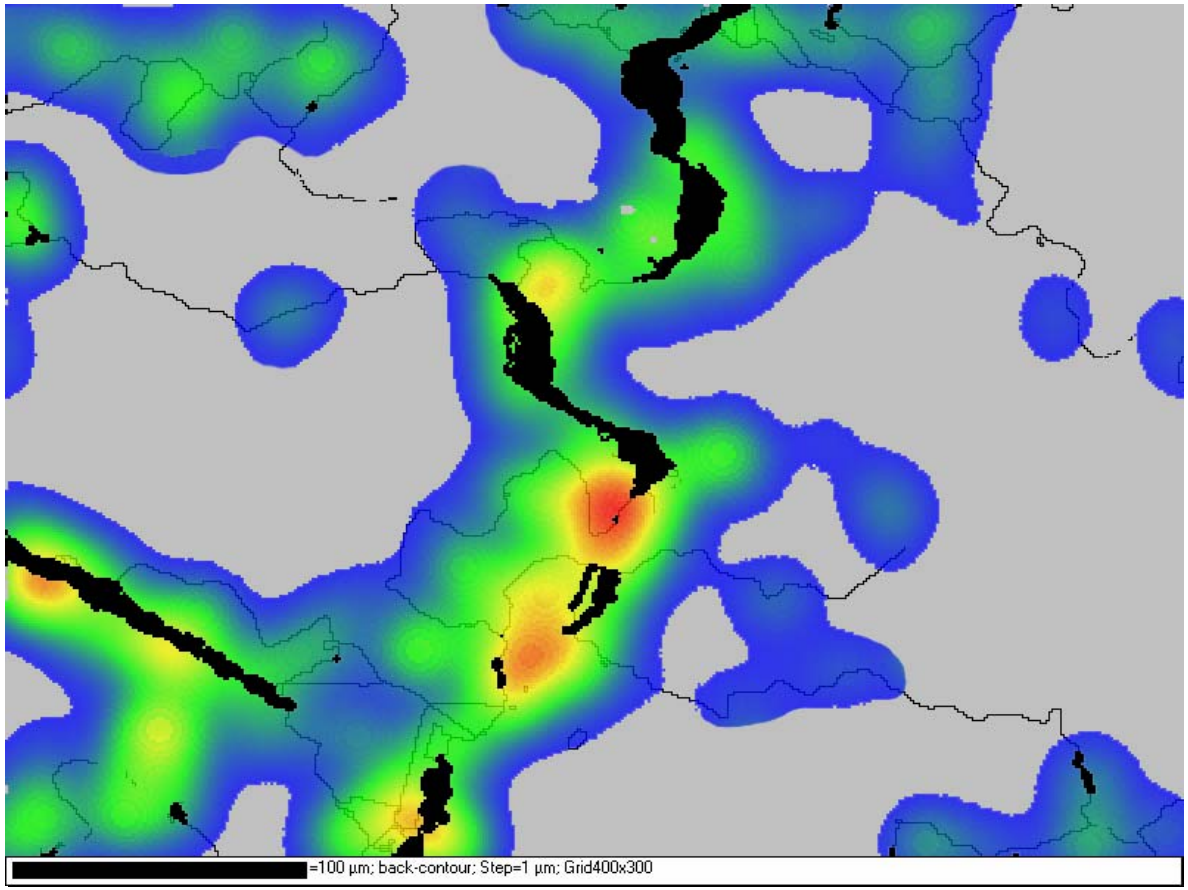

1147 °C
Strain: 11.3%

FM-82
Heat – YN6830

Strain Distribution

Welding and Joining Metallurgy Group

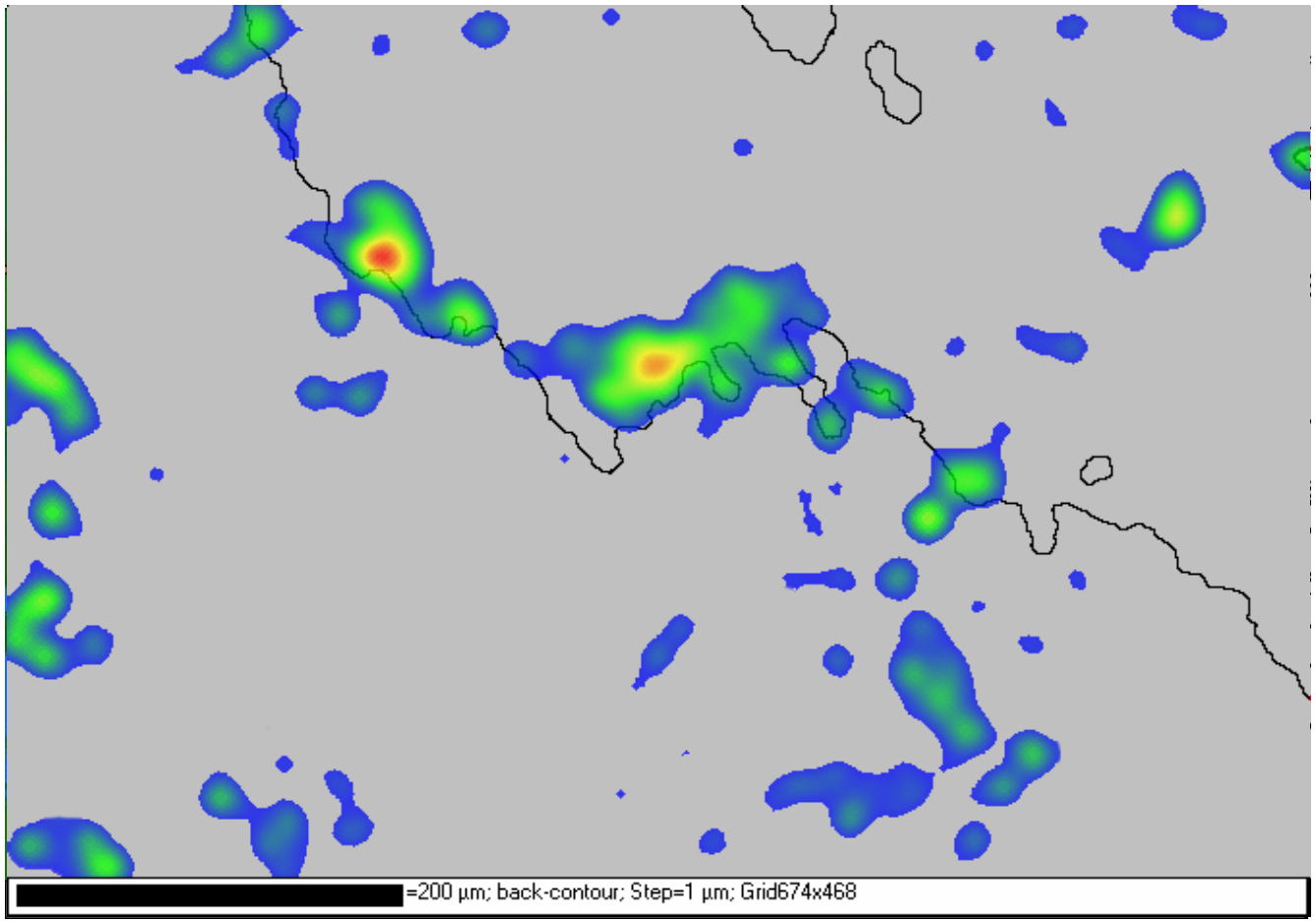

985 °C
Strain: 8.1%

FM-82
Heat – YN6830

Comparison

- **Filler Metal 52**
  - Long, straight grain boundaries (not tortuous)
  - Sporadic intergranular large carbides and nitrides
  - The nitrides are not enough to avoid grain growth
  - Consistent medium size $M_{23}C_6$ distribution
  - Small amount of intragranular precipitates

- **Filler Metal 82**
  - Very tortuous grain boundaries
  - Consistent inter- and intra-granular eutectic large (Nb,Ti)C distribution (1-3 μm)
  - Sporadic intergranular medium size and small (NbTi)C carbides
  - Small amount of intragranular carbides
  - No $M_{23}C_6$ observed

Insight Into the Mechanism

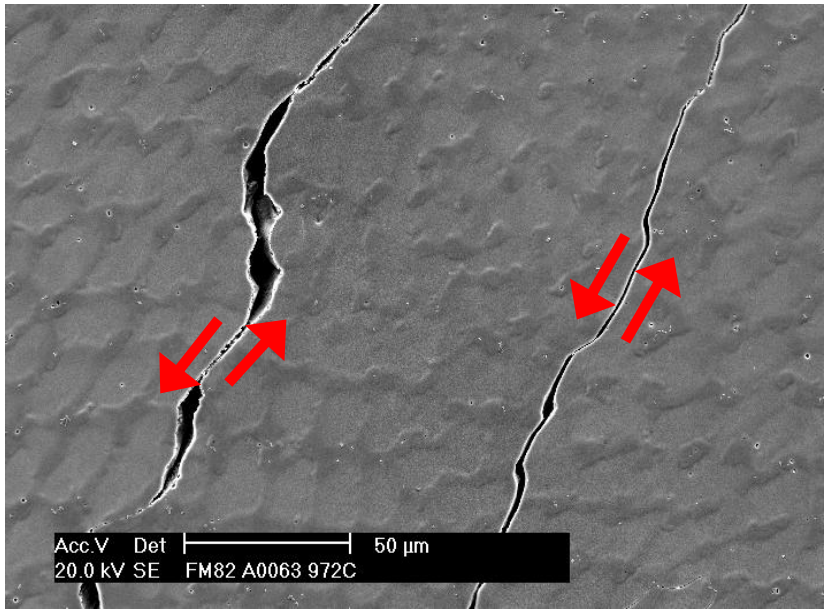

FM-82
972 °C

Grain Boundary Sliding

FM-52
986 °C

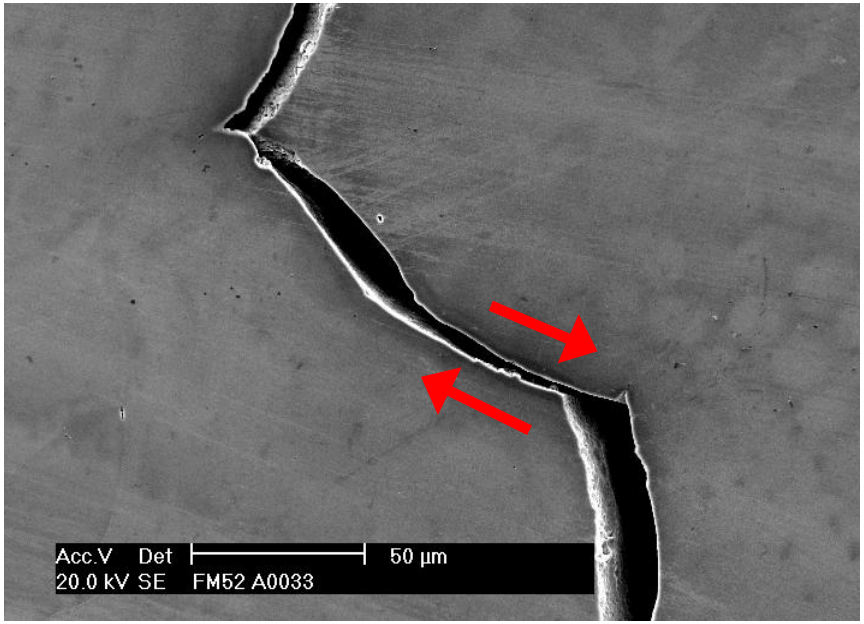

Insight Into the Mechanism

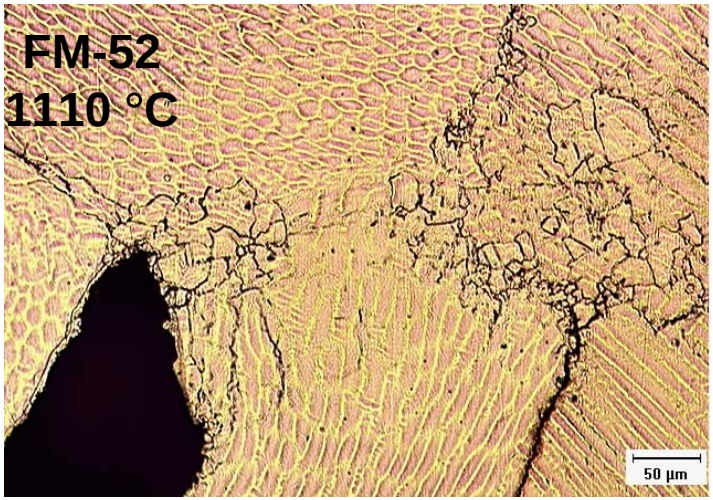

Dynamic recrystallization at high temperatures

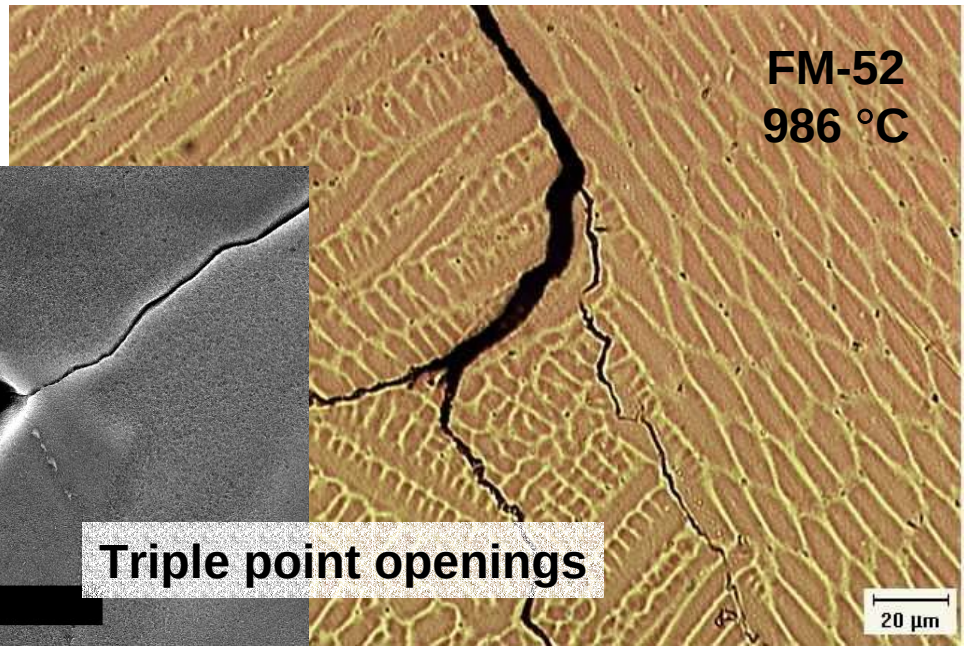

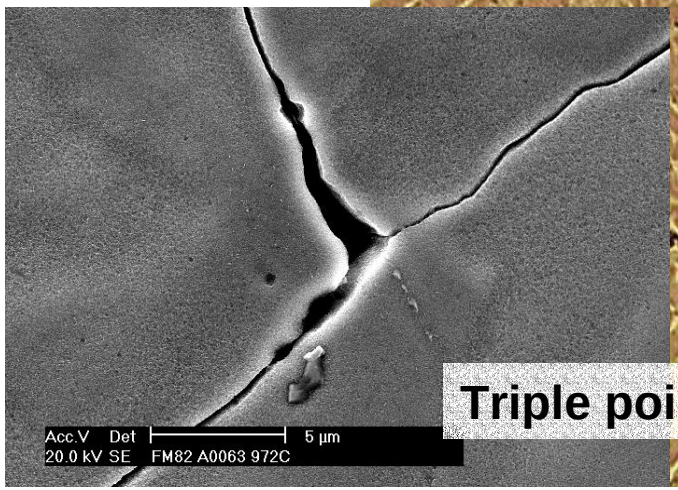

FM-82
972 °C

Triple point openings

DDC Mechanism Insight

- **Effect of grain boundary precipitates**
  - **"Locks" GB and/or "pins" GB migration**
  - **Increases GB tortuosity**
  - **Restricts grain growth**
  - **Reduces GB sliding**
  - **Reduces deformation accumulation at triple points**
  - **May be crack initiators (precipitate itself or interface)**
  - **Interaction with impurities**

- **Effect depends on**
  - **When and where the precipitate forms**
  - **Precipitate properties (MN - MC - $M_{23}C_6$)**
  - **Interface properties**
  - **Distribution**
  - **Size**

DDC Mechanism Insight

- **Grain boundary tortuosity**
  - **Increases GB area versus straight grain boundaries**
  - **GB “locking” effect**
  - **Reduce deformation accumulation at triple points**
  - **Favors cracks arrest process**

- **Hydrogen Effect**
  - **Increases GB/Interface decohesion**
  - **Interaction with precipitates**
  - **Enhances GB sliding**

Vessel Head Penetration Inspection, Cracking, and Repairs Conference

Impact of PWSCC and Current Leak Detection on Leak-Before-Break

607

D. Rudland [(1)], R. Wolterman [(1)], G. Wilkowski [(1)], and R. Tregoning[(2)]

(1) Engineering Mechanics Corporation of Columbus

(2) U.S. Nuclear Regulatory Commission, Office of Nuclear Reactor Research

Acknowledgements

- ***Work supported by NRC-RES through subcontract from Battelle to Emc²***

  R. Tregoning is NRC project manager

  P. Scott is Battelle Project Manager

LB-LOCA Redefinition Program

- *This effort small part of larger program*
- *On-going elicitation to assess failure probabilities*
- *Next generation of probabilistic pipe fracture code under development*
  - *Discussion with many people during this meeting to get updated subcritical crack initiation and growth models*
  - *Including many of the piping fracture analysis aspects from NRC's Degraded Piping Program, Short Cracks programs, IPIRG-1 and –2 programs*

609

Background

- *PWSCC in Ringhal and VC Summer hot legs, as well as more recent Belgium and Japanese PWSCC piping experiences raised concern about past LBB approvals for lines that at one time were thought to be free of any cracking mechanism.*

- *SRP 3.6.3 has a screening criterion to ensure that lines susceptible to potentially large cracks cannot be accepted for LBB relief of dynamic load effects of pipe whip supports and jet impingements shields.*
  - *"..requirement that corrosion resistance of piping be demonstrated….".*

- *Fortunately the PWSCC cracks to date have been primarily axial and a few small circumferential cracks; nevertheless, it was desirable to see if LBB could be satisfied if circumferential through-wall cracks occurred.*

Background

- ***V.C. Summer PWSCCs in hot-leg***

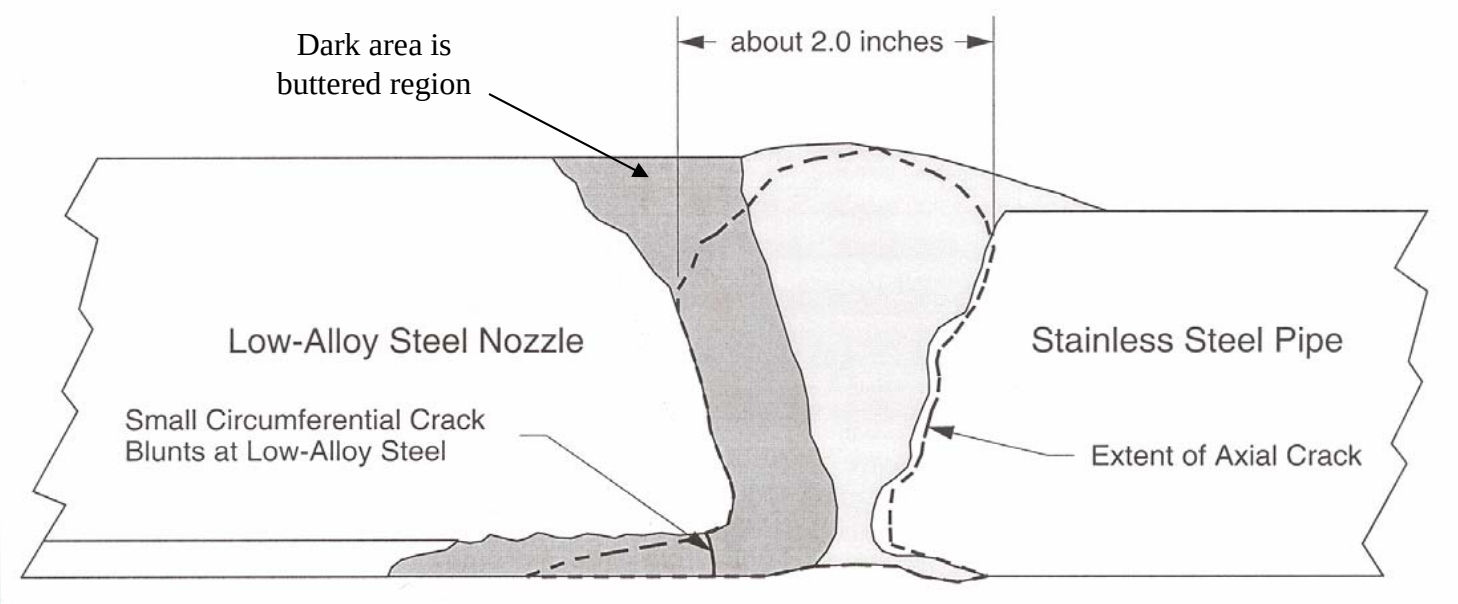

611

Background

- *Inconel 82/182 bimetallic weld locations that might be susceptible to PWSCC*
  - *RPV main coolant nozzles, core flood nozzles*
  - *Pressurizer nozzle, spray nozzles, and surge lines*
  - *Steam generator nozzles and RCP nozzles*
  - *Many branch line connections*
- *Locations vary by NSSS supplier since main coolant piping could be stainless or clad carbon steels*

Revised LBB Analysis

- *As part of the LB-LOCA redefinition program and the technical support for a new LBB Regulatory Guide, many past LBB submittals were reviewed*
- *LBB analysis conducted in this effort using typical LBB loads and recalculating how the leakage size crack may change if it was a PWSCC crack, i.e., PWSCC cracks have a more tortuous flow path than fatigue cracks used in many past LBB submittals.*
  - *Need to define PWSCC crack-morphology parameters (roughness, number of turns, actual flow path-to-thickness ratio) from cracks removed from service.*
  - *Photomicrographs of several PWSCC service-removed cracks were available.*
- *Recalculated leakage cracks for LBB cases and determined margins on leakage crack size versus critical crack size at N+SSE or other critical transient load (i.e., start-up/shut-down thermal loads for a surge line)*

Crack Morphology Parameters

- ***Surface roughness, number of turns, and actual flow path length are key crack morphology parameters.***

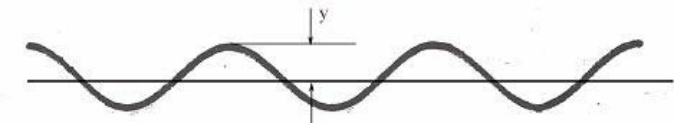

$$R_q = \sqrt{\left(\frac{1}{L}\int_{x=0}^{x=L} y^2 dx\right)}$$

- ***Surface roughness and number of turns can depend on the magnitude of the crack-opening displacement (μ_G = global surface roughness, μ_L = local surface roughness).***

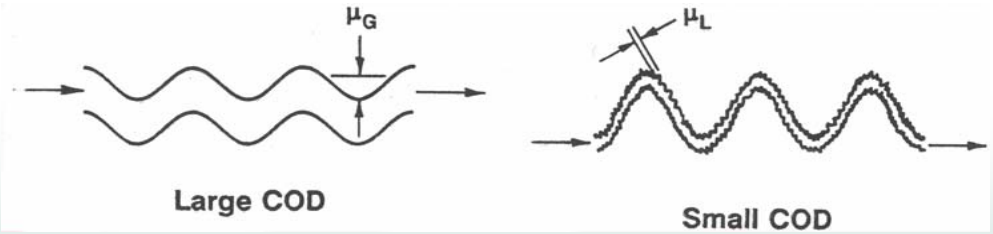

Crack Morphology Parameters

- ***Actual flow path length can depend on number of turns and will be greater than just the thickness of the pipe.***

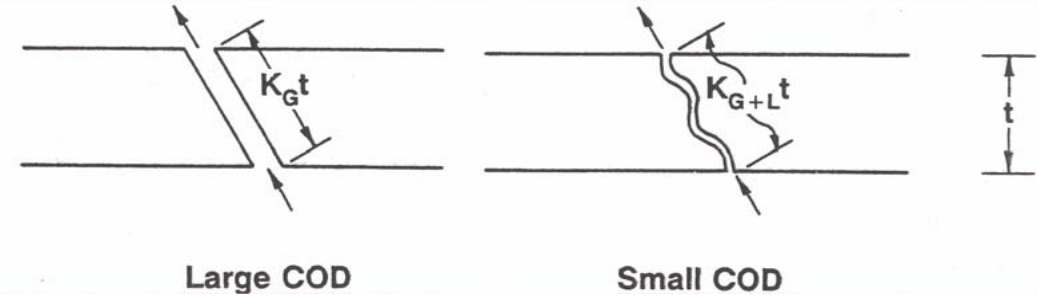

Crack Morphology Parameters

- ***Interpolation procedure used to account for effect of COD on transition from:***
  - ***very tight cracks (lower surface roughness, many turns, longer flow path length) to***
  - ***large COD crack cases (higher roughness, fewer turns, and shorter effective flow length)***

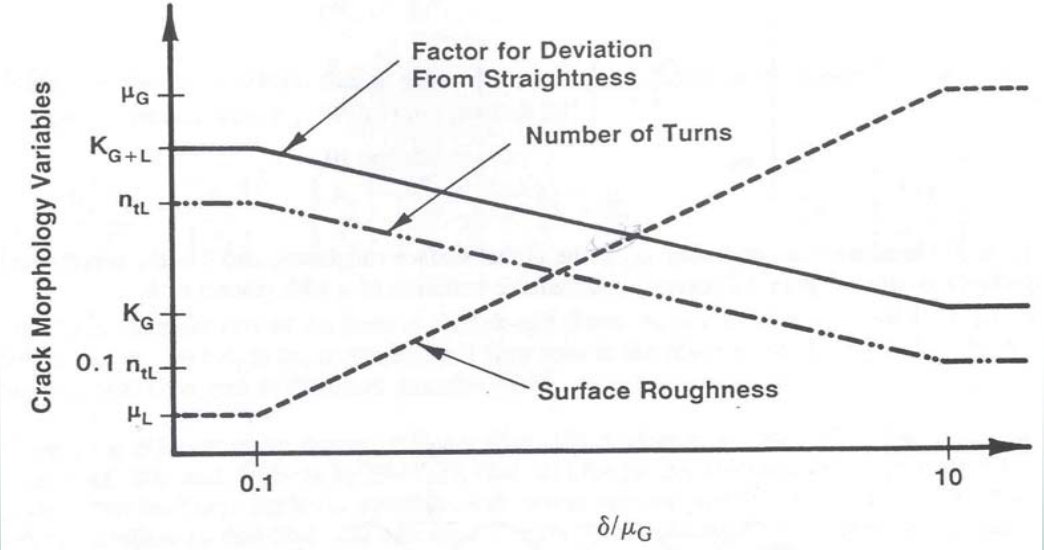

Crack Morphology Parameters

- ***Interpolation procedure is approximate and could be improved with detailed CFM analysis***

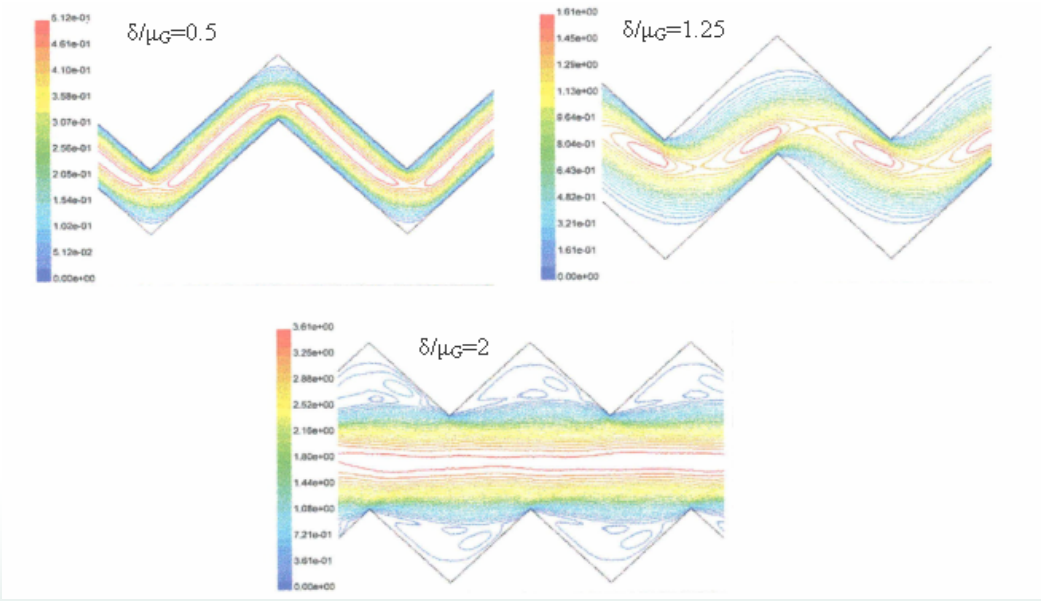

Unique aspects of PWSCC in bimetallic welds

- ***Weld bead orientation may affect crack morphology parameters, i.e., cracks grow parallel to dendritic grains faster***

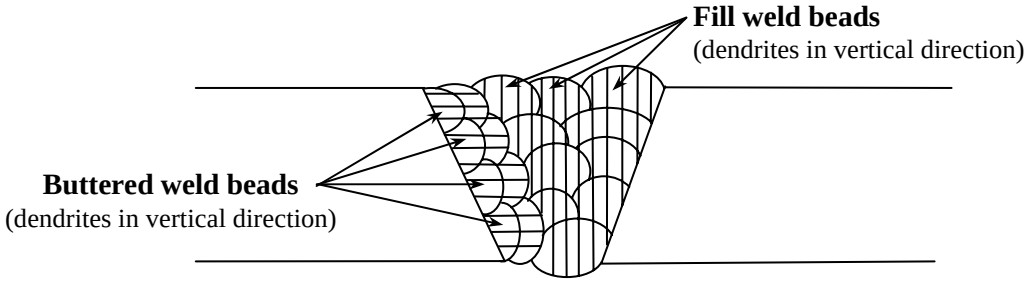

Statistical analysis of crack morphology for different types of cracks

- ***Evaluated service removed cracks in NUREG/CR-6004 "Probabilistic Pipe Fracture Evaluations for Leak-Rate-Detection Applications"***

Air fatigue crack

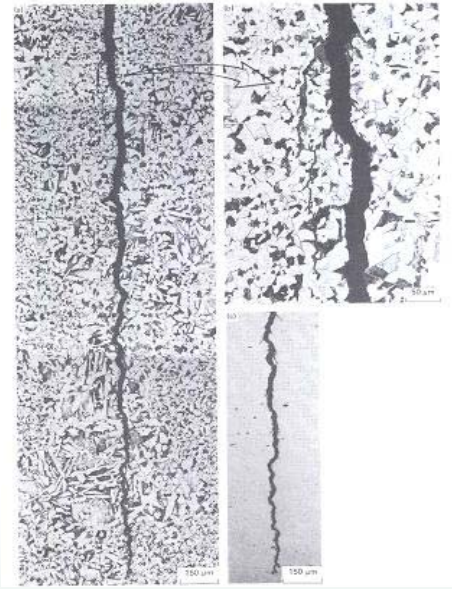

Corrosion fatigue crack

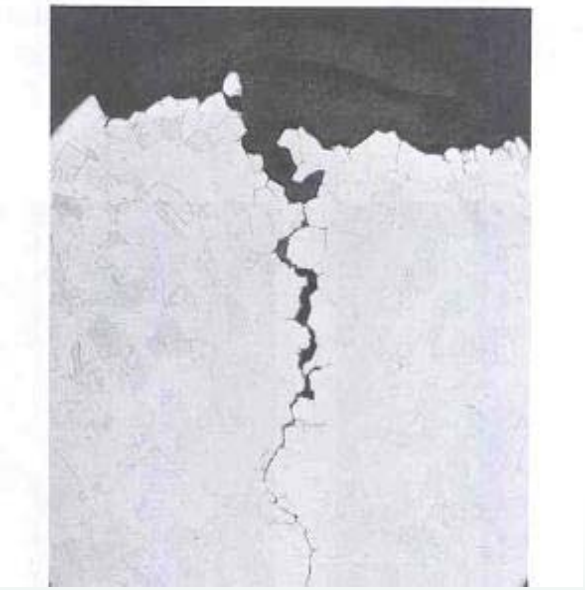

IGSCC crack

PWSCC cracks examined from metallographic sections

- *Inconel 600 base metal (CRDM nozzle)*

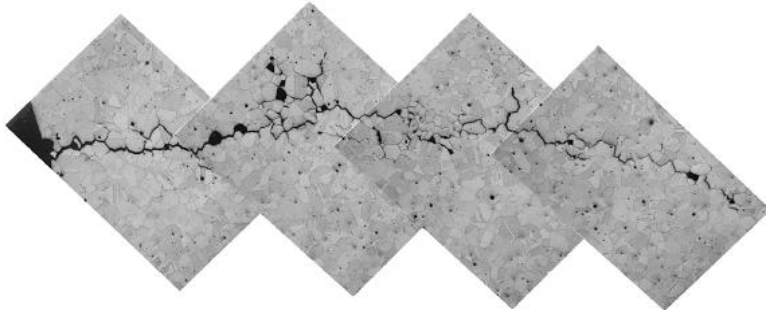

- *Inconel 600 base and weld metal (CRDM nozzle)*

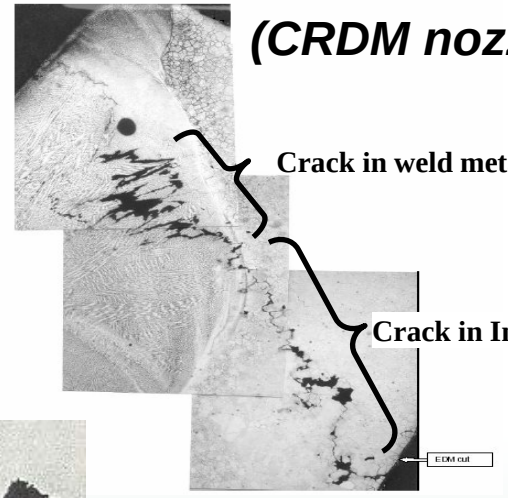

- *In 82/182 weld in pipe*

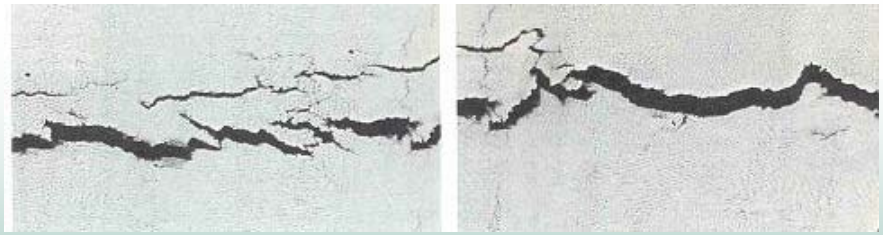

Example of determining crack morphology parameters

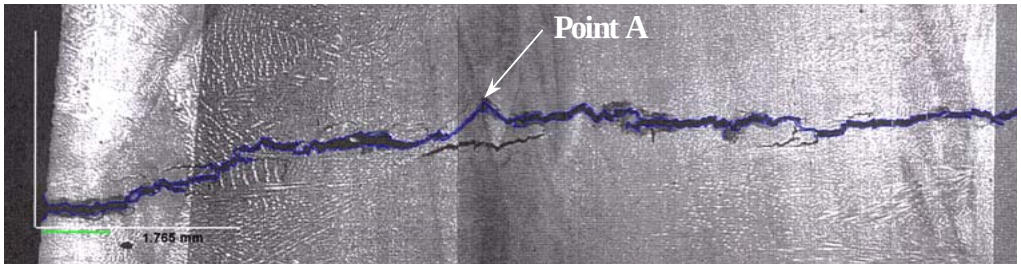

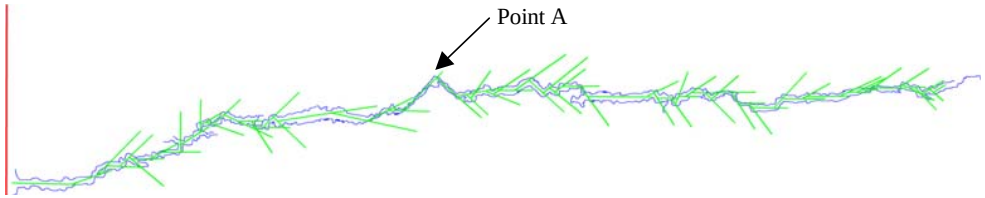

# of turns

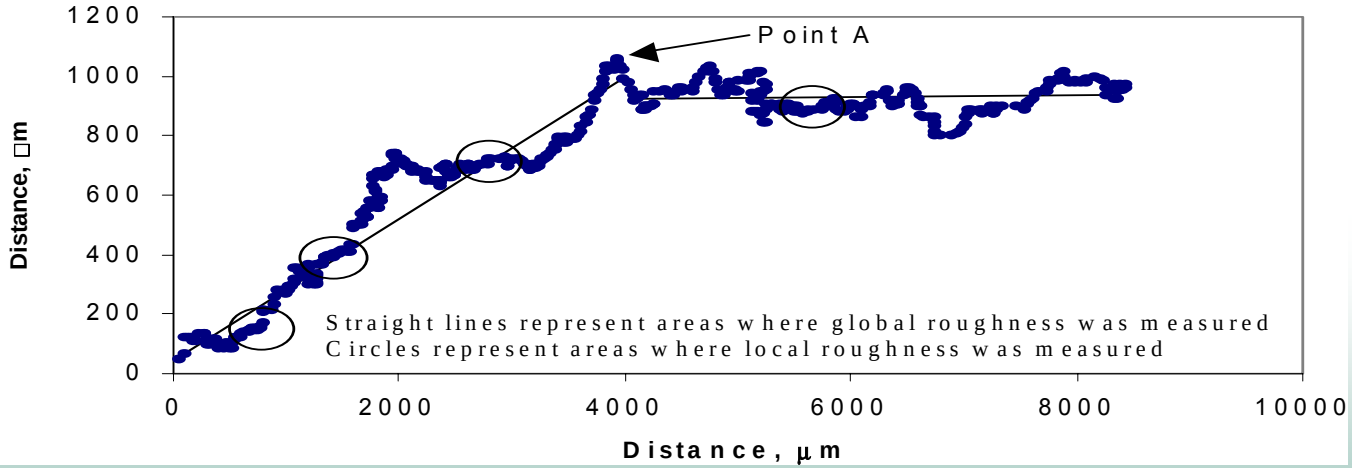

Roughness

Comparison of Parameters for Various Cracking Mechanisms

- ***PWSCC crack results***

Location	μ_L (μm)	μ_G (μm)	n_{tL} (mm^{-1})	K_G	K_{G+L}
Hot-leg Inconel 82/182 weld Parallel to dendritic grain	7.5	52	3.95	1.022	1.132
	4.75	40	12.4	1.000	1.245
Hot-leg Inconel 82/182 weld Parallel to dendritic grain	21	125.5	5.42	1.015	1.278
	34.2	238	1.97	1.000	1.315
CRDM nozzle Inconel 82/182 weld Transverse to dendritic grains	10.2	282	8.3	1.500	2.487
CRDM tube Inconel 600 base metal	4.3	71	5.72	1.001	1.165
CRDM tube Inconel 600 base metal	22	166	9.56	1.170	1.614
CRDM tube Inconel 600 base metal	5.57	41	8.85	1.010	1.203

Mean and standard deviation of crack morphology parameters

Crack Morphology Variable	Corrosion Fatigue		IGSCC		PWSCC – Base		PWSCC – Weld[(a)]	
	Mean	Standard Dev	Mean	Standard Dev	Mean	Standard Dev	Mean	Standard Dev
μ_L, μm	8.814	2.972	4.70	3.937	10.62	9.870	16.86	13.57
μ_G, μm	40.51	17.65	80.0	39.01	92.67	65.26	113.9	90.97
n_L, mm^{-1}	6.730	8.070	28.2	18.90	8.043	2.043	5.940	4.540
K_G	1.017	0.0163	1.07	0.100	1.060	0.095	1.009	0.011
K_{G+L}	1.060	0.0300	1.33	0.170	1.327	0.249	1.243	0.079

(a) Crack growth ***parallel*** to long direction of dendritic grains.

Typical LBB Cases Analyzed

Case Number	Piping System	Bimetallic Weld Location	OD, mm (inch)	Wall thickness, mm (inch)
1	Surge line	Surge line to pressurizer	356 (14.0)	35.7 (1.41)
2	Hot leg	Hot-leg safe end to reactor vessel nozzle	879 (34.6)	68.6 (2.70)
3	Hot leg	Hot-leg safe end to reactor vessel nozzle	878 (34.6)	68.3 (2.69)
4	Surge Line	Surge line to hot leg	406 (16.0)	40.4 (1.59)
5	Surge Line	Surge line to pressurizer	356 (14.0)	35.8 (1.41)
6	Surge Line	Surge line to pressurizer	305 (12.0)	33.3 (1.31)

Typical LBB Cases Analyzed

Case Number	Normal Operating Conditions				Faulted Conditions (N+SSE)			
	Pressure, MPa (psi)	Temp., C (F)	F_x w/press, MN (kips)	M_{eff}, kN-m (in-kips)	Pressure, MPa (psi)	Temp., C (F)	F_x w/press, kN (kips)	M_{eff}, kN-m (in-kips)
1	16.0 (2,327)	345 (653)	1.04 (234)	200 (1,770)	16.0 (2,327)	345 (653)	1,078 (242)	241.6 (2,138)
2	15.4 (2,235)	323 (614)	6.61 (1490)	1720 (15,200)	15.4 (2,235)	323 (614)	7,126 (1,602)	1,861 (16,470)
3	15.4 (2,235)	323 (613)	6.19 (1,390)	3,680 (32,600)	15.4 2,235)	322.8 (613)	7,864 (1,768)	4,397 (38,910)
4	14.8 (2,150)	316 (600)	1.29 (290)	209 (1,853)	14.8 (2,150)	316 (600)	NA	NA
5	14.8 (2,150)	316 (600)	0.98 (221)	243 (2,147)	14.8 (2,150)	316 (600)	NA	NA
6	15.5 (2,250)	345 (653)	0.689 (155)	220 (1,950)	15.5 (2,250)	345 (653)	NA	NA

Case Number	Average Properties						Minimum Properties					
	Yield MPa (ksi)	Ultimate MPa (ksi)	E GPa (msi)	ε_o	α	n	Yield MPa (ksi)	Ultimate MPa (ksi)	E GPa (msi)	ε_o	α	n
1[a]	155 (22.4)	474 (68.7)	179.3 (26.0)	0.000863	6.50	3.80	130 (18.8)	454 (65.8)	179.3 (26.0)	0.000723	9.11	3.80
2[b]	146 (21.1)	453 (65.7)	179.3 (26.0)	0.000812	8.10	3.35	142 (20.6)	434 (62.9)	175.8 (25.5)	0.000808	8.04	5.55
3[a]	169 (24.5)	469 (68)	175.8 (25.5)	0.000961	3.75	4.82	163 (23.7)	427 (61.9)	175.8 (25.5)	0.000929	7.30	8.90
4[c]	229 (33.2)	501 (72.7)	172.7 (25.05)	0.001325	12.1	2.83	NA	NA	NA	NA	NA	NA
5[c]	229 (33.2)	501 (72.7)	172.7 (25.05)	0.001325	12.1	2.83	NA	NA	NA	NA	NA	NA
6[b]	146 (21.1)	453 (65.7)	179.3 (26.0)	0.000812	8.10	3.35	142 (20.6)	434 (62.9)	175.8 (25.5)	0.000808	8.04	5.55

LBB Results – Leakage flaw lengths

- ***PWSCC parallel to dendritic grain – main part of weld***

Case	Applicants'/ Published leakage size flaw, mm (inch)	Leakage crack size, mm (inch) (Using GE/EPRI with original h functions - COD dependence)			
		Air-fatigue crack (300-μinch roughness no turns)	IGSCC	Corrosion-fatigue	PWSCC[(a)]
1[(b)]	71 (2.80)	88.6 (3.49)	178 (6.99)	133 (5.25)	156 (6.13)
2[(c)]	132 (5.20)	142 (5.61)	321 (12.6)	218 (8.52)	291 (11.4)
3[(c)]	85 (3.35)	110 (4.35)	234 (9.23)	166 (6.54)	216 (8.50)
4[(c)]	213 (8.40)	128 (5.03)	253 (9.98)	188 (7.39)	224 (8.81)
5[(c)]	261 (10.26)	214 (8.44)	345 (13.59)	283 (11.13)	306 (12.03)
6[(c)]	76 (3.00)	53.6 (2.11)	104 (4.11)	80.0 (3.15)	90.2 (3.55)

(a) Crack growing ***parallel*** to long direction of dendritic grains in Inconel 82/182 weld.
(b) 5 gpm leak rate – Factor of safety of 10 on 0.5 gpm leakage detection capability.
(c) 10 gpm leak rate – Factor of safety of 10 on 1 gpm leakage detection capability.

626

Comparison of length of leaking corrosion cracks with the length of air-fatigue cracks

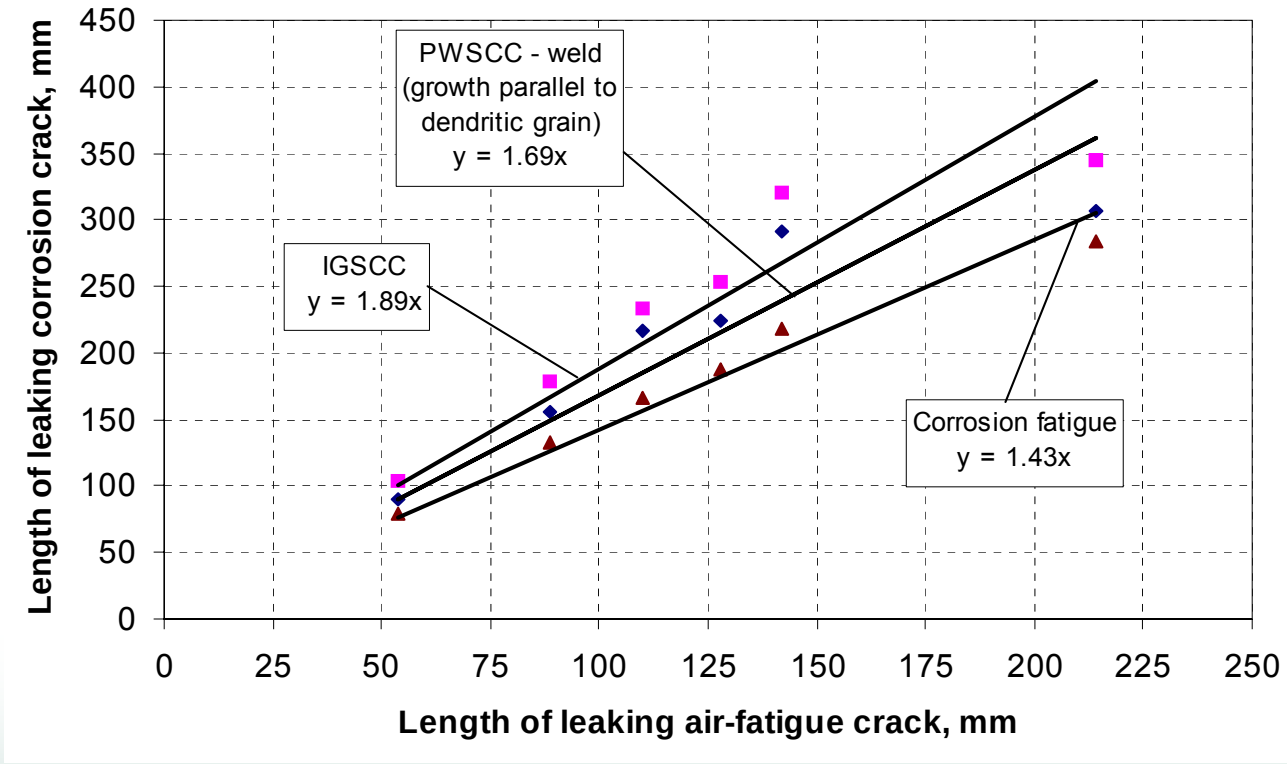

LBB Results – Margins on crack size

- ***PWSCC parallel to dendritic grain – main part of weld***

Case	Applicant/ Published critical flaw size, mm (inch)	Margin on leakage crack size				
		Applicants'/ Published margin	Calculations from this report			
			Air-fatigue crack (300-μinch roughness no turns)	IGSCC	Corrosion -fatigue	PWSCC[(a)]
1	427 (16.8)	6.0	4.82	2.40	3.21	2.74
2	NA[(b)]	>2	5.51	2.45	3.63	2.70
3	190 (7.5)	2.24	1.72	0.81	1.15	0.88
4	396 (15.6)	1.86	3.10	1.56	2.11	1.77
5	462 (18.2)	1.77	2.16	1.34	1.64	1.51
6	163 (6.4)	2.13	3.03	1.56	2.03	1.80

(a) Crack growing ***parallel*** to long direction of dendritic grains.
(b) Applicant's critical flaw size was not available. Critical flaw size was calculated using NRCPIPE Version 3.0. For this case, the critical flaw size was calculated as 785 mm (30.9 inch).

PWSCC growth across the long direction of the dendritic grains – buttered region

Crack growth and shortest path leakage direction

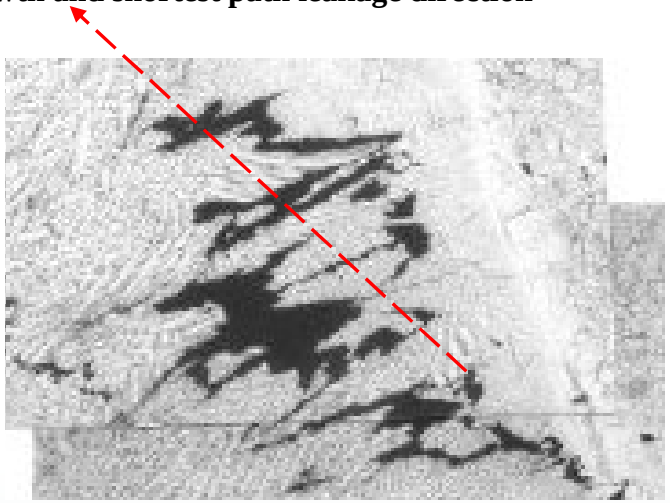

LBB Results – Leakage flaw lengths

- ***PWSCC perpendicular to dendritic grain – buttered region crack***

Case	Applicants'/ Published Leakage Size Flaw, mm (inch)	Leakage crack size, mm (inch) (Using GE/EPRI with original h functions & SQUIRT with COD dependence)	
		Air-fatigue crack (300-μinch roughness with no turns)	PWSCC[(a)] (with crack growing *perpendicular* to long direction of dendritic grains)
1[(b)]	71 (2.80)	88.7(3.49)	187 (7.35)
2[(c)]	132 (5.20)	142 (5.61)	356 (14.02)
3[(c)]	85 (3.35)	110 (4.35)	287 (11.28)
4[(c)]	213 (8.40)	128 (5.03)	271 (10.68)
5[(c)]	261 (10.26)	214 (8.44)	353 (13.89)
6[(c)]	76 (3.00)	53.6 (2.11)	120 (4.72)

(a) Crack morphology parameters are derived from only one photomicrograph, Figure 19 of Reference 12.
(b) 5 gpm leak rate – Factor of safety of 10 on 0.5 gpm leakage detection capability.
(c) 10 gpm leak rate – Factor of safety of 10 on 1 gpm leakage detection capability.

LBB Results – Margins on crack size

- ***PWSCC perpendicular to dendritic grain – buttered region crack***

Case	Applicants'/ Published Critical Flaw Size, mm (inch)	Margin on leakage crack size		
		Applicants'/ Published margin	Margins from analysis in this report	
			Air fatigue crack (300-µinch roughness with no turns)	PWSCC[(b)] (with crack growing *perpendicular* to long direction of dendritic grains)
1	427 (16.8)	6.0	4.82	2.28
2	NA[(a)]	>2	5.51	2.21
3	190 (7.5)	2.24	1.72	0.66
4	396 (15.6)	1.86	3.10	1.46
5	462 (18.2)	1.77	2.16	1.31
6	163 (6.4)	2.13	3.03	1.35

(a) Applicant's critical flaw size was not available. Critical flaw size was calculated using NRCPIPE Version 3.0. For this case, the critical flaw size was calculated as 785 mm (30.9 inch).

(b) Crack morphology parameters are derived from only one photomicrograph, Figure 19 of Reference 15.

Conclusions

- ***PSWCC cracks have a more tortuous flow path than air fatigue cracks that were frequently used in past LBB submittals***

- ***PWSCC crack morphology parameters determined from a few limited service cracks***

- ***PWSCC crack morphology slightly less severe than IGSCC if crack grow parallel to dendritic grains, but could be worse if going perpendicular to dendritic grain – buttered region***

Conclusions

- ***An updated LBB analysis was conducted using typical LBB submittals***
  - ***J-R curves for In82/182 in progress***

633

- ***PWSCC cracks have leakage crack lengths that are longer than air fatigue cracks (used in many LBB submittals) at the same leakrate***
  - ***~70% longer if PWSCC is parallel to dendritic grain – main weldment***
  - ***~110% longer if PWSCC is perpendicular to dendritic grain – buttered region***

Conclusions

- *Average margin on LBB crack length decreased from 3.39 for air-fatigue crack to*
  - *1.9 for the PWSCC crack growing parallel to the long direction of the dendritic grains*
  - *1.55 for the PWSCC crack growing transverse to the long direction of the dendritic grains*

- *LBB difficult to satisfy for PWSCC crack cases using draft SRP 3.6.3 procedures*

- *PWSCCs could result in long circumferential surface cracks, which could make breaks more likely to occur than by using the simple circumferential through-wall crack analysis*
  - *LBB screening criteria not satisfied*